A CDC48 COFACTOR AFFECTS UBIQUITINATED PROTEIN LEVELS, ENDOPLASMIC RETICULUM ASSOCIATED DEGRADATION AND PROTEASOME SUBTYPES

by

Joseph Riley Tran

Bachelor's of Science, University of Pittsburgh at Johnstown, 2000

Master's of Science, Indiana University of Pennsylvania, 2003

Submitted to the Graduate Faculty of

The School of Medicine in partial fulfillment

of the requirements for the degree of

Doctor of Philosophy

University of Pittsburgh

2012

UNIVERSITY OF PITTSBURGH

SCHOOL OF MEDICINE

This dissertation was presented

by

Joseph Riley Tran

It was defended on

August 17, 2012

and approved by

Dr. Raymond A. Frizzell, Professor and Director of Cystic Fibrosis Research Center

Dr. Rebecca P. Hughey, Professor, Cell Biology and Molecular Physiology

Dr. Martin C. Schmidt, Associate Professor, Microbiology and Molecular Genetics

Dr. Thomas E. Smithgall, William S. McEllroy Professor and Chair, Microbiology and Molecular Genetics

Dissertation Advisor: Dr. Jeffrey L. Brodsky, Professor and Avinoff Chair of Biological Sciences, Biological Sciences

A CDC48 COFACTOR AFFECTS UBIQUITINATED PROTEIN LEVELS, ENDOPLASMIC RETICULUM ASSOCIATED DEGRADATION AND PROTEASOME SUBTYPES

Joseph Riley Tran, Ph.D.

University of Pittsburgh, 2012

The ubiquitin proteasome system (UPS) maintains cellular homeostasis by controlling the turnover of important regulatory enzymes and by the removal of damaged or misfolded proteins. The UPS serves as the basic framework of many specific catabolic pathways, including the Endoplasmic Reticulum-Associated Degradation (ERAD) pathway, which in particular helps to maintain the homeostasis of the early secretory pathway. An important component of the ERAD pathway is a complex containing the AAA ATPase, Cdc48p. The Cdc48p complex couples ATP hydrolysis with the physical dislocation of ubiquitinated substrates from the endoplasmic reticulum prior to degradation by a multi-subunit catabolic protease known as the 26S proteasome. Here I show that the loss of a Cdc48p cofactor, VCP/Cdc48p-associated Mitochondrial Stress-responsive-1 (Vms1p), negatively affects the turnover of the model ERAD substrate, the Cystic Fibrosis Transmembrane Conductance Regulator (CFTR), but does not affect the ubiquitination of CFTR. Strains lacking both the *VMS1* gene and other select Cdc48p cofactors, namely genes encoding members of the Ubiquitin Regulatory X and Ubiquitin Fusion Degradation families, are hypersensitive to certain chemical stressors, and also display additive ERAD defects for certain substrates. Curiously, *VMS1* mutants show increased accumulation of ubiquitinated proteins in total cell extracts, and also in complex with Cdc48p. These data suggest that Vms1p functions after substrate ubiquitination. In support of this hypothesis, I found that

VMS1 mutants show a decrease in the amount of proteasome that handles ubiquitinated substrates and an increase in the amount of free, latent 20S proteasome holoenzyme. This phenomenon is not a result of the altered expression of proteasome components. Additionally, the restoration of ubiquitinated protein accumulation and the distribution of proteasome subtypes to near wild-type levels require the physical interaction between Vms1p and Cdc48p. Furthermore, Cdc48p may be important for recruitment of Vms1p to the proteasome. Using yeast genetics I provide supporting evidence that indicates that Vms1p does not appear to function with various proteasome assembly chaperones. Quantitative mass spectrometry indicates that Cdc48p-associated proteasome is unaffected by loss of *VMS1*. Together my data indicates that Vms1p functions with Cdc48p to regulate proteasome subtypes that are required to degrade ubiquitinated substrates.

TABLE OF CONTENTS

LIST OF TABLES

LIST OF FIGURES

PREFACE

Accomplishing a doctorate is really the work of many people. True, I did the experiments and quite a bit of thinking, but this type of journey requires guidance, a guidance that not only shapes the project, but also the person doing the work. I'd like to thank Jeff Brodsky – my doctoral mentor. You helped think critically and clearly about my work. You also helped me develop my public speaking – something that was quite disorganized when I joined the lab. I'm infinitely thankful for these things (and many others). I would like to thank my dissertation committee (Drs. Ray Frizzell, Becky Hughey, Tom Smithgall, and Martin Schmidt) for their insightful guidance. I appreciate and thank my past and present lab mates for making the lab a wonderful environment: Sarah Grubb, Karen Hecht, Stacy Alex Kolb, Sandlin Seguin and Shruthi Vembar; the postdocs: Teresa Ninehouser (nee: Buck), Annette Chiang, Chris Guerriero, Cristy Gelling, Kunio Nakatasukasa Patrick Needham, and Lucia Zacchi, our lab manager Jen Goeckeler-Fried, and our undergrads, especially Kurt Weiberth, Kasia Mikoluk and Joe Clay. I also especially want to thank Kunio who provided his guidance, and Jen for making everyday lab life smooth. I also thank the lab of Roger Hendrix and Bob Duda for pleasantry and reagents; the lab of Karen Arndt (Peggy Shirra) for help with yeast genetics; Tom the coffee guy for soup and bagels; Cathy Barr, Cindy Duffy and Kristin DiGiacomo for the behind-the-scenes work in the main office. I am indebted to my past: Drs. Clair Francomano (GBMC), David Schlessinger (NIA/NIH), Ramaiah Nagaraja (NIA/NIH) and Bob Hinrichsen (IUP). Your endless support is

greatly appreciated. Finally, I want to thank my family and friends for their endless support. To mom and dad for everything you've done to guide me, and for never giving up even when I quit. To my brothers and sisters, David, Martin, Christine, Mark, and Cindy, we've always done it together, so congrats!

1.0 INTRODUCTION TO THE UBIQUITIN PROTEASOME SYSTEM

Life is a balance between anabolic and catabolic pathways. However, for much of the 1950s through the 1970s, research in biology was largely skewed towards the study of anabolic processes such as nucleic acid and protein production with little regard to how these biomolecules were turned over. It was thought that protein turnover was a generally non-specific process, and that degradation occurred within a specialized, acidic organelle known as the lysosome in mammals, or the vacuole in lower eukaryotes and plants. However, a series of discoveries from the mid to late 1970s changed the scientific view of protein catabolism - the process was energy dependent and highly regulated. In the last 30 or so years, a tremendous amount of work has been done on the ubiquitin proteasome system, and we now know that this system is as important to the birth of proteins as it is to their death. In this Chapter, I will introduce the basic components of the ubiquitin proteasome system followed by a description of a specialized branch of this system at the endoplasmic reticulum (ER).

1.1 UBIQUITIN

The ubiquitin proteasome system (UPS) is the major eukaryotic catabolic pathway tasked with regulating cellular enzymes and protecting the cell from damaged or misfolded proteins. The targets of the UPS are modified most commonly by the covalent attachment of a highly-

conserved 76 amino acid protein known as ubiquitin via its carboxy-terminal glycine to the ε-amino group of a lysine residue on a recipient protein (HERSHKO and CIECHANOVER 1998). The fate of a ubiquitinated substrate is largely dependent on whether the target is modified by one (monoubiquitination) or many ubiquitin (multiubiquitination and polyubiquitination) moieties (**Figure 1**) (HICKE 2001; HOCHSTRASSER 1996). The monoubiquitination of a substrate normally alters a protein's function or localization and is well documented for processes such as gene transcription, DNA repair, membrane trafficking, and protein endocytosis (HAGLUND *et al.* 2003; HICKE 2001; OSLEY 2004). In contrast, substrate polyubiquitination is most commonly associated with substrate degradation by a multi-subunit ATP-dependent protease known as the 26S proteasome (HOCHSTRASSER 1996). Polyubiquitination, however, has an additional and rather complex layer of regulation. The polyubiquitin polymer is formed by the successive linking of one ubiquitin to another ubiquitin via one of eight different linkages between the ubiquitin moieties (**Figure 2**) (WALCZAK *et al.* 2012). Seven of these linkages are based on internal lysine residues within ubiquitin while the eighth is an amino-terminal linkage that leads to the formation of a linear ubiquitin chain (WALCZAK *et al.* 2012). Of these eight possible linkages, two ubiquitin linkages are highly abundant and well characterized (HERSHKO and CIECHANOVER 1998). The lysine 48 (K48)-linked polyubiquitin chain is the most common type and leads to the most recognizable consequence of ubiquitination, substrate degradation by the 26S proteasome (CHAU *et al.* 1989; VAN NOCKER and VIERSTRA 1993). The lysine 63 (K63)-linkage, alternatively, directs proteins primarily to non-degradative fates (ARNASON and ELLISON 1994; HOCHSTRASSER 2006; SPENCE *et al.* 1995). Not surprisingly, the structures of K48- and K63-linked chains are very different. K48-chains are compact while K63-chains appear extended, and these structures suggest that their recognition by ubiquitin-binding proteins is a

strong determinant of their fate (**Figure 3**) (KIM and RAO 2006; PICKART and FUSHMAN 2004; WICKLIFFE *et al.* 2011). There is also very compelling evidence indicating that all ubiquitin-linkages, aside from linear and K63 chains are candidates for proteasome-mediated degradation (XU *et al.* 2009). Though some of these linkages are highly abundant (e.g., K11 and K63), they cannot rescue the inviability of strains lacking the K48 linkage (XU *et al.* 2009). Intriguingly, "atypical" ubiquitin chains with mixed linkages have been detected, some of which result from ubiquitin chain editing (BEN-SAADON *et al.* 2006; IKEDA and DIKIC 2008; KIM *et al.* 2007; NEWTON *et al.* 2008; WINBORN *et al.* 2008). One exciting possibility is that a ubiquitin chain of mixed linkages may couple temporal and spatial information for protein function prior to degradation.

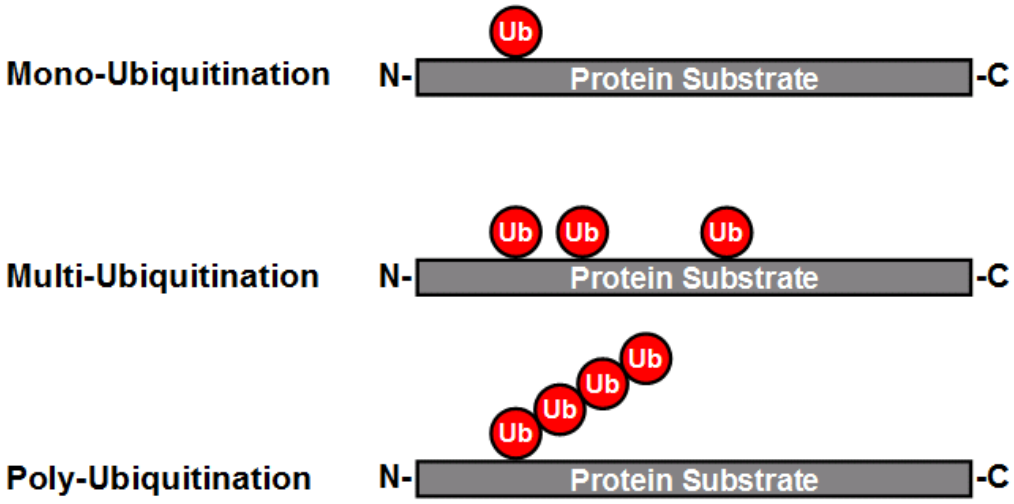

Figure 1. Mono, multi, and polyubiquitination

In monoubiquitination, a ubiquitin (red circle) peptide is attached to a substrate. Multiubiquitination is monoubiquitination, but at many different sites. Polyubiquitination describes the formation of a ubiquitin-ubiquitin chain on a substrate.

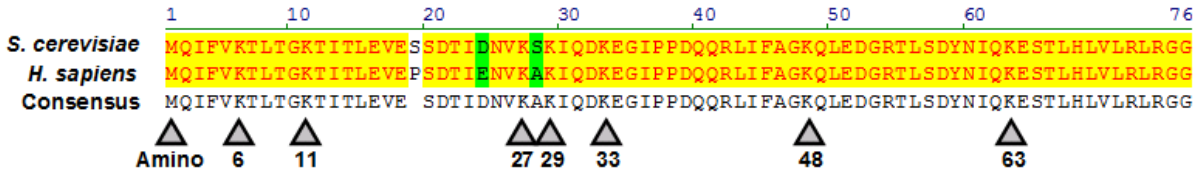

Figure 2. Conservation of Ubiquitin

Pair-wise alignment of full-length ubiquitin from *Homo sapiens* and *Saccharomyces cerevisiae* using Vector NTI. Identical residues are highlighted in yellow and conserved changes are in green. Inverted arrowheads indicate residues used to forming linkages in a polyubiquitin chain.

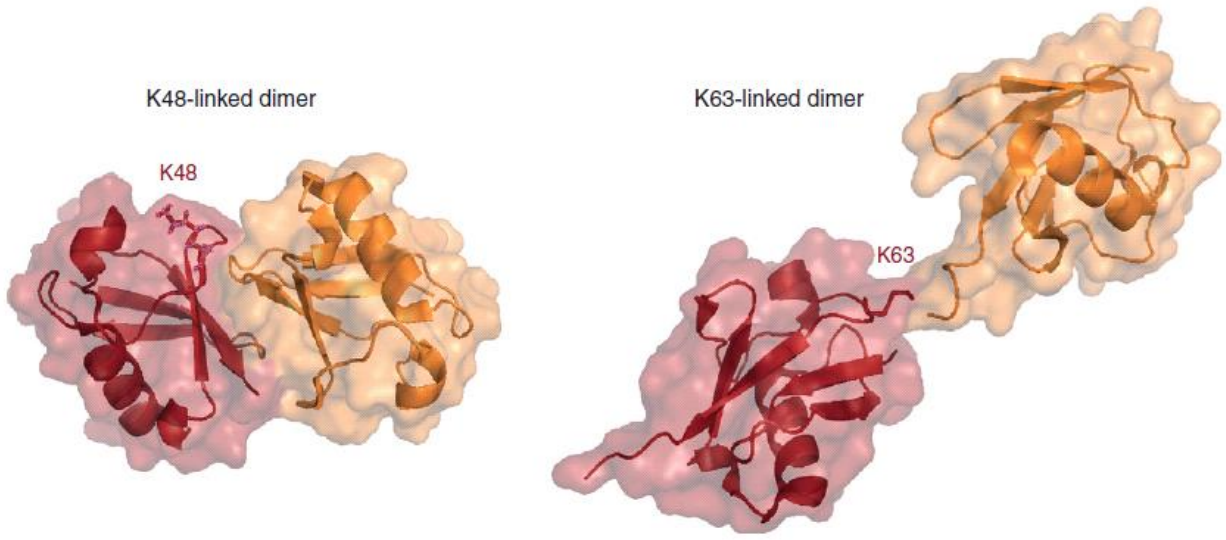

Figure 3. The Structure of K48 and K63-linked diubiquitin

Ribbon diagrams of K48- and K63-linked diubiquitin. K48 diubiquitin adopts a compact structure while K63 diubiquitin is extended. K48-linkage is a classic degradation signal. The K63-linkage is involved primarily in non-degradative fates (WICKLIFFE *et al.* 2011).

1.1.1 ENZYMES OF THE UBIQUITIN PROTEASOME SYSTEM

The process leading to substrate ubiquitination occurs in a step-wise fashion (**Figure 4**), and starts with the initial formation of a ubiquitin-adenylate intermediate by the adenylation domains of the E1 activating enzyme (SCHULMAN and HARPER 2009). Next, a covalent thioester bond is formed between the terminal glycine of the ubiquitin-adenylate intermediate and the Second Catalytic Cysteine Half-domain (SCCH) of the E1-activating enzyme by attack from a cysteine residue found within this domain (SCHULMAN and HARPER 2009). Upon thioester bond formation, the E1 enzyme undergoes a conformational change that exposes E2-conjugating enzyme interaction surfaces in the Ubiquitin Fold Domain (HUANG *et al.* 2007; LEE and SCHINDELIN 2008). The ubiquitin in the E1-ubiquitin complex is next transferred to an E2-conjugating enzyme by a transthioesterification reaction that is mediated by attack from a cysteine residue in the highly-conserved UBiquitin Conjugating (UBC) domain of the E2 enzyme (LEE and SCHINDELIN 2008). The E2-ubiquitin complex then transfers its ubiquitin moiety to a substrate via one of two important families of E3 ubiquitin ligases whose mechanisms of action are distinct (FINLEY 2009) (see below).

The three step process shown in **Figure 4** is highly conserved with only a few variations; one example is the ability of select E2 enzymes to directly monoubiquitinate some ubiquitin binding proteins (HOELLER *et al.* 2007). The initial activation of an ubiquitin moiety by an E1 enzyme occurs at a quicker rate than that of substrate ubiquitination, and for good reason: most eukaryotes possess a single E1 enzyme (MCGRATH *et al.* 1991). The fact that E1 enzymes are

efficient machines is in part because they can interact with two ubiquitin moieties: one at the active site cysteine in the SCCH and a second at the site of ubiquitin-adenylate intermediate formation (SCHULMAN and HARPER 2009). By comparison, E2-conjugating enzymes are more abundant than E1 enzymes, but are far less common than E3 ubiquitin ligases (PICKART 2001). In humans, there are two E1s, ~38 E2s, and greater than 600 E3 enzymes, while yeast has a single E1, 13 E2, and ~60 E3 enzymes (CREWS 2003; YE and RAPE 2009). Given the number of potential substrates, the functional hierarchy of the UPS, and the large number of E3 ubiquitin ligases, it is not a surprise that the E3 enzymes are largely responsible for selecting substrates.

The two important families of E3 ubiquitin ligases are the Really Interesting New Gene (RING) zinc finger and Homologous to the E6-AP Carboxy Terminus (HECT) domain families (FREEMONT *et al.* 1991; HUIBREGTSE *et al.* 1995). The RING and HECT domain families differ in their mode of action. RING finger E3 ligases promote the attachment of ubiquitin to a substrate directly from an E2-ubiquitin complex, and never come in contact with the ubiquitin moiety itself (BAILLY *et al.* 1997; KWON *et al.* 1998). The RING-E3 ligases do this by acting as a molecular scaffold that brings the active site of the E2-ubiquitin spatially closer to a lysine on a substrate (DESHAIES and JOAZEIRO 2009). It is worth noting the existence of a minor subfamily of E3 ubiquitin ligases possessing a variation of the RING zinc finger, called a U-box domain. U-box E3 ligases, unlike the RING zinc finger domain E3s, do not contain the key cysteine residues needed for zinc ion coordination (HATAKEYAMA and NAKAYAMA 2003; PATTERSON 2002). Interestingly, some U-box family members possess a ubiquitin-extending, or E4 activity (KOEGL *et al.* 1999; NAKATSUKASA *et al.* 2008). The mechanism of U-box ligase activity is similar to that of RING E3 ligases, and both require structural flexibility to place the charged E2

in close proximity to a substrate for efficient polyubiquitination (QIAN *et al.* 2009). HECT E3 ligases, on the other hand, directly form a thioester bond with the ubiquitin moiety prior to transferring the ubiquitin to a substrate (ROTIN and KUMAR 2009; SCHEFFNER *et al.* 1995). All HECT E3s have an invariant cysteine residue in the HECT domain that forms this bond, and the sequences surrounding the HECT domain are important for mediating interaction with E2s and substrate (LEE *et al.* 2009; ROTIN and KUMAR 2009). Like the RING domain E3s, HECT E3s are also structurally flexible (VERDECIA *et al.* 2003). While the domains that define an E3 ubiquitin ligase may be conserved, there can be variability in the surrounding sequences. These variable regions are likely determinants for E2 and substrate specificity (DESHAIES and JOAZEIRO 2009; ROTIN and KUMAR 2009).

In a clever twist in E3 evolution, a very abundant group of RING-like domain E3 ligases has evolved structural flexibility by becoming entirely modular. This group of E3s is generically called the Skp1-Cullin-Fbox (SCF)-family of RING-like E3 ubiquitin ligases. SCF family E3s have both substrate recognition and E3 ligase activity in separate protein complexes that then assemble onto a scaffold protein (DESHAIES and JOAZEIRO 2009). In yeast, the scaffold (Cullin portion), substrate recognition protein (Fbox portion), and the RING E3 are encoded by the *CDC53*, *CDC4*, and *HRT1* genes, respectively. A protein encoded by the *SKP1* gene connects the substrate binding Fbox to the Cullin scaffold and an E2 conjugating enzyme, Cdc34p supplies the activated ubiquitin. SCF mediated protein degradation is particularly important for the regulation of the cell cycle (SKAAR and PAGANO 2009).

The E3 ligases are processive enzymes and can successively add ubiquitin moieties to form the polyubiquitin chain on a substrate (DESHAIES and JOAZEIRO 2009; ROTIN and KUMAR 2009). This feat can be accomplished by oligomerization of the E3s, or by repeated association/dissociation of the E2/E3 complex in addition to other mechanisms that have yet to be defined (CHENG *et al.* 2009; KLEIGER *et al.* 2009). In some instances, an entire polyubiquitin chain can be formed on an E3, or in solution, and at least *in vitro* can be added to a substrate by the E3 ligase (LI *et al.* 2007a; PARKER and ULRICH 2009; WANG and PICKART 2005). It is unknown if E3s add entire polyubiquitin chains en bloc *in vivo*, but this is a formal possibility since di-, tri-, and tetra-ubiquitin chains can exist as free entities *in vivo*.

As introduced above, ubiquitin linkage is an important determinant of ubiquitinated substrate fate. There is compelling evidence that the formation of specific linkages is mediated primarily by the E2 enzyme in combination with an E3, but evidence also suggests that the determinants for linkage may lie within the E3 itself (KIM and HUIBREGTSE 2009; KIM *et al.* 2007; MASTRANDREA *et al.* 1999; YOU and PICKART 2001). It is quite likely that there are many more factors involved in determining what type of ubiquitin linkage is formed, and we are only beginning to understand this.

Aside from these enzymes, the cell possesses additional ubiquitin-specific enzymes that help to modify the outcome of ubiquitination. For example, deubiquitinating (DUB) enzymes are a large group of proteins that can 1) remove ubiquitin from substrates and prevent degradation, 2) process ubiquitin precursors, 3) recycle ubiquitin, or 4) assist in editing the linkage of the ubiquitin chain on a protein (AMERIK and HOCHSTRASSER 2004; CROSAS *et al.* 2006; MAYER and

WILKINSON 1989; NEWTON *et al.* 2008; PAPA and HOCHSTRASSER 1993; PICKART and ROSE 1985). DUB enzymes are classified either as papain-like cysteine or zinc-metalloproteases (REYES-TURCU *et al.* 2009). And, examples of select DUBs in yeast illustrate the varied roles of this enzyme class. Doa4p, for instance, is involved in recycling ubiquitin and is also important in the process of ubiquitin-mediated endocytosis (AMERIK *et al.* 2000; SWAMINATHAN *et al.* 1999). Another example, Otu1p, is involved in regulated turnover of ubiquitin-fusion degradation substrates associated with the ATPase, Cdc48p (RUMPF and JENTSCH 2006). Otu1p and a protein known as Ufd3p compete with Ufd2p for binding to Cdc48p. The Ufd2p protein belongs to a group of the aforementioned E4 polyubiquitin-extending enzymes and promotes the efficient degradation of various substrates by extending the polyubiquitin chain (HOPPE 2005; KOEGL *et al.* 1999; NAKATSUKASA *et al.* 2008; SHI *et al.* 2009). This "tug-of-war" battle between deubiquitination and polyubiquitin chain extension is also demonstrated for the DUB, Ubp6p and the E4 enzyme, Hul5p at the 26S proteasome (CROSAS *et al.* 2006). Ultimately, the regulated turnover of the vast majority of UPS substrates is governed by the balance between the addition, extension, and removal of ubiquitin.

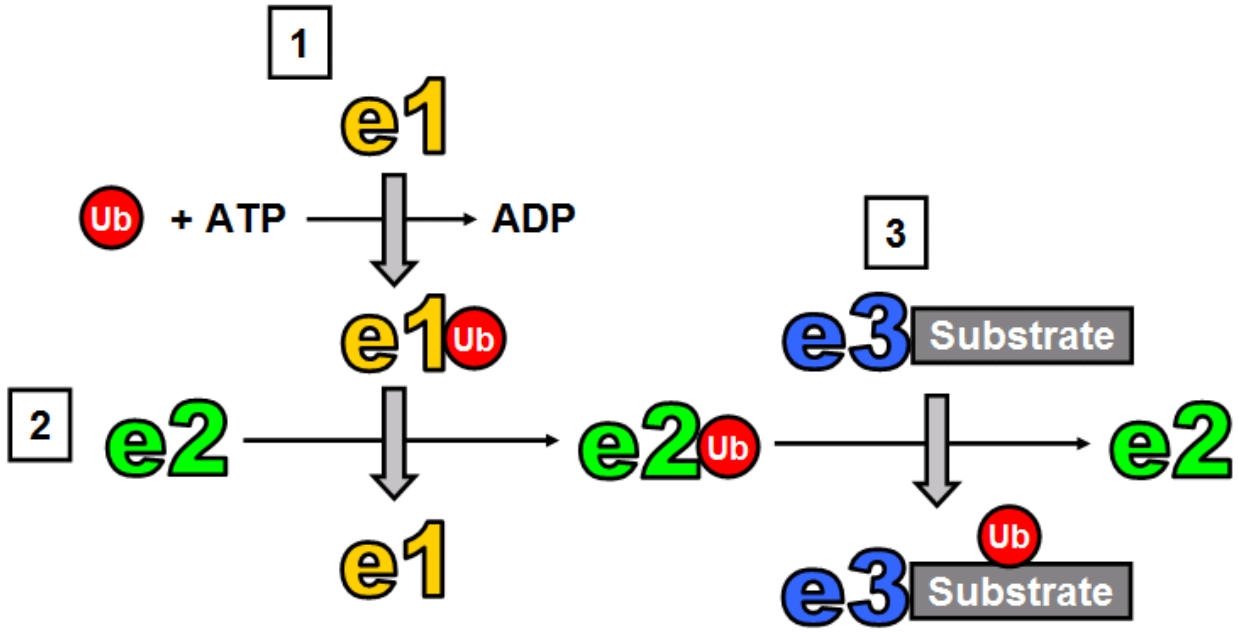

Figure 4. Ubiquitin cascade

Ubiquitin (red circle) is first activated by an E1-activating enzyme (yellow) in an ATP-dependent process. The ubiquitin-E1 complex then passes the ubiquitin to an E2-conjugating enzyme (green). The E2-ubiquitin complex works with an E3-substrate (blue/grey) complex resulting in substrate ubiquitination.

1.1.2 UBIQUITIN INDEPENDENT DEGRADATION

A chain of four ubiquitin moieties is minimally required for proteasomal degradation (THROWER *et al.* 2000). It is not entirely clear why an extended polyubiquitin chain is needed, but one can speculate that having a long chain of ubiquitins, with perhaps mixed linkages, can potentially serve as recruitment platform for a large number of processing factors. Interestingly, there are a select number of substrates that undergo proteasomal degradation without being ubiquitinated. For instance, the tumor suppressor p53 can be degraded by both ubiquitin-dependent and independent mechanisms, while ornithine decarboxylase is degraded by the proteasome in an entirely ubiquitin-independent manner (ASHER *et al.* 2005; HOYT *et al.* 2003). Some proteins that possess ubiquitin-like or -associated domains can also be degraded independent of ubiquitination (BAUGH *et al.* 2009). And, localization to the proteasome appears to be sufficient to trigger protein degradation independent of ubiquitin (JANSE *et al.* 2004). The proteasome has also been shown to retrotranslocate a non-ubiquitinated substrate for degradation from the ER (LEE *et al.* 2004).

1.2 THE 26S PROTEASOME

The K48-linked polyubiquitinated substrate is the prototypical degradation substrate of the 26S proteasome. The 26S proteasome is a large multi-subunit ATP-dependent protease that is composed of two main parts, a 20S proteolytic core particle (20S core, or CP) and the 19S

regulatory particle (19S cap, PA700, or RP), which accepts and processes ubiquitinated substrates (LIU *et al.* 2002; PICKART and COHEN 2004; VOGES *et al.* 1999). In the cell, the proteasome exists as three major forms: the 20S core alone and the 20S core flanked by either one 19S cap (RPCP) or two 19S caps (RP_2CP, **Figure 5**) (VOGES *et al.* 1999). Though it is unknown if there are functional distinctions between the RP1CP and RP2CP forms, both versions are considered to be active towards ubiquitinated substrates as they are readily detectable with artificial fluorogenic reporters (HOUGH *et al.* 1986; HOUGH *et al.* 1987). Conversely, the 20S core is considered inactive under normal circumstances and undetectable by fluorogenic reporter substrates unless low concentrations of detergent or fatty acids are added (ARRIBAS and CASTANO 1990; DAHLMANN *et al.* 1985; MCGUIRE *et al.* 1989). The 20S core is also a latent enzyme in the presence of cellular concentrations of select cations, such as potassium, further suggesting inactivity (KOHLER *et al.* 2001; WILK and ORLOWSKI 1983).

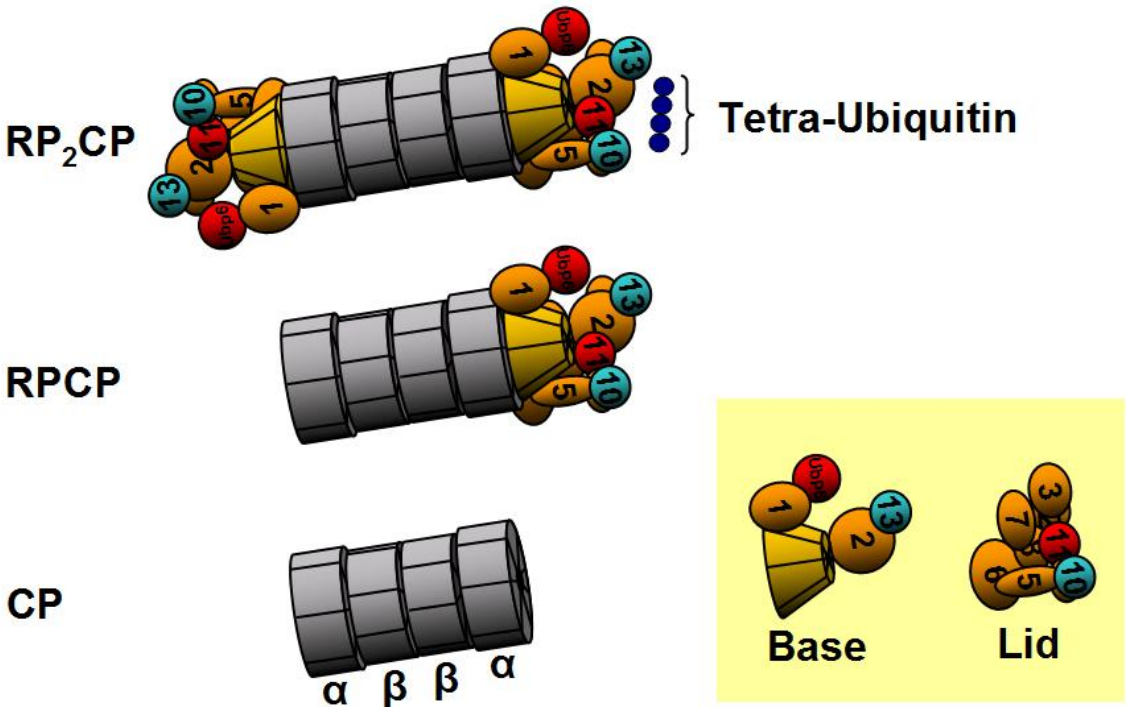

Figure 5. Three forms of the proteasome

The proteasome exists in three dominant forms. The 20S core particle (CP, grey barrel) is composed of four-stacked seven member rings (αββα). The CP can be flanked by one "base" and "lid" subassembly (boxed in yellow, RPCP) or two subassemblies (RP_2CP).

1.2.1 Proteasome localization

The activation of the 20S by fatty acids is intriguing given the fact that the mammalian 26S proteasome is found associated with the ER – a major site of lipid and protein biosynthesis (ENENKEL *et al.* 1998; FRICKE *et al.* 2007; RIVETT *et al.* 1992). The ER/nucleus is postulated to be the site of the proteasome biogenesis (FRICKE *et al.* 2007; GORBEA *et al.* 2004; LEHMANN *et al.* 2002). In yeast, components of the 19S cap were shown to be more abundant at the ER than components of the 20S core (KALIES *et al.* 2005). The juxtanuclear quality control compartment, which is a major site of protein degradation in yeast and mammals, is situated near the ER (KAGANOVICH *et al.* 2008). In both yeast and mammals, the 26S proteasome is localized throughout the cytosol, nucleus, and at the surface of many endomembrane systems (RIVETT 1998; WOJCIK and DEMARTINO 2003). Proteasomes are quite abundant in the nucleus where they are associated with both degradative and, surprisingly, non-degradative roles (VON MIKECZ 2006). The roles of nuclear proteasomes include nucleotide excision repair and regulation of gene expression (GONZALEZ *et al.* 2002; RUSSELL *et al.* 1999). Intriguingly, a protein known as Sts1p may act as a proteasome receptor and aid in localizing proteasomes within the nucleus (CHEN *et al.* 2011). The localization of the proteasome has even been noted to change during different stages of the cell cycle (WOJCIK and DEMARTINO 2003). Overall, however, the regulation of proteasome localization and dynamics are currently poorly understood.

1.2.2 The 20S core particle

The 20S core particle is a cylindrical, chambered protease that is composed of four-stacked heteroheptameric rings (GRZIWA *et al.* 1991; KOPP *et al.* 1986; LOWE *et al.* 1995). The two outer-most rings are largely structural and are composed of alpha subunits while the inner-most pair of rings contains the proteolytic activity and are composed of beta subunits (**Figure 5**). The chambered protease is an evolutionarily conserved structure. The 20S proteasome of archaebacteria, eubacteria, and eukaryotes all share this structure along with the unrelated chambered proteases of prokaryotes (PICKART and COHEN 2004). Although there is evidence suggesting that the free 20S core particle can process select types of substrates, the 20S is an inactive enzyme because the aperature leading into the barrel is closed by the amino-termini of the alpha subunits that serve as a gate (BAUGH *et al.* 2009; DAHLMANN *et al.* 1985; GROLL *et al.* 1997; JUNG and GRUNE 2008). In *Saccharomyces cerevisiae*, the amino-terminus of the alpha3 subunit plays an important role in 20S gating by coordinating the amino termini of other select alpha subunits (alpha1, 2, 6, 7) (GROLL *et al.* 2000; GROLL *et al.* 1997). Curiously, the yeast alpha3 subunit is the only non-essential subunit of the 20S core, and can be replaced by an additional alpha4 subunit (HILT and WOLF 1995; KUSMIERCZYK *et al.* 2008; VELICHUTINA *et al.* 2004). As expected, this alternate version of the 20S core has increased basal 20S activity (VELICHUTINA *et al.* 2004). This paradigm is not uncommon as naturally-occurring alternative versions of select 20S subunits exist in higher eukaryotes, with some subunits being known to alter the proteolytic activity of the proteasome (DRISCOLL *et al.* 1993; GACZYNSKA *et al.* 1993; VELICHUTINA *et al.* 2004).

The constitutive catalytic subunits of the 20S core are the beta1, beta2, and beta5 subunits, and each subunit possesses an evolutionarily-conserved but distinct proteolytic activity. The beta1, beta2, and beta5 subunits contain: 1) peptidylglutamyl peptide hydrolyzing, 2) trypsin-like and 3) chymotrypsin-like activities which cleave after: 1) acidic, 2) basic and 3) hydrophobic residues, respectively. In addition to these three subunits, humans have a group of inducible beta subunits known as beta1i, beta2i, and beta5i, which are expressed by many cell types in response to interferon-gamma signaling and are incorporated into the proteasome. This results in the formation of the immunoproteasome, or i-proteasome (DRISCOLL *et al.* 1993; GACZYNSKA *et al.* 1993). The i-proteasome helps process host and pathogen proteins for display by the Major Histocompatibility Complex I (MHCI), but also has a major function in the degradation of the defective ribosomal products that can occur as a result of increased protein translation (KINCAID *et al.* 2012; SEIFERT *et al.* 2010). As expected, the i-proteasome subunits confer enhanced proteolytic activity to the 26S and 20S proteasome (DRISCOLL *et al.* 1993; GACZYNSKA *et al.* 1993).

1.2.3 The 19S cap and accessory complexes

The 20S core particle can be flanked by any number of accessory complexes (HOFFMAN *et al.* 1992). The accessory complex associated with ubiquitinated protein degradation, and also the most recognizable is the 19S cap. The highly-conserved 19S cap is composed of two main parts, the base and lid (**Figure 5**) (GLICKMAN *et al.* 1998a). In yeast, the base of the cap is composed of a heterohexameric ring of ATPases (Rpt1p-6p), which drives a deubiquitinated substrate into the 20S core barrel, and a quartet of proteins that are involved in stabilizing the 19S cap structure and ubiquitin-substrate binding (Rpn1p, 2p, 10p, 13p) (ELSASSER *et al.* 2002; GLICKMAN *et al.*

1998a; GLICKMAN *et al.* 1998b; HUSNJAK *et al.* 2008; VAN NOCKER *et al.* 1996). Rpn10p, in particular has been proposed to be important in stabilizing the complete 19S cap structure, and recent cryo-electron microscopy studies of yeast 26S proteasomes with and without the Rpn10p and Rpn13p suggest that these two ubiquitin receptors determine the requirement of tetraubiquitin as a degradation signal (GLICKMAN *et al.* 1998a; LANDER *et al.* 2012; SAKATA *et al.* 2012; THROWER *et al.* 2000). The base subassembly sits on top of the 20S core particle, forming contacts between the ATPase ring and the alpha subunits (PETERS *et al.* 1993; WALZ *et al.* 1998). The ring of ATPases contributes to the opening of the 20S gate via an evolutionarily-conserved "hydrophobic-tyrosine-X" (HbYX) motif at the carboxy terminus (KOHLER *et al.* 2001; SMITH *et al.* 2007). Many other factors also contribute to the opening of the 20S core, possibly by binding to and modulating the activity of the ATPase ring, or affecting the assembly of the 19S-20S subunits (BECH-OTSCHIR *et al.* 2009; LI and DEMARTINO 2009; PETH *et al.* 2009).

Traditionally, the base subassembly was thought to be positioned below the lid subassembly. However, recent cryo-electron microscopy studies indicate that the lid components are on the side of the base and even contact the 20S core (LANDER *et al.* 2012). Nevertheless, the lid subassembly in yeast is composed of nine proteins, Rpn3p, 5p-9p, 11p, 12p, and Sem1p (FUNAKOSHI *et al.* 2004; GLICKMAN *et al.* 1998b; SONE *et al.* 2004). Many lid components (e.g., Rpn3p, 5p, 6p, 7p, 9p, 11p, 12p, and Sem1p) appear to be necessary for the biogenesis and stability of the 19S lid structure, and the 26S proteasome (CHANDRA *et al.* 2010; FUKUNAGA *et al.* 2010; FUNAKOSHI *et al.* 2004; ISONO *et al.* 2004; ISONO *et al.* 2005; JOSHI *et al.* 2011; PATHARE *et al.* 2012; SONE *et al.* 2004; TOMKO and HOCHSTRASSER 2011; YU *et al.* 2011). One structural component, Rpn11p, however, contains a specific activity. Rpn11p is one of two DUB

enzymes associated with the proteasome in yeast; the other is Ubp6p (see above) (GUTERMAN and GLICKMAN 2004; LEGGETT *et al.* 2002; VERMA *et al.* 2002; VERMA *et al.* 2000; YAO and COHEN 2002). As a core component of the 19S lid, Rpn11p is required for the stability of the 19S cap and as a DUB enzyme can remove ubiquitin *en bloc* from a substrate (LANDER *et al.* 2012). Ubp6p, on the other hand, has a processive ubiquitin trimming activity, and also a DUB-independent function that modulates the activity and assembly of the proteasome (HANNA *et al.* 2006; PETH *et al.* 2009; SAKATA *et al.* 2011). Cryo-electron microscopy of the 19S indicates that Rpn11p is well-positioned between the two ubiquitin receptors and nearest the entrance of the ATPase base subassembly, a position where the *en bloc* removal of an entire ubiquitin chain is important (LANDER *et al.* 2012). On the other hand, Ubp6 is at the periphery of the 19S which is consistent with its involvement in ubiquitin chain trimming and thus rescuing substrates from degradation (**Figure 5**) (CROSAS *et al.* 2006; LANDER *et al.* 2012).

In addition to the 19S cap, the 20S core can be flanked by other accessory complexes, of which many seem to increase the proteolytic activity of the 20S core (HOFFMAN *et al.* 1992; MA *et al.* 1992; SCHMIDT *et al.* 2005). For example, the yeast Blm10 protein promotes the efficient degradation of a number of protein substrates by gating the proteasome in a manner similar to that of the HbYX motif of the 19S base (DANGE *et al.* 2011; LOPEZ *et al.* 2011). Interestingly, there are other proteins that possess this HbYX motif, most notably the multifunctional hexameric ATPase, p97, which is the mammalian homolog of yeast Cdc48p (see below, Dave Smith, West Virginia University, personal communication). Indeed it does appear that Cdc48 and 20S form a stable and functional complex (BARTHELME and SAUER 2012). It will be

interesting to find out if other HbYX motif-ATPase complexes modulate the activity of this important protease.

1.2.4 Proteasome assembly

The multitude of proteasomal accessory complexes, cofactors, and alternate proteasomal subunits suggests that there are specialized assembly pathways. Additionally, the composition of the proteasome is known to change under certain stress conditions (HANNA *et al.* 2007; WANG *et al.* 2010; XIE and VARSHAVSKY 2001). Early hints of a proteasome assembly pathway were demonstrated in reconstitution experiments that originally aimed to prove that the 20S core was a component of the 26S proteasome (DRISCOLL and GOLDBERG 1990; EYTAN *et al.* 1989; GANOTH *et al.* 1988; HOFFMAN *et al.* 1992; ORINO *et al.* 1991). These experiments showed that the 19S cap was composed of two chief parts, the lid and base, that when mixed together with the third fraction containing the 20S formed the 26S particle (DRISCOLL and GOLDBERG 1990; EYTAN *et al.* 1989; HOFFMAN *et al.* 1992; ORINO *et al.* 1991). Preincubating these three fractions with ATP to promote assembly prevented a delay in model substrate degradation (GANOTH *et al.* 1988). Work from the late 1990s has since uncovered a host of dedicated assembly chaperones for the assembly of both the 20S core and 19S cap.

The assembly of the 20S core particle is well-defined and evolutionarily-conserved between man and yeast (MURATA *et al.* 2009). In yeast, five different chaperones contribute to different stages of 20S core formation. Two heterodimeric complexes, Pba1p-Pba2p and Pba3p-Pba4p, cooperate to form the alpha ring which then serves as a template for subsequent chaperone-assisted incorporation of the beta subunits (LE TALLEC *et al.* 2007; LI *et al.* 2007b).

This alpha and the partially-complete beta ring pair is known as the "half-mer" (**Figure 6**). It is worth noting that the Pba1p-Pba2p and Pba3p-Pba4p chaperones appear to have specific functions in the formation of the half-mer. For instance, Pba1p-Pba2p mutants have a specific defect in chymotryptic-like (beta5) activity, suggesting a specific role in beta ring formation (LI *et al.* 2007b; SCOTT *et al.* 2007). Pba4p mutants lead to the incorporation of the alpha4 subunit in place of the alpha3 subunit, suggesting a role in alpha ring formation (KUSMIERCZYK *et al.* 2008; MURATA *et al.* 2009). Intriguingly, Pba3p-Pba4p mutants form the alternate 20S proteasome that is observed when alpha3 is deleted (see above). It is still not clear if this alternative, more active 20S core exists naturally in yeast. As mentioned, the half-mer is incomplete, and in yeast, the beta7 subunit is not incorporated until the dimerization of two half-mers to form the 20S core (**Figure 7**) (LI *et al.* 2007b; MARQUES *et al.* 2007). The incorporation of beta subunits and dimerization of the two half-mers is assisted by a fifth chaperone, Ump1p (RAMOS *et al.* 1998). Half-mer dimerization results in the encapsulation and degradation of Ump1p after the processing of the catalytic beta subunit propeptides, as well as the noncatalytic beta6 and beta7 subunits (CHEN and HOCHSTRASSER 1996; HEINEMEYER *et al.* 1997; RAMOS *et al.* 1998; SEEMULLER *et al.* 1996).

Interestingly, mutations in the genes-encoding Pba3p, Pba4p, Ump1p, and alpha3 lead to the accumulation of 19S cap precursors, suggesting that the 20S core particle can serve a scaffold for 19S cap formation (HENDIL *et al.* 2009; KUSMIERCZYK *et al.* 2008). Like the 20S core, the 19S cap is also assembled by chaperone-like proteins (**Figure 8**). The assembly of the base of the 19S has only been recently described. Here, four proteasome-dedicated chaperones, Nas2p, Nas6p, Hsm3p, and Rpn14p bind different Rpt-Rpn subunits of the 19S base to facilitate their

assembly (FUNAKOSHI *et al.* 2009; KANEKO *et al.* 2009; LE TALLEC *et al.* 2009; PARK *et al.* 2009; ROELOFS *et al.* 2009; SAEKI *et al.* 2009). These chaperones bind near the carboxy terminus of their respective Rpt subunits, and are displaced by the presence of the 20S core particle (ROELOFS *et al.* 2009). The binding of the chaperone probably prevents the premature proteolytic activation by the formation of a stable complex between an unregulated, base assembly and the 20S core particle (BESCHE *et al.* 2009b; HENDIL *et al.* 2002; KRIEGENBURG *et al.* 2008). Surprisingly, the simultaneous deletion of all four chaperones does not completely abolish the formation of the 26S proteasome (SAEKI *et al.* 2009). These data indicate that there are alternative back-up methods to assemble this essential protease.

The assembly of the lid is very poorly characterized, and no dedicated chaperones have been identified thus far. However, analyses of the lid intermediates that accumulate in various lid mutants have identified two main lid modules, one containing Rpn5p, 6p, 8p, 9p, 11p and a second consisting of Rpn3p, 7p and Sem1p (FUKUNAGA *et al.* 2010; ISONO *et al.* 2004). This provides evidence that Rpn12p is the last lid component to incorporate when these two modules form (**Figure 9**) (FUKUNAGA *et al.* 2010; ISONO *et al.* 2004). This conclusion is supported by the finding that mutations in the Rpn12p carboxy terminus accumulate the entire lid subassembly without Rpn12p (TOMKO and HOCHSTRASSER 2011). *In vitro* reconstitution experiments indicate that the carboxy terminus of Rpn12p drives the association of the lid and base subassemblies in the presence of 20S core particles (TOMKO and HOCHSTRASSER 2011).

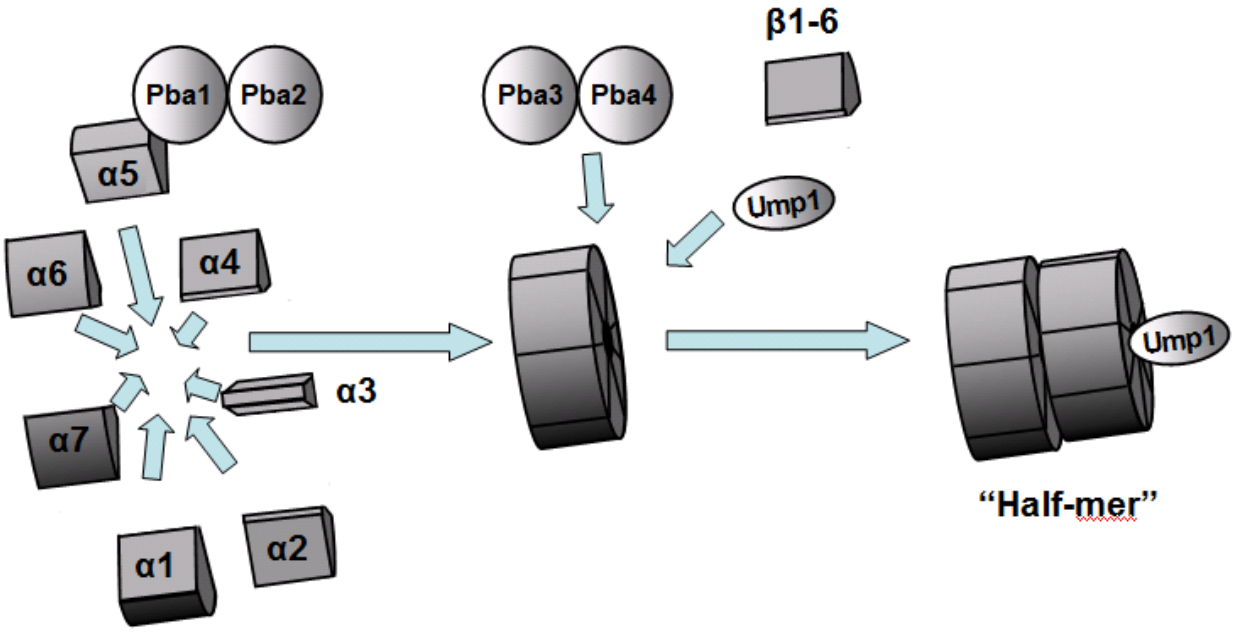

Figure 6. Assembly of the 20S half-mer

Two chaperones, Pba1p and Pba2p, facilitate the assembly of the alpha ring. The assembled alpha ring then serves as a template for beta ring assembly. Beta ring assembly is assisted by the Pba3p, Pba4p and Ump1p chaperones and is incomplete as the beta7 subunit is not incorporated. This incomplete structure is called the "half-mer".

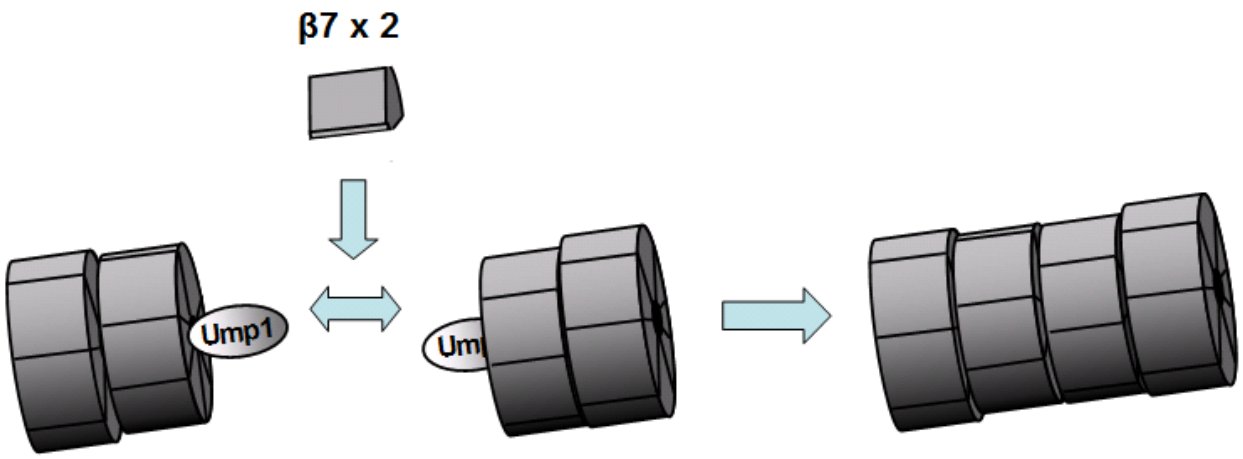

Figure 7. Assembly of the 20S core

Two half-mers are joined together and incorporate two copies of the beta 7 subunit. This encapsulates Ump1p which is then degraded after catalytic subunit propeptide maturation and formation of the 20S core particle.

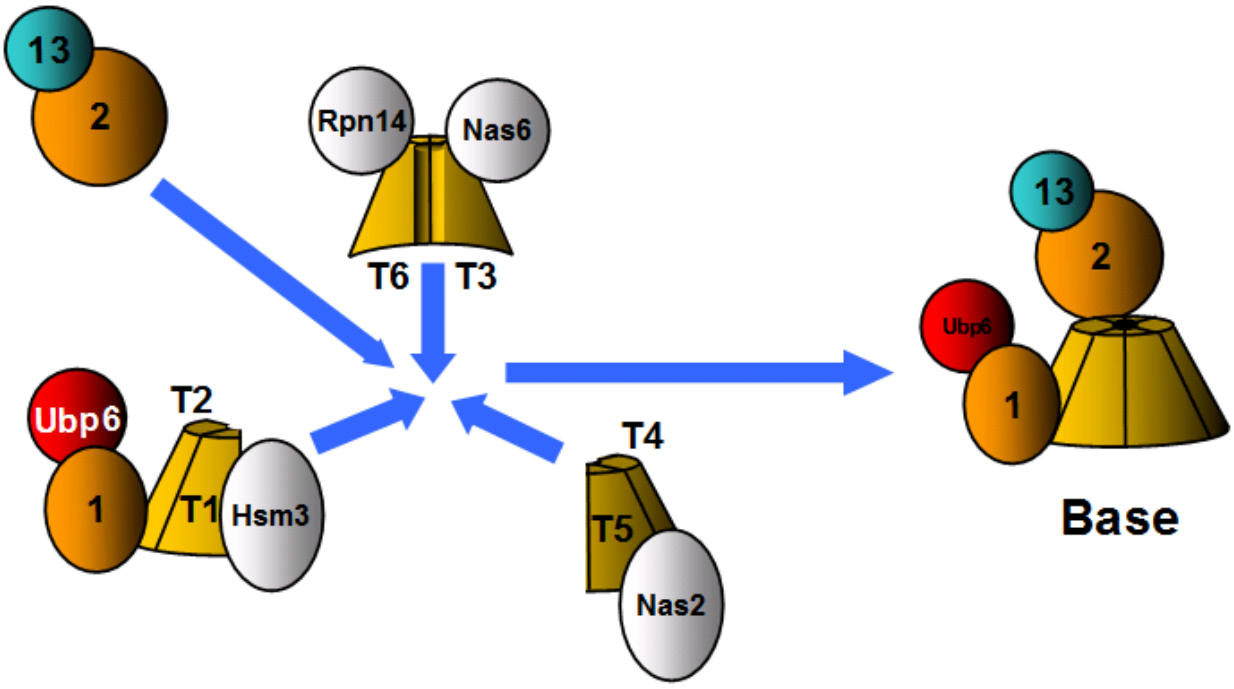

Figure 8. Assembly of the 19S base

Hsm3p , Nas2p, and the Rpn14p/Nas6p pair facilitate the assembly of the base. Hsm3p interacts with Rpt1p (T1), Rpt2p (T2), Rpn1p (1) and Ubp6p. Nas6p interacts with Rpt5p (T5) and Rpt4p (T4). Rpn14p and Nas6p interact with Rpt6p (T6) and Rpt3p (T3), respectively. White indicates proteasome chaperone, red indicates deubiquitinating enzyme, blue indicates ubiquitin receptor, orange indicates non-ATPase subunit and yellow indicates ATPase subunit.

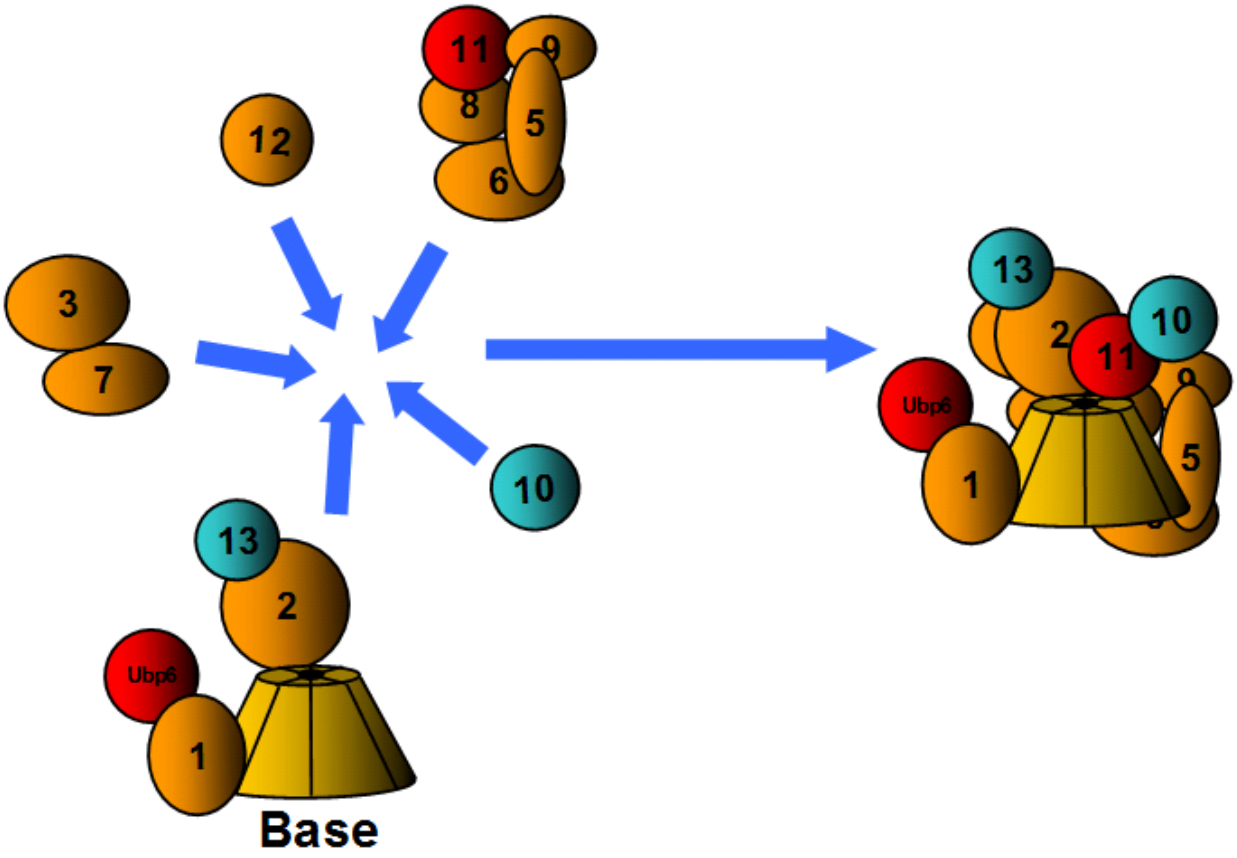

Figure 9. Assembly of the 19S lid

Two intermediates of the 19S lid subassembly 1) Rpn3p (3) and Rpn7p (7), and 2) Rpn5p (5), Rpn6p (6), Rpn8p (8), and Rpn11p (11) are joined together by Rpn12p (12). This subassembly is then joined to the 19S base by Rpn10p (10). Red indicates deubiquitinating enzyme, blue indicates ubiquitin receptor, orange indicates non-ATPase subunit and yellow indicates ATPase subunit.

1.2.5 Additional Factors

Other factors also appear to be involved in the assembly and function of the proteasome. For instance, yeast Hsp90 mutants or Hsp90 inhibitor treatment (geldanamycin) has been reported to reduce the levels of 26S proteasome (IMAI *et al.* 2003). Ubiquitinated substrates have been shown to promote the stability of the 26S proteasome, and ATP hydrolysis may destabilize the yeast proteasome (BABBITT *et al.* 2005; KLEIJNEN *et al.* 2007). Specific proteins such as Ecm29p, Not4p, and Nob1p have partially characterized roles in proteasome biology (LEHMANN *et al.* 2010; PANASENKO and COLLART 2011; TONE and TOH 2002; WANG *et al.* 2010). For example, Ecm29p is involved in the joining of the 19S cap and 20S core, and binds to both 19S cap and 20S core particles (LEHMANN *et al.* 2010). Ecm29p also serves as a quality control checkpoint and appears to inhibit improperly assembled proteasomes (LEE *et al.* 2011). This implies that there is some assembly of the proteasome can occur after the 19S and 20S particles are joined. The proteasome is also subject to environmental factors. For instance, ubiquitin depletion promotes the expression of the DUB, Ubp6p, which is then loaded onto the 26S proteasome to promote the recycling of ubiquitin (HANNA *et al.* 2007). Hydrogen peroxide, or reactive oxygen species-triggered stress promotes the disassembly of the proteasome (WANG *et al.* 2010). Organelle stress, such as that from misfolded proteins at the ER leads to changes in the expression of the proteasome, which is mediated by the proteasomal transcription factor Rpn4p (METZGER and MICHAELIS 2009; XIE and VARSHAVSKY 2001). The proteasomal stress response is generally conserved, but the equivalent of Rpn4p in mammals, Nrf1, has only recently been identified (RADHAKRISHNAN *et al.* 2010).

1.2.6 Chemical targeting of the Proteasome

Chemical modulation of the proteolytic activity of the proteasome has received considerable interest since it was discovered to have positive effects in the treatment of certain cancers (ADAMS and KAUFFMAN 2004; TAN *et al.* 2006). Currently, there are five proteasomal inhibitors in clinical trial, and one (Bortezomib/Velcade) is FDA-approved for use as a frontline cancer treatment for certain types of cancers, such as multiple myeloma and some types of lymphoma (MOLINEAUX 2012). These inhibitors are either natural beta-lactones or protected peptides with groups that are reactive towards the proteasome active site (MOLINEAUX 2012). These inhibitors take advantage of the fact that these cancers are caused by professional secretory cells that are under high levels of ER stress; therefore reducing proteasomal activity pushes these cells towards apoptosis (KISSELEV *et al.* 2012).

1.3 ENDOPLASMIC RETICULUM ASSOCIATED DEGRADATION (ERAD)

The function of the UPS underlies many cellular protein degradation pathways. These pathways are largely defined by specific E2, E3, DUB and E4 enzyme combinations in addition to other specific adaptor proteins. Some of these pathways are further divided depending on the location (e.g., cytoplasmic versus intraorganellar) and nature (e.g., misfolded protein versus a naturally regulated substrate) of a given substrate. One of the most thoroughly examined models of UPS-mediated protein degradation is with regard to misfolded protein substrates in the ER.

The ER is the site of protein synthesis and folding for both transmembrane and secreted proteins in eukaryotes. The volume of protein traffic that enters the ER, and thus the early secretory pathway is very large and accounts for 20-30% of the total proteome (GHAEMMAGHAMI *et al.* 2003; LANDER *et al.* 2001). Proteins enter the secretory pathway by one of two modes, co-translationally or post-translationally, both of which utilize the highly-conserved Sec61 translocation channel complex (RAPOPORT *et al.* 1999). The yeast Sec61p translocation channel is a membrane-spanning multi-protein complex that contains two additional proteins, Sbh1p and Sss1p and is the docking site of the translating ribosome (ROMISCH 1999). The central pore of Sec61p is gated closed by the molecular chaperone, BiP/Kar2p, which allows the environment of the secretory pathway to be different from that found in the cytoplasm (HAMMAN *et al.* 1998). Proteins that enter the secretory gateway can be subject to: 1) proteolytic cleavage of the ER-targeting signal sequence, 2) Asparagine-linked (Asn or N-linked) glycosylation, 3) disulfide bond formation, 4) chaperone-assisted protein folding and 5) propeptide processing (BRODSKY and SKACH 2011).

The environment of the ER differs from the cytoplasm in a number of ways. For example, the ER is an oxidizing environment that allows the formation of disulfide bonds, and is a major site of lipid metabolism and calcium storage (CSALA *et al.* 2006; RAINA and MISSIAKAS 1997). The ER also acts as a protein concentrating organelle prior to secretory protein transport (MIZUNO and SINGER 1993). These factors can present a hurdle to proper protein folding, especially if the protein is mutated or damaged. Fortunately, the early secretory pathway is protected from misfolded proteins by a protein quality-control/processing pathway known as Endoplasmic Reticulum-Associated Degradation (ERAD) (MCCRACKEN and BRODSKY 1996; VEMBAR and

BRODSKY 2008). The ERAD pathway is composed of a cooperating set of sequential events: substrate recognition and targeting, ubiquitination by membrane-anchored E3 ubiquitin ligases, substrate retrotranslocation, and finally degradation by the 26S proteasome. Substrate recognition is the starting point for the ERAD surveillance pathway and is based largely on the location of the offending lesion (ISMAIL and NG 2006; SMITH *et al.* 2011; VASHIST and NG 2004; VEMBAR and BRODSKY 2008).

1.3.1 ERAD-Lumenal (ERAD-L)

Misfolded proteins inside the ER are recognized by a specific set of molecular chaperones, and are targeted to the protein degradation machinery that comprises the ERAD-Lumenal (ERAD-L) pathway (**Figure 10**) (BUCK *et al.* 2007; CARVALHO *et al.* 2006; DENIC *et al.* 2006; VASHIST and NG 2004). The primary ERAD-L chaperone is a 72 KDa protein known as BiP, or Kar2p in yeast. Kar2p is a member of the abundant Heat Shock Protein 70 (HSP70) family and couples ATP hydrolysis with protein binding. The ATPase activity of HSP70 proteins, as well as their substrate binding ability can be modulated by cofactors such as HSP40 co-chaperones (BRODSKY 2007). The activity of HSPs can be either pro-folding or pro-degradation. In addition, chaperone-like lectins such as Yos9p and Htm1p monitor the status of the N-linked glycosylation signals on ERAD-L substrates (BHAMIDIPATI *et al.* 2005; KIM *et al.* 2005; NAKATSUKASA *et al.* 2001; SZATHMARY *et al.* 2005). N-linked glycosylation occurs on proteins that possess the Asn-X-Ser/Thr (NXS/T) consensus motif inside the ER lumen (HELENIUS and AEBI 2004). The N-linked glycosylation signal serves a dynamic timer of substrate folding and is based on the removal and addition of glucose residues (by glucosidases and glycosyl transferases, respectively), and the trimming of mannoses from the parent oligosaccharide (N-acetylglucosamine$_2$ - mannose$_9$ -

glucose$_3$) (HELENIUS and AEBI 2004). Molecular chaperones and these lectins target misfolded ERAD-L substrates to the ER membrane via physical interactions with the transmembrane ubiquitin ligase complex. Here, they are presented to the catalytic portion of the E3 ubiquitin ligase found on the cytosolic side of the ER by a "retrotranslocation" mechanism that is poorly understood.

The ubiquitin ligase of the yeast ERAD-L pathway is a transmembrane RING E3 known as Hrd1p (**Figure 10**) (BAYS *et al.* 2001a; HAMPTON *et al.* 1996). Hrd1p interacts with a number of different proteins to form a multi-protein complex that appears to regulate its ubiquitin ligase activity (CARVALHO *et al.* 2010; GARDNER *et al.* 2000). One key interactor with the Hrd1p E3 enzyme is Cue1p, a transmembrane tether for the cytosolic E2-conjugating enzyme, Ubc7p (BIEDERER *et al.* 1997). Cue1p is part of a larger and poorly-characterized family of proteins defined by the monoubiquitin-binding CUE domain (SHIH *et al.* 2003). The ERAD-L pathway is defined by this particular E2 (Ubc7p) -E3 (Hrd1p) pairing. Hrd1p receives substrates via a physical interaction with second key partner, Hrd3p, which is a transmembrane receptor for the lumenal lectin-like chaperone and chaperone Yos9p and Kar2p/BiP, respectively (CARVALHO *et al.* 2006; DENIC *et al.* 2006; GARDNER *et al.* 2000; GAUSS *et al.* 2006). Hrd1p substrates are then linked to the cytosolic protein degradation machinery by a Hrd1p interaction with the transmembrane protein, Ubx2p (CARVALHO *et al.* 2006; DENIC *et al.* 2006; SCHUBERTH *et al.* 2004). Ubx2p possesses a Ubiquitin Regulatory X (UBX) domain that is needed to recruit an abundant hexameric ATPase complex that contains Cdc48p (see below) (BUCHBERGER *et al.* 2001; NEUBER *et al.* 2005; SCHUBERTH and BUCHBERGER 2005; SCHUBERTH *et al.* 2004; WILSON *et al.* 2006). The Cdc48p hexamer and Npl4p/Ufd1p cofactors provide the specificity

and mechanical force needed to retrotranslocate a substrate from the ER (see below) (BAYS *et al.* 2001a; HITCHCOCK *et al.* 2001; JAROSCH *et al.* 2002; RABINOVICH *et al.* 2002; YE *et al.* 2001). This simplified ERAD-L model indicates that the Hrd1p complex serves as a central hub for receiving, ubiquitinating and recruiting the necessary cytosolic factors for substrate retrotranslocation from the ER.

The Hrd1p protein has additional interaction partners that have incompletely characterized roles in the ERAD-L complex and pathway. For instance, Hrd1p interacts with Der1p, which from studies of the mammalian homolog Derlin-1 was proposed to be part of an undefined proteinaceous channel that allows substrates to pass from inside the ER to the cytosol (LILLEY and PLOEGH 2004; YE *et al.* 2004). While data supporting the Derlin-1/Der1p translocation channel model in yeast (and mammals) are lacking, yeast Der1p mutants have a rather significant protein degradation defect for many ERAD-L substrates, indicating an important and conserved role for this protein (HORN *et al.* 2009; KNOP *et al.* 1996; PLEMPER *et al.* 1999; SATO and HAMPTON 2006). Recently, the human Derlin-1 protein, which bears a resemblance to the rhomboid protease family, has been linked to ERAD, although the catalytic residue in Derlin-1 is mutated (GREENBLATT *et al.* 2011; ZETTL *et al.* 2011). The interaction between Hrd1p and Der1p is mediated by Usa1p, a transmembrane protein that contains a Ubiquitin-Like (UBL) domain (**Horn 09**). In the absence of Hrd3p, Hrd1p self-ubiquitination occurs *in trans* through a Usa1p-mediated oligomerization of Hrd1p (CARROLL and HAMPTON 2010; GARDNER *et al.* 2000). The self-ubiquitination of Hrd1p ultimately leads to degradation but is largely independent of Der1p (CARROLL and HAMPTON 2010; HORN *et al.* 2009). In yeast, Dfm1p is a Der1p homolog which itself is an unstable protein that depends on Usa1p (HITT and WOLF 2004; STOLZ *et al.* 2010).

Unlike Der1p, Dfm1p mutants do not show defects in the ERAD-L pathway, but, conflictingly, may show a defect for a model, mutated transmembrane substrate (HITT and WOLF 2004; SATO and HAMPTON 2006; STOLZ *et al.* 2010). Genetic interaction studies suggest that Dfm1p may also function in a non-ERAD process that involves Cdc48p (SATO and HAMPTON 2006). And Dfm1p, but not Der1p genetically interacts with Cdc48p (SATO and HAMPTON 2006). While Hrd1p is best known for its role in the ERAD-L pathway, it was originally discovered as a protein required for the degradation of the transmembrane protein, Hmg2p (HAMPTON *et al.* 1996). This example is not isolated, as Hrd1p is necessary for the degradation of other transmembrane proteins such as a mutated versions of the translocation channel, Sec61p, and the multi-drug resistance pump, Pdr5p (BIEDERER *et al.* 1997; PLEMPER *et al.* 1998). While there is still confusion about the roles of Hrd1p interaction partners, the simplest model is that the Hrd1p complex plays two roles in ERAD that are both mediated by Usa1p: a Der1p-dependent ERAD-L, and a Der1p-independent ERAD-Membrane (ERAD-M) pathway (CARROLL and HAMPTON 2010; HORN *et al.* 2009; SATO and HAMPTON 2006). In general, transmembrane proteins represent a complex class of ERAD substrates as they can have misfolded protein signatures on either side, or even within the lipid bilayer of the ER membrane.

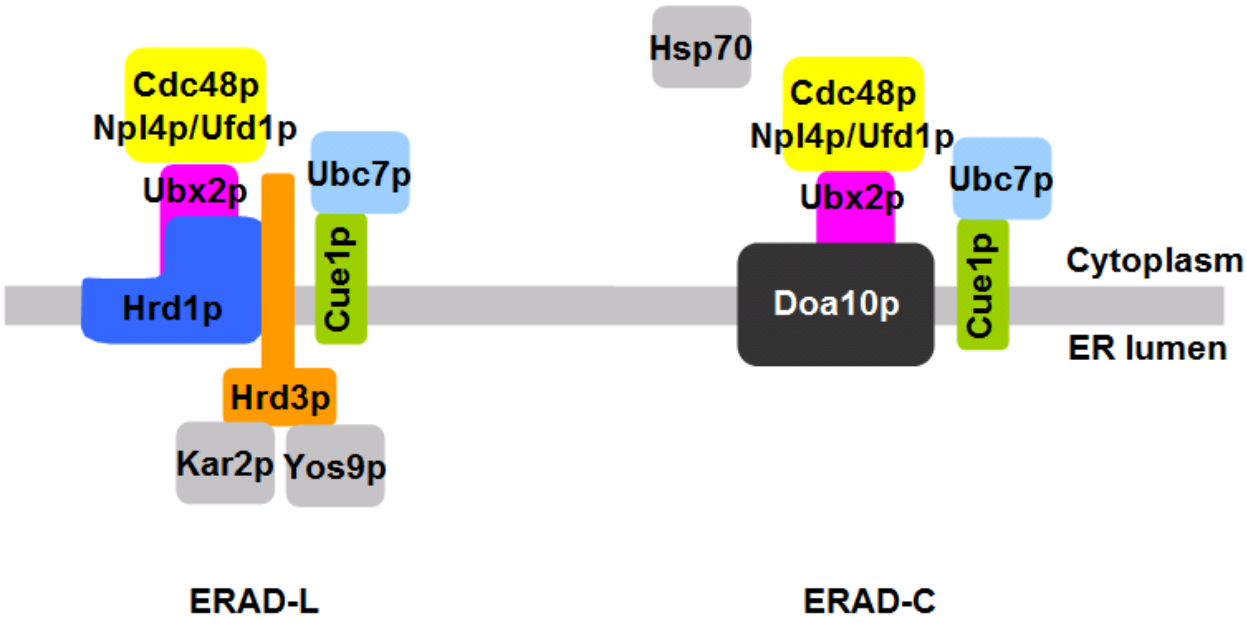

Figure 10. The ERAD-L and ERAD-C Complexes

The ERAD-L surveillance complex is composed of the chaperones Kar2p and Yos9p (grey), their receptor Hrd3p (orange), the ubiquitination machinery Hrd1p, Cue1p, and Ubc7p (dark blue, green, and light blue), and the retrotranslocation machinery, Cdc48p-Npl4p-Ufd1p and its receptor Ubx2p (yellow and magenta). The ERAD-C complex is composed of the chaperones of the HSP70 family (grey), the ubiquitination machinery Doa10p, Cue1p, and Ubc7p (black, green, and light blue, respectively), and the retrotranslocation machinery Cdc48p-Npl4p-Ufd1p (yellow). In both cases, chaperones bring substrates to the ubiquitination machinery. Ubiquitinated substrates are then retrotranslocated into the cytosol for degradation by the 26S proteasome.

1.3.2 ERAD-Cytosol (ERAD-C)

Proteins with offending lesions on the cytosolic side of the ER are targeted to the ERAD-Cytosol (ERAD-C) pathway. The ERAD-C pathway is quite similar in design to the ERAD-L pathway (**Figure 10**) (ISMAIL and NG 2006). In yeast, ERAD-C substrates are first recognized by cytosolic molecular chaperones (BUCK *et al.* 2007; HUYER *et al.* 2004; VASHIST and NG 2004). These chaperones include small HSPs, HSP70 (Ssa1p) and the Heat Shock Cognate 70 (HSC70) families of molecular chaperones (BRODSKY 2007). These cytosolic chaperones facilitate the interaction of the substrate with a second ER E3 ubiquitin ligase complex known as the Doa10p complex (HAN *et al.* 2007; NAKATSUKASA *et al.* 2008; SWANSON *et al.* 2001). It is unknown if there is a chaperone receptor analogous to Hrd3p, but given the location of ERAD-C substrates and their known interactions with chaperones, there may not be a requirement for such. Regardless, the Doa10p RING E3 ligase is linked to the E2-conjugating enzymes Ubc7p (through Cue1p), and to a transmembrane E2 known as Ubc6p (CARVALHO *et al.* 2006; SWANSON *et al.* 2001). Doa10p interacts with Ubx2p and Dfm1p, both of which are known to recruit the retrotranslocating ATPase, Cdc48p (SCHUBERTH and BUCHBERGER 2005; STOLZ *et al.* 2010). Interestingly, some substrates appear to teeter between the ERAD-C and ERAD-L pathways. For instance, complicated transmembrane proteins such as the 12-transmembrane pass Ste6p and Cystic Fibrosis Transmembrane Conductance Regulator (CFTR) show dependence on both Hrd1p and Doa10p, and on Ubc6p and Ubc7p (GNANN *et al.* 2004; HUYER *et al.* 2004; VASHIST and NG 2004; ZHANG *et al.* 2001). Regardless of which ERAD pathway is used, ubiquitinated substrates are removed from the ER for degradation by the homohexameric Cdc48p ATPase complex.

1.4 CELL DIVISION CYCLE 48 (CDC48)

The yeast Cdc48p protein is an evolutionarily-conserved ATPase of the ATPases Associated with various cellular Activities (AAA) family. *CDC48* was first identified in a yeast screen for temperature-sensitive mutants of the cell cycle (MOIR *et al.* 1982). In mammals, a 25-amino acid peptide known as Valosin was identified from porcine intestine (SCHMIDT *et al.* 1985). Valosin was later discovered to be a proteolytic artifact, as its sequence corresponded to the second AAA-ATPase domain of a larger, 97 KDa protein called, Valosin-Containing Protein (VCP) (KOLLER and BROWNSTEIN 1987). The Cdc48p and p97/VCP proteins were identified as homologs in 1991, and both were found to form a homohexameric ring structure (FROHLICH *et al.* 1991; KOLLER and BROWNSTEIN 1987). Cdc48p is an extremely abundant protein, with some estimates of its abundance at over 1% of total cellular protein (LATTERICH *et al.* 1995). The cellular functions of Cdc48p/p97/VCP are also incredibly diverse and include cell division, DNA repair, RNA transcription, protein translation, nuclear envelope/ER reformation, vesicle fusion, protein transport, endosome size formation, cell-wall integrity, autophagy, and protein quality control at both the ER (ERAD) and mitochondria (CAO *et al.* 2003; FROHLICH *et al.* 1991; FUJII *et al.* 2012; HETZER *et al.* 2001; HITCHCOCK *et al.* 2001; HSIEH and CHEN 2011; JAROSCH *et al.* 2002; JU *et al.* 2009; KRICK *et al.* 2010; LATTERICH *et al.* 1995; MEERANG *et al.* 2011; MIYACHI *et al.* 2004; MOIR *et al.* 1982; PLEASURE *et al.* 1993; RAMADAN *et al.* 2007; RAPE *et al.* 2001; TRESSE *et al.* 2010; UCHIYAMA *et al.* 2006; VERMA *et al.* 2011; YE *et al.* 2001). The common theme in all these processes is ubiquitinated-protein processing.

1.4.1 The medical relevance of Cdc48p/p97/VCP

The human p97/VCP is of considerable medical interest. For instance, the upregulation of p97/VCP mRNA and protein is associated with negative outcomes in many cancers (BERTRAM *et al.* 2008; VALLE *et al.* 2011; YAMAMOTO *et al.* 2003). Mutations in p97/VCP are known to directly cause two muscle-related diseases: Inclusion Body Myopathy associated with Paget's disease of bone and Frontotemporal Dementia (IBMPFD) and a subtype of familial Amyotrophic Lateral Sclerosis (ALS) (JOHNSON *et al.* 2010; WATTS *et al.* 2004). Both diseases have overlapping molecular phenotypes, such ubiquitin-positive inclusions and the aggregation of TAR DNA binding Protein-43 (TDP-43) (GUINTO *et al.* 2007; JOHNSON *et al.* 2010; SCHYMICK *et al.* 2007). The mutations that cause IBMPFD and ALS are also commonly found the amino terminus or the first of two AAA-ATPase domains (see below, **Figure 11**) in p97/VCP (HALAWANI *et al.* 2009). In fact, some IBMPFD and ALS mutations are exactly the same (e.g., R155H and R191Q), strongly suggesting the presence of additional phenotype-modifying genetic loci (HALAWANI *et al.* 2009; JOHNSON *et al.* 2010; WATTS *et al.* 2004). The R191Q mutation in p97/VCP has also been recently linked to a third muscular disorder called Facioscapulohumeral Muscular Dystrophy-1 (SACCONI *et al.* 2012). Neuromuscular dysfunction seems to be a commonality of disease-causing p97/VCP mutations and suggests a shared molecular mechanism. IBMPFD may ultimately result from defects in autophagy and ERAD (JU *et al.* 2009; WEIHL *et al.* 2006).

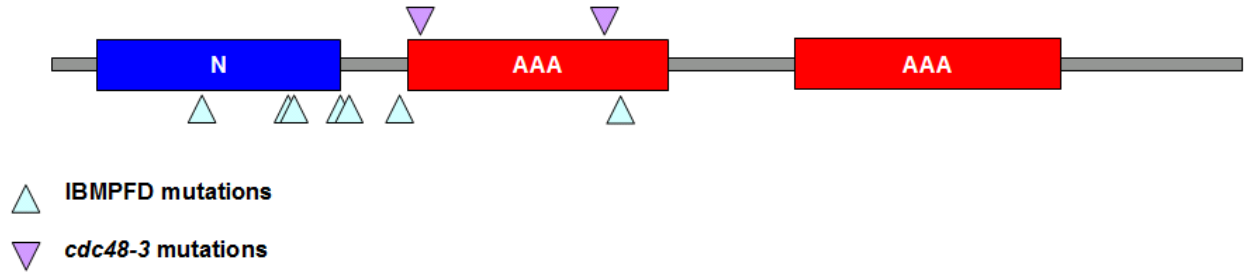

Figure 11. Domain map of Cdc48p

Cdc48p is composed of three domains, the N-domain (blue) and two-AAA ATPase domains (red). The location of IBMPFD mutations are marked by upward-pointing arrowheads (light blue) and mutations found in the commonly used *CDC48* allele, *cdc48-3*, are marked by the downward pointing arrowheads (purple).

1.4.2 Cdc48p/p97/VCP ATPase activity

Each monomer of yeast Cdc48p and mammalian p97/VCP contains: 1) a cofactor binding amino-terminal domain (termed N domain), 2) two AAA-ATPase domains (termed D1 and D2) and 3) a carboxy terminal end that can also bind select cofactors (**Figure 12**). The AAA-ATPase domains each contain a Walker A and a Walker B motif which coordinate the binding and hydrolysis of ATP, respectively (HANSON and WHITEHEART 2005). ATP hydrolysis occurs at both ATPase domains, and is most extensively studied using the mammalian p97/VCP as a model (PYE *et al.* 2006). The purification of p97/VCP hexamers for structural studies, however, indicates that the D1 domain remains tightly bound to ADP while the D2 domain can be empty, or bound to ADP or to transition state analogs (PYE *et al.* 2006). This finding has been validated by biochemical and genetic experiments supporting the idea that the bulk of p97/VCP ATPase activity comes from the D2 ATPase domain (SONG *et al.* 2003; WANG *et al.* 2003; YE *et al.* 2003). The D1 ATPase domain is believed to be mainly involved in some aspect of Cdc48p/p97/VCP hexamerization (SONG *et al.* 2003; WANG *et al.* 2003; YE *et al.* 2003). Structural data indicate that these two ATPase domains do not function in isolation, and that ATPase hydrolysis in one domain contributes to structural changes in the other domain within the same protomer and also between neighboring protomers (DELABARRE and BRUNGER 2003; LI *et al.* 2012). ATPase activity also contributes to conformational changes in the cofactor-binding amino-terminal N domain (NIWA *et al.* 2012; PYE *et al.* 2006; ROUILLER *et al.* 2002). This is an attractive way of converting ATP hydrolysis to mechanical work on a substrate. Indeed, Cdc48p/p97/VCP has been suggested to aid in protein unfolding, possibly by funneling proteins through the central pore of the hexamer (DELABARRE *et al.* 2006). Definitive evidence

for this is still lacking, and the reality is we still have very little idea as to how Cdc48p/p97/VCP acts to retrotranslocate a substrate during ERAD. Interestingly, all IBMPFD mutants tested by Niwa and colleagues (**2012**) showed increased D2 domain ATPase activity, and in at least one known mutant (A232E), the increased ATPase activity required the presence of the N domain. The carboxy terminus was also required for D2 ATPase. In addition, in *Arabidopsis*, a Ubiquitin-Regulatory X (UBX) domain protein known as AtPUX1 was shown to down-regulate ATPase activity and promote hexamer disassembly (PARK *et al.* 2007; RANCOUR *et al.* 2004). Similarly, the mammalian UBX protein TUG down-regulates p97/VCP ATPase activity and promotes hexamer disassembly (ORME and BOGAN 2012). Other mammalian UBX protein such as p47 and SAKS1 have also been shown to negatively regulate p97/VCP vesicle formation and ERAD function, respectively, but it is unknown if either affects hexamer stability (BRUDERER *et al.* 2004; LALONDE and BRETSCHER 2011; MEYER *et al.* 1998). Only one example of cofactor binding increases ATPase activity: Synaptotagmin, which is a tramsmembrane protein involved in vesicle fusion, may increase the ATPase activity of p97/VCP, but the relevance of this phenomena is not currently understood (DELABARRE *et al.* 2006; MARTENS *et al.* 2007). Finally, cofactor binding to p97 has also been demonstrated to induce major conformational changes and likely modulates the activity of either the D1 or D2 ATPase domain (BEURON *et al.* 2006).

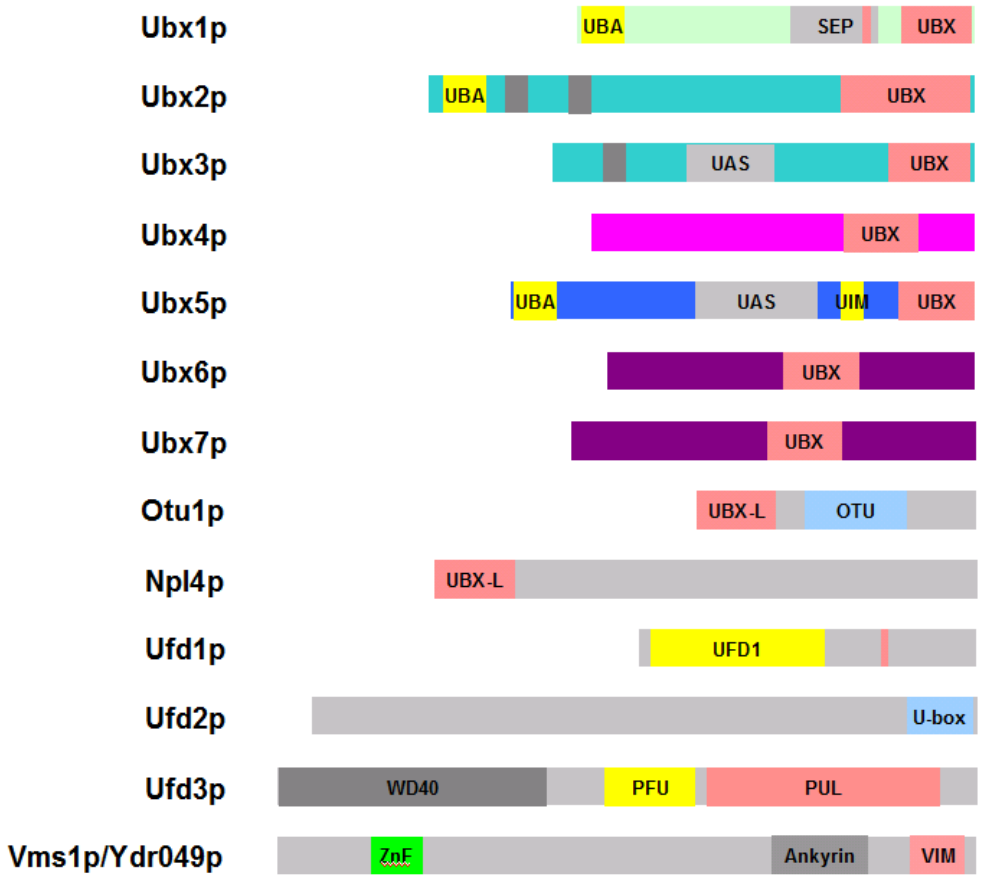

Figure 12. Cdc48p cofactors

An abbreviated list of cofactors and their functional domains. Ubiquitin interacting domains (yellow) include Ubiquitin-Associated (UBA), Ubiquitin Interacting Motif (UIM), PLAA family ubiquitin binding domain (PFU), and Ubiquitin Fusion Degradation domain (UFD). Cdc48p interaction domains (pink) include Ubiquitin Regulatory X (UBX) and UBX-like (UBX-L), PLAP, UFD3 and Lub1 (PUL), and VCP/p97 Interacting Motif (VIM). Uncharacterized domains (grey) include Shp1, Eyc and p47 (SEP) and UAS. E3 or DUB domains (light blue) include the Ovarian Tunor (OUT) and Ubox modified ring finger (UBOX). Scaffold domains (dark grey) include WD-40 and the Ankyrin repeat. The C2H2 zinc finger motif is in green. Adapted from (SCHUBERTH and BUCHBERGER 2008).

1.4.3 Cdc48p/p97/VCP cofactors

While Cdc48p has an innate ability to recognize unfolded proteins, the overwhelming majority of Cdc48p/p97/VCP-associated functions relies on its interaction partners (THOMS 2002; YEUNG *et al.* 2008). In this section, I will focus primarily on yeast Cdc48p interaction partners that are relevant to the ERAD pathway, and highlight examples from higher organisms as necessary.

1.4.3.1 UBX-domain cofactors

The UBX domain family of proteins represents the most abundant group of Cdc48p cofactors (see above, **Figure 12**) (SCHUBERTH and BUCHBERGER 2008). The UBX domain is an 80 amino acid motif that structurally resembles ubiquitin (BUCHBERGER *et al.* 2001). Seven UBX domain-containing proteins exist in *S. cerevisiae* (*UBX1-7*), but only two are functionally characterized. The first, Ubx1p (also known as Shp1p), was originally isolated as a suppressor of lethality caused by the overexpression of the phosphatase Glc7p (ZHANG *et al.* 1995). Insights into Ubx1p function came from studies of the mammalian version of Ubx1p, p47 (see above) and showed that a complex of p97 and p47 regulated Golgi-vesicle membrane fusion (KONDO *et al.* 1997). In yeast, Ubx1p was found to be involved in the vacuolar degradation of fructose-1,6-bisphosphatase and regulated autophagosome formation (CUI *et al.* 2004; KRICK *et al.* 2010). One of the earliest discovered roles for yeast Cdc48p was homotypic ER membrane fusion (LATTERICH *et al.* 1995). In addition, Ubx1p is required for the degradation of model ubiquitin-fusion degradation substrates, the UV-response mediated degradation of RNA Polymerase II, and the degradation of a classic ERAD-L substrate (SCHUBERTH *et al.* 2004; TRAN *et al.* 2011;

VERMA *et al.* 2011). Ubx2p was also first characterized as being involved in ubiquitin-fusion substrate degradation (SCHUBERTH *et al.* 2004). A series of papers in 2005 and 2006 showed that Ubx2p is a transmembrane protein that acts as a recruitment factor for Cdc48p (NEUBER *et al.* 2005; SCHUBERTH and BUCHBERGER 2005; WILSON *et al.* 2006). Ubx2p was found as an associated component of the ER E3 ubiquitin ligases, Hrd1p and Doa10p, and is required for the retrotranslocation of select ERAD substrates (see above) (CARVALHO *et al.* 2006; DENIC *et al.* 2006; GARZA *et al.* 2009). Recent data suggest that Ubx2p, and the human homolog, UBXD8, are involved in ERAD substrate retrotranslocation through lipid droplets – an organelle that provides both storage and metabolic functions (FARESE and WALTHER 2009; SUZUKI *et al.* 2012; WANG and LEE 2012).

In contrast to these two UBX proteins, relatively little is known about the yeast Ubx3p-7p proteins. Some data suggest that Ubx4p is involved in protein degradation either on its own or with other cofactors such as the UBX proteins, Ubx6p and Ubx7p (ALBERTS *et al.* 2009; DECOTTIGNIES *et al.* 2004; TRAN *et al.* 2011). Ubx4p is the yeast version of TUG (**see above**), a protein linked to the trafficking of GLUT4 upon insulin stimulation (BOGAN *et al.* 2003). Additionally, the mammalian version of Ubx7p, Erasin/UBXD2 localizes to the ER, is found in complex with ERAD components, and affects the degradation of a model substrate (LIANG *et al.* 2006; LIM *et al.* 2009). The mammalian version of Ubx5p, UBXD7, has recently been linked to SCF-RING mediated protein degradation (ALEXANDRU *et al.* 2008). In addition, one study suggests that Ubx5p-7p plays a role in DNA damage response (LIS and ROMESBERG 2006). Overall, UBX domain-containing proteins contribute significantly to Cdc48p/p97/VCP functional diversity.

1.4.3.2 Ubiquitin Fusion Degradation (UFD) cofactors

The Ubiquitin Fusion Degradation (UFD) group of cofactors was originally identified in a screen for mutants that stabilized a normally short-lived version of beta-galactosidase (JOHNSON *et al.* 1995). A majority of *UFD* genes encoded for Cdc48p interaction partners, but not all. For instance, Ufd4p and Ufd5p are linked to proteasome function. Ufd4p is an E3 ligase associated with the 19S base of the proteasome and Ufd5p is Rpn4p, the transcription factor responsible for controlling proteasome levels (see section 1.2.6.) (XIE and VARSHAVSKY 2000; XIE and VARSHAVSKY 2001). Ufd1p, Ufd2p, and Ufd3p have since been identified as Cdc48p interaction partners (**Figure 12**).

The *UFD3* gene was found to be identical to the "*Degradation of Alpha 1*" (*DOA1*) gene, and encodes a WD-40 repeat protein that appears to be involved in regulating ubiquitin homeostasis (GHISLAIN *et al.* 1996; JOHNSON *et al.* 1995). Most recently, Ufd3p was implicated in the bulk degradation of ribosomes (ribophagy), DNA damage response, and the sorting of ubiquitinated plasma membrane proteins (LIS and ROMESBERG 2006; OSSAREH-NAZARI *et al.* 2010; REN *et al.* 2008). Ufd3p does not seem to play a role in ERAD (MULLALLY *et al.* 2006). While the exact function of Ufd3p remains unclear, Ufd3p is one of the few Cdc48p cofactors that binds at the carboxy terminus, via a PLAP, UFD3 and Lub1, or PUL domain (ZHAO *et al.* 2009). The Ufd3p-Cdc48p complex can bind the DUB, Otu1p (see above) and excludes the binding of a second PUL-domain containing protein, Ufd2p (RUMPF and JENTSCH 2006). This competitive binding occurs at the same site in the Cdc48p carboxy terminus, and leads to a Cdc48p complex that can either remove or add ubiquitin moieties to a substrate (BOHM *et al.* 2011; RUMPF and JENTSCH 2006). Ufd2p is a U-box containing protein that extends K48

polyubiquitin chains and was discussed briefly in section 1.1.2 (KOEGL *et al.* 1999; NAKATSUKASA *et al.* 2008; SAEKI *et al.* 2004). *UFD2* mutants, alone or when deleted with other Cdc48p cofactors, stabilize select ubiquitin proteasome substrates (LIU *et al.* 2011; NAKATSUKASA *et al.* 2008; TRAN *et al.* 2011). The mammalian version of Ufd2p, UBE4B, is involved in the degradation of the tumor suppressor p53 and in the pathology of certain neurological conditions (CONFORTI *et al.* 2000; WU *et al.* 2011).

Perhaps the most recognizable UFD group member is Ufd1p. Ufd1p is an essential protein that forms a heterodimeric complex with Npl4p (JOHNSON *et al.* 1995; MEYER *et al.* 2000). This heterodimeric complex binds to the N-domain of Cdc48p and can directly bind to ubiquitinated substrates (MEYER *et al.* 2000; MEYER *et al.* 2002; YE *et al.* 2001). Ufd1p and Npl4p mutants were initially linked to the proteasomal activation of ER-bound transcription factors, Spt23p/Mga2p (HITCHCOCK *et al.* 2001; HOPPE *et al.* 2000). A series of papers in 2001 and 2002 further connected the Cdc48p-Npl4p-Ufd1p complex to the retrotranslocation of ubiquitinated ERAD substrate (BAYS *et al.* 2001b; HITCHCOCK *et al.* 2001; JAROSCH *et al.* 2002; RABINOVICH *et al.* 2002; YE *et al.* 2001). It is clear that these proteins, in complex with Cdc48p, are important for many ubiquitin-dependent processes in addition to ERAD (**see above**). Moreover, the Cdc48p complex is proposed to have the ability to separate ubiquitinated substrates from unmodified proteins, and probably reflects the segregase activity of the complex (BRAUN *et al.* 2002; SHCHERBIK and HAINES 2007).

1.4.3.3 Additional Cofactors that function with Cdc48p

During ERAD, UBX proteins, such as Ubx2p, can recruit the Cdc48p-Npl4p/Ufd1p to sites of protein ubiquitination. In this model, the Cdc48p-Npl4p-Ufd1p complex can then

retrotranslocate the ubiquitinated substrate and the presence of additional cofactors like Ufd2p can further extend the polyubiquitin chain (NAKATSUKASA *et al.* 2008). Nevertheless, a polyubiquitinated substrate that has been retrotranslocated requires additional proteins to facilitate proteasomal degradation. This is surprising given the fact that the proteasome has receptors for ubiquitin itself (see above). Moreover, the Cdc48p complex can be found associated with the proteasome (VERMA *et al.* 2000). Three proteins that fit this role are Rad23p, Dsk2p, and Ddi1p. All three proteins possess a Ubiquitin-Like (UBL) domain that mediates interaction with the 26S proteasome and a Ubiquitin-Associated (UBA) domain for interaction with ubiquitinated substrate (DANTUMA *et al.* 2009). Rad23p was originally described as a DNA repair protein and was the first of these proteins linked to the 26S proteasome (SCHAUBER *et al.* 1998). Rad23p and Dsk2p were found as a complex that could bind to ubiquitinated substrates and to the Rpn1p subunit of the proteasome (ELSASSER *et al.* 2002; RAO and SASTRY 2002; SAEKI *et al.* 2002). Rad23p-Dsk2p could also be purified with Ufd2p and competitive binding experiments suggested that Rpn1p competes with Ufd2p for Rad23p (KIM *et al.* 2004; RICHLY *et al.* 2005). A complex of Cdc48p-Rad23p-Ufd2p was also isolated (RICHLY *et al.* 2005). Interestingly, Rad23p was also found in complex with Png1p, a cytosolic enzyme that can deglycosylate a misfolded protein (KIM *et al.* 2006). Relevant to this discussion, Rad23p-Dsk2p mutants showed an ERAD defect (MEDICHERLA *et al.* 2004; RICHLY *et al.* 2005). These data ultimately suggest a model in which the substrate has its polyubiquitin chain extended by Cdc48p-Ufd2p, possibly in complex with Rad23p-Dsk2p. This is followed by Rpn1p competition, leading to the loss of Ufd2p and proteasomal degradation of the substrate.

Table 1. Relevant factors of the ERAD pathway

Yeast	Human	Function
CDC48	VCP	Multifunctional AAA ATPase, forms hexamer.
NPL4	NPLOC4	Dimerizes with Ufd1p/UFD1L.
UFD1	UFD1L	Dimerizes with Npl4p/NPLOC4.
UFD2	UBE4A & UBE4B	E4 polyubiquitin extending enzyme.
UFD3/DOA1	PLAA	Involved in regulating ubiquitin levels. WD40 repeat protein.
UFD4	TRIP12	E3 ubiquitin ligase associated with the proteasome.
UBX1/SHP1	NSFL1C	UBX domain protein. Involved in homotypic vesicle fusion
UBX2	UBXD8/ETEA	UBX domain protein. Recruits Cdc48p to the Endoplasmic Reticulum
UBX3	-	UBX domain protein. Transmembrane.
UBX4	TUG/ASPL	UBX domain protein. Potentially involved in ERAD.
UBX5	UBXD7	UBX domain protein.
UBX6	-	UBX domain protein. Potential role in ubiquitin-mediated proteolysis
UBX7	UBXD2/Erasin	UBX domain protein. Potential role in ubiquitin-mediated proteolysis
VMS1	ANKZF1	Cdc48p/VCP cofactor. Involved in ubiquitin-mediated proteolysis.
HRD1	SYVN1	E3 ubiquitin ligase of the Endoplasmic Reticulum.
HRD3	SEL1L	Protein of the Endoplasmic Reticulum, involved in ERAD. Part of the Hrd1p complex.
USA1	-	Protein of the Endoplasmic Reticulum, involved in ERAD. Part of the Hrd1p complex.
YOS9	OS9	Lectin of the ER lumen. Part of the Hrd1p complex.
DOA10	MARCH VI	E3 ubiquitin ligase of the Endoplasmic Reticulum.
UBC6	UBE2J2	E2 ubiquitin conjugating enzyme. Involved in ERAD.
UBC7	UBE2G2	E2 ubiquitin conjugating enzyme. Involved in ERAD.
DER1	DER2L, DER3L	Protein of the Endoplasmic Reticulum. Involved in ERAD.
CUE1	-	Protein of the Endoplasmic Reticulum. Involved in ERAD.
RPT1	PSMC2	AAA ATPase subunit of the 19S base.
RPT2	PSMC1	AAA ATPase subunit of the 19S base.
RPT3	PSMC4	AAA ATPase subunit of the 19S base.
RPT4	PSMC6	AAA ATPase subunit of the 19S base.
RPT5	PSMC3	AAA ATPase subunit of the 19S base. Candidte ubiquitin receptor.
RPT6	PSMC5	AAA ATPase subunit of the 19S base.
RPN1	PSMD2	Non-ATPase component of 19S base. Candidate ubiquitin receptor.
RPN2	PSMD1	Non-ATPase component of 19S base. Binds to Rpn13
RPN10	PSMD4	Non-ATPase component of 19S base. Ubiquitin receptor.
RPN3	PSMD3	Non-ATPase component of 19S basse.
RPN5	PSMD12	Component of the 19S lid.
RPN6	PSMD11	Component of the 19S lid.
RPN7	PSMD6	Component of the 19S lid.
RPN8	PSMD7	Component of the 19S lid.
RPN9	PSMD13	Component of the 19S lid.
RPN11	PSMD14	Component of the 19S lid. Deubiquitinating enzyme.
RPN12	PSMD8	Component of the 19S lid.
RPN13	ADRM1	Component of the 19S lid. Deubiquitinating enzyme.
RPN14	PAAF1	Chaperone of the 19S Regulatory Particle.
RPN15/SEM1	SHFM1	Non-ATPase component of 19S base.
HSM3	PSMD5	Chaperone of the 19S Regulatory Particle.

NAS2	PSMD9	Chaperone of the 19S Regulatory Particle.
NAS6	PSMD10	Chaperone of the 19S Regulatory Particle.
RAD23	RAD23A/RAD23B	Ubiquitinated substrate escort factor. Also involved in DNA damage repair.
DSK2	UBQLN1	Ubiquitinated substrate escort factor.
DDI1	DDI1/DDI2	Possible ubiquitinated substrate escort factor. DNA damage inducible.
PBA1	PSMG1	Chaperone of the 20S core particle.
PBA2	PSMG2	Chaperone of the 20S core particle.
PBA3	PSMG3	Chaperone of the 20S core particle.
PBA4	PSMG4	Chaperone of the 20S core particle.
UMP1	POMP1	Chaperone of the 20S core particle.
ECM29	ECM29	Stabilizer of the proteasome.
BLM10	PSME4	Activator of the proteasome. Human version also called PA200.
UFD5/RPN4	-	Transcription factor regulating proteasome levels. Functional homolog is NRF1.
SCL1	PSMA6	20S core subunit alpha 1.
PRE8	PSMA2	20S core subunit alpha 2.
PRE9	PSMA4	20S core subunit alpha 3.
PRE6	PSMA7	20S core subunit alpha 4.
PUP2	PSMA5	20S core subunit alpha 5.
PRE5	PSMA1	20S core subunit alpha 6.
PRE10	PSMA3	20S core subunit alpha 7.
PRE3	PSMB6	20S core subunit beta 1.
PUP1	PSMB7	20S core subunit beta 2.
PUP3	PSMB3	20S core subunit beta 3.
PRE10	PSMB2	20S core subunit beta 4.
PRE2	PSMB5	20S core subunit beta 5.
PRE7	PSMB1	20S core subunit beta 6.
PRE4	PSMB4	20S core subunit beta 7.

1.5 PREVIEW OF CHAPTERS 2 THROUGH 4

While our view of the ERAD pathway is becoming more and more complete, there are still lingering questions concerning the role of Cdc48p during ERAD. For instance, Cdc48p/p97/VCP has been found in a stable complex with the 26S proteasome, which is counter to the processive and transient nature of protein degradation (BESCHE *et al.* 2009a; DAI *et al.* 1998; DUBIEL *et al.* 1995; VERMA *et al.* 2000). Additionally, Cdc48p is known to bind to many cofactors, most of which are uncharacterized (KROGAN *et al.* 2006). One of these cofactors, encoded by the *YDR049W* gene, was isolated from a gene expression profile study of yeast expressing a model misfolded substrate (AHNER *et al.* 2007). Ydr049p was found in a large multi-protein complex with Cdc48p and was also linked to the DOA pathway, which includes the ERAD-C E3 ligase Doa10p (KROGAN *et al.* 2006; RAVID *et al.* 2006). The Ydr049p protein contains a C2H2-type zinc finger, an Ankyrin repeat, and a "VCP/p97-Interacting Motif" (VIM). In Chapter 2, I will present data indicating that Ydr049p functions at a post-ubiquitination step in the ERAD pathway. I specifically found that deleting the yeast *YDR049W* gene leads to a modest defect in the ERAD of a model substrate, the Cystic Fibrosis Transmembrane Conductance Regulator. I will also present data indicating that Ydr049p plays a redundant role with other Cdc48p cofactors. And finally, I show that loss of *YDR049W* does not affect ERAD substrate ubiquitination, and leads to accumulation of Cdc48p-associated ubiquitinated proteins. During the course of my work, an independent group led by Dr. Jared Rutter from the University of Utah discovered that the Ydr049 protein was involved in Cdc48p-dependent mitochondrial protein

degradation (HEO *et al*. 2010). They termed the *YDR049W* gene, *VCP/Cdc48-associated Mitochondrial Stress-responsive*, or *VMS1*. From this point on, I shall use their nomenclature for this gene. In Chapter 3, I will present data that indicates that Vms1p functions in proteasome biology. First I demonstrate that *VMS1* deletion causes an increased accumulation of ubiquitinated proteins in total cell extracts. Second, *VMS1* deletion changes the distribution of proteasome subtypes. Specifically, there is an increase in free latent 20S core particle and a decrease in the ubiquitin-processing capped forms of the proteasome. Both of these phenomena can be restored to near wild-type conditions with a version of Vms1p that maintains its interaction with Cdc48p. I also provide evidence indicating that Cdc48p recruits Vms1p to the proteasome, and that Vms1p does not function with select proteasome chaperones. Finally, I present data that Cdc48p interaction with the proteasome is preserved in *VMS1* mutants. Cumulatively, this work suggests that Cdc48p-Vms1p aids in the efficient turnover of ubiquitinated proteins by promoting the stability of ubiquitin substrate-competent proteasomes. In Chapter 4, I will summarize my finding and detail some potential future goals.

2.0 VMS1 FUNCTIONS AT A POSTUBIQUITINATION STEP IN THE ERAD PATHWAY

Endoplasmic Reticulum-Associated Degradation (ERAD) clears the early secretory pathway of misfolded proteins, and can be sub-divided into distinct stages of substrate recognition and membrane targeting, retrotranslocation from the ER into the cytoplasm, ubiquitination, and degradation by the 26S proteasome (VEMBAR and BRODSKY 2008). Given the volume and diversity of protein traffic through the ER, it is not surprising that the cell has evolved unique ERAD pathways (e.g., ERAD-L, ERAD-C, and ERAD-M) that handle substrates based on the location of the offending lesion (SMITH *et al.* 2011; VASHIST and NG 2004; VEMBAR and BRODSKY 2008). Irrespective of the ERAD pathway employed, the retrotranslocation of most substrates relies upon the Cdc48p complex, which consists of the homohexameric Cdc48p ring and two adaptor proteins, Npl4p and Ufd1p (BAYS *et al.* 2001b; HITCHCOCK *et al.* 2001; JAROSCH *et al.* 2002; RABINOVICH *et al.* 2002; YE *et al.* 2001). Cdc48p, the yeast homolog of p97/Valosin Containing Protein (p97/VCP), is a multifunctional member of the ATPases Associated with various Activities (AAA) family. This family also includes the ATPase ring of the 26S proteasome and the MCM complex, which is involved in DNA replication. Like other AAA proteins, Cdc48p is thought to couple ATP hydrolysis with changes in the conformation of its targets (NIWA *et al.* 2012; PYE *et al.* 2006; ROUILLER *et al.* 2002). The specificity of Cdc48p function relies on the cofactors to which it binds (BUCHBERGER *et al.* 2010).

While many Cdc48p cofactors have been identified in recent years, very few of these are functionally characterized. Of the ones that are, it is not uncommon to find that the cofactor functions in many different processes. For example, Ubx1p, also known as Shp1p, was originally isolated as a suppressor of phosphoprotein phosphatase 1 overexpression, but was later found to participate in Golgi vesicle fusion, ubiquitin-mediated degradation of select substrates, and autophagy (CUI *et al.* 2004; KONDO *et al.* 1997; KRICK *et al.* 2010; SCHUBERTH *et al.* 2004; TRAN *et al.* 2011; ZHANG *et al.* 1995). Ubx1p is one member of a larger group of generally uncharacterized UBX-domain containing proteins (BUCHBERGER *et al.* 2010). The UBX domain mediates binding to Cdc48p, and its tertiary structure resembles ubiquitin (BUCHBERGER *et al.* 2001). Other members of the UBX family have also been linked to ubiquitin-mediated protein degradation. For example, Ubx2p recruits the Cdc48p-Npl4p-Ufd1p complex to the ER membrane and *ubx2*Δ yeast exhibit ERAD defects (NEUBER *et al.* 2005; SCHUBERTH and BUCHBERGER 2005; WILSON *et al.* 2006).

Another group of Cdc48p-associated proteins were first isolated as mutants that impaired the degradation of Ubiquitin Fusion Degradation (UFD) substrates (JOHNSON *et al.* 1995). As noted above, Ufd1p is a Cdc48p partner and is required for ERAD. Ufd2p is a Cdc48p-associated ubiquitin chain assembly factor, catalyzing the extension of ubiquitin chains (KOEGL *et al.* 1999; NAKATSUKASA *et al.* 2008). Additionally, a deubiquitinating enzyme (DUB), known as Otu1p, binds the Cdc48p complex and antagonistic interactions amongst Ufd2p, and Ufd3p-Otu1p have been observed (RUMPF and JENTSCH 2006). Nevertheless, it is unknown how

Cdc48p's function during ERAD is altered by most of these partners, and whether additional, ill-characterized partners of Cdc48p also impact ERAD.

In this Chapter, I report on the characterization of a new Cdc48p cofactor that is encoded by the *VMS1*/*YDR049W* open reading frame in the yeast, *Saccharomyces cerevisiae*. Large-scale yeast proteomic studies uncovered Vms1p in a multi-protein complex that contains Cdc48p (KROGAN *et al.* 2006). Deletion of *VMS1* was also observed to exhibit mild synthetic growth defects in yeast compromised for the Degradation of Alpha (DOA) pathway (RAVID *et al.* 2006). Moreover, yeast lacking *VMS1* were reported to exhibit synthetic interactions in karmellae-forming yeast, suggesting a role in ER membrane homeostasis (WRIGHT *et al.* 2003). Here, I demonstrate that *VMS1* deletion affects the ERAD of a model transmembrane substrate, the Cystic Fibrosis Transmembrane Conductance Regulator (CFTR), and that *VMS1* exhibits genetic interactions with select members of the UBX and UFD pathway. In some cases, the genetic interaction is supported by increased sensitivity to ER- and oxidative stressors and in other cases by synergistic ERAD defects. Finally, I show that increased levels of ubiquitinated species are associated with Cdc48p in *vms1*Δ yeast.

2.1 EXPERIMENTAL PROCEDURES

2.1.1 Yeast strains, plasmids, and growth assays

Most yeast strains employed in this study (**Table 2**) were in the BY4742 background, and were obtained from Open Biosystems (Thermo Scientific, USA) or were made by disrupting the gene

by homologous recombination using resistance marker cassettes amplified from the plasmids pRS400 (KanMX4) or pFA6-His3MX (His3MX) (54,55). Synthetic primers used to construct linear DNA strands for gene disruption contained 50-100bp of sequence homology as well as sequences to amplify the cassette. A complete list of primers used to make the strains in this study is provided in **Table 3**. Yeast harboring multiple gene deletions were made by standard genetic techniques (ADAMS 1997). In brief, strains were mated on rich media (YPD: 1% yeast extract, 2% peptone, 2% dextrose), and after 4-6 h at 30ºC diploids were selected on synthetic complete (SC) media lacking both lysine and histidine. Diploids were nitrogen-starved for 3-7 d in sporulation media (1% KOAc, 0.1% Bacto yeast extract, 0.05% dextrose) prior to tetrad dissection. The resulting germinated spores were screened on the appropriate media and deletions were confirmed by PCR. To introduce the *cdc48-3* allele into the BY background, a *cdc48-3* strain (MATa, *his4-619*, *leu2,3,-112*, *ura3*, *pep4*Δ::*URA3*, *cdc48-3*) in a S288C background was crossed against a BY strain of the opposite mating type. The resulting *cdc48-3* strain from this genetic cross was backcrossed three additional times against the BY background. The *cdc48-3* strain derived from these backcrosses was then used.

The plasmids used in the study (**Table 4**) were described previously, or created by PCR amplification and cloned as follows. For the construction of C-terminal HA- or myc-tagged Cdc48p constructs, two-PCR fragments were generated and ligated together into the desired plasmid. The first fragment was amplified with the forward primer: 5'-TTGCGGCCGCGGTGGCCAGCCCAAGAAACGGA and the reverse primer: 5'-ACGGATCCACTATACAAATCATCATCTTCC. These primers were synthesized with a NotI restriction site in the forward primer and a BamHI restriction site in the reverse primer

(underlined). The resulting PCR product started 437bp upstream of the ORF and contained the entire *CDC48* ORF minus the termination codon. The second fragment was PCR amplified in a reaction with either the forward primer: 5'ACGGATCC**TACCCATACGACGTCCCA GACTACGCT**TAGTAGTTATATGCCAGGTATATTTTTATTTTAAATCG for the HA-tagged constructs (the HA tag sequence is in boldface), or the forward primer 5'-ACGGATCC**GAACAAAAACTCATCTCAGAAGAGGATCTG**TAGTAGTTATATGCCAG GTATATTTTTATTTTAAATCG for myc-tagged constructs (the myc tag sequence is in boldface), paired with the reverse primer 5'-AGCTCGAGACGACCGAGGTCCTACAGCCT. Both forward primers contained a BamHI site while the reverse primer contained an XhoI site (underlined). The resulting PCR fragments encoded either a single in-frame copy of the HA or myc epitope tag followed by the termination codon in duplicate, and 221bp of the 3' intergenic sequence. The PCR fragments were restriction digested and gel extracted prior to ligation into a pRS315 plasmid that was similarly digested with NotI and XhoI (SIKORSKI and HIETER 1989). Sequence verified constructs were used to create a library of expression vectors in the pRS316, pRS425 and pRS426 backbones (CHRISTIANSON *et al.* 1992; SIKORSKI and HIETER 1989).

To generate plasmids for the expression of an untagged form of Cdc48p, the forward primer: 5'-TTGCGGCCGCGGTGGCCAGCCCAAGAAACGGA and the reverse primer 5'-AGCTCGAGACGACCGAGGTCCTACAGCCT were used in a PCR reaction. The PCR fragment, which contained the full-length, untagged *CDC48* gene, was digested with NotI and XhoI (underlined) and cloned into pRS315 (SIKORSKI and HIETER 1989). Sequence verified constructs were used to create a library of expression vectors in the pRS316, pRS425, and pRS426 backbones (CHRISTIANSON *et al.* 1992; SIKORSKI and HIETER 1989). A similar ligation strategy was used to clone the tagged and untagged versions of *VMS1*. The first fragment was

amplified using the forward primer: 5'-CTGCGGCCGCTTCTTGGAGGAGTGCCACAG and the reverse primer: 5'-ACGGATCCGTATTTCTTTTTCATCCTTTCTTCTGCG. The forward primer contains a NotI site while the reverse primer contains a BamHI site (underlined). This PCR fragment contains 341bp upstream of the ORF and the entire *VMS1* ORF except the termination codon. For the second fragment, either the forward primer: 5'-ACGGATCC**TACCCATACGACGTCCCAGACTACGCT**TGATGAGGAATATCTCATAT TCAAATTTTTAGG for the HA-tagged construct (in boldface) or the forward primer: 5'-ACGGATCC**GAACAAAAACTCATCTCAGAAGAGGATCTG**TGATGAGGAATATCTCA TATTCAAATTTTTAGG for the myc-tagged construct (in boldface) was used in a PCR reaction with the reverse primer: 5'- CGGTCGACGGCGTCATTTTCGCGTTGAG. Both forward primers contained BamHI sites (underlined) while the reverse primer contained a SalI restriction site (underlined). The resulting PCR fragment contained the HA or Myc-tag followed by a termination codon in duplicate and 227bp of the 3' intergenic sequence. For untagged *VMS1* constructs, the forward primer: 5'-CTGCGGCCGCTTCTTGGAGGAGTGCCACAG and the reverse primer: 5'- CGGTCGACGGCGTCATTTTCGCGTTGAG were paired in the PCR reaction. The primers contained a NotI and SalI restriction site, respectively. Cloning was done as described for the tagged and untagged forms of *CDC48*.

To examine the growth of yeast under various conditions, log-phase cells grown at 26ºC were harvested and resuspended in sterile water to a final A_{600} of 1.0. Ten-fold serial dilutions were spot plated on the indicated media and grown for 2 to 6 d at 30° or 38°C.

Table 2. List of strains used in this study

All strains were in the BY4742 background.

Strain	Genotype	Reference
BY4742	*MATα, his3Δ1, leu2Δ0, ura3Δ0, lys2Δ0, MET15*	Open Biosystems
vms1Δ::HIS3	*MATα, his3Δ1, leu2Δ0, ura3Δ0, lys2Δ0, MET15, vms1Δ::HIS3*	This study
vms1Δ::KanMX	*MATα, his3Δ1, leu2Δ0, ura3Δ0, lys2Δ0, MET15, vms1Δ::KanMX*	Open Biosystems
vms1Δ	*MATα/A, his3Δ1, leu2Δ0, ura3Δ0, lys2Δ0, MET15, vms1Δ::KanMX, vms1Δ::HIS3*	This study
ufd2Δ	*MATα, his3Δ1, leu2Δ0, ura3Δ0, lys2Δ0, MET15, ufd2Δ::KanMX*	Open Biosystems
ufd2Δvms1Δ	*MATα, his3Δ1, leu2Δ0, ura3Δ0, lys2Δ0, MET15, vms1Δ::HIS3, ufd2Δ::KanMX*	This study
ufd3Δ	*MATα, his3Δ1, leu2Δ0, ura3Δ0, lys2Δ0, MET15, ufd3Δ::KanMX*	Open Biosystems
ufd3Δvms1Δ	*MATα, his3Δ1, leu2Δ0, ura3Δ0, lys2Δ0, MET15, vms1Δ::HIS3, ufd3Δ::KanMX*	This study
ubx1Δ	*MATα, his3Δ1, leu2Δ0, ura3Δ0, lys2Δ0, MET15, ubx1Δ::KanMX*	Open Biosystems
ubx1Δvms1Δ	*MATα, his3Δ1, leu2Δ0, ura3Δ0, lys2Δ0, MET15, vms1Δ::HIS3, ubx1Δ::KanMX*	This study
ubx2Δ	*MATα, his3Δ1, leu2Δ0, ura3Δ0, lys2Δ0, MET15, ubx2Δ::KanMX*	Open Biosystems
ubx2Δvms1Δ	*MATα, his3Δ1, leu2Δ0, ura3Δ0, lys2Δ0, MET15, vms1Δ::HIS3, ubx2Δ::KanMX*	This study
ubx3Δ	*MATα, his3Δ1, leu2Δ0, ura3Δ0, lys2Δ0, MET15, ubx3Δ::KanMX*	Open Biosystems
ubx3Δvms1Δ	*MATα, his3Δ1, leu2Δ0, ura3Δ0, lys2Δ0, MET15, vms1Δ::HIS3, ubx3Δ::KanMX*	This study
ubx4Δ	*MATα, his3Δ1, leu2Δ0, ura3Δ0, lys2Δ0, MET15, ubx4Δ::KanMX*	Open Biosystems
ubx4Δvms1Δ	*MATα, his3Δ1, leu2Δ0, ura3Δ0, lys2Δ0, MET15, vms1Δ::HIS3, ubx4Δ::KanMX*	This study
ubx5Δ	*MATα, his3Δ1, leu2Δ0, ura3Δ0, lys2Δ0, MET15, ubx5Δ::KanMX*	Open Biosystems
ubx5Δvms1Δ	*MATα, his3Δ1, leu2Δ0, ura3Δ0, lys2Δ0, MET15, vms1Δ::HIS3, ubx5Δ::KanMX*	This study
ubx6Δ	*MATα, his3Δ1, leu2Δ0, ura3Δ0, lys2Δ0, MET15, ubx6Δ::KanMX*	Open Biosystems
ubx6Δvms1Δ	*MATα, his3Δ1, leu2Δ0, ura3Δ0, lys2Δ0, MET15, vms1Δ::HIS3, ubx6Δ::KanMX*	This study
ubx7Δ	*MATα, his3Δ1, leu2Δ0, ura3Δ0, lys2Δ0, MET15, ubx7Δ::KanMX*	Open Biosystems
ubx7Δvms1Δ	*MATα, his3Δ1, leu2Δ0, ura3Δ0, lys2Δ0, MET15, vms1Δ::HIS3, ubx7Δ::KanMX*	This study
cdc48-3	*MATα, his3Δ1, leu2, ura3, lys2Δ0, MET15, cdc48-3*	This study
cdc48-3 vms1Δ	*MATα, his3Δ1, leu2, ura3, lys2Δ0, MET15, cdc48-3, vms1Δ::KanMX*	This study
pdr5Δ	*MATα, his3Δ1, leu2Δ0, ura3Δ0, lys2Δ0, MET15, pdr5Δ::KanMX*	Open Biosystems
pdr5Δvms1Δ	*MATα, his3Δ1, leu2Δ0, ura3Δ0, lys2Δ0, MET15, vms1Δ::HIS3, pdr5Δ::KanMX*	This study

Table 3. List of oligonucleotide primers used in this study

Restriction enzyme recognition sites are underlined and the sequences encoding epitope tags are in bold.

Oligo	Sequence
*vms1*Δ::KanMX-F	ggattttcaaaagatctgcacgcctgttgacaagcttccaatagcatctgtgcggtatttcacaccg
*vms1*Δ::KanMX-R	gcaaatgctaagaaaaatcctaaaaatttgaatatgagatattccagattgtactgagagtgcac
*vms1*Δ::HIS3-F	ggattttcaaaagatctgcacgcctgttgacaagcttccaatagcatcggatccccgggttaattaa
*vms1*Δ::HIS3-R	gcaaatgctaagaaaaatcctaaaaatttgaatatgagatattccgaattcgagctcgtttaaac
VMS1 screen-F	ttcttggaggagtgccacag
VMS1 screen-R	ggcgtcattttcgcgttgag
*ufd2*Δ::His3-F	ccaatagaaaggtaaagttgaccacaagttgtttaaggggaaaagttaactttgaaagtagaaccctcattccatagatccggatccccgggttaattaa
*ufd2*Δ::His3-R	aaatataagacacattgagcgatgaaataagccttatttgattagggtcaattttgcaatttattctatcacttattcatgaattcgagctcgtttaaac
UFD2 screen-F	ccagtttcgagaatctagtgctg
UFD2 screen-R	gaagcaaatcgctttcccacaa
UBX1 screen-F	gtagtgacaaacatgcctctggat
UBX1 screen-R	gcagcagttattcatgatgctggt
UBX2 screen-F	tggctgaggattgccgccaagctg
UBX2 screen-R	actataaaggtaggccccagctcc
UBX3 screen-F	agaccgcctaattggatcatcg
UBX3 screen-R	aaactgatgcacgtgacactt
UBX4 screen-F	aagatagcgggcgcctcaaccgct
UBX4 screen-R	gtacaagttacggaaggcggagct
UBX5 screen-F	ctcgatgtctctgcagaagcga
UBX5 screen-R	caacagcggcagatgcatcgct
UBX6 screen-F	ggatttacctctagcgcgtcaacc
UBX6 screen-R	aaccaggatttgcacgagcca
UBX7 screen-F	gtgctgcccatatacagcaactt
UBX7 screen-R	gctgagttcttttgcggtgat
CDC48-NotI-F1	ttgcggccgcggtggccagcccaagaaacgga
CDC48-XhoI-R1	agctcgagacgaccgaggtcctacagcct
CDC48-Cterm-BamHI-R1	acggatccactatacaaatcatcatcttcc
CDC48-Myc-BamHI-F1	acggatccg**aacaaaaactcatctcagaagaggatctg**tagtagttatatgccaggtatatttttattttaaatcg
CDC48-HA-BamHI-F1	acggatcc**tacccatacgacgtcccagactacgct**tagtagttatatgccaggtatatttttattttaaatcg
vms1-NotI-F	ctgcggccgcttcttggaggagtgccacag
vms1-SalI-R	tcggtcgacggcgtcattttcgcgttgag
vms1-Cterm-BamHI-R1	acggatccgtatttctttttcatcctttcttctgcg
vms1-Myc-BamHI-F1	acggatccg**aacaaaaactcatctcagaagaggatctg**tgatgaggaatatctcatattcaaatttttagg
vms1-HA-BamHI-F1	acggatcc**tacccatacgacgtcccagactacgct**tgatgaggaatatctcatattcaaatttttagg

Table 4. Plasmids used in the study

Unless referenced, all plasmids were constructed by PCR amplification and cloning as detailed in the Materials and Methods section.

Plasmid name	Description	Reference
pSM1152	PGK1 promoter, CFTR-HA expression plasmid, 2 micron	Zhang, et al., 2002
pSM1911	PGK1 promoter, Ste6p*-HA expression plasmid, 2 micron	Huyer, et al., 2006
CPY*-3xHA	Endogenous promoter, CPY* 3xHA expression plasmid, CEN	Bhamidipati, et al., 2005
pRS316-CDC48	Endogenous promoter, untagged CDC48, CEN	This study
pRS426-CDC48	Endogenous promoter, untagged CDC48, 2 micron	This study
pRS316-CDC48myc	Endogenous promoter, c-terminal 1xmyc CDC48, CEN	This study
pRS316-CDC48HA	Endogenous promoter, c-terminal 1xHA tagged CDC48, CEN	This study
pRS426-CDC48myc	Endogenous promoter, c-terminal 1xmyc tagged CDC48, 2 micron	This study
pRS426-VMS1	Endogenous promoter, untagged VMS1, CEN	This study
pRS315-VMS1HA	Endogenous promoter, c-terminal 1xHA tagged VMS1, CEN	This study
pRS316-VMS1HA	Endogenous promoter, c-terminal 1xHA tagged VMS1, CEN	This study
pRS426-VMS1HA	Endogenous promoter, c-terminal 1xHA tagged VMS1, 2 micron	This study
pRS426-UFD2	Endogenous promoter, untagged UFD2, 2 micron	This study

2.1.2 Assays for ER-associated degradation (ERAD) and the degradation of other substrates

To assess the rate of CFTR and Ste6p* degradation, the appropriately transformed strains were grown to log-phase (A_{600}=0.5-1.5) in selective media at 26°C. The cells were then harvested and resuspended to a final A_{600} of 1.0. One ml of cells was taken as the zero time point. Next, cycloheximide was added to a final concentration of 100-200μg/ml and cells were incubated at 30°C for Ste6p* or 40°C for CFTR (NAKATSUKASA *et al.* 2008; ZHANG *et al.* 2002). Aliquots were removed at the indicated time points. Samples were mixed with NaN_3 (final concentration, 10μM) and the cells were centrifuged at 16,000g for 1 min. The resulting supernatant was aspirated and the pellet was snap frozen in liquid nitrogen and stored at -80°C until use. Total protein was extracted from cell according to a previously established protocol (ZHANG *et al.* 2002). Briefly, aliquots were thawed and resuspended in 1ml of freshly prepared alkaline lysis solution (0.2M NaOH, 0.11M beta-mercaptoethanol). The mixture was agitated briefly on a Vortex mixer and incubated on ice for 10 min. Next, 150μl of 50% TCA was added, agitated on a Vortex mixer and incubated on ice for an additional 10 min. The mixture was then centrifuged at 16,000g for 10 min. The supernatant was carefully aspirated and the pellet washed with 500μl of ice-cold acetone. The pellet was resuspended in SDS-PAGE sample buffer (80mM Tris-HCl pH 8.0, 8mM EDTA, 3.5% SDS, 15% glycerol, 0.08% Tris base, 0.01% bromophenol blue) containing freshly added DTT (100mM) to a final concentration of 10 OD/ml. The samples were solubilized by grinding with a Kontes mini-hand-held pestle. Samples were resolved by SDS-PAGE, transferred to a nitrocellulose membrane, and detected by western blotting with the

appropriate antibodies. Data were quantified using ImageJ v1.42q software (ABRAMOFF *et al.* 2004). The degradation of an HA epitope tagged form of CPY* (BHAMIDIPATI *et al.* 2005) was also assessed by cycloheximide chase analysis, as described above, except that the cells were incubated at 30°C during the chase.

The pulse chase analysis of CFTR-HA was performed as previously described (GNANN *et al.* 2004). Briefly, 30 ml of cells were grown overnight to log-phase, harvested, and resuspended in media lacking methionine and cysteine to a final A_{600} of 6/ml. Cells were labeled for 1 h with ^{35}S-labeled methionine (New England Nuclear, USA) at a final concentration of 100μCi/ml. A zero time point was then taken, and cells were chased with cold methionine and cysteine. Cells were disrupted by glass-bead lysis and the crude lysate was solubilized in 12.5mM Tris-HCl, pH 7.5, 150mM NaCl, 1% SDS. The lysate was then diluted with IP buffer (50mM Tris-HCl, pH 7.5, 150mM NaCl, 1% deoxycholic acid, 1% Triton X-100) so that the final concentration of SDS was 0.1%. CFTR-HA was immunoprecipitated from the solubilized lysate with anti-HA agarose (Roche, USA) and immunoprecipitated material was separated by SDS-PAGE and subject to autoradiography.

The degradation of a galactose-inducible version of a ubiquitin-proline β-galactosidase chimera was measured by pulse-chase analysis as previously described (BACHMAIR *et al.* 1986). In brief, cells were grown to saturation, harvested, and resuspended to an A_{600} of ~3/ml in media lacking methionine. Next, ^{35}S-labeled methionine (New England Nuclear, USA) was added to a final concentration of 11μCi/μl and total protein was labeled for 15 min at 30°C. Cycloheximide was added to a final concentration of 500μg/ml, aliquots were removed at the indicated time

points, and samples were processed. The precipitated chimeric protein was visualized by phosphorimager analysis on a Fujifilm BAS-2500 and the data were quantified using ImageJ v1.42q software (ABRAMOFF *et al.* 2004). The degradation of a Deg1-β-galactosidase fusion was assessed by cycloheximide chase analysis, as published (HOCHSTRASSER and VARSHAVSKY 1990).

2.1.3 Preparation of yeast subcellular fractions and indirect immunofluorescence microscopy

Yeast cytosol was prepared by liquid nitrogen lysis as described previously (MCCRACKEN and BRODSKY 1996). In brief, 4-6 l of cells were grown to log-phase, harvested, and resuspended in Buffer 88 (20mM HEPES pH 6.8, 150mM KOAc, 250mM sorbitol, 5mM MgOAc). The suspension was then poured into liquid nitrogen and pulverized in a Waring blender for 10 min. The resulting mixture was thawed and clarified by centrifugation at 300,000g. The final concentration of cytosol was ~20-30mg/ml and was stored at -80°C. Yeast microsomes were prepared as previously described from 1-2 l of log-phase cells that were spheroplasted, lysed in a Potter-Elvehjem homogenizer, and isolated by differential centrifugation (BRODSKY and SCHEKMAN 1993; DESHAIES and SCHEKMAN 1989; NAKATSUKASA *et al.* 2008). The ER-enriched microsomes were resuspended in Buffer 88 to a final A_{280} of 40 (as measured in 2% SDS) and stored at -80°C.

The subcellular localization of Vms1p was determined by a previously reported method (KABANI *et al.* 2002) in which log-phase cells were harvested, washed, and lysed with glass beads. After unbroken cells were removed by centrifugation at 3,000g for 5 min, a crude

membrane fraction was obtained as the pellet after a 16,000g centrifugation for 15 min and the supernatant constituted a crude cytosolic fraction. The crude cytosolic fraction was clarified by centrifugation at 150,000g for 15 min. Ten microliters of total lysate and each membrane and cytosol fraction was subject to SDS-PAGE and western blotting with the indicated antibodies.

The subcellular residence of Vms1p was also determined by indirect immunofluorescence microscopy, as previously described (COUGHLAN *et al.* 2004). Diploid strains lacking *VMS1* and expressing an HA-tagged form of Vms1p from an episomal CEN plasmid were grown to log-phase. Cells were fixed by adding a 1/10th volume of 37% formaldehyde and incubation at room temperature for 60 min. Cells were harvested and washed twice with Solution A (1.2M sorbitol, 50mM KPO4, pH 7.0) and were then treated with 2μg/ml of Zymolyase 20T (MP Biomedicals, USA) resuspended in Solution A for 30-40 min. Following treatment, cells were pelleted and washed twice with Solution A and resuspended in 200μl of Solution A. A total of 25-30μl of cells were pipetted onto polylysine-treated slides and allowed to adhere for 30 min at room temperature. Loose cells were aspirated and the slides were washed once with PBS, 0.1% BSA, followed by two washes with PBS, 0.1% BSA, 0.1% NP-40. The samples were incubated overnight at 4ºC with primary antibodies against yeast BiP/Kar2p (1:2000) and the HA epitope tag (1:500) that were resuspended in PBS, 0.1% BSA. Next, the samples were washed one time each with PBS, 0.1% BSA and PBS, 0.1% BSA, 0.1% NP-40. Samples were then incubated with a 1:2000 dilution of Alexa-Fluor-conjugated secondary antibodies (Invitrogen, USA, goat anti-rabbit, 594 and goat anti-mouse, 488) resuspended in PBS, 0.1% BSA, for 1-2 h at room temperature. The slides were then washed once with PBS, 0.1% BSA, twice, with PBS, 0.1% BSA, 0.1% NP-40, and once with PBS, 0.1% BSA. Anti-fade mounting medium plus DAPI

(Invitrogen, USA) was laid on top of each sample before applying a coverslip that was sealed with nail polish. Images were captured by QED software using a Hamamamatsu camera attached to an Olympus BX-60 microscope (Olympus, Japan). Images were analyzed using ImageJ v1.42q (ABRAMOFF *et al.* 2004).

2.1.4 Measurements of substrate ubiquitination

In vitro ubiquitination reactions were performed as previously described (NAKATSUKASA *et al.* 2008). In brief, microsomes, cytosol, an ATP regenerating system and ^{125}I-labeled ubiquitin were mixed and incubated at room temperature for 1 h. Yeast membranes were then solubilized with detergent and the ERAD substrate was immunoprecipitated with a mixture of anti-HA antibody and protein-A sepharose (GE Healthcare, USA). The precipitated material was washed with 50mM Tris-HCl, pH 7.4, 150mM NaCl, 5mM EDTA, 1% Triton X-100, 0.2% SDS, and then released from the beads with SDS-PAGE sample buffer (80mM Tris-HCl, pH 8.0, 8mM EDTA, 3.5% SDS, 15% glycerol, 0.08% Tris base, 0.01% bromophenol blue) containing freshly added DTT (100mM) and heating at 37°C for 30 min. The resulting ^{125}I-ubiquitinated material was resolved on a 6% SDS-polyacrylamide gel and was detected by phosphorimager analysis, as described above. Unmodified CFTR was visualized by western blotting using anti-HA antibody. Data were quantified using Image Gauge v4.0 or ImageJ v1.42q (ABRAMOFF *et al.* 2004).

The immunoprecipitation and detection of in vivo ubiquitinated CFTR was carried-out as previously described (AHNER *et al.* 2007). A total of 100ml of cells were grown overnight to log-phase and were harvested and disrupted by glass bead lysis. Unbroken cells were sedimented by low-speed centrifugation, and membranes were sedimented at 18,000g for 20 min in a

refrigerated table top centrifuge and resuspended in Buffer 88 to an A_{280} of 40 as measured in 2% SDS. Membranes were solubilized in 1% SDS at 37ºC for 30 min, and the solubilized ERAD substrate was immunoprecipitated with anti-HA-conjugated agarose (Roche, USA). The immunoprecipitated substrate was released with SDS-PAGE sample buffer containing freshly added DTT and heating at 37°C for 30 min. The protein was then resolved by SDS-PAGE, and transferred to nitrocellulose as in a standard western blot except with the following modification. After the transfer to nitrocellulose was complete, the nitrocellulose membrane was sandwiched between two sheets of Whatmann filter paper and placed in a boiling water bath for 45 min. The sandwiched blot was allowed to cool to room temperature and after blocking, the ubiquitinated species were detected using anti-ubiquitin antibody.

2.1.5 Immunoprecipitation of Cdc48p and detection of Cdc48p-associated ubiquitinated proteins

To monitor the association between Cdc48p and Vms1p, cells lacking *VMS1* were transformed with CEN plasmids containing a C-terminal Myc-tagged version of Cdc48p and/or a C-terminal HA-tagged version of Vms1p (**Table 4**), or the vectors lacking an insert. The transformed cells were grown in selective media to log-phase, harvested by low-speed centrifugation, resuspended in Buffer 88—which was supplemented with 1mM PMSF, 1µg/ml leupeptin, 0.5µg/ml pepstatin A, and 10mM NEM—and then disrupted with glass beads by vigorous agitation on a Vortex mixer 10 times for 30 sec, followed by a 30 sec incubation on ice. The extract was removed and reserved, and the beads were washed with an equal volume of Buffer 88, which was then pooled with the reserved extract. Unbroken cells were removed by centrifugation at 1,500g for 5 min at 4°C. A portion of the resulting supernatant represented the total lysate, and the protein

concentration was estimated by adjusting the A_{280} in 2% SDS such that the absorbance was 40 (i.e., a protein concentration of ~10 mg/ml). To separate membrane and cytosolic fractions, the total lysate was centrifuged at 150,000g for 20 min at 4ºC. The resulting membrane fraction was washed one time with Buffer 88 and then resuspended in Buffer 88 such that the final A_{280} in 2% SDS was 40 (i.e., a protein concentration of ~10 mg/ml). The protein concentration of the cytosol was estimated using the BioRad protein assay kit. To immunoprecipitate the tagged proteins, 200µg of lysate, cytosol, and membrane proteins were treated as follows: The total and membrane fractions were solubilized on ice for 30 min in Buffer A (20mM HEPES, pH 7.4, 150mM NaCl, 1% Triton X-100). Then, an equal amount of Buffer B (20mM HEPES, pH 7.4, 150mM NaCl) was added so that the final concentration of Triton X-100 was 0.5%. For consistency the cytosolic extract was treated on ice for 30 min by adding Triton X-100 to a final concentration of 0.5%. For each fraction, insoluble material was removed by centrifugation at 16,000g for 10 min at 4°C and the volume was brought-up to 500µl with Buffer C (20mM HEPES, pH 7.4, 150mM NaCl, 0.5% Triton X-100) prior to immunoprecipitation with anti-HA- or anti-Myc-conjugated agarose The immunoprecipitate was washed once with Buffer C, and three times with Buffer D (20mM HEPES, pH 7.4, 300mM NaCl, 0.5% Triton X-100), and the bound proteins were released with SDS-PAGE sample buffer, as described above.

To examine Cdc48p association with ubiquitinated proteins, yeast cultures containing 100ml of log-phase cells harboring the Cdc48p-HA expression vector or a vector control either were left untreated or treated with 50µM MG132 for 1 h. Cell disruption was performed using the medium-scale preparation, as described previously (NAKATSUKASA *et al.* 2008), and all buffers, including SDS-PAGE sample buffer were supplemented with 1mM PMSF, 1µg/ml

leupeptin, 0.5 μg/ml pepstatin A, and 10 mM NEM. The cells were harvested, disrupted with glass-beads, and following the removal of unbroken cells the crude extract was loaded onto a 1.0M sucrose cushion and the mixture was centrifuged at 6,900g in a Sorvall HB-6 swinging bucket rotor for 10 min at 4°C. The material residing above the cushion is enriched for ER-microsomes and this was collected by centrifugation at 20,200g for 10 min at 4°C in a Sorvall SS-34 rotor. The microsomes were washed and resuspended in Buffer 88 to a final A_{280} (measured in 2% SDS) of 40. To immunoprecipitate epitope-tagged Cdc48p, 20μl of membranes were solubilized with 1% Triton X-100 in Buffer A (see above) for 30 min on ice. The solubilized material was then diluted with Buffer B (see above) so that the final concentration of Triton X-100 was 0.5%. Insoluble material was pelleted by centrifugation at 16,000g for 10 min at 4°C and the clarified, soluble material was brought to a final volume of 500μl with Buffer C (see above) prior to immunoprecipitation with anti-HA agarose (Roche, USA). The immunoprecipitate was washed three times with Buffer C, and the bound proteins were eluted with SDS-PAGE sample buffer, as described above. After SDS-PAGE, the resolved proteins were transferred to a nitrocellulose membrane, and the membrane was treated as described above.

2.1.6 Assays to measure autophagy

The effect of *VMS1* deletion on autophagy was assessed by two established methods (CHEONG and KLIONSKY 2008). In the first method, the processing of Ape1p/Lap4p was measured by western blot analysis. Wild-type and *vms1*Δ yeast were grown in 5ml YPD (1% yeast extract, 2% peptone, 2% dextrose) cultures to log-phase at 30°C. An aliquot (1ml) of the log-phase culture was taken and mixed with sodium azide (final concentration 10mM). This aliquot was

centrifuged at 16,000g for 1 min in a refrigerated centrifuge to pellet the cells. The supernatant was next aspirated and the remaining pellet was snap frozen in liquid nitrogen and stored at -80°C until use. The remaining 4ml culture was centrifuged at 1,000g for 5 min in a clinical centrifuge. The media was decanted and the cells were washed with and resuspended in an equal volume of SC-N (1.7% Yeast nitrogen base without ammonium sulfate, 2% glucose). The final resuspension was placed at 30°C and grown for 4 h to induced starvation. At 4 h an aliquot (1ml) was taken and processed as described above in section 2.2.2.

In the second method, the processing of GFP-Atg8p was measured. Wild-type and *vms1*Δ yeast expressing GFP-Atg8p were grown to log-phase. An aliquot (1ml) was taken and processed as described for the Ape1p/Lap4p assay. The remaining log-phase culture was centrifuged at 1,000g for 5 min in a clinical centrifuge. The media was decanted and the cells were washed with and resuspended in an equal volume of SC-N. The final resuspension was placed at 30°C and grown for 2 h to induced starvation. Aliquots of 1ml were taken at the 1 and 2 h time points. The aliquots were processed as described in section 2.2.2.

2.1.7 Antibodies and western oblot analysis

Antibodies used in this study included: Anti-HA (Roche, USA), anti-Myc (Santa Cruz, USA), anti-Ubiquitin (Santa Cruz, USA), anti-GFP (Roche, USA), anti-Cdc48p (*S. pombe*, a kind gift from Dr. Rasmus Hartmann-Petersen), anti-Cdc48p (*S. cerevisiae*), Ufd2p, Ufd3p, Ubx1p, Ubx2p (a kind gift from Dr. Alexander Buchberger), anti-Otu1p, Ufd1p (a kind gift from Dr. Stefan Jentsch), anti-Ufd1p (a kind gift from Dr. Claire Moore), anti-Ape1p (a kind gift from Dr. Daniel Klionsky), and monoclonal anti-yeast BiP/Kar2p (a kind gift from Dr. Mark Rose).

Western blots were decorated with the indicated primary antibodies and appropriate HRP-conjugated anti-mouse or anti-rabbit IgG secondary antibodies. The HRP-chemiluminescent signal was visualized by enhanced chemiluminescence (Pierce, USA). Images were captured on a Kodak Image Station 440CF (Kodak, USA) and were analyzed using ImageJ v1.42q (ABRAMOFF *et al.* 2004).

2.2 RESULTS

2.2.1 Vms1p resides primarily in the cytoplasm

To probe the localization of Vms1p in yeast during normal cell growth, I constructed a C-terminal, HA-epitope-tagged version of Vms1p. The protein's expression was controlled by the endogenous promoter and the gene was maintained on a low-copy CEN plasmid. By taking advantage of the fact that yeast lacking *VMS1* are cycloheximide sensitive (**Parsons AB Boone C 04**), I established that Vms1p-HA was functional since it rescued the growth of *vms1*Δ cells in the presence of cycloheximide (**Figure 13A**). Next, I used differential centrifugation to assess the localization of Vms1p. As shown in **Figure 13B**, Vms1p appears to reside in both membrane-associated and soluble fractions, but is predominantly a cytosolic protein. In this experiment, I also monitored the localization of Sec61p, which is an ER membrane protein (STIRLING *et al.* 1992), and Sse1p, which like Vms1p is primarily a cytosolic protein but exhibits partial membrane residence (GOECKELER *et al.* 2002). To further analyze Vms1p's residence, I performed indirect immunofluorescence microscopy with the help of a colleague, Dr. Christopher Guerriero. As seen in **Figure 13C**, Vms1p-associated fluorescence was primarily

cytoplasmic and in some cases enriched in large intracellular punctae. In some cells these bodies appeared to reside just at the periphery of the ER, as evidenced by the signal corresponding to yeast BiP, Kar2p. These bodies did not colocalize with mitochondrial-derived DAPI staining (**Figure 13C**). As assessed by indirect immunofluorescence, the localization of Cdc48p is also primarily cytosolic - except in late G1 - and can also be visualized in large bodies that reside periphery to the ER in some cells (MADEO *et al.* 1998).

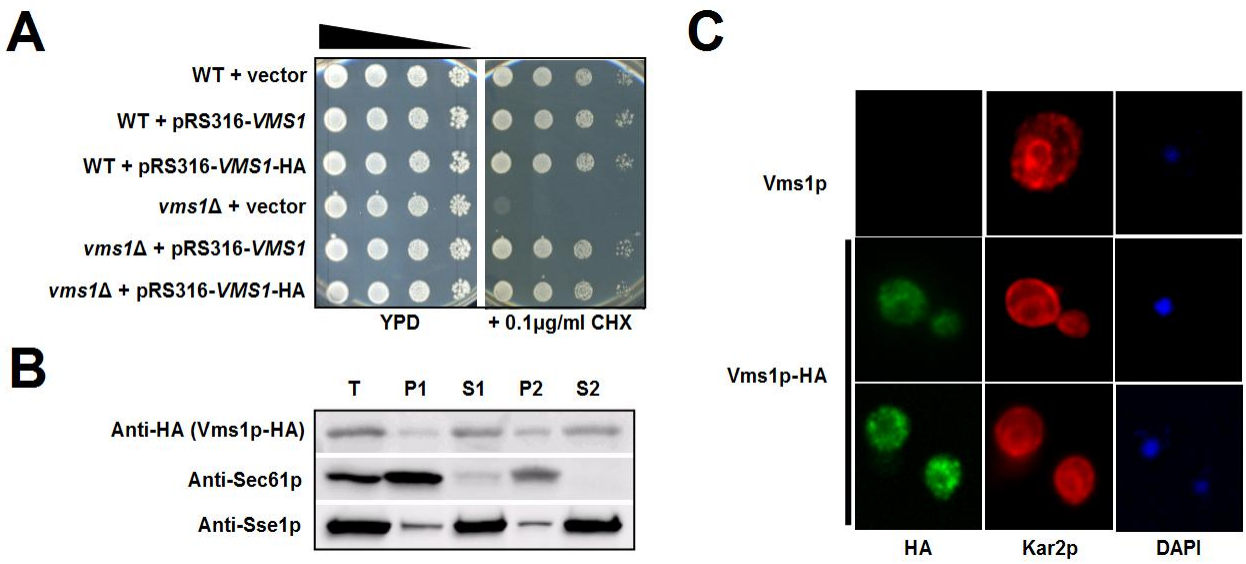

Figure 13. Vms1p is found in the cytoplasm and at the membrane

A. Wild-type and *vms1*Δ yeast cells harboring an empty vector, or a construct designed to express *VMS1* or a *VMS1-HA* under its endogenous promoter were tested for cycloheximide sensitivity. Cells were spot tested as 10-fold serial dilution on either YPD, or YPD + 0.1µg/ml cycloheximide. The plates were incubated at 30ºC for 4 d. **B.** *VMS1* encodes a cytosolic protein with limited membrane association. Yeast cells deleted for *VMS1* were transformed with a low-copy *VMS1-HA* expression vector whose expression is under the control of the endogenous promoter. Yeast cells were disrupted and lysates were processed for SDS-PAGE and western blot analysis. The ER membrane protein, Sec61p, and the cytosolic chaperone, Sse1p, served as controls. "T" represents total lysate, "P1" is the membrane pellet after a 16,000*g* centrifugation, "S1" is the supernatant after 16,000*g*, "P2" is the membrane pellet derived from "S1" after 160,000*g*, and "S2" is the supernatant derived from "S1" after the 160,000*g* spin. A total of 10µl of each fraction was analyzed. **C.** Yeast cells were fixed and decorated with anti-HA antibody to detect Vms1p and anti-BiP (Kar2p), an ER resident protein, and the appropriate secondary

fluorescent-conjugated antibodies. DAPI staining was used to detect nuclear and mitochondrial DNA.

2.2.2 Vms1p is associated with Cdc48p in both cytosol and membrane fractions

Large-scale proteomic studies identified Vms1p as a component of a multi-protein complex that included Cdc48p (KROGAN *et al.* 2006). Because false-positives can arise from proteomic analyses, experiments were designed to determine if Vms1p and Cdc48p can be co-precipitated. I therefore performed reciprocal co-immunoprecipitations with a C-terminal Myc-tagged version of Cdc48p and the HA-tagged form of Vms1p. Expression of the epitope tagged version of Cdc48p rescued the growth of *cdc48-3* yeast at a non-permissive temperature (**Figure 14A**), indicating that Cdc48p-Myc is active. I then isolated cytosolic and membrane fractions from cells grown in the absence of stress to determine whether Cdc48p and Vms1p co-precipitate. As shown in **Figure 14B**, Vms1p and Cdc48p can be co-precipitated when a total yeast lysate is examined (T), and when both membrane (M) and cytosolic (C) fractions are examined. As controls for this experiment, co-precipitation was absent when cells expressed untagged versions of either protein. I also noted that significantly more Cdc48p resided in the cytosol than at the membrane, and that the amount of Vms1p associated with Cdc48p reflected this distribution (**Figure 14B, top**). In contrast, when Vms1p was precipitated (**Figure 14B, bottom**), approximately equal amounts of the protein resided at the membrane and in the cytosol, but in both cases again Cdc48p co-precipitated with Vms1p. Further evidence for the functional significance of Vms1p-Cdc48p interaction is provided by a synthetic growth phenotype in *vms1*Δ yeast that simultaneously harbor a temperature sensitive allele of *CDC48* (**Figure 14C**). Given that Vms1p can localize and associate with the Cdc48p complex at the mitochondrial membrane in the presence of mitochondrial and oxidative stressors (HEO *et al.* 2010), I also

tested directly whether Vms1p associates with the Cdc48p complex at the ER membrane. To this end, Vms1p-HA was immunoprecipitated from highly enriched ER membranes and the resulting precipitate was blotted for Cdc48p. As shown in **Figure 14D**, Cdc48p was coimmunoprecipitated with Vms1p-HA from ER-enriched membranes but not from strains that contained an untagged version of Vms1p. Because Vms1p contains a VCP/p97 Interacting Motif (VIM) domain (HEO *et al.* 2010), which is known to mediate direct interactions with VCP/p97 (BALLAR *et al.* 2006), it is likely that Vms1p and Cdc48p directly associate. I also observed reproducible interactions between Vms1p-HA and Ubx2p and Ufd3p, which are known Cdc48p partners (see Chapter 1) (**Figure 15**). Together, these data indicate that that Vms1p is a component of a Cdc48p complex that exists in both the cytosol and at the ER membrane.

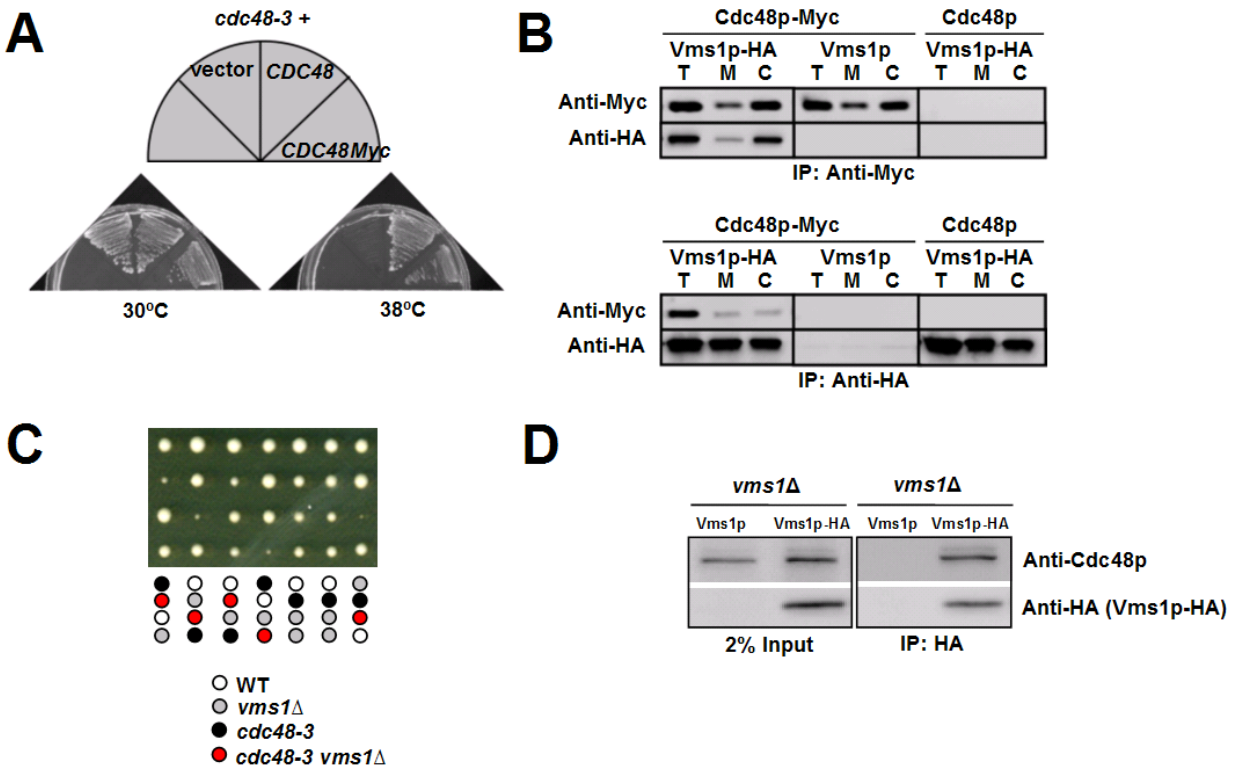

Figure 14. Vms1p co-immunoprecipitates with Cdc48p

A. The classic temperature sensitive mutant, *cdc48-3*, was transformed with an empty vector, or a vector designed to express *CDC48* or *CDC48-Myc* from its endogenous promoter. Strains were streaked onto selective media and incubated at 30 or 38°C to test for the rescue of the conditional allele. **B.** *VMS1*-deleted cells were transformed with a plasmid engineered for the expression of a functional, Myc-tagged version of Cdc48p and/or with the HA-tagged version of Vms1p. As controls, untagged versions of each protein were introduced into each strain. The resulting transformants were disrupted and a portion of the total lysate (T), the membrane fraction (M), and the cytosolic fraction (C) were subject to immunoprecipitation with anti-Myc or anti-HA antibodies. The immunoprecipitated proteins were resolved by SDS-PAGE and subjected to western blot analysis with the indicated antibodies. **C.** To test for a genetic interaction between *VMS1* and *cdc48-3*, the individual strains were mated on rich media followed by sporulation in nutrient poor media. The genotypic results of tetrad dissection are

shown in the circles beneath the image. White is wild-type, grey is *vms1*Δ, black is *cdc48-3*, and red is *cdc48-3vms1*Δ. **D.** *VMS1* deleted cells were transformed with a plasmid engineered for the expression of untagged or HA-tagged versions of Vms1p. ER-microsomes were enriched through sucrose gradient and Vms1p was immunoprecipitated with anti-HA resin. The immunoprecipitate was resolved by SDS and subject to western blot analysis with anti-Cdc48p and anti-HA.

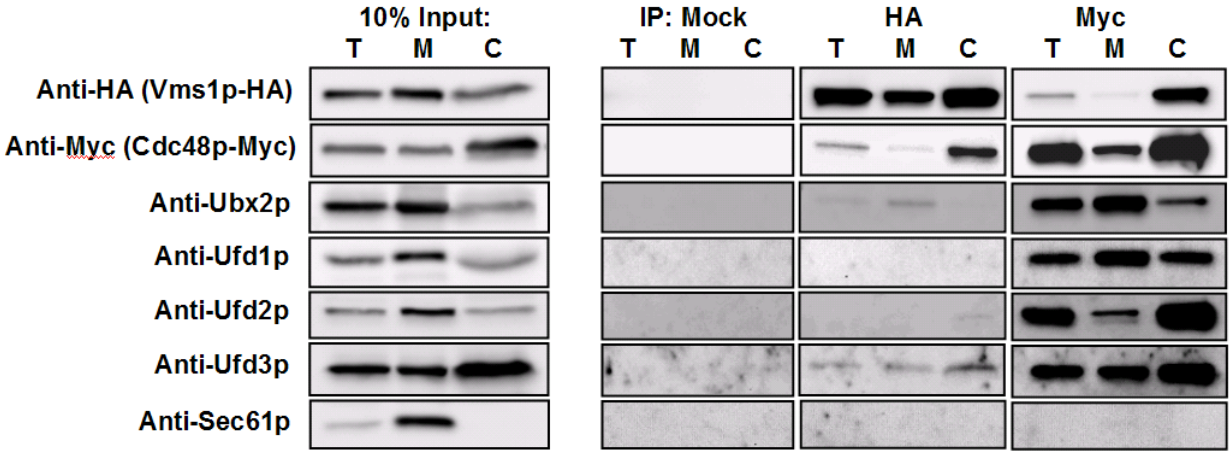

Figure 15. Vms1p physically associates with other members of the Cdc48p complex

Total lysate (T), membrane (M), and cytosolic (C), fractions were prepared from cells expressing Vms1p-HA from a 2μ plasmid the under control of its endogenous promoter. Vms1p-HA was immunoprecipitated with anti-HA agarose and Cdc48p-Myc was immunoprecipitated with anti-Myc agarose. A mock control using protein-A sepharose was included. The immunoprecipitated material was eluted with SDS-PAGE sample buffer, resolved by SDS-PAGE and followed by western blot analysis with the indicated antibodies.

2.2.3 Yeast lacking *VMS1* exhibit slowed degradation of CFTR, an integral membrane ERAD substrate

As described in Section 2.1, Cdc48p plays a well-defined role during ERAD. To test if Vms1p function is also important for ERAD, I performed degradation assays with a panel of well-established ERAD substrates. I found first that CFTR degradation was modestly slowed in *vms1*Δ yeast (**Figure 16A**, compare filled versus unfilled squares), and that the CFTR degradation defect was fully recoverable when an extrachromosomal copy of *VMS1* was introduced (**Figure 16A**, gray squares). The CFTR degradation defect caused by *VMS1* loss was reproducible by pulse-chase analysis, which unlike cycloheximide chase follows the degradation of a newly synthesized subpopulation of CFTR (**Figure 16B**). Interestingly, *vms1*Δ yeast proficiently degraded several other ERAD substrates, including Ste6p* and CPY* (**Figure 17A and B**). Moreover, the degradation of an N-end rule substrate, the ubiquitin-proline β-galactosidase chimera, and the DOA pathway substrate, Deg1-β-galactosidase, were unaffected (**Figure 17C and D**). Based on these results, I conclude that loss of *VMS1* modestly affects the ERAD of select substrates.

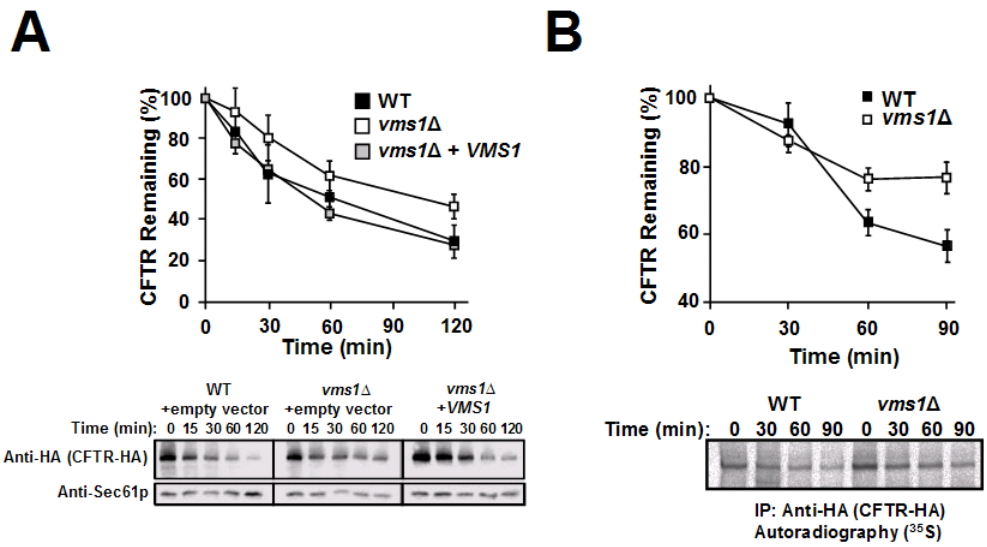

Figure 16. Loss of VMS1 results in compromised ERAD efficiency of the model substrate, CFTR

A. The degradation of the model substrate CFTR was assessed by cycloheximide chase assay. Each cell type was transformed with a CFTR-HA expression plasmid and was co-transformed with either an empty vector, or a plasmid containing *VMS1* driven by its endogenous promoter. Wild-type cells containing the empty vector control are represented by black squares, *vms1*Δ cells containing an empty vector are represented by white squares, and *vms1*Δ yeast containing the extrachromosomal copy of *VMS1* are represented by gray squares. Data represent the means of 6 independent experiments, $\pm$SE. T-test statistic is $p < 0.01$ for the 120 min time point, and $p < 0.05$ for the 60 min time point when comparing the extent of degradation between wild type and *vms1*Δ strains. A representative set of images corresponding to this experiment are shown in the bottom panels. **B.** Loss of *VMS1* affects the ERAD of CFTR as assessed by pulse-chase analysis. Wild type and *vms1*Δ cells expressing CFTR-HA were radio-labeled for 1 hour with ^{35}S-methionine and cysteine and chased with unlabeled amino acids. Aliquots were taken at the indicated time points, the cells were lysed and CFTR-HA was immunoprecipitated with anti-HA agarose. The immunoprecipitate was resolved SDS-PAGE and subject to radiography. Data

were quantitated relative to the zero time point. n = 10, ±SEM. Wild-type (WT) cells are denoted by the filled squares and *vms1*Δ cells are represented by the unfilled squares.

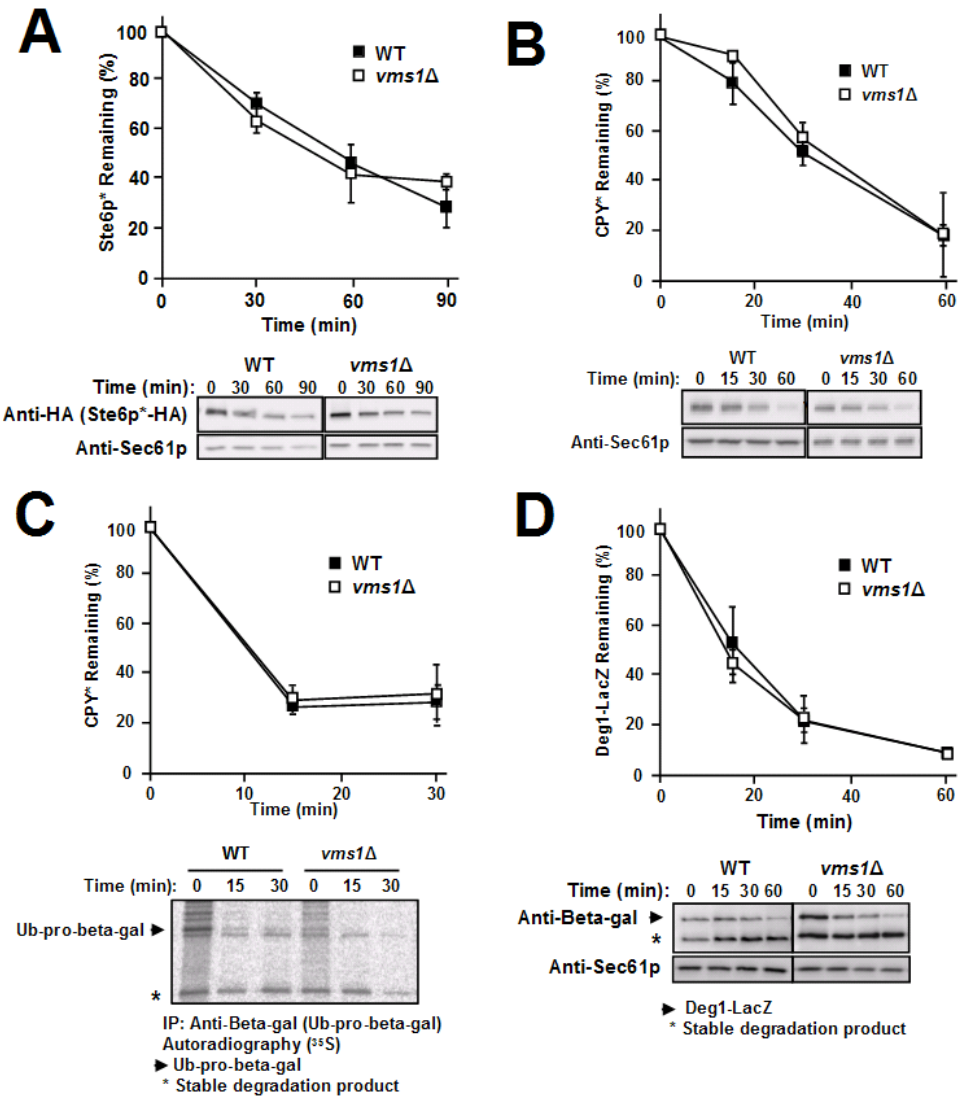

Figure 17. Loss of VMS1 has no effect on the degradation of two model ERAD and two model non-ERAD substrates

A., B. The degradation of the classic ERAD-C substrate, Ste6p* and the classic ERAD-L substrate, CPY* were assessed by cycloheximide chase in both wild-type and *vms1*Δ. **C., D.** The degradation of the N-end rule pathway substrate, Ub-pro-beta-gal, and the DOA pathway substrate, Deg1-LacZ were assessed by pulse- and cycloheximide chase, respectively. In all cases, the wild-type is represented by filled squares and *vms1*Δ is represented by open squares. Representative images are shown below the graphs.

2.2.4 Autophagy is unaffected in yeast lacking *VMS1*

Cdc48p function was recently linked to autophagy (JU *et al.* 2009; KRICK *et al.* 2010; TRESSE *et al.* 2010). To rule out the possibility that the degradation defects were a result of other catabolic mechanisms such as autophagy, I looked at the processing of Ape1p/Lap4p and GFP-Atg8p as a measure of Cytoplasmic to Vacuole Transport (CVT) and autophagic induction, respectively (CHEONG and KLIONSKY 2008). As seen in **Figure 18A**, Ape1p/Lap4p processing was apparent in both wild-type and *vms1*Δ cells and under both optimal growth and nitrogen-starved conditions. As anticipated, processing was absent in a strain lacking *ATG8*. Thus, it appears that the CVT pathway is not affected by the loss of *VMS1*. When a GFP-Atg8p reporter was used to measure autophagic induction, I observed no obvious impairment in the *vms1*Δ background. As expected, *atg14*Δ, was unable to process GFP-Atg8p (**Figure 18B**). I conclude that *vms1*Δ has no obvious role in autophagy.

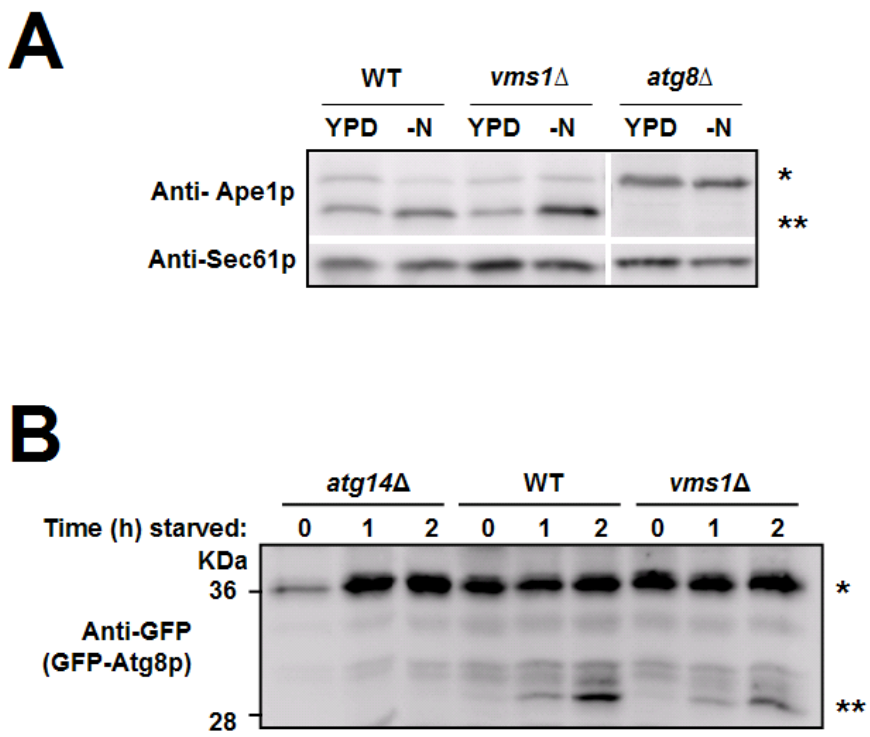

Figure 18. Strains lacking VMS1 do not exhibit a defect in the Cytoplasmic-to-Vacuole Transport (CVT) or autophagic pathways

A. Wild-type (WT), *vms1*Δ, and *atg8*Δ cells were grown in rich medium (YPD) and then shifted to nitrogen-poor medium (-N) for four hours. Total lysates were prepared by TCA precipitation, and equal amounts of lysate were resolved by SDS-PAGE for western blotting with a marker of CVT activity, anti-Ape1p. Autophagic induction increases the amount of processed Ape1p. Sec61p was analyzed as a loading control. **B.** Wild-type, *vms1*Δ, and *atg14*Δ were transformed with a reporter expressing GFP-Atg8p, which is processed during the early steps of autophagy. Cell were grown in rich media and then shifted to nitrogen-poor media for the indicated times. Total protein was prepared by TCA precipitation, resolved by SDS-PAGE, and the western blotted with anti-GFP. Induction of autophagy by nitrogen starvation results in the processing of the GFP-Atg8p. In both experiments, the * denotes the unprocessed formed and the ** denotes the processed form.

2.2.5 *VMS1* genetically interacts with members of the UBX and UFD gene families during ERAD

Cdc48p is a multifunctional protein that physically interacts with a large number of cofactors. It is unlikely that all of these cofactors are bound simultaneously to Cdc48p (SCHUBERTH and BUCHBERGER 2008). Indeed, evidence indicates competition between distinct cofactors (RUMPF and JENTSCH 2006). However, the many complex genetic interactions between Cdc48p partners have not been fully explored.

Based on the data presented above, I hypothesized that Vms1p might act in parallel and/or complementary with established Cdc48p partners during ERAD and in the presence of specific stress-inducing agents. Therefore, Lauren Tomsic (undergraduate, University of Pittsburgh) and I performed genetic crosses between *vms1*Δ yeast and strains lacking the genes encoding select Cdc48p cofactors (**Table 5**). I focused on UBX-domain containing proteins since yeast lacking the genes encoding some members of the UBX (*UBX1* and *UBX4*) family share phenotypes with *vms1*Δ (e.g., cycloheximide and rapamycin sensitivity) and because most of the UBX and UFD proteins have not been examined for their roles during ERAD. Therefore, the resulting tetratype progeny were first screened for growth on tunicamycin and cadmium-containing media, which respectively induce ER and heavy metal stress. Under each condition, an exaggerated requirement for the protein quality control machinery is evident. In these assays, yeast deleted for *IRE1*, which is required to induce the unfolded protein response (COX *et al.* 1993), were used as a positive control for sensitivity on tunicamycin, and yeast deleted for

RPN4, which is required for the induction of genes encoding proteasome subunits (XIE and VARSHAVSKY 2001), were used as a positive control for sensitivity on cadmium. Consistent with previous data, I observed that yeast deleted for *UBX1* were sensitive to tunicamycin (PARSONS *et al.* 2006), but I also noted that deletion of *VMS1* exacerbated the growth defect (see **Table 5**; growth defects are denoted by a "+", and a heightened defect is denoted by a "++"; also see **Figure 19A** for select examples of synergistic growth defects). This result suggests that Ubx1p, which is the yeast homolog of the p97 partner, p47, may contribute to ER homeostasis (see below). In addition, I discovered that *VMS1* interacted genetically with other genes encoding Cdc48p cofactors, including *UBX2*, *UBX3*, *UBX4*, and *UFD3*, when growth was assessed in the presence of cadmium (**Table 5, Figure 19**). These data suggest that Vms1p functions in parallel with several Cdc48p-associated proteins and helps mitigate the toxic effects of oxidative stress.

Because loss of *VMS1* led to a substrate-specific ERAD defect (see above), I reasoned that the simultaneous deletion of *VMS1* and other Cdc48p partners would result in synthetic effects on ERAD. To date, the coordinated action of Cdc48p partners during ERAD has not been examined. Therefore, the degradation of CFTR, as a representative misfolded membrane protein was examined, and the turnover of CPY*, a model misfolded soluble ERAD substrate, was assessed in each of the tetratype progeny. The most striking example of a synergistic ERAD defect was observed when *VMS1* and *UFD2* were simultaneously deleted. Specifically, I found that CFTR was significantly stabilized when *UFD2* was disrupted in *vms1*Δ cells (**Figure 20A**, open triangles). This strong effect is comparable to the CFTR degradation defect observed when Cdc48p function is disabled or when the Hrd1p and Doa10p ubiquitin ligases are both absent (GNANN *et al.* 2004). Furthermore, I found that *ufd2*Δ yeast exhibit a modest delay during the

CFTR degradation time course (**Figure 20A**, compare closed triangles and closed squares), which is reminiscent of the *ufd2*Δ defect when Ste6p* degradation was assessed (NAKATSUKASA *et al.* 2008). Finally, I discovered that *vms1*Δ*ufd2*Δ yeast proficiently degraded CPY* and robust growth was noted on stress-inducing media. One explanation for these data is that the ERAD defect in this mutant strain is confined to ERAD-C substrates. A summary of the degradation assays for the ERAD substrates Ste6p* and CPY*, and the N-end rule substrate and Ub-Pro β-galactosidase in these strains is provided in **Table 6**.

That Vms1p contributes to the ERAD pathway in a substrate-specific manner was also evident in *vms1*Δ*ubx4*Δ yeast. Although CPY* degradation proceeded maximally when *VMS1* and *UBX4* were individually deleted, the proteolysis of CPY* was slowed in the double mutant (**Figure 20B**). In other cases, I observed that ERAD defects were notable in mutants lacking a single Cdc48p cofactor, but the absence of *VMS1* had no further effect on ERAD efficiency. For example, the degradation of CPY* is significantly attenuated in *ubx2*Δ yeast (NEUBER *et al.* 2005), but the magnitude of the defect was not exacerbated in *vms1*Δ*ubx2*Δ yeast (**Figure 20C, Table 6**). This phenomenon was also apparent when the degradation of CPY* was examined in *ubx1*Δ and *ubx1*Δ*vms1*Δ yeast (**Figure 20D, Table 6**): An ERAD defect in *ubx1*Δ yeast has, to our knowledge, not previously been reported, and the effect on the degradation of an ERAD-L substrate in the *ubx1*Δ strain is consistent with the tunicamycin sensitive growth phenotype observed in this strain (**Table 5 and Figure 19**).

A variety of other *vms1*Δ combined mutants were also examined. In brief, I confirmed first that the deletion of *UFD2* slows the degradation of Ste6p* (NAKATSUKASA *et al.* 2008) and

I found that the loss of *VMS1* in the strain had no further effect on degradation. Second, I discovered the loss of both *UBX1* and *VMS1* slowed the degradation of Ste6p* (**Table 6**). Finally, as anticipated, loss of *UBX1*, *UBX2*, or *UFD2* slowed degradation of Ub-Pro β-galactosidase and that the deletion of *VMS1* in these backgrounds was without an added effect on degradation. I observed no effect of *VMS1* deletion on the degradation of the Deg1-LacZ substrate (**Table 6**).

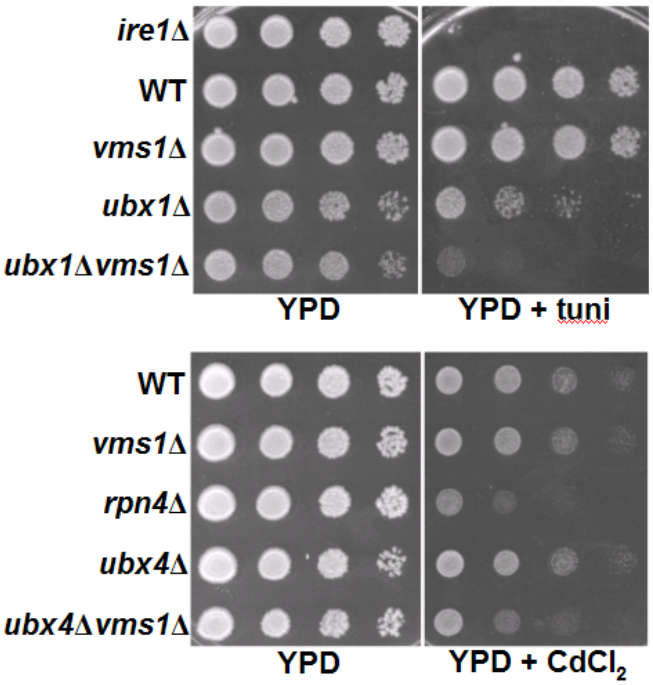

Figure 19. VMS1 genetically interacts with genes encoding several Cdc48p partners

Yeast cells with the indicated genotypes were grown to log-phase and harvested. The cells were then serially diluted and spot-plated on rich media (YPD) or rich media containing either tunicamycin (tuni) or cadmium ($CdCl_2$). The plates were incubated at 30°C for 2-6 d. The images are representative of several independent experiments.

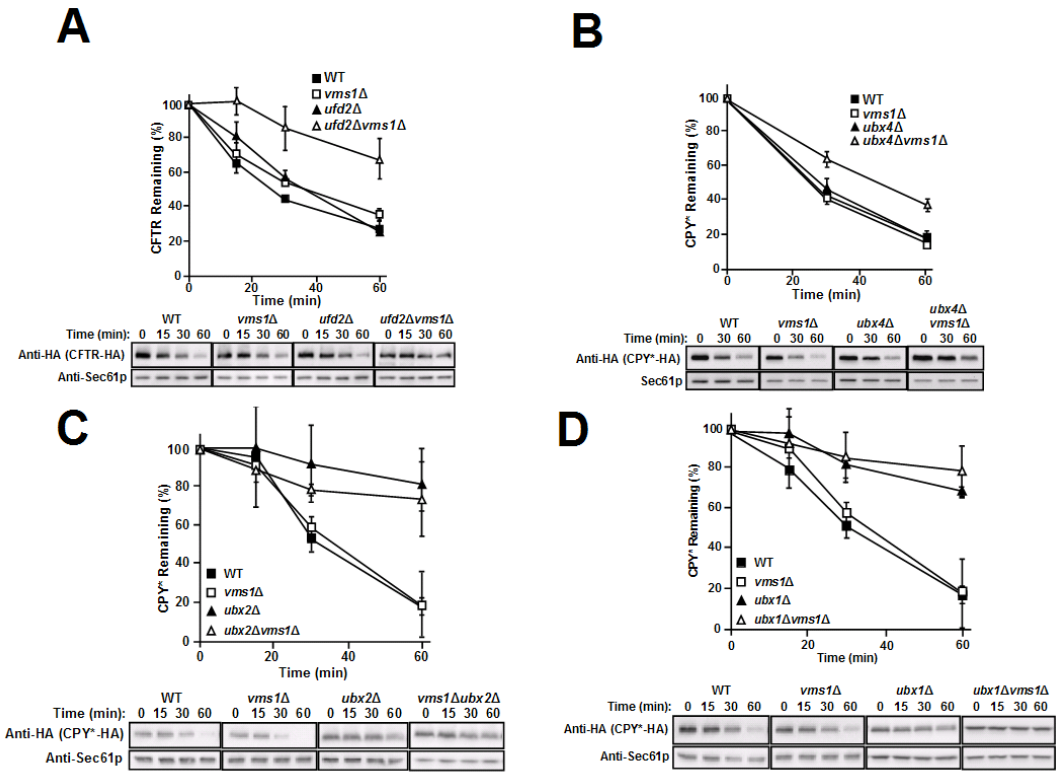

Figure 20. ERAD defects are exacerbated in yeast lacking VMS1 and UFD2 or UBX4 but not UBX1 or UBX2

A. The stability of CFTR was examined by cycloheximide chase analysis as described for Figure 16. Anti-HA antibody was used to detect each epitope-tagged ERAD substrate and Sec61p served as a loading control. **B-D.** The ERAD of CPY* was assessed in the indicated strains. Anti-HA was used to detect the substrate and Sec61p was used as a loading control. For all graphs, wild type cells are represented by black squares and *vms1*Δ yeast is represented by white squares. Black triangles represent *ufd2*Δ in the graph seen in **A.**, *ubx4*Δ in **B.**, *ubx2*Δ in **C.**, and *ubx1*Δ in **D.** The white triangles represent *ufd2*Δ*vms1*Δ in the graph seen in **A.**, *ubx4*Δ*vms1*Δ in **B.**, *ubx2*Δ*vms1*Δ in **C.**, and *ubx1*Δ*vms1*Δ in **D.** The panels at the bottom of each graph are representative western blots. Data represent the means of at least three independent experiments, ±SD.

Table 5. A summary of genetic interactions observed when double deletions between VMS1 and genes-encoding select Cdc48p cofactors were tested on chemical stressors

The "+" indicates sensitivity, "++" indicates additive sensitivity and "-" indicates no sensitivity.

	Tunicamycin		Cadmium	
Strain	**Single**	***+vms1Δ***	**Single**	***+vms1Δ***
ubx1Δ	+	++	+	+
ubx2Δ	-	-	-	+
ubx3Δ	-	-	-	+
ubx4Δ	-	-	-	+
ubx5Δ	-	-	-	-
ubx6Δ	-	-	-	-
ubx7Δ	-	-	-	-
ufd2Δ	-	-	-	-
ufd3Δ	-	-	-	+

Table 6. A summary of protein degradation assays for the indicated substrates

The strains either lacked *VMS1*-only or lacked both *VMS1* and a gene encoding a select Cdc48p cofactor. The "+" indicates a protein degradation defect and "-" indicates no effect.

	Ste6p*		CPY*		Ub-pro-beta-gal		Deg1-LacZ	
Strain	**Single**	**+*vms1*Δ**	**Single**	**+*vms1*Δ**	**Single**	**+*vms1*Δ**	**Single**	**+*vms1*Δ**
***ubx1*Δ**	-	+	+	+	+	+	-	-
***ubx2*Δ**	-	-	+	+	+	+	-	-
***ubx3*Δ**	-	-	-	-	-	-	-	-
***ubx4*Δ**	-	-	-	-	-	-	-	-
***ubx5*Δ**	-	-	-	+	-	-	-	-
***ubx6*Δ**	-	-	-	-	-	-	-	-
***ubx7*Δ**	-	-	-	-	-	-	-	-
***ufd2*Δ**	+	+	-	-	+	+	-	-

2.2.6 Substrate ubiquitination is proficient in yeast deleted for *VMS1*

The results presented above implicate Vms1p as a contributing factor during the ERAD of specific substrates, and highlight the complex functional interplay amongst Cdc48p-associated factors. One mechanism by which loss of Vms1p might inhibit ERAD is by impeding substrate ubiquitination. However, because Cdc48p acts after ERAD substrates have been ubiquitinated, I instead predicted that the loss of Vms1p would have no effect on substrate ubiquitination, nor would the loss of *VMS1* lead to synergistic effects on ubiquitination in mutant strains with known defects in the ubiquitin pathway.

To test this hypothesis, I assessed the extent of CFTR ubiquitination in the *ufd2*Δ*vms1*Δ strain due to the significant stabilization of this substrate in the double mutant (**Figure 20A**). I also wished to investigate whether the extent of CFTR ubiquitination decreased in *ufd2*Δ yeast because Ufd2p is required for ubiquitin chain extension, and the loss of *UFD2* results in reduced Ste6p* ubiquitination (NAKATSUKASA *et al.* 2008). To this end, CFTR was immunoprecipitated from wild type cells and from *vms1*Δ, *ufd2*Δ, and *ufd2*Δ*vms1*Δ yeast (**Figure 21A**). As a positive control for this experiment, the amount of ubiquitinated CFTR in *doa10*Δ*hrd1*Δ yeast was also measured. As anticipated, I first noted that CFTR ubiquitination decreased in the *doa10*Δ*hrd1*strain compared to wild type cells (compare lanes 1 and 3),Δ and that a signal corresponding to ubiquitinated CFTR was absent when immunoprecipitations in the absence of anti-HA antibody were performed ("Mock", lane 2). In addition, I noted that the amount of polyubiquitinated CFTR decreased by ~30% and there appeared to be a shift to lower molecular

weight ubiquitinated species when CFTR was examined in *ufd2*Δ-derived lysates. As predicted, the loss of *VMS1* did not decrease the extent of CFTR ubiquitination, consistent with Vms1p acting in the ERAD pathway after substrate ubiquitination. In fact, the loss of *VMS1* led to a small but reproducible increase in the amount of ubiquitinated CFTR, in either the presence (compare lanes 3 and 4) or absence (compare lanes 5 and 6) of Ufd2p. Similar results were obtained when the ubiquitination of Ste6p* was monitored in these strains and in an *in vitro* ubiquitination assay (NAKATSUKASA *et al.* 2008). Together, these data are consistent with the notion that Vms1p acts in the ERAD pathway after substrate ubiquitination.

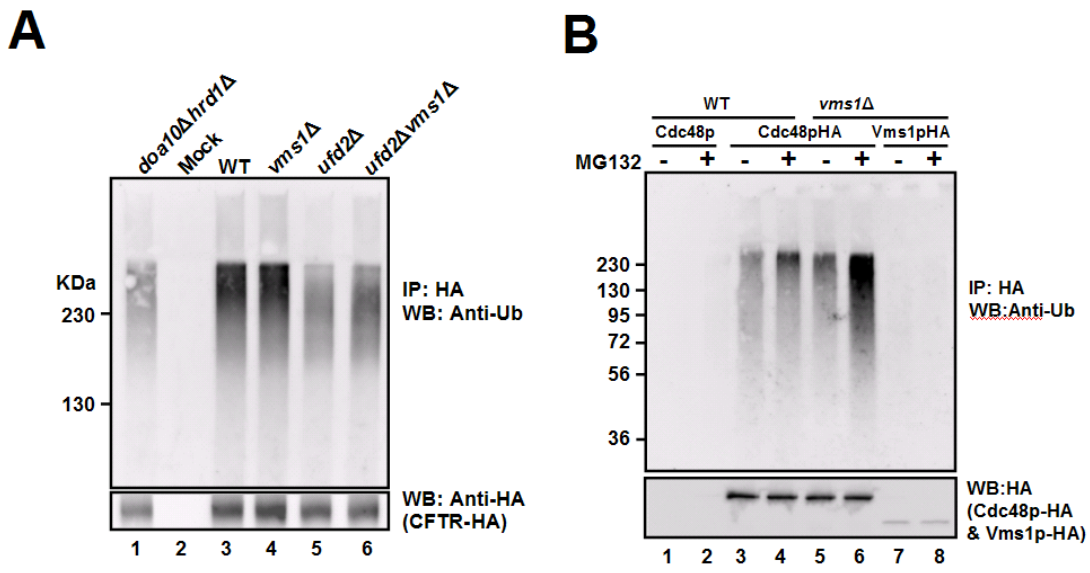

Figure 21. Increased levels of ubiquitinated proteins are associated with the Cdc48p complex in yeast lacking Vms1p

A. The indicated yeast strains expressing CFTR-HA were grown to log-phase, collected and processed for immunoprecipitation. Immunoprecipitated material was resolved by SDS-PAGE and subjected to anti-ubiquitin (top) and anti-HA (CFTR, bottom) western blotting. Polyubiquitinated CFTR resolves by SDS-PAGE as a smear ≥140 kDa, which is the approximate molecular mass of CFTR. **B.** Wild type ("WT") and *vms1*Δ cells in which the *PDR5* locus was also disrupted were transformed with either an untagged or HA-tagged version of Cdc48p. The *vms1*Δ strain was also transformed an HA-tagged version of Vms1p. Each indicated cell type was treated with MG132 (100μM) or an equal volume of DMSO for 1 h. ER fractions were isolated and the Cdc48p or Vms1p complexes were immunoprecipitated with anti-HA agarose after Triton X-100-solubilization. The isolated proteins were resolved by SDS-PAGE and processed for western blot analysis. The top panel depicts the results of the western blot with anti-ubiquitin antibody and the bottom panel depicts the results of the western blot with anti-HA antibody.

2.2.7 Polyubiquitinated species associated with Cdc48p increase in *vms1*Δ yeast

Based on the data presented in **Figure 21A**, and because Vms1p associates with the Cdc48p complex (**Figure 14B**), I next asked whether Vms1p regulates the ability of the Cdc48p complex to bind ubiquitinated substrates or the ability of the complex to release substrates. If Vms1p is required for the association of ubiquitinated substrates with the Cdc48p complex, then decreased amounts of these substrates should be associated with the Cdc48p complex in the *vms1*Δ mutant. In contrast, if Vms1p aids in a post-ubiquitination step, then increased levels of ubiquitinated proteins should associate with the Cdc48p complex in *vms1*Δ yeast.

To differentiate between these models I immunoprecipitated Cdc48p under native conditions from ER-enriched membranes. I then performed an anti-ubiquitin immunoblot to detect Cdc48p-associated ubiquitinated species. This protocol was conducted in a wild type and *vms1*Δ strain. In addition, to bias the analysis toward the spectrum of proteasome-targeted, Cdc48p substrates, the wild type and *vms1*Δ strains also lacked the gene encoding the multidrug resistance pump, *PDR5*, which sensitizes yeast to proteasome inhibitors (FLEMING *et al.* 2002). In a control experiment, a signal corresponding to ubiquitinated proteins was absent when an anti-HA immunoprecipitate from lysates containing an untagged version of Cdc48p was examined (**Figure 21B**, lanes 1 and 2). Also, as expected, the addition of MG132 resulted in increased association of ubiquitinated species with the Cdc48p complex (compare lanes 3 and 4). Most striking, I observed an increase in the amount of ubiquitinated-species in association with Cdc48p when solubilized ER-enriched membranes from *vms1*Δ yeast were examined (compare

lanes 3 and 5), an effect that was significantly enhanced when proteasome-mediated degradation was blocked with MG132 (compare lanes 4 and 6). When the co-immunoprecipitation was performed in the presence of SDS, no ubiquitin signal was detected, indicating that the ubiquitin profile was not attributable to ubiquitin-modified Cdc48p. Additionally, I immunoprecipitated a carboxy terminus HA-tagged version of Vms1p under these same conditions and found that Vms1p was not detectably associated with ubiquitinated proteins (lanes 7 and 8). I therefore conclude that Vms1p plays a role in regulating the population of proteasome-targeted, ubiquitinated species in association with Cdc48p, but itself does not detectably associate with ubiquitinated proteins.

2.3 DISCUSSION

A large and increasing number of Cdc48p-associated partners in yeast have been identified, and with few exceptions the activities of most of these partners is not clear. Notable partners with established activities include Otu1p, a DUB, Ufd2p, a ubiquitin extension enzyme (also referred to as an E4), and Ufd3p, which competes with Ufd2p and can consequently rescue ubiquitinated proteins from being destroyed (RICHLY *et al.* 2005; RUMPF and JENTSCH 2006). Ubx2p has been reported to help anchor the Cdc48p complex to the ER membrane, although the magnitude of Cdc48p release from the membrane in *ubx2*Δ yeast is variable (NEUBER *et al.* 2005; SCHUBERTH and BUCHBERGER 2005; WILSON *et al.* 2006). The Cdc48p complex has also been found in association with multi-protein membrane complexes that include Hrd1p and Doa10p (CARVALHO *et al.* 2006; DENIC *et al.* 2006; GAUSS *et al.* 2006). And, Ufd1p-Npl4p, which compete with Ubx1p/p47, aid in the binding of ubiquitinated substrates and designate Cdc48p function for

ERAD. In contrast, the functions of most other Cdc48p partners are ill-defined, and the list of Cdc48p/p97 partners is more complex in higher eukaryotes.

2.3.1 Vms1p is linked to ERAD and protein quality control

In this study, I report on the characterization of a new Cdc48p partner, the product of the *YDR049W* gene, which is now termed *VMS1* (HEO *et al.* 2010). Vms1p is a conserved, soluble, cytosolic protein that exhibits limited residence on membranes in non-stressed cells and is found in the Cdc48p-containing complex. Heo and colleagues (2010) also found that Vms1p is localized throughout the cytosol, and partially relocalizes, under mitochondrial stress conditions, to the mitochondrial membrane where it plays a role in protein degradation (HEO *et al.* 2010).

In my hands, the loss of *VMS1* leads to a modest ERAD defect that is significantly enhanced when either *UFD2* or *UBX4* are deleted. Based on the growth phenotypes of the *vms1*Δ allele in the context of mutations in the genes encoding diverse Cdc48p partners (i.e., *UBX1*, *UBX2*, *UBX3*, *UBX4*, and *UFD3*), I suggest that Vms1p participates in other quality control and stress-relief pathways in yeast, besides ERAD. Indeed, the recent discovery of Vms1p as a contributor to Cdc48p-associated mitochondrial protection under conditions of mitochondrial stress (HEO *et al.* 2010) is consistent with this hypothesis. Of note, an increasing body of data indicates that cellular quality control processes that operate under both stressed and unstressed conditions affect lifespan (BALCH *et al.* 2008).

2.3.2 *VMS1* genetically interacts with genes encoding Cdc48p cofactors

In accordance with this proposal, one UBX protein that was recently shown to contribute to Cdc48p function and to alter ERAD efficiency is Ubx4p. Alberts and colleagues (2009) recently reported that *ubx4*Δ yeast exhibit a defect in the degradation of both CPY* and Ste6p* which results in a build-up of ubiquitinated proteins on Cdc48p (ALBERTS *et al.* 2009). Thus, Ubx4p may cooperate with Vms1p as a release factor. Notably, I observed a genetic interaction between *VMS1* and *UBX4*, and a CPY* degradation defect was enhanced in the double mutant. However, I failed to observe an ERAD defect for CPY* or CFTR in the *ubx4*Δ mutant (**Figure 20B**), possibly because of the unique strain backgrounds used in this study and in the previously published report. The importance of strain background in analyzing the phenotypes in strains deleted for Cdc48p partners is highlighted by the fact *UBX1* is an essential gene in the W303 strain (CHENG and CHEN 2010), but the knock-out is viable in the BY background, as employed in this study. Additionally, the single deletion of *UBX2* is not sensitive to cadmium in the BY background, but is sensitive in another genetic background (SCHUBERTH *et al.* 2004).

In our hands, the strongest effect on ERAD was apparent in the *vms1*Δ*ufd2*Δ strain. The loss of *VMS1* did not exacerbate the decrease in ubiquitinated proteins or alter the profile of ubiquitinated proteins observed in the *ufd2*Δ strain. However, the synergistic effect may best be explained by positing that Ufd2p and Vms1p regulate unique steps in the ERAD pathway. For example, Ufd2p is required for ubiquitin chain elongation, and consistent with its role as a processivity factor the absence of this enzyme does not alter the extent of ubiquitination but only the rate at which polyubiquitination is achieved. ERAD is, therefore, initially delayed in the *ufd2*Δ strain but over time the amount of degradation catches-up with that observed in wild type

yeast (**Figure 20A**) (NAKATSUKASA *et al.* 2008). If Vms1p also catalyzes a relatively slow but non-essential step in the ERAD pathway, then the combined effect of deleting *VMS1* and *UFD2* may result in synergism. It is also formally possible that the loss of Vms1p reduces the cellular levels of Ufd2p, or that its absence prevents Ufd2p association with the Cdc48p complex. I have tested these hypotheses but observed wild type levels of Ufd2p in *vms1*Δ yeast and in the Cdc48p complex.

2.3.3 Vms1p affects a post-ubiquitination event

By developing new genetic and biochemical tools, I have also obtained data consistent with a role for Vms1p in a post-ubiquitination event. I find that: 1) there is a synthetic ERAD defect when both *VMS1* and *UFD2* are deleted and 2) that there is an increase in the amount of Cdc48p-associated ubiquitinated proteins in *vms1*Δ cells (**Figure 21B**). Other factors that may contribute to this critical step are Rad23p and Dsk2p, which contain both ubiquitin-like domains and ubiquitin-binding domains (ELSASSER *et al.* 2002; RAO and SASTRY 2002) and help link the Cdc48p complex and the proteasome. Future efforts may indicate whether Vms1p functions in tandem with Rad23p-Dsk2p to affect the release of ubiquitinated substrates from the Cdc48p complex. The loss of *VMS1* might lead to the absence of the bona fide release factor(s). In addition, future efforts may identify the spectrum of substrates that are enriched in complex with Cdc48p when the proteasome is disabled and Vms1p function is ablated. I suspect that ERAD substrates, as well as cytoplasmic substrates en route to the proteasome, will be present in association with the Cdc48p complex under these conditions.

In sum, I provide genetic evidence that a previously uncharacterized, Cdc48p partner performs an important house-keeping function during ER and cellular homeostasis. Consistent with our genetic data that suggest a role for *VMS1* in the ubiquitin-proteasome system, Costanzo and colleagues (2011) showed that *VMS1*, *UBX1*, *UBX4*, and *UFD2* negatively interact with genes that encode non-essential components of the 19S proteasome particle and *PRE9*, the only nonessential component of the 20S core (COSTANZO *et al.* 2011). These data suggested that Vms1p, Ubx1p, Ubx4p and Ufd2p may play a role in substrate recognition, transfer of substrate to the proteasome, and/or deubiquitination. When combined with our genetic and biochemical data, we favor the view that Vms1p is a regulator of an important but poorly defined step in the ubiquitin-proteasome pathway.

3.0 VMS1 PROTEIN IS INVOLVED IN REGULATING THE PROTEASOME

In Chapter 2, I showed that 1) loss of *VMS1* affected the ERAD of a model substrate but not its ubiquitination, 2) Vms1p physically interacts with Cdc48p in both membrane and cytosolic fractions, 3) *VMS1* genetically interacts with genes encoding Cdc48p cofactors, and that this led to additive ERAD defects and exaggerated sensitivity to stress agents, and 4) loss of *VMS1* led to an accumulation of ubiquitinated proteins bound to Cdc48p. These data suggest that Vms1p functions at a post-ubiquitination step in the ERAD pathway. In this chapter, I demonstrate that loss of *VMS1* increases the total cellular level of ubiquitinated proteins. Further, I provide evidence to indicate that this arises because the loss of *VMS1* also decreases the amount of ubiquitin-processing 26S proteasome, and increases the free, inactive 20S proteasome core particle. Both of these phenomena can be restored to near wild-type levels, but only with a version of Vms1p that can interact with Cdc48p.

3.1 EXPERIMENTAL PROCEDURES

3.1.1 Yeast strains, growth conditions, and plasmids

Yeast strains were from either the BY4741 or BY4742 genetic backgrounds and were grown at either room temperature (~24 ºC) or 30 ºC, as indicated. All strains used in this study are listed in

Table 7. Strain construction was identical to that described in Chapter 2. Plasmids used in this study are listed in **Table 8**. The construct expressing Vms1p-ΔVIM HA was a generous gift from Dr. Jared Rutter (University of Utah).

Table 7. List of strains used in this study.

All strains were in BY4742 background, unless noted otherwise.

Strain	Genotype	Reference
BY4742	*MATα, his3Δ1, leu2Δ0, ura3Δ0, lys2Δ0, MET15*	Open Biosystems
BY4741	*MATA, his3Δ1, leu2Δ0, ura3Δ0, LYS2, met15Δ0*	Open Biosystems
KFY100	*MATA, his4-619 leu2-3,112 ura3-52*	Dr. Kai Uwe Frohlich
KFY100-*vms1*Δ	*MATA, his4-619 leu2-3,112 ura3-52, vms1Δ::KanMX*	This study
YPH500	*MATα, his3Δ200, leu2Δ1, ura3-52, lys2-801, ade2-101, trp1Δ63*	ATCC
YPH500-*vms1*Δ	*MATα, his3Δ200, leu2Δ1, ura3-52, lys2-801, ade2-101, trp1Δ63, vms1Δ::KanMX*	This study
vms1Δ::HIS3	*MATα, his3Δ1, leu2Δ0, ura3Δ0, lys2Δ0, MET15, vms1Δ::HIS3*	This study
vms1Δ::KanMX	*MATα, his3Δ1, leu2Δ0, ura3Δ0, lys2Δ0, MET15, vms1Δ::KanMX*	Open Biosystems
vms1Δ::KanMX	*MATA, his3Δ1, leu2Δ0, ura3Δ0, LYS2, met15Δ0, vms1Δ::KanMX*	Open Biosystems
cdc48-3	*MATα, his3Δ1, leu2, ura3, lys2Δ0, MET15, cdc48-3*	This study
vms1Δcdc48-3	*MATα, his3Δ1, leu2, ura3, lys2Δ0, MET15, cdc48-3, vms1Δ::KanMX*	This study
*ubx2*Δ	*MATα, his3Δ1, leu2Δ0, ura3Δ0, lys2Δ0, MET15, ubx2Δ::KanMX*	Open Biosystems
ubx2Δvms1Δ	*MATα, his3Δ1, leu2Δ0, ura3Δ0, lys2Δ0, MET15, vms1Δ::HIS3, ubx2Δ::KanMX*	This study
*rad23*Δ*dsk2*Δ	*MATA, his3Δ1, leu2Δ0, ura3Δ0, LYS2, met15Δ0, rad23Δ::KanMX, dsk2Δ::KanMX*	Dr. Susan Michaelis
rad23Δdsk2Δvms1Δ	*MATA, his3Δ1, leu2Δ0, ura3Δ0, LYS2, met15Δ0, rad23Δ::KanMX, dsk2Δ::KanMX, vms1Δ::HIS3*	This study
*rpn4*Δ	*MATα, his3Δ1, leu2Δ0, ura3Δ0, lys2Δ0, MET15, rpn4Δ::KanMX*	Open Biosystems
rpn4Δvms1Δ	*MATα, his3Δ1, leu2Δ0, ura3Δ0, lys2Δ0, MET15, vms1Δ::HIS3, rpn4Δ::KanMX*	This study
hsm3Δ	*MATα, his3Δ1, leu2Δ0, ura3Δ0, lys2Δ0, MET15, hsm3Δ::KanMX*	Open Biosystems
hsm3Δvms1Δ	*MATα, his3Δ1, leu2Δ0, ura3Δ0, lys2Δ0, MET15, vms1Δ::HIS3, hsm3Δ::KanMX*	This study
ump1Δ	*MATα, his3Δ1, leu2Δ0, ura3Δ0, lys2Δ0, MET15, ump1Δ::KanMX*	Open Biosystems
ump1Δvms1Δ	*MATα, his3Δ1, leu2Δ0, ura3Δ0, lys2Δ0, MET15, vms1Δ::HIS3, ump1Δ::KanMX*	This study
rpn10Δ	*MATα, his3Δ1, leu2Δ0, ura3Δ0, lys2Δ0, MET15, rpn10Δ::KanMX*	Open Biosystems
rpn10Δvms1Δ	*MATα, his3Δ1, leu2Δ0, ura3Δ0, lys2Δ0, MET15, vms1Δ::HIS3, rpn10Δ::KanMX*	This study
rpn13Δ	*MATα, his3Δ1, leu2Δ0, ura3Δ0, lys2Δ0, MET15, rpn13Δ::KanMX*	Open Biosystems
rpn13Δvms1Δ	*MATα, his3Δ1, leu2Δ0, ura3Δ0, lys2Δ0, MET15, vms1Δ::HIS3, rpn13Δ::KanMX*	This study
rpn14Δ	*MATα, his3Δ1, leu2Δ0, ura3Δ0, lys2Δ0, MET15, rpn14Δ::KanMX*	Open Biosystems
rpn14Δvms1Δ	*MATα, his3Δ1, leu2Δ0, ura3Δ0, lys2Δ0, MET15, vms1Δ::HIS3, rpn14Δ::KanMX*	This study
otu1Δ	*MATα, his3Δ1, leu2Δ0, ura3Δ0, lys2Δ0, MET15, otu1Δ::KanMX*	Open Biosystems
otu1Δvms1Δ	*MATα, his3Δ1, leu2Δ0, ura3Δ0, lys2Δ0, MET15, vms1Δ::HIS3, otu1Δ::KanMX*	This study
cdc48Δ	*MATα, his3Δ1, leu2Δ0, ura3Δ0, lys2Δ0, MET15, cdc48Δ::KanMX, pRS315-CDC48MYC*	This study
cdc48Δvms1Δ	*MATα, his3Δ1, leu2Δ0, ura3Δ0, lys2Δ0, MET15, vms1Δ::HIS3, cdc48Δ::KanMX, pRS315-CDC48MYC*	This study

Table 8. Plasmids used in the study.

Unless referenced, all plasmids were constructed by PCR amplification and cloning as detailed in the Materials and Methods section of Chapter 2.

Plasmid name	Description	Reference
pRS316-*VMS1*	Endogenous promoter, c-terminal 1xHA tagged *VMS1*, CEN	This study
pRS316-*VMS1HA*	Endogenous promoter, c-terminal 1xHA tagged *VMS1*, CEN	This study
pRS416-*VMS1*-Δ*VIM-HA*	Endogenous promoter, c-terminal 3xHA tagged *VMS1*-Δ*VIM*, CEN	Dr. Jared Rutter

3.1.2 Measurements of total cellular ubiquitin levels

The indicated yeast strains were grown overnight to log phase (OD_{600} = ~0.6-0.8). A total of 1ml was dispensed into 10mM sodium azide and harvested by centrifugation in a refrigerated tabletop centrifuge at 18000g for 2 min. The supernatant was aspirated and the pellets were snap-frozen in liquid nitrogen. Thawed cell pellets were precipitated with 10% trichloroacetic acid, resuspended in SDS-sample buffer (80mM Tris-HCl, pH 8.0, 8mM EDTA, 3.5% SDS, 15% glycerol, 0.08% Tris base, 0.01% bromophenol blue) containing 100µM DTT to a final concentration of 10 OD_{600}/ml and resolved by SDS-PAGE (10% or 12.5% polyacrylamide gels). Proteins were transferred onto a piece of nitrocellulose that was then sandwiched between two sheets of filter paper and placed in a boiling water bath for 30 min. Blots were probed with anti-ubiquitin and anti-GPD antibodies and visualized as described in section 3.2.7, below.

3.1.3 In gel proteasome assay

An in gel proteasome assay was performed as described, but with minor modification (ELSASSER *et al.* 2005). All steps were performed on ice or at 4 ºC unless indicated otherwise. First, yeast were grown overnight in liquid culture (100ml) to log-phase (OD_{600} = 0.6-0.8) and harvested by centrifugation at 1000g for 5 min in a room temperature clinical centrifuge. Cell pellets were used immediately to prepare lysates, or snap frozen in liquid nitrogen and stored at -80 ºC. In each case, cell pellets were thoroughly resuspended in buffer containing 50mM Tris-Cl, pH 7.4, 5mM $MgCl_2$, 5mM ATP and 1mM DTT and disrupted by glass bead lysis (6 x 1 min pulses with 1 min rests on ice) on a Vortex mixer. Unbroken cells were removed by centrifugation at 1000g

for 5 min, and the lysate as clarified by centrifugation in a refrigerated centrifuge at 18000g for 30 min. The protein concentration of the final lysate was measured by BioRad assay. The typical protein concentration was ~10mg/ml, and the prepared lysates were immediately used.

Native 3.5% polyacrylamide gels were prepared in 90mM Tris-base, pH 8.0, 90mM boric acid, 5mM $MgCl_2$, 0.5mM EDTA, 5mM ATP, and 1mM DTT. Ammonium sulfate and TEMED were used to polymerize the gel. The gels were prepared at room temperature but were allowed to polymerize at 4 ºC. The running buffer was the same as the gel buffer, but lacked the polyacrylamide. A total of 60µg of lysate was mixed with an appropriate volume of 5x sample buffer (250mM Tris-Cl, pH 7.4, 50% glycerol, 60ng/ml xylene cyanol) and gels were loaded and run at 110V at 4 ºC until the ferritin (~440KDa) marker was three-fourths of the way to the bottom of the gel. The gel was then carefully transferred to a clean dish containing room temperature developer solution (50mM Tris-Cl, pH 7.4, 5mM $MgCl_2$, 0.5mM EDTA, and 5mM ATP) and briefly incubated to bring the gel to room temperature. This solution was then carefully decanted and fresh developer solution containing 100µM of the proteasome substrate Suc-LLVY-AMC (Enzo) was added and the gel was incubated with gentle rocking for 30 min at 37 ºC. Proteasome activity was visualized using a Kodak Image Station 440CF (Kodak). To visualize the activity of the 20S core particle, the gel was placed back into the developer solution, SDS was added to a final concentration of 0.02%, and the gel was incubated with gentle rocking at 37 ºC for 10-15 min. The activity was visualized as above. For western blot analysis, the native gels were preincubated with transfer buffer (0.025M Tris, 0.192M glycine pH 8.3, 0.1% SDS, and 20% methanol) for 10-15 min and transferred overnight onto nitrocellulose. Gels were probed with the indicated antibodies and visualized as described in section 3.2.7.

3.1.4 Real-time proteasome activity assay

Cell growth conditions and lysate preparation were identical to that described in section 3.2.3. To measure proteasome activity in solution, 60μg of lysate/ml was brought to a final volume of 2ml with a buffer containing 50mM Tris-Cl, pH 7.4, 5mM $MgCl_2$, 5mM ATP, 1mM DTT, and 10% glycerol. At this point, additives such as MG132 and SDS (0.02%) were added as indicated, to inhibit the proteasome or visualize the contribution of the 20S core particle, respectively. These lysates were preincubated at 30 ºC for 30 min. The fluorogenic proteasome substrate, Suc-LLVY-AMC was next added to a final concentration of 100μM and fluorescence (excitation 380nm, emission 460nm, bandpass = 4) was manually read using an Aminco-Bowman Series 2 Luminescence Spectrometer over the course of 2 h. The reaction was kept at 30 ºC for the duration of the experiment. Data were plotted and analyzed in Microsoft Excel 2003.

3.1.5 Glycerol gradient fractionation

Cell growth conditions and lysate preparation was identical to those described in section 3.2.3 and 3.2.4. To fractionate proteasomes, a 10-30% linear glycerol gradient was prepared in 50mM Tris-Cl, pH 7.5, 5mM $MgCl_2$, and 5mM ATP using a Gradient Master (BioComp Instruments) according to the manufacturer's instruction. The gradients were used either immediately, or stored overnight at 4 ºC before use. A total of 10mg of cell lysate was layered on top of the gradient and centrifuged at 83,000g for 24 h. Fractions (1ml) were collected from the top, and were TCA precipitated and resolved by SDS-PAGE as described above. Western blotting was performed using the indicated antibodies as described in 3.2.7, below.

3.1.6 Immunoprecipitation and Stable Isotopic Labeling by Amino acids in Cell culture (SILAC) analysis

Immunoprecipitation of Cdc48p-Myc was performed as described in Chapter 2, section 2.1.5. Briefly, transformed cells were grown in selective media to log-phase, harvested by low-speed centrifugation, resuspended in Buffer 88 (20mM HEPES pH 6.8, 150mM KOAc, 250mM sorbitol, 5mM MgOAc) supplemented with 1mM PMSF, 1µg/ml leupeptin, 0.5µg/ml pepstatin A, and 10mM NEM. Cells were disrupted with glass beads by vigorous agitation on a Vortex mixer 10 times for 30 sec, followed by a 30 sec incubation on ice between each agitation. Unbroken cells were removed by centrifugation at 1,500g for 5 min at 4°C. Total lysate was separated into membrane and cytosol fractions by centrifugation at 150,000g for 20 min at 4ºC. The supernatant (cytosol) was collected and the protein concentration was estimated using the BioRad protein assay kit. The membrane fraction was washed one time with Buffer 88 and then resuspended in Buffer 88 such that the final A_{280} in 2% SDS was 40, which corresponds to a protein concentration of ~10mg/ml. Both fractions were stored at -80 ºC. To immunoprecipitate Cdc48p-Myc, 1mg of cytosol and resuspended membrane protein were treated as follows: The membrane fractions were solubilized on ice for 30 min in Buffer A (20mM HEPES, pH 7.4, 150mM NaCl, 1% Triton X-100). Then, an equal amount of Buffer B (20mM HEPES pH 7.4, 150mM NaCl) was added so that the final concentration of Triton X-100 was 0.5%. The cytosolic extract was treated on ice for 30 min by adding Triton X-100 to a final concentration of 0.5%. For each sample, insoluble material was removed by centrifugation at 16,000g for 10 min at 4°C and the volume was brought-up to 500µl with Buffer C (20mM HEPES, pH 7.4, 150mM NaCl, 0.5% Triton X-100) prior to immunoprecipitation with anti-HA- or anti-Myc-conjugated agarose (Santa Cruz). The immunoprecipitate was washed once with Buffer C, and three times

with Buffer D (20mM HEPES, pH 7.4, 300mM NaCl, 0.5% Triton X-100), and the bound proteins were released with SDS-PAGE sample buffer, as described above.

For the Stable Isotopic Labeling with Amino acids in Culture (SILAC) experiment, wild-type cells expressing Cdc48p-Myc from a low-copy plasmid were grown to log phase in standard minimal medium containing unlabeled L-Lysine-2HCl (Cambridge Isotope Labs) and *vms1*Δ cells expressing Cdc48p-Myc were grown in minimal medium containing L-Lysine-2HCl $^{13}C_6$,$^{15}N_2$ (Cambridge Isotope Labs). Cells were processed and the immunoprecipitations were carried out as described above. Immunoprecipitated proteins were eluted by incubating the beads four times with 100µl of 0.1M glycine, pH 2.2 for 10 min at room temperature. The combined eluate was methanol/chloroform (4:1) extracted and lyophilized prior to mass spectrometry. The mass spectrometry was performed by our collaborators, Drs. Woong Kim and Steven Gygi (Harvard Medical School).

3.1.7 Antibodies and western blot analysis

Antibodies used in this study included: Anti-HA (Roche, USA), anti-Myc (Santa Cruz, USA), anti-FLAG M2 (Sigma), anti-Ubiquitin (Santa Cruz, USA), anti-Hsm3p (a generous gift from Dr. Daniel Finley, Harvard Medical School), anti-Blm10p (Enzo), anti-Rpt5p (Enzo), anti-Rpn10p (a generous gift from Dr. Dorota Skowyra, St. Louis University), anti-Rpn3 (Abcam), anti-yeast alpha and beta 20S subunits (Enzo), and anti-GPD (Sigma). Bound antibodies were visualized with HRP-conjugated anti-mouse (Roche) or anti-rabbit (Roche) IgG. Western blot detection was performed as described in Chapter 2, section 2.1.7.

3.2 RESULTS

3.2.1 Loss of *VMS1* leads to the accumulation of cellular ubiquitinated proteins

In Chapter 2, I showed that loss of *VMS1* led to an increase in the amount of ubiquitinated species that was associated with an epitope-tagged version of Cdc48p (**Figure 21B**). In order to assess if the effect of Vms1p was specific for Cdc48p bound species, or represented a more global phenomenon, I compared the levels of ubiquitinated proteins found in total cellular extracts from a panel of strains possessing or lacking *VMS1* and that were mutated for other genes. Specifically, these strains represent a range of defects at various stages of the ERAD pathway: *ubx2*Δ shows reduced recruitment of the Cdc48p complex to the ER membrane, the *cdc48-3* mutant exhibits retrotranslocation defects, and *rad23*Δ*dsk2*Δ has defects in shuttling ubiquitinated substrates to the 26S proteasome (ELSASSER *et al.* 2002; JAROSCH *et al.* 2002; RAO and SASTRY 2002; SCHUBERTH and BUCHBERGER 2005). As seen in **Figure 22A**, I found that strains lacking *VMS1* consistently showed an increase in the amount of total cellular ubiquitinated protein regardless of genotype. This was evident regardless of strain background or mating type (**Figure 22B and C**). Select double mutants had pronounced levels of ubiquitin accumulation. For example, the *ubx2*Δ*vms1*Δ accumulated ubiquitinated proteins to a greater extent than other combinations tested. On the other hand, the *rad23*Δ*dsk2*Δ*vms1*Δ strain showed only a modest accumulation. Regardless, this result suggests two things. First, it suggests that Vms1p functions in a parallel pathway with Ubx2p, Cdc48p, and Rad23p/Dsk2p. Second, it suggests that Vms1p may function in a pathway separate from its involvement in ERAD.

Based on these findings, I decided to test whether the accumulation of polyubiquitinated proteins required Vms1p-Cdc48p interaction by using a well-characterized mutant version of Vms1p that is unable to physically interact with Cdc48p. In this experiment, strains lacking *VMS1* were supplemented with an empty vector and either a low-copy plasmid harboring a wild-type, HA-epitope tagged version of Vms1p or an HA-epitope tagged version lacking the VCP/p97 Interacting Motif (VIM) (BALLAR *et al.* 2006; HEO *et al.* 2010; STAPF *et al.* 2011). The *VMS1* deletion harboring an empty vector shows the expected increase in total ubiquitinated protein when compared to a wild-type strain, or to a *vms1*Δ strain harboring a wild-type copy of *VMS1* (**Figure 23B)**. However, when *vms1*Δ strains were supplied with a copy of Vms1p that cannot physically interact with Cdc48p (ΔVIM), the level of cellular ubiquitinated protein was similar to that seen in the *vms1*Δ strain harboring an empty vector. In addition, I examined whether protein expressed from these plasmids can also rescue the cycloheximide-sensitive phenotype of *vms1*Δ cells (PARSONS *et al.* 2006). I found that rescue also requires the VIM domain of *VMS1* (**Figure 23A**). It is noteworthy to mention that I consistently observed that the level of "VIM-less" Vms1p appears to be somewhat higher than that of the wild-type version (**Figure 23B**), so that the inability to rescue this phenotype does not arise from poor protein expression. These data suggest that Vms1p interaction with Cdc48p is required to off-set the accumulation of ubiquitinated proteins in the cell.

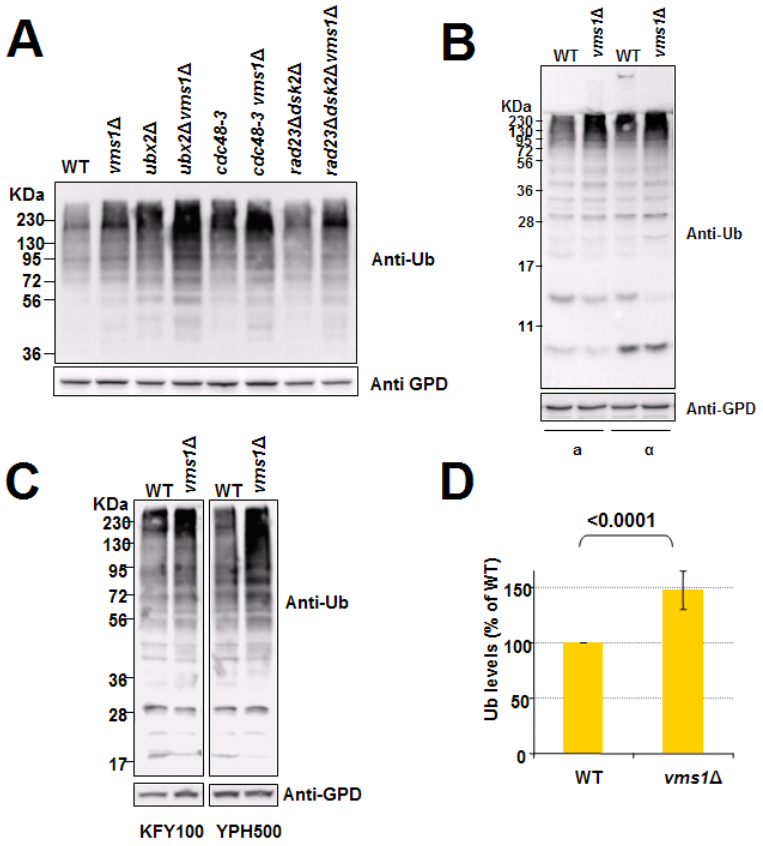

Figure 22. Loss of VMS1 leads to an accumulation of ubiquitinated proteins in the cell

A. Whole cell extracts from strains containing or lacking *VMS1* were examined for total ubiquitinated proteins by western blotting with anti-ubiquitin antibody. Strains examined include those defective for various steps in the ERAD pathway, such as Cdc48p localization (*ubx2*Δ), retrotranslocation (*cdc48-3*), and ubiquitinated substrate escort (*rad23*Δ*dsk*Δ). Anti-GPD was used as a loading control. **B.** Lysates from BY4741 ("a") and BY4742 ("α") were separated by SDS-PAGE and subjected to western blotting as described in part A. Ubiquitin levels in *vms1*Δ strains increased approximately 50%. **C.** Lysates from wild-type and *vms1*Δ strains from the KFY100 and YPH500 genetic backgrounds were resolved by SDS-PAGE and subject to western blotting with anti-ubiquitin and anti-GPD (loading control). **D.** Quantitation of polyubiquitin (>72KDa) signal from wild-type and *vms1*Δ strains. Sample size is 6.

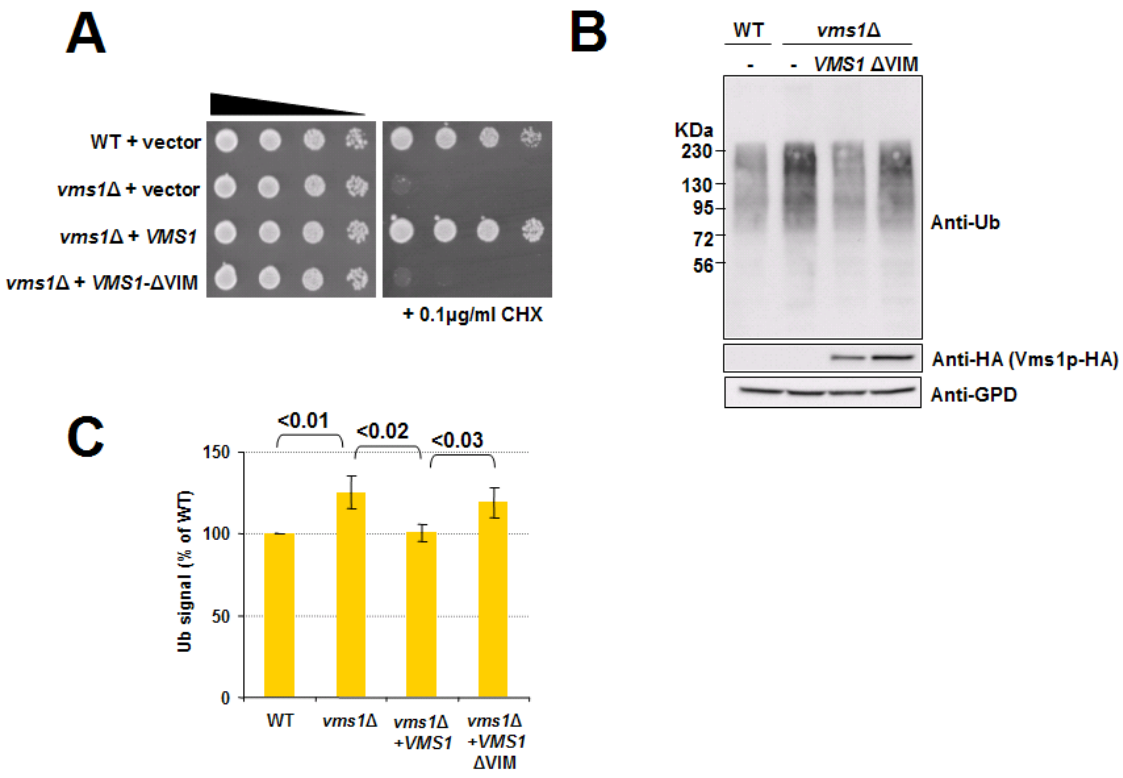

Figure 23. Vms1p regulation of ubiquitinated protein homeostasis requires interaction with Cdc48p

A. The function of the wild-type Vms1p-HA and Vms1p-ΔVIM-HA proteins was assessed by 10-fold serial dilution spot plating onto either YPD or YPD plus 0.1µg/ml cycloheximide. **B.** To assess whether Vms1p-Cdc48p interaction was required for the recovery of the ubiquitinated protein accumulation phenotype, whole cell extracts were prepared from strains harboring an empty vector, or a vector engineered for the expression of either wild-type Vms1p-HA or Vms1p-ΔVIM-HA (ΔVIM, a generous gift from Dr. Jared Rutter) and western blotted with anti-ubiquitin. Blots were also probed with anti-HA to detect the expression of the tagged forms of Vms1p and with anti-GPD as a loading control. **C.** Quantitation of ubiquitin signal (>72KDa) in B. Sample size is 4.

3.2.2 Loss of *VMS1* alters the distribution of proteasome subtypes

The data from Chapter 2 and section 3.3.1 of this chapter suggest that Vms1p functions at a late stage (i.e., post-ubiquitination event) in protein degradation. Therefore, I examined the architecture and activity of the proteasome from total cell lysates using a previously established in gel proteasome activity assay (ELSASSER *et al.* 2005; HOUGH *et al.* 1987). As seen in **Figure 24A**, lysates from *vms1*Δ cells showed a reproducible increase in the amount and activity of free 20S core particles (CP) and a corresponding reduction in the amount and activity of capped proteasome particles (RPCP, RP_2CP). The results of several experiments were quantified and these differences were found to be statistically significant (**Figure 24B**). To confirm these results, 20S CP activity was assessed in solution and over time using fluorometry and again there was a significant increase in the activity of the 20S CP (**Figure 24C**).

Since there is more free 20S core particle in the *vms1*Δ, it is a formal possibility that *vms1*Δ mutant cells upregulate the protein levels of proteasome components, including the alpha and beta subunits of the 20S core particle, which in turn leads to a decrease in the relative amount of 26S particle. To rule out this possibility, I performed western blotting with a panel of antibodies against different components of the proteasome. As observed in **Figure 25A**, wild-type and *vms1*Δ mutant cells have similar levels of all proteasome components tested. To further support these data, I compared the proteasome profile in *rpn4*Δ strains possessing or lacking *VMS1* by the in gel proteasome overlay assay. Rpn4p is a transcription factor that regulates the expression of proteasome subunits, and in *rpn4*Δ cells there is a reduction in the amount of

proteasome subunits (XIE and VARSHAVSKY 2001). I observed that *rpn4*Δ strains show the expected reduction in the amount of total proteasome, but when *rpn4*Δ strains were also deleted for *VMS1*, lysates prepared from this strain again showed an increase in the amount and activity of the free 20S CP (**Figure 25B and C**). I conclude that the gene product of *VMS1* plays a role in regulating the distribution of proteasome subtypes, but does not regulate the expression or translation of proteasome components.

So far, I have shown in this chapter that loss of *VMS1* leads to: 1) the accumulation of ubiquitinated proteins in total cell lysates and 2) a change in the distribution of proteasome subtypes. However, ubiquitin accumulation can be decreased back to approximate wild-type levels when the *vms1*Δ strain is supplied with a full-length copy of wild-type *VMS1*, but not with a version that fails to interact with Cdc48p. To examine whether the ubiquitin accumulation and proteasome distribution phenotypes correlated, I performed an in gel proteasome activity assay using lysates from *vms1*Δ strains that were supplemented with an empty vector or vectors for the expression of wild-type Vms1p-HA or Vms1p-HA lacking the VIM domain. As shown in **Figure 26A and B**, *vms1*Δ strains harboring an empty vector yielded the expected increase in the free 20S CP activity when compared to a wild-type strain. When *vms1*Δ strains were supplemented with a plasmid carrying wild-type Vms1p-HA, the amount of 20S CP activity decreased to near wild-type levels. However, *vms1*Δ strains expressing Vms1p-HA lacking the VIM domain did not show a significant decrease in 20S CP activity. These effects on the activities of the 20S CP were correlated to the levels of alpha and beta subunits by western blotting analysis.

Interestingly, a western blot against the HA-tag on Vms1p indicated that Vms1p-HA co-migrates with capped proteasomes (**Figure 26A, lower right**). In addition, the Vms1p-HA mutant lacking the VIM domain showed a reproducible decrease in the amount of HA-signal co-migrating with the capped proteasome. These results suggest that Vms1p is in a complex with the 26S proteasome and that the inability to interact with Cdc48p reduces the amount of associated Vms1p. Thus, Cdc48p may bridge Vms1p to the 26S proteasome.

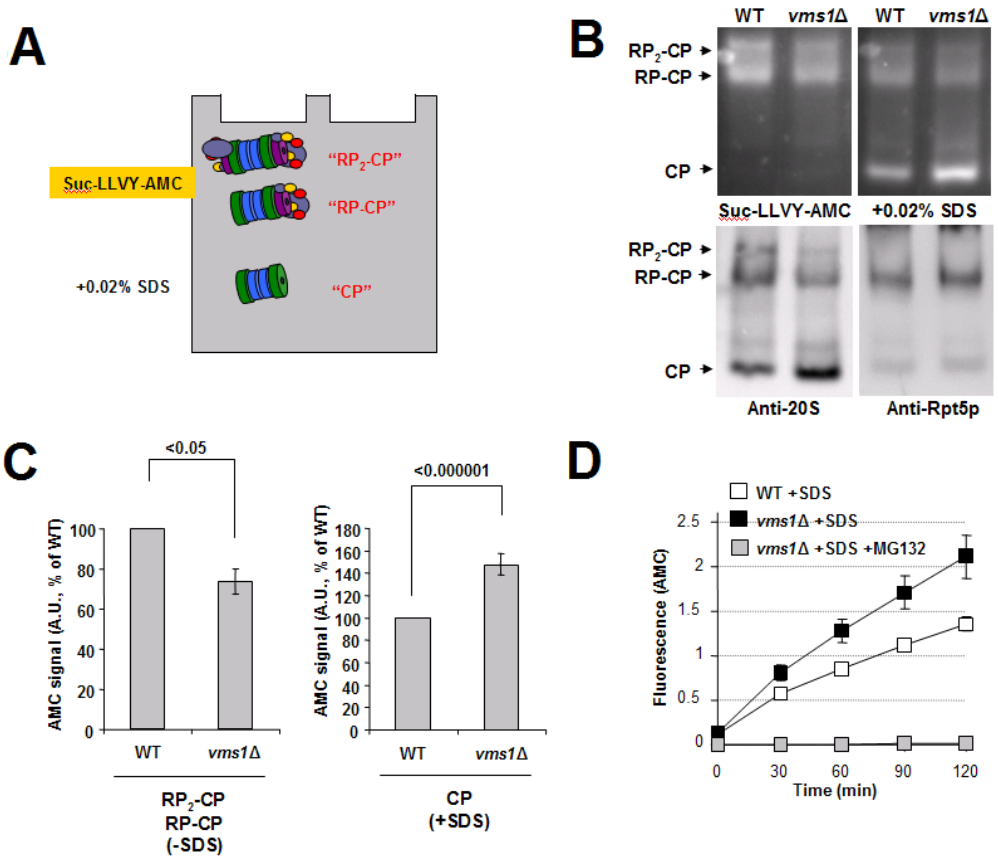

Figure 24. The vms1Δ strain shows increased levels of 20S core particles

A. Lysates from wild-type and *vms1*Δ cells (60µg) were resolved on a 3.5% native gel and the gels were incubated in a solution containing ATP and the fluorogenic chymotrypsin-like proteasome substrate, Suc-LLVY-AMC (100µM) to assess capped proteasomes. After imaging, the gels were incubated with the same solution, but with the addition of 0.02% SDS to visualize 20S core activity. **B.** Wild-type and *vms1*Δ cell extracts were resolved on a 3.5% native gel and proteasome activity was visualized as described in A. Western blotting with antibodies against yeast 20S core alpha and beta particles and the 19S cap subunit, Rpt5p (bottom two panels, B). **C.** The left graph represents capped proteasome signal while the graph on the right represent signal corresponding to the 20S core. The units are arbitrary and the error bars represent $\pm$ standard error ($n \geq 10$). Quantitation was performed using ImageJ v4.16e. The activity from the

wild-type strain was set as 100%. **D.** The proteasome activity from lysates prepared from wild-type or *vms1*Δ cells (60μg) were assessed in solution by fluorometry. Reactions were prepared in a buffer containing ATP and 100μM of the proteasome substrate Suc-LLVY-AMC. Where indicated, MG132 was added to a final concentration of 100μM. The error bars represent ± standard error from at three independent experiments.

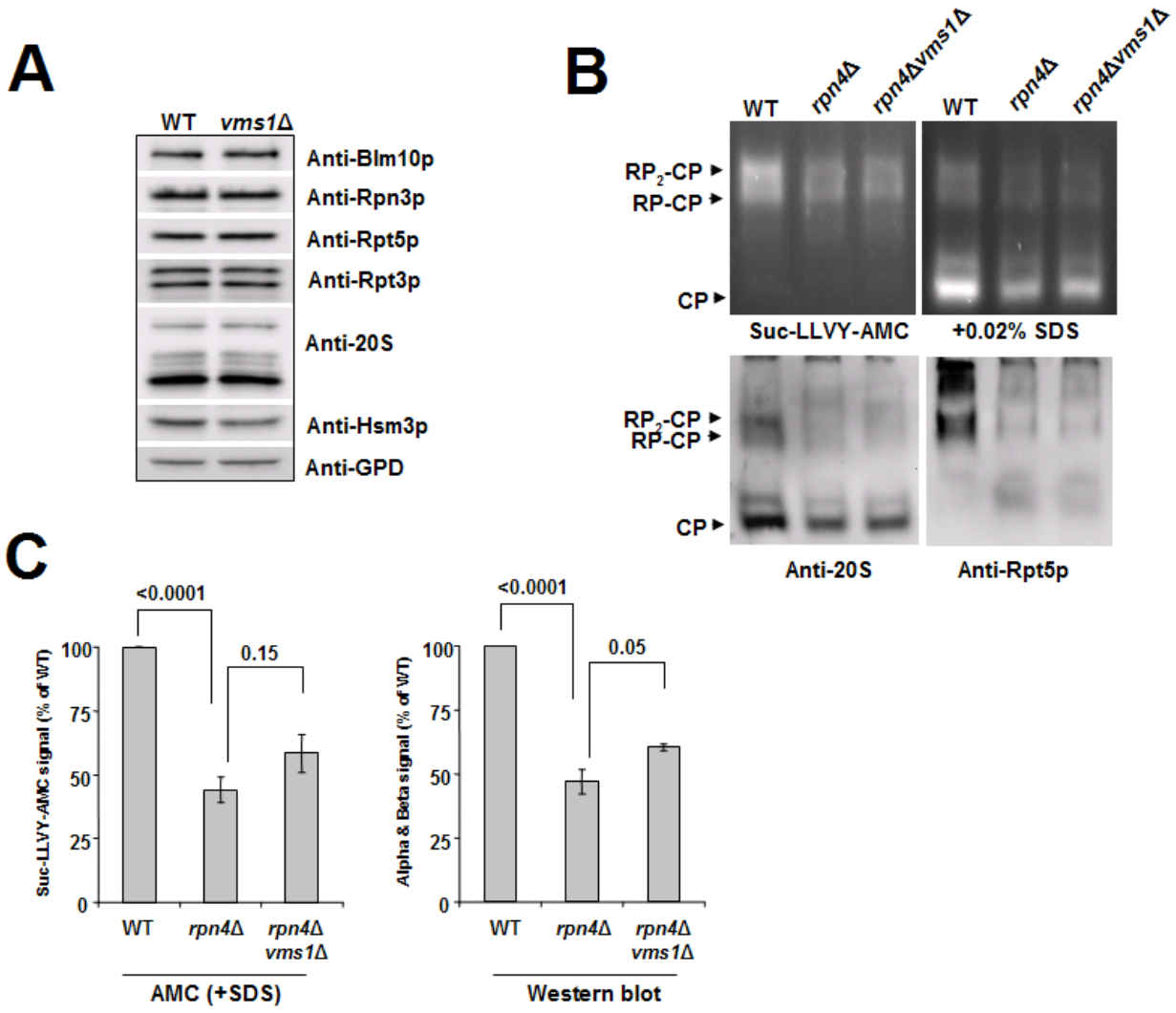

Figure 25. Maintenance of proteasome components are unaffected in vms1Δ strains

A. Equal amounts of whole cell extracts from wild-type and *vms1*Δ strains were resolved by SDS-PAGE. Western blot analysis was used to detect the levels of the proteasomal activator (Blm10p), 19S cap components (Rpn3p, Rpt5p, and Rpt3p), a proteasome chaperone (Hsm3p), and the 20S core particle (alpha and beta Subunits). Anti-GPD was used as a loading control. **B.** In gel proteasome activity assay was performed to assess the effect of *VMS1* deletion in strains lacking the proteasome transcription factor, Rpn4p. Wild-type, *rpn4*Δ, and *rpn4*Δ*vms1*Δ yeast lysates were resolved by native gel. The gel was incubated in a solution containing ATP and Suc-LLVY-AMC (100μM) to assess capped proteasome activity (upper left panel, B). Next, the

gel was incubated in the same solution except 0.02% SDS was added to assess 20S core activity (right upper panel, B). Western blot analysis was performed with anti-yeast 20S CP and anti-Rpt5p to assess the amount of 20S core and 19S cap, respectively. **C.** Quantitation of 20S CP activity (left) and anti-alpha and beta proteins corresponding to the 20S CP (right) from four independent experiments. The error bars indicate $\pm$ standard error. The difference between *rpn4*Δ and *rpn4*Δ*vms1*Δ in the in gel activity assays (corresponding to 20S core) was not statistically significant. The rpn4vms1 strain is being validated. Sample size is 4.

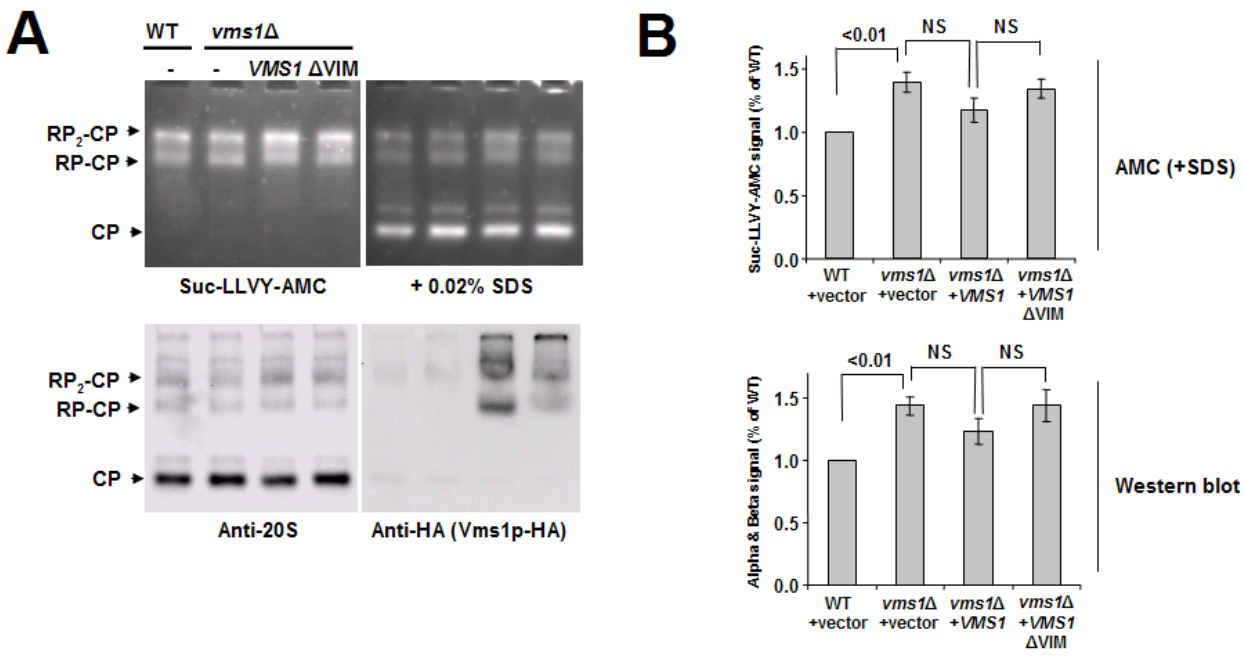

Figure 26. Proteasome architecture requires Vms1p-Cdc48p interaction

A. Proteasome activity in lysates (60μg) from wild-type or *vms1*Δ cells containing an empty vector, or a vector expressing either wild-type Vms1p-HA or Vms1p-ΔVIM-HA (ΔVIM) were examined by native gel and Suc-LLVY-AMC (100μM) substrate overlay assay. The activity of the capped proteasome (RP2CP, RPCP, left panel A) and 20S core (CP, right panel A) were both assessed. Western blotting for Vms1p-HA (anti-HA) and 20S CP (alpha and beta) was also performed. **B.** Quantitation of 20S activity (top) and anti-20S CP signal (bottom) from four independent experiments in the indicated strains. The error bars represent ± standard error of four independent experiments. Sample size is 4. "NS" means not significant.

3.2.3 *VMS1* function appears to be independent of proteasome assembly chaperones

To determine if Vms1p facilitates proteasome assembly or stability, I examined ubiquitinated protein levels and proteasome distribution phenotypes in a panel of double deletion mutants that lacked *VMS1* and genes known to be involved in proteasome assembly/stability. The genes tested were: *RPN10* – a ubiquitin receptor that is involved in connecting the base and lid of the 19S cap (GLICKMAN *et al.* 1998a), *RPN13* – a ubiquitin receptor and core component of the 19S particle (HUSNJAK *et al.* 2008), *RPN14* - a chaperone of the 19S cap (FUNAKOSHI *et al.* 2009; LE TALLEC *et al.* 2009; PARK *et al.* 2009; ROELOFS *et al.* 2009; SAEKI *et al.* 2009), *HSM3* – another chaperone of the 19S cap (FUNAKOSHI *et al.* 2009; LE TALLEC *et al.* 2009; PARK *et al.* 2009; ROELOFS *et al.* 2009; SAEKI *et al.* 2009), and *UMP1* – a chaperone of the 20S core (RAMOS *et al.* 1998). The analysis presented in **Figure 27A** revealed that loss of *VMS1* resulted in an additive increase in ubiquitinated protein levels in most of the genotypes tested. This result suggests that Vms1p functions in parallel to Rpn13p, Rpn14p, Hsm3p, and Ump1p. The exception to this finding, however, was the *rpn10*Δ and *rpn10*Δ*vms1*Δ strains, which both showed similar levels of ubiquitinated protein accumulation. Rpn10p is a ubiquitin receptor that also helps link the 19S base and lid (GLICKMAN *et al.* 1998a). This intriguing result suggests that these two gene products function in series. To further support this hypothesis, I examined the distribution of proteasome subtypes in these same mutants. As seen in **Figure 27B**, the accumulation of 20S CP was evident in all strains examined, as assessed with the fluorogenic substrate and by western blotting. Finally, I used glycerol gradient analysis to examine the distribution of proteasome components. Western blotting with antibodies against the 19S cap (Rpt5p), accessory proteins

(Blm10p), Cdc48p, 19S chaperone (Hsm3p) and the core components indicated that the sedimentation distribution was not significantly altered by the deletion of *VMS1* (**Figure 27C**). On occasion, I have observed that both 20S core particle subunits and Rpn10p distributed differently (**Figure 27D. see upward bracket**). These data collectively suggest that Vms1p functions in a parallel and possibly independent proteasome assembly/stability pathway, and that Rpn10p and Vms1p may function in series.

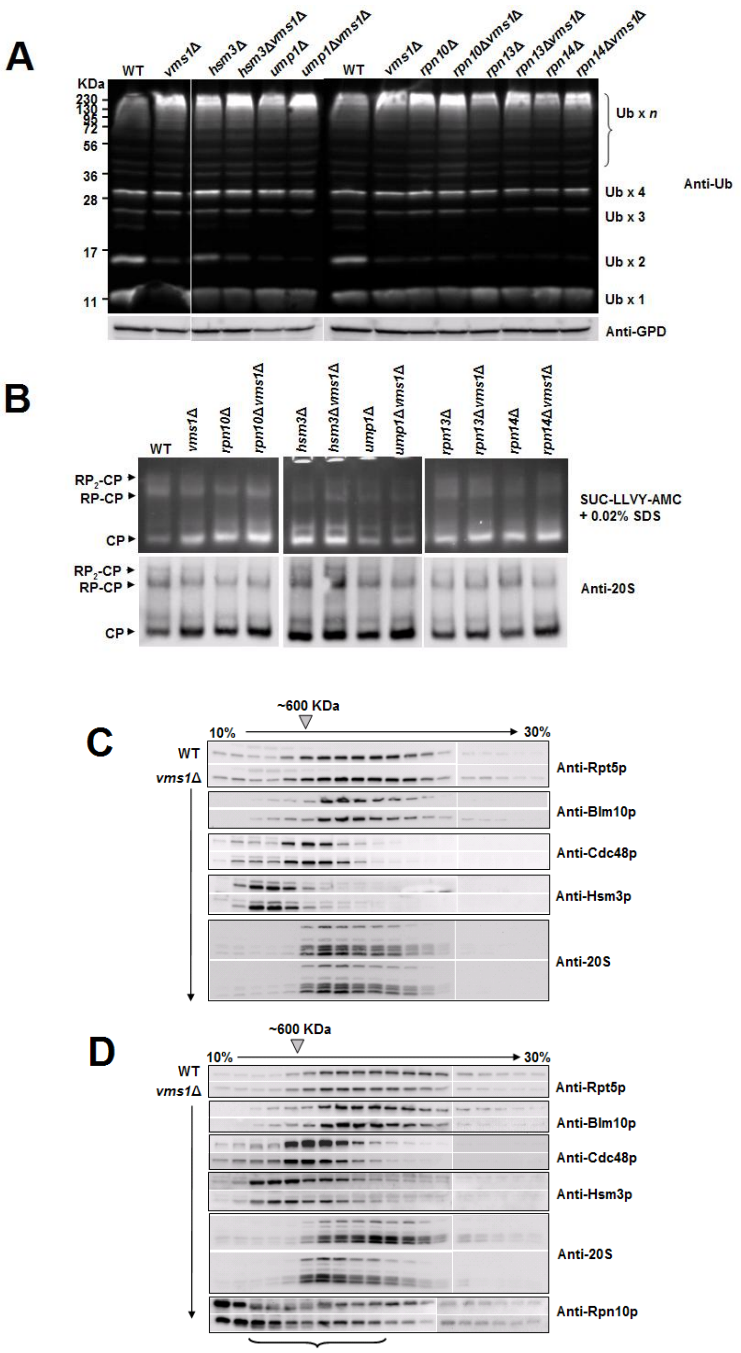

Figure 27. Loss of VMS1 does not appear to affect proteasome assembly

A. The effect of *VMS1* deletion on ubiquitinated cellular proteins was assessed in different strains representing a panel of defects in proteasome stability (*rpn10*Δ, *rpn13*Δ) and assembly (*hsm3*Δ, *ump1*Δ, *rpn14*Δ). Wild-type and *vms1*Δ strains were also assessed. Equal amounts of whole cells extracts were resolved by SDS-PAGE and western blotted with anti-

ubiquitin. Anti-GPD was used as a loading control. **B.** Proteasome activity from the strains used in (A) was assessed by native gel overlay assay with Suc-LLVY-AMC followed by the addition of 0.02% SDS to assess 20S core activity. The 20S core particle components were assessed by western blotting with an antibody against yeast 20S alpha and beta subunits. **C.** Whole cell extracts (5mg) from wild-type and *vms1*Δ strains were resolved on a glycerol gradient (10-30%). To examine the distribution of proteasome components, individual fractions were collected, precipitated and resolved by SDS-PAGE. Western blotting was performed with antibodies against the 19S cap (Rpt5p), the proteasome activator (Blm10p), Cdc48p, the proteasome chaperone (Hsm3p) and the 20S core (alpha and beta subunits). **D.** An independent example of the glycerol gradient analysis. The antibodies used in this experiment are Rpt5p (19S cap), Blm10p (proteasome activator), Cdc48p (ERAD-associated ATPase), Hsm3p (proteasome cap chaperone), alpha and beta subunits (20S core) and Rpn10p (ubiquitin receptor).

3.2.4 *VMS1* does not significantly affect the Cdc48p association with the proteasome

Based on the data presented in section 3.3.2, the Vms1p-ΔVIM mutant shows reduced co-migration with capped proteasomes, which suggests two intriguing possibilities. 1) Cdc48p is at the proteasome at normal levels and the Vms1p-ΔVIM mutant shows reduced binding or 2) the Vms1p-ΔVIM mutant shows a reduced association and Cdc48p interaction with capped proteasomes is also lower. To begin to differentiate between these two possibilities, I performed immunoprecipitation experiments with an epitope-tagged version of Cdc48p from strains containing or lacking *VMS1*. I examined Cdc48p-Myc precipitates from both crude membrane and cytosolic fractions. The immunoprecipitated proteins were identified by mass spectrometry in collaboration with the laboratory of Dr. Steven Gygi (Harvard Medical School), and with the help of Dr. Kim Woong (Harvard Medical School). Cdc48p immunoprecipitations from the cytosolic fraction yielded ~400 interactors while material from the membrane fraction yielded ~350 interactors (**Table 9**). Of these interactions, only 126 and 95 unique interactions were identified from the cytosol and membrane fractions, respectively. This indicates that the vast majority of interactors overlap. Additionally, I only observed 27 of the 79 (34.1%) known Cdc48p physical interactions annotated on the *Saccharomyces* Genome Database (www.yeastgenome.org, Biogrid) (STARK *et al.* 2006). Of the 79 known Cdc48p interactors, 54 were identified by mass spectrometry. Thus, I was able to identify 50% of the known Cdc48p interactions that were detectable by mass spectrometry.

When I focused on specific UPS/ERAD relevant interactions and their peptide (spectral) counts, I noted that Cdc48p-Myc interactions with the 20S core appeared to be reduced in the cytosol of *vms1*Δ yeast (**Table 10**). In contrast, interactions with the 19S cap were largely similar. To test this possibility in a quantitative manner, I performed a Stable Isotope Lableing by Amino acids in Cell culture (SILAC) experiment, which is a form of quantitative mass spectrometry. In the SILAC experiment, wild-type cells were grown under normal conditions and *vms1*Δ yeast were grown in the presence of heavy, isotopic lysine. Cdc48p-Myc was immunoprecipitated from these the strains and again mass spectrometry was performed by the Gygi lab. The relative amount of "normal" (WT) and "heavy, isotopic" (*vms1*Δ) signal was compared between shared co-precipitating proteins. Unexpectedly, and in contrast to the spectral counting, I discovered that the interaction between Cdc48p and the proteasome was largely unaffected by the *vms1*Δ genotype (**Figure 28**). Rpt3p may be enriched in *VMS1* mutants, but this is likely an outlier. Rpt3p has no known function outside of the proteasome. These data further support a model in which Cdc48p binds independent of Vms1p function to the proteasome, and most likely then recruits Vms1p.

Table 9. Complete list of membrane and cytosolic fraction Cdc48p interactors from wild-type and vms1Δ strains

Cdc48p-Myc was immunoprecipitated from 2-3mg of cytosol or membrane from wild-type and *vms1*Δ strains. The Cdc48p-Myc was the only copy of Cdc48p in these strains. The immunoprecipitated material was methanol/chloroform extracted, lyophilized and subject to mass spectrometry in collaboration with Drs. Steven Gygi and Woong Kim (Harvard Medical School). Included with the gene name are unique peptide counts, which represents how many different proteolyzed fragments of a protein were observed, and total peptide counts, which represents the absolute total number of peptides seen in the experiment. This is sorted by unique peptide counts and the most abundant are shown at the top.

CYTOSOL					
WT			*vms1* Δ		
Gene	Unique	Total	Gene	Unique	Total
CDC48	64	288	CDC48	77	319
SSA2	27	39	SSA2	33	54
CDC19	24	60	MET6	31	40
HSP82	22	28	HSP82	30	38
TFP1	21	27	MET10	30	37
THS1	20	25	THS1	29	34
ENO2	19	31	ECM17	29	31
PGK1	19	25	CDC19	28	58
DDR48	16	74	TFP1	27	31
NUP2	16	21	TDH2	22	41
MET6	16	17	FAS2	22	26
TDH2	15	39	RPO21	22	24
NPL4	15	22	ENO2	21	37
PAN1	15	18	ADH1	20	38
RPB2	15	18	YHR020W	20	26
SHP1	14	53	PGK1	20	26
LEU2	14	31	PDC1	20	25
GPM1	14	23	ILS1	20	23
SPT5	14	19	CHC1	20	22
ADH1	14	19	LEU2	19	37
GPH1	14	17	VMA2	19	30
ALA1	14	16	EFT1	18	22
EFT1	13	18	SHP1	17	30
GSY2	13	17	HSP60	17	22
PAB1	13	15	MES1	17	19
PGI1	13	15	SSE1	17	19
PDC1	12	17	SPT5	17	19
HSP60	12	15	FAS1	17	18
SUP35	12	13	ALA1	17	18
SAH1	12	12	MET3	16	25
TPI1	11	13	GPM1	16	22
SES1	11	12	GSY2	16	21
RPO21	11	12	GPH1	16	18
CHC1	11	11	NPL4	16	17
RPN2	11	11	DDR48	15	30
KAR2	10	13	DPS1	15	21
SSA1	10	12	CYS4	15	17
HXK2	10	12	NUP2	15	16
TEF1	9	16	SES1	15	15
SSC1	9	12	CPA2	14	18
SSB2	9	11	PAB1	14	16
MES1	9	11	RPB2	14	16
HIS4	9	10	KAR2	14	15
CYS4	9	9	ADE3	14	15
VMA2	8	23	VAS1	14	14
ILV5	8	11	ALD6	13	18
UFD1	8	11	PYC1	13	18
ACT1	8	11	SSA1	13	17
YHR020W	8	10	SSC1	13	17
SHM1	8	10	PFK1	13	16
BMH1	8	9	SSB2	13	15
ADE3	8	9	HIS4	13	15
URA2	8	9	SAH1	13	14
TIF1	8	9	GDB1	13	13
DEF1	7	15	RPN1	12	13
PSA1	7	12	RPA190	12	13
DPS1	7	12	ACT1	12	13
ATP1	7	9	CLC1	11	16
ALD6	7	9	TEF1	11	16
ATP3	7	7	SAM1	11	14
SSE1	7	7	PGI1	11	14
PYC1	7	7	GRS1	11	13
PIN4	6	10	ATP2	11	13
RHR2	6	10	PAN1	11	12
RPS31	6	9	TRP3	11	12
SAM1	6	8	HOM6	11	11
IPP1	6	8	SHM1	11	11
GUS1	6	8	TPI1	10	12
ASN1	6	8	TRM1	10	11
CLC1	6	7	FRS2	10	10
ILS1	6	7	TDH1	10	10
RPN1	6	6	ENO1	9	18
VAS1	6	6	ILV5	9	13
TRP3	6	6	PSA1	9	12

MEMBRANE					
WT			*vms1* Δ		
Gene	Unique	Total	Gene	Unique	Total
CDC48	42	124	CDC48	54	133
SSA2	28	39	SSA2	27	32
CDC19	21	26	HSP82	23	28
HSP82	20	24	KAR2	17	20
ENO2	15	17	FKS1	15	17
KAR2	14	21	NPL4	15	17
NPL4	14	18	ENO2	14	20
EFT1	14	18	TDH2	13	17
PGK1	11	12	CDC19	13	15
TEF1	10	17	SSB2	13	14
ADH1	10	10	PGK1	12	12
FKS1	9	16	EFT1	11	14
TDH2	9	13	ECM17	11	12
TIF1	9	10	PAB1	11	11
SSA1	8	11	MET6	11	11
NUP2	8	10	SSA1	10	12
SSB2	8	9	TRM1	10	11
DEF1	7	11	PAN1	10	11
RPL3	7	11	DDR48	9	19
LEU2	7	9	DEF1	9	16
RPS6A	7	9	TFP1	9	11
GPM1	7	9	TEF1	9	11
URA2	7	8	SSE1	9	10
UBX2	7	7	SPT5	9	9
HRD3	7	7	SSC1	8	10
RPS31	6	15	LEU2	8	9
PIL1	6	9	ADH1	8	9
ILV2	6	8	CBR1	8	9
PAB1	6	7	SUP35	8	8
UFD1	6	7	CHC1	8	8
CHC1	6	6	CHS1	7	8
RPL27A	6	6	ILV2	7	8
RPL19A	6	6	UFD1	7	8
SHP1	5	12	RPL1A	7	8
TPI1	5	7	HRD3	7	8
RVB1	5	7	PDI1	7	7
RPS18B	5	6	YEF3	7	7
PDC1	5	6	ACT1	7	7
RPL25	5	6	SHP1	6	11
SPT5	5	5	VMA2	6	9
RPL4B	5	5	RPL3	6	8
RPL7B	5	5	GPM1	6	8
RPL2B	5	5	RPS6A	6	7
PMA2	5	5	RPL8B	6	7
GCN20	5	5	PHO88	6	7
LSP1	5	5	TIF1	6	7
VMA2	4	8	FAA1	6	6
RPS14B	4	6	URA2	6	6
SSC1	4	5	RPL7B	6	6
RPL1A	4	5	RPS31	5	13
PET9	4	5	HSC82	5	8
RPL6B	4	5	VMA4	5	7
FAA1	4	4	BMH1	5	6
RPN1	4	4	PDC1	5	6
SEC21	4	4	TPI1	5	5
SUP35	4	4	NUP2	5	5
GCD11	4	4	GCN20	5	5
RPS3	4	4	RPL19A	5	5
PGA3	4	4	RPL2B	5	5
THS1	4	4	TRP5	5	5
CHO2	4	4	PET9	4	6
RPS4A	4	4	PIN4	4	5
RPL21B	4	4	RPS18B	4	5
ABP1	3	6	PMA2	4	5
FBA1	3	6	RPL20B	4	5
RPL17A	3	5	RPL10	4	5
USA1	3	5	RPS14B	4	5
RPL16B	3	5	RPL6B	4	5
URA7	3	4	STM1	4	5
RPT5	3	4	RPL16B	4	5
LCB1	3	4	RPL17A	4	4
RPL8B	3	4	TRX2	4	4
HSC82	3	4	POR1	4	4
PMA1	3	4	RPL4B	4	4

RPN7	6	6
FBA1	5	10
APA1	5	9
RTG2	5	9
RPT5	5	8
ALF1	5	8
DED81	5	7
NAP1	5	7
FAS1	5	7
FAS2	5	7
GFA1	5	7
CTS2	5	6
RPT6	5	6
ABP1	5	6
GSY1	5	6
GCD11	5	6
PYC2	5	6
PDI1	5	6
ENO1	5	6
TRM1	5	6
RPS18B	5	6
LEU1	5	6
TKL1	5	6
GRS1	5	5
YDR341C	5	5
GDB1	5	5
HOM6	5	5
AAP1	5	5
YEF3	5	5
RPA190	5	5
TAL1	5	5
GDH1	5	5
ERG13	5	5
DLD3	5	5
ADH3	5	5
HSC82	4	6
SAM2	4	5
END3	4	5
CDC60	4	5
YAK1	4	5
ADE13	4	5
RPP2A	4	4
FRS2	4	4
GLE2	4	4
TRR1	4	4
ARO2	4	4
TRP2	4	4
VMA4	4	4
GLN4	4	4
KAP123	4	4
ASC1	4	4
ATP2	4	4
DAK1	4	4
CPA2	4	4
RPL27A	4	4
RPS20	3	5
RPS6A	3	5
RNR4	3	5
TUB3	3	5
RPT2	3	4
TMA19	3	4
CPR1	3	4
RPL17A	3	4
AAH1	3	4
PNC1	3	4
RPN9	3	4
RPL25	3	4
YHB1	3	4
ERG10	3	3
FKS1	3	3
RPP2B	3	3
LYS4	3	3
CDC33	3	3
SRP1	3	3
TRX1	3	3

DLD3	9	12
GFA1	9	12
DED81	9	11
PDI1	9	9
YDR341C	9	9
APE2	9	9
LEU1	9	9
DUG2	9	9
FBA1	8	15
ALF1	8	14
IPP1	8	11
BMH1	8	10
UFD1	8	10
GSY1	8	9
TKL1	8	9
PYC2	8	8
PFK2	8	8
GDH1	8	8
CDC60	8	8
DEF1	7	9
HXK2	7	9
RPT5	7	8
EFB1	7	8
TAL1	7	8
YGR117C	7	8
PIN4	7	7
YOL098C	7	7
RPT6	7	7
TRR1	7	7
AAP1	7	7
ADO1	7	7
ATP3	7	7
END3	7	7
URA2	7	7
ADE13	7	7
ASC1	7	7
RPN7	7	7
GUS1	7	7
ADH3	7	7
HSC82	6	10
CPR1	6	9
NAP1	6	8
RHR2	6	8
MET17	6	8
TIF1	6	8
RNR2	6	7
THR4	6	7
ERG13	6	7
SUP35	6	6
SOD2	6	6
LYS4	6	6
RPS6A	6	6
YEF3	6	6
YBR056W	6	6
ATP1	6	6
TYS1	6	6
ARO8	6	6
ACC1	6	6
SAM2	5	9
RPS31	5	8
AAT2	5	7
RPT2	5	6
RPS18B	5	6
SGM1	5	6
HEM1	5	6
DUG3	5	6
DED1	5	6
RPN6	5	6
CTS2	5	5
ERG10	5	5
GCD11	5	5
RPA135	5	5
TRX2	5	5
KRS1	5	5
WTM1	5	5

CBR1	3	4
RPL20B	3	4
RPL28	3	4
RPL13B	3	4
HRD1	3	3
SEC4	3	3
CDC33	3	3
YOS9	3	3
RPT2	3	3
SGM1	3	3
ACT1	3	3
POR1	3	3
SRP1	3	3
RPN2	3	3
HSP60	3	3
RPS12	3	3
YEF3	3	3
YPR158W-B	3	3
BMH1	3	3
RPL6A	3	3
RPS17A	3	3
TRP5	3	3
RPL16A	3	3
RPL11A	3	3
RPT6	3	3
PFK2	3	3
GGC1	3	3
RPS19A	3	3
RPG1	3	3
RPN9	3	3
GUS1	3	3
RPS9A	3	3
HTB1	3	3
IST2	2	4
RPL15B	2	4
PHO84	2	3
RPS20	2	3
PGI1	2	3
OLE1	2	3
ERG26	2	3
SSE1	2	3
DDR48	2	3
RPL30	2	3
LEU1	2	3
YPT1	2	3
RPL33A	2	3
SCS2	2	3
DFM1	2	3
RPP0	2	3
RPS1B	2	3
ARO2	2	2
SEC26	2	2
NAP1	2	2
SUB2	2	2
KAP123	2	2
RPS2	2	2
YDR341C	2	2
RTN1	2	2
TMA19	2	2
PHO88	2	2
RPP2A	2	2
RPP2B	2	2
RPN5	2	2
BMH2	2	2
RPL12A	2	2
YGR117C	2	2
RNA1	2	2
ARC1	2	2
RPN7	2	2
YKT6	2	2
SPF1	2	2
TFP1	2	2
UBX7	2	2
RPL35A	2	2
RPS15	2	2

RPN1	4	4
ERG6	4	4
RPL12A	4	4
ERG11	4	4
RPS20	4	4
RPP0	4	4
YOS9	4	4
UBX2	4	4
RPO21	4	4
THS1	4	4
PSA1	4	4
GGC1	4	4
SAM1	4	4
MIR1	4	4
RPL25	4	4
SAH1	4	4
RPS17A	4	4
RPS12	4	4
RPL27A	4	4
RPL28	4	4
RPL21B	4	4
END3	4	4
RPL6A	4	4
ILV5	4	4
GSY2	4	4
PMR1	4	4
RPL13B	3	5
SEC4	3	4
RPT5	3	4
YPR158W-B	3	4
RPL33A	3	4
UBX7	3	4
CDC33	3	4
RPL24B	3	4
PMA1	3	4
GAS1	3	4
RPL32	3	4
TDH3	3	4
RPL26A	3	4
RPS1B	3	4
SEC27	3	3
FBA1	3	3
TRX1	3	3
RNR4	3	3
RPP2A	3	3
SEC21	3	3
MET10	3	3
CLC1	3	3
GCD11	3	3
EFB1	3	3
ARC1	3	3
ARO2	3	3
RPB2	3	3
DED1	3	3
PIL1	3	3
PGA3	3	3
RPL11A	3	3
HSP60	3	3
SCS2	3	3
RPL9B	3	3
ILV1	3	3
GUA1	3	3
ERG26	3	3
SEC63	3	3
RPL14A	3	3
LEU1	3	3
GSP2	3	3
YKT6	3	3
RPL5	3	3
RPS4A	3	3
SHM2	3	3
TEF4	3	3
CCT8	3	3
TIF4631	3	3
VMA13	3	3

EFB1	3	3	PGM1	5	5
ERG20	3	3	RTG2	5	5
HOM2	3	3	APA1	5	5
CYS3	3	3	RPN12	5	5
SHM2	3	3	UBA1	5	5
YOL098C	3	3	TRP5	5	5
HIS1	3	3	RPN2	5	5
RPL3	3	3	TDH3	4	25
RNR2	3	3	LIA1	4	6
TRP5	3	3	AAH1	4	6
RPS3	3	3	SEC53	4	5
GSP2	3	3	NAB3	4	5
YGR117C	3	3	CYS3	4	5
RPN6	3	3	HOM2	4	5
GUA1	3	3	ARC1	4	5
TYS1	3	3	GSP2	4	5
URA5	3	3	GND1	4	5
RPL21B	3	3	RPP2A	4	4
KRS1	3	3	RPP2B	4	4
PDC5	3	3	SSA4	4	4
BET4	3	3	YMR315W	4	4
RPT1	3	3	GUA1	4	4
SEC13	3	3	RPP0	4	4
STI1	3	3	GLE2	4	4
PRO2	3	3	ADK1	4	4
ACC1	3	3	ERG20	4	4
RPS9A	3	3	PRO3	4	4
APE3	3	3	RPS12	4	4
HSP10	2	4	HIS7	4	4
RPB4	2	4	ARG5	4	4
THR4	2	4	STI1	4	4
PDC6	2	4	PRD1	4	4
YMR226C	2	4	SHM2	4	4
RPB11	2	4	GLN4	4	4
NUP100	2	3	IKI3	4	4
SGT2	2	3	MET13	4	4
ADK1	2	3	APE3	4	4
ADO1	2	3	RPT1	4	4
HIS7	2	3	TUB3	4	4
RPL4B	2	3	AHP1	3	7
RPN3	2	3	TEF4	3	4
PRO3	2	3	SPE3	3	4
WTM1	2	3	MAE1	3	4
NAB3	2	3	GCD10	3	4
UBA1	2	3	YMR226C	3	4
AAT2	2	3	RPB5	3	3
ARO8	2	3	HNT1	3	3
RPP0	2	3	RPB3	3	3
RPL16B	2	3	RNR4	3	3
RPP1B	2	2	BSP1	3	3
GUK1	2	2	YPL247C	3	3
RPN5	2	2	TMA19	3	3
NSP1	2	2	TRX1	3	3
ARC1	2	2	HSP10	3	3
COF1	2	2	HSP26	3	3
LIA1	2	2	HEM2	3	3
TRX2	2	2	RPS20	3	3
NUP116	2	2	COF1	3	3
PRE9	2	2	NSP1	3	3
VMA10	2	2	RPN5	3	3
ADE12	2	2	SRP1	3	3
MET17	2	2	TSA1	3	3
EDE1	2	2	ILV3	3	3
SEC18	2	2	YLR301W	3	3
MMF1	2	2	DAK1	3	3
MDE1	2	2	HTS1	3	3
RPS14B	2	2	YHB1	3	3
LYS21	2	2	LYS9	3	3
PRT1	2	2	WHI4	3	3
RPS15	2	2	RPS17A	3	3
SGM1	2	2	CCT8	3	3
RNA1	2	2	DLD2	3	3
ARP3	2	2	RPN9	3	3
RVB2	2	2	BLM10	3	3
BMH2	2	2	ADE2	3	3

RPL5	2	2	GUS1	3	3
GAS1	2	2	RPN2	3	3
RPS8B	2	2	RPS11A	3	3
GSP2	2	2	ERV41	3	3
RPL32	2	2	CHO2	3	3
WHI4	2	2	IST2	2	4
RVB2	2	2	RAS2	2	4
RVS161	2	2	OLE1	2	3
FAS2	2	2	SPF1	2	3
TDH3	2	2	ALF1	2	3
NDE1	2	2	PHO84	2	3
RPL9B	2	2	RPL15B	2	3
TIF4631	2	2	SAM3	2	3
RPL42A	2	2	RPN7	2	3
RPS25B	2	2	SEC26	2	3
RPL26A	2	2	ATP1	2	3
ERG1	2	2	ALA1	2	3
RPL18A	2	2	SAM2	2	3
PMR1	2	2	PEP4	2	2
FAA4	2	2	HYP2	2	2
ARF1	2	2	TOM70	2	2
YET3	1	2	HRD1	2	2
AHA1	1	2	SEC28	2	2
RPS9B	1	2	ABP1	2	2
CHS1	1	2	RHR2	2	2
UGP1	1	2	YET3	2	2
EGD2	1	2	SRV2	2	2
HXT4	1	2	ASC1	2	2
RPL24B	1	2	NAP1	2	2
YJR015W	1	2	VMA5	2	2
RPL14A	1	2	RPL16A	2	2
SEC27	1	2	RPS7A	2	2
USO1	1	2	LCB1	2	2
TRM1	1	2	RTN1	2	2
RPS24B	1	2	YDR341C	2	2
PRS2	1	2	VAS1	2	2
TOM70	1	1	YGR117C	2	2
MKT1	1	1	TSA1	2	2
STM1	1	1	GET1	2	2
CLC1	1	1	NSP1	2	2
TSA1	1	1	TMA19	2	2
SUR4	1	1	AHA1	2	2
SUP45	1	1	YKL100C	2	2
PRE9	1	1	FAS2	2	2
GET1	1	1	SUB2	2	2
ALG2	1	1	RPP2B	2	2
SEC11	1	1	RPT6	2	2
ASC1	1	1	YCP4	2	2
CHS3	1	1	RPS15	2	2
RPS5	1	1	CUE5	2	2
RPS13	1	1	COF1	2	2
ALF1	1	1	GET3	2	2
ECM33	1	1	USA1	2	2
RPN13	1	1	ALD6	2	2
RFA2	1	1	ARO4	2	2
UBX6	1	1	RPS3	2	2
MIR1	1	1	GSF2	2	2
RAS2	1	1	FPR1	2	2
SCS7	1	1	RPS19A	2	2
ECM10	1	1	SUR4	2	2
RNR2	1	1	RNR2	2	2
FEN1	1	1	RPL35A	2	2
CSE1	1	1	RVB2	2	2
RHR2	1	1	PMT4	2	2
TRX2	1	1	RVB1	2	2
RPS7B	1	1	KAP123	2	2
ATP3	1	1	NRP1	2	2
RPO21	1	1	MET17	2	2
GCN1	1	1	RPL36B	2	2
SAM1	1	1	ERG9	2	2
PEP4	1	1	RPL37A	2	2
ADE3	1	1	RPN6	2	2
PIM1	1	1	RPS5	2	2
BFR1	1	1	WHI4	2	2
EDE1	1	1	YDJ1	2	2

RPS4A	2	2	CCT5	3	3
ALD4	2	2	GUK1	3	3
FPR1	2	2	MMF1	3	3
YKT6	2	2	LSC2	3	3
PRE1	2	2	BET4	3	3
ARG5	2	2	HIS1	3	3
ZEO1	2	2	IDI1	3	3
RPL32	2	2	UBX4	3	3
LYS9	2	2	FRS1	3	3
ILV3	2	2	SUB2	3	3
GCD10	2	2	ARC35	3	3
WHI4	2	2	SEC13	3	3
RVB1	2	2	URA1	3	3
AHP1	2	2	ACO1	3	3
RPA135	2	2	PDC6	2	4
SPE3	2	2	VMA4	2	3
SPT6	2	2	TUB2	2	3
RPS17A	2	2	RPB11	2	3
YPL247C	2	2	GCD14	2	3
CCT8	2	2	IMD3	2	2
RPL35A	2	2	SEC27	2	2
GPR1	2	2	RPP1B	2	2
APE2	2	2	ARO2	2	2
TDH1	2	2	NUP116	2	2
YRB1	2	2	MDE1	2	2
ASP1	2	2	RPN8	2	2
RPL9B	2	2	MAM33	2	2
CPR6	2	2	ADE5	2	2
HSP104	2	2	PNC1	2	2
RPS19A	2	2	YDL124W	2	2
SOD2	2	2	ABP1	2	2
PMA2	2	2	CDC33	2	2
ARC35	2	2	YAK1	2	2
RPL34B	2	2	BMH2	2	2
TDH3	1	3	ILV2	2	2
TUB2	1	2	YGL039W	2	2
SNF7	1	2	DUG1	2	2
ECM10	1	2	RAD9	2	2
ENP1	1	2	RPS14B	2	2
RPL11A	1	2	URA7	2	2
TIF3	1	2	DYS1	2	2
SSA4	1	2	YNL134C	2	2
GAS1	1	2	PRT1	2	2
SEC4	1	2	YJR096W	2	2
TUB1	1	2	RPS15	2	2
YPR158W-B	1	2	KAP123	2	2
LSB3	1	2	ARO9	2	2
IMD3	1	1	TRP2	2	2
TSA1	1	1	ALD5	2	2
CDC53	1	1	URA4	2	2
KAP95	1	1	ZEO1	2	2
SOD1	1	1	HEM13	2	2
YJL055W	1	1	ARP2	2	2
RNR1	1	1	PMI40	2	2
AHA1	1	1	RPS16A	2	2
RPL16A	1	1	APT1	2	2
PIN3	1	1	ADE6	2	2
SUP45	1	1	HXK1	2	2
RPL30	1	1	FPR1	2	2
YMR315W	1	1	RPS3	2	2
NPL3	1	1	YGP1	2	2
THR1	1	1	ASP1	2	2
RPL33A	1	1	SVF1	2	2
PAN5	1	1	RPS21A	2	2
YEL007W	1	1	UBP14	2	2
SEC26	1	1	RPS11A	2	2
YPT1	1	1	MET14	2	2
ACF4	1	1	ASN1	2	2
YBR056W	1	1	LEU9	2	2
RPL24B	1	1	ARP3	2	2
HYR1	1	1	YPR158W-B	2	2
EGD2	1	1	ARG4	2	2
NAM8	1	1	URA5	2	2
VPS74	1	1	PAA1	2	2
RPS12	1	1	ARO1	2	2

RPS10A	1	1	FAA4	2	2
RPL33B	1	1	PUB1	2	2
ITR1	1	1	PFK2	2	2
SEC63	1	1	DPS1	2	2
YKL100C	1	1	ARF1	2	2
ZEO1	1	1	MRH1	2	2
PSD1	1	1	DFM1	2	2
SOD1	1	1	FSF1	2	2
ACC1	1	1	RPS9A	2	2
RPL23B	1	1	RPL18A	2	2
FPR1	1	1	HXK2	2	2
PDR5	1	1	RAS1	2	2
RPT1	1	1	ERG3	2	2
ERG11	1	1	TPO3	2	2
FSF1	1	1	LCB2	2	2
PDI1	1	1	ERG1	2	2
RPS26A	1	1	ANB1	2	2
OLA1	1	1	RPS23B	2	2
IRC22	1	1	ENO1	1	3
SEC28	1	1	RPP1B	1	2
RPL10	1	1	RPL30	1	2
TOM22	1	1	VPH1	1	2
RPL22A	1	1	ALO1	1	2
ILV1	1	1	MNN2	1	2
RPB2	1	1	RPL8A	1	2
CTS2	1	1	PMT2	1	2
TIF11	1	1	HSP26	1	1
HXK2	1	1	RPS2	1	1
RPL21A	1	1	YNL208W	1	1
MES1	1	1	NAB3	1	1
LYS20	1	1	KAP95	1	1
PTP2	1	1	RFA2	1	1
YPR158C-C	1	1	RPB5	1	1
RPL7A	1	1	PGI1	1	1
TVP38	1	1	MET3	1	1
PMT1	1	1	YEL007W	1	1
HTA1	1	1	YPT1	1	1
HCH1	1	1	ALG2	1	1
ALA1	1	1	NPL3	1	1
ILV5	1	1	RPN5	1	1
RNR4	1	1	RPS9B	1	1
RPS11A	1	1	CYS4	1	1
SMI1	1	1	EDE1	1	1
CAM1	1	1	ECM33	1	1
SHM2	1	1	EPT1	1	1
PDC6	1	1	SPT6	1	1
RRB1	1	1	VPS74	1	1
PYK2	1	1	TIF3	1	1
RPN12	1	1	EBP2	1	1
MGM101	1	1	RPL33B	1	1
ENO1	1	1	RPS13	1	1
RPS30B	1	1	SKG6	1	1
ERG3	1	1	SEC17	1	1
YJR003C	1	1	UBP14	1	1
RPL34B	1	1	DBP5	1	1
TEF4	1	1	PMT1	1	1
TPO3	1	1	SEC11	1	1
ATP1	1	1	RPS7B	1	1
ILV3	1	1	CAP2	1	1
RPL15A	1	1	HYR1	1	1
HSP104	1	1	RPS16A	1	1
GUA1	1	1	YJR015W	1	1
YDJ1	1	1	RPN13	1	1
CHL1	1	1	YOP1	1	1
PDC5	1	1	ECM10	1	1
FAS1	1	1	CHS3	1	1
CPR1	1	1	TAF14	1	1
ARO1	1	1	SGM1	1	1
RPS0B	1	1	ALG5	1	1
TRX1	1	1	GNP1	1	1
RPS16A	1	1	MBF1	1	1
ENP1	1	1	ACC1	1	1
UBX3	1	1	GCN1	1	1
ACS2	1	1	VBA4	1	1
SAC1	1	1	VTC4	1	1

RPS12	1	1
URA7	1	1
RPB3	1	1
RPS7B	1	1
CAF16	1	1
IDH2	1	1
BSP1	1	1
IMD4	1	1
ECM33	1	1
SEC21	1	1
HNT1	1	1
RPS1A	1	1
RPL14A	1	1
OLA1	1	1
ADE5	1	1
TIF34	1	1
RPS21A	1	1
MED2	1	1
CRM1	1	1
PHO3	1	1
RPS13	1	1
DUG3	1	1
YER156C	1	1
RPN13	1	1
PFK1	1	1
HEM1	1	1
RDI1	1	1
ADE6	1	1
ADE17	1	1
SCS2	1	1
FBP26	1	1
LSC2	1	1
RPN12	1	1
NUP60	1	1
SUB2	1	1
RPL12A	1	1
MET10	1	1
YPR1	1	1
NRP1	1	1
UBX7	1	1
UBP14	1	1
ARB1	1	1
RPL1A	1	1
SAP185	1	1
SIT4	1	1
DED1	1	1
BNA1	1	1
RPS11A	1	1
SAC6	1	1
MAM33	1	1
APT1	1	1
PMI40	1	1
PYK2	1	1
CTS1	1	1
TOM1	1	1
YMR099C	1	1
LYS20	1	1
RPS5	1	1
PTC3	1	1
RPL8B	1	1
RPL6A	1	1
GRE3	1	1
HXK1	1	1
HMF1	1	1
RPC40	1	1
HAT2	1	1
YJR096W	1	1
ASF1	1	1
RPL2B	1	1
PFK2	1	1
PTP2	1	1
ACS2	1	1
PIL1	1	1
NPA3	1	1
RPS29A	1	1

ARO1	2	2
HOR2	2	2
CCT3	2	2
HMF1	2	2
CPR6	2	2
ADH6	2	2
RPS4A	2	2
SUI3	2	2
RPL3	2	2
PDX3	2	2
RNA1	2	2
YRB1	2	2
RPL25	2	2
LSP1	2	2
HIS2	2	2
ELP3	2	2
RPS9A	2	2
ARF1	2	2
HEF3	2	2
YNL010W	2	2
RPN11	2	2
PDC5	1	3
YEL007W	1	2
TAF14	1	2
PIL1	1	2
AHA1	1	2
ARO4	1	2
NRD1	1	2
LAP3	1	1
RPB4	1	1
RNR1	1	1
NAM8	1	1
BNA3	1	1
PIN3	1	1
MDH1	1	1
PRE9	1	1
KAP95	1	1
HAM1	1	1
PEP4	1	1
RPS9B	1	1
RPL24B	1	1
NPL3	1	1
CCP1	1	1
EDE1	1	1
CAF16	1	1
CAP2	1	1
DOA1	1	1
RTN1	1	1
RPL11A	1	1
ZWF1	1	1
HYR1	1	1
GET3	1	1
THR1	1	1
RPT3	1	1
SUP45	1	1
PAN5	1	1
ECM10	1	1
TUB1	1	1
SNF7	1	1
RPS1A	1	1
PRE10	1	1
TIF4631	1	1
RPS13	1	1
ACO2	1	1
SOD1	1	1
BAT1	1	1
ECM33	1	1
UBX7	1	1
CIA1	1	1
RPA12	1	1
RPS7A	1	1
RVB2	1	1
SGT2	1	1
RPG1	1	1
PRO1	1	1

SAC1	1	1
ADK1	1	1
RPL24A	1	1
UBX4	1	1
RPN6	1	1
DHH1	1	1
ATP2	1	1
MMF1	1	1
SEC13	1	1
SUR2	1	1

VTC4	1	1
MES1	1	1
MNN5	1	1
CTS2	1	1
IRC22	1	1
TSC13	1	1
FEN1	1	1
YMR046C	1	1
TOM5	1	1
RPT2	1	1
PSD1	1	1
RPT1	1	1
HTB1	1	1
MET14	1	1
ARB1	1	1
SCD6	1	1
TIF11	1	1
DIC1	1	1
ENT2	1	1
VMA8	1	1
YMR124W	1	1
NUP100	1	1
APT1	1	1
FRE1	1	1
MNN9	1	1
YGR001C	1	1
ERG25	1	1
RPS25B	1	1
SAC1	1	1
DBP2	1	1
SES1	1	1
RPS24B	1	1
SSA4	1	1
PYK2	1	1
ADE5	1	1
CPR1	1	1
ZRT1	1	1
RFA1	1	1
RPB3	1	1
ERV46	1	1
RPL24A	1	1
RPN8	1	1
BMH2	1	1
RPL37B	1	1
RPS25A	1	1
RPS29A	1	1
TIM44	1	1
KRE9	1	1
MAE1	1	1
ZRT2	1	1
BUG1	1	1
HCH1	1	1
YPT7	1	1
EMC4	1	1
CAM1	1	1
ARP2	1	1
LAG1	1	1
YPR158C-C	1	1
TUB3	1	1
PRE9	1	1
TAL1	1	1
DED81	1	1
TFC4	1	1
PIS1	1	1
GND1	1	1
RPB11	1	1
SCM4	1	1
NDE1	1	1
TRR1	1	1
APE3	1	1
CPR6	1	1
HSP104	1	1
APA1	1	1
ELO1	1	1
SSZ1	1	1

FRS1	1	1
NGL2	1	1
OYE2	1	1
FUR1	1	1
DBP2	1	1
HCH1	1	1
CIC1	1	1
PAA1	1	1
TEF4	1	1
UBR1	1	1
RPL10	1	1
RPL20B	1	1
HTB1	1	1
ILV2	1	1
RPS24B	1	1
YLR301W	1	1
NFU1	1	1
RPS16A	1	1
PPH22	1	1
PMA1	1	1
MAE1	1	1
RPS0B	1	1
RPS30B	1	1
VMA7	1	1
RPS25B	1	1
PAN3	1	1
RPC10	1	1
RPL6B	1	1
RPL42A	1	1
ARO9	1	1
CHL1	1	1
IDI1	1	1
CAM1	1	1
RPT4	1	1
SEC53	1	1
RPL24A	1	1
UBX4	1	1
FAA4	1	1
RPL7B	1	1
RPL15B	1	1
FET4	1	1
CCT5	1	1
ASN2	1	1
HTA1	1	1
DHH1	1	1
CPR3	1	1
RPL28	1	1
URA1	1	1
MOT3	1	1
SEC27	1	1

SER33	1	1
RPN13	1	1
SSZ1	1	1
YPR1	1	1
GCY1	1	1
SIT4	1	1
YJL055W	1	1
MGE1	1	1
RPL14A	1	1
RPL16B	1	1
CPS1	1	1
VPS74	1	1
ARG1	1	1
YLR179C	1	1
BNA1	1	1
YMR099C	1	1
RPS25A	1	1
PRE8	1	1
SAM4	1	1
RVB1	1	1
GCN20	1	1
CPR3	1	1
PRI1	1	1
NRP1	1	1
ATP15	1	1
UBP15	1	1
RPC10	1	1
MET8	1	1
YKR070W	1	1
NUP100	1	1
ILV1	1	1
RPN10	1	1
SER1	1	1
PKP1	1	1
SCW4	1	1
RIB4	1	1
VMA7	1	1
GLY1	1	1
SEC21	1	1
YKL215C	1	1
TUF1	1	1
LSM4	1	1
PYK2	1	1
LSC1	1	1
BUD14	1	1
LSB1	1	1
RPS19A	1	1
QCR2	1	1
CAM1	1	1
PRS2	1	1
ASN2	1	1
PPH22	1	1
RPC19	1	1
MEU1	1	1
FUR1	1	1
FRE1	1	1
PRE1	1	1
RPC40	1	1
RPL6A	1	1
PGM2	1	1
PRC1	1	1
MRH1	1	1
POR1	1	1
NOP58	1	1
OYE2	1	1
GLC7	1	1
CFT2	1	1
ADE12	1	1
SPT6	1	1
RPP1A	1	1
TFC4	1	1
PRO2	1	1
TRM7	1	1
RPL21B	1	1
MOT3	1	1

FAS1	1	1
SER1	1	1
RPL26B	1	1
FKS3	1	1
SSM4	1	1
NUP116	1	1
ATP2	1	1
SNL1	1	1
CCT5	1	1
YOR342C	1	1
CCC1	1	1
YTA12	1	1
GBP2	1	1
RPN12	1	1
COP1	1	1
BNA1	1	1
WTM1	1	1
RPL23B	1	1
ARV1	1	1
RPS0B	1	1
PRO2	1	1
RNA1	1	1
CCT6	1	1
GLE2	1	1
GFA1	1	1

Table 10. Select ERAD/UPS-related interactions found in Table 9

Data from Table 8 were mined for relevant interactions related to ERAD/UPS process. Included with the gene name are unique and total peptide counts.

CYTOSOL						MEMBRANE						
WT			*vms1* Δ			WT			*vms1* Δ			
Gene	Unique	Total	Gene	Unique	Total	Gene	Unique	Total	Gene	Unique	Total	
CDC48	64	288	CDC48	77	319	CDC48	42	124	CDC48	54	133	**Cdc48p**
NPL4	15	22	NPL4	16	17	NPL4	14	18	NPL4	15	17	**complex**
UFD1	8	11	UFD1	8	10	UFD1	6	7	UFD1	7	8	
SHP1	14	53	SHP1	17	30	SHP1	5	12	SHP1	6	11	**UBX**
UBX2			UBX2			UBX2	7	7	UBX2	4	4	
UBX3			UBX3			UBX3	1	1	UBX3			
UBX4	1	1	UBX4	3	3	UBX4	1	1	UBX4			
UBX5			UBX5			UBX5			UBX5			
UBX6			UBX6			UBX6	1	1	UBX6			
UBX7	1	1	UBX7	1	1	UBX7	2	2	UBX7	3	4	
RPT1	3	3	RPT1	4	4	RPT1	1	1	RPT1	1	1	**19S base**
RPT2	3	4	RPT2	5	6	RPT2	3	3	RPT2	1	1	
RPT3	1	1	RPT3	1	1	RPT3	1	1	RPT3			
RPT4	1	1	RPT4			RPT4	2	2	RPT4			
RPT5	5	8	RPT5	7	8	RPT5	3	4	RPT5	3	4	
RPT6	5	6	RPT6	7	7	RPT6	3	3	RPT6	2	2	
RPN1	6	6	RPN1	12	13	RPN1	4	4	RPN1	4	4	
RPN2	11	11	RPN2	5	5	RPN2	3	3	RPN2	3	3	
RPN10			RPN10	1	1	RPN10			RPN10			
RPN3	2	3	RPN3			RPN3			RPN3			**19S lid**
RPN5	2	2	RPN5	3	3	RPN5	2	2	RPN5	1	1	
RPN6	3	3	RPN6	5	6	RPN6	1	1	RPN6	2	2	
RPN7	6	6	RPN7	7	7	RPN7	2	2	RPN7	2	3	
RPN8			RPN8	2	2	RPN8			RPN8	1	1	
RPN9	3	4	RPN9	3	3	RPN9	3	3	RPN9			
RPN11			RPN11	2	2	RPN11			RPN11			
RPN12	1	1	RPN12	5	5	RPN12	1	1	RPN12	1	1	
RPN13	1	1	RPN13	1	1	RPN13	1	1	RPN13	1	1	
SCL1	6	8	SCL1			SCL1			SCL1			**20S**
PRE8	2	4	PRE8	1	1	PRE8			PRE8			**(alpha)**
PRE9	2	2	PRE9	1	1	PRE9	1	1	PRE9	1	1	
PRE6	2	2	PRE6			PRE6			PRE6			
PRE2	2	2	PRE2			PRE2			PRE2			
PRE5	7	7	PRE5			PRE5	1	1	PRE5			
PRE10	3	5	PRE10	1	1	PRE10			PRE10			
PUP1	2	2	PUP1			PUP1			PUP1			**20S**
PUP3	2	3	PUP3			PUP3			PUP3			**(beta)**
PRE1	2	2	PRE1	1	1	PRE1			PRE1			
PRE2	2	2	PRE2			PRE2			PRE2			
BLM10			BLM10	3	3	BLM10			BLM10			
CIC1	1	1	CIC1			CIC1			CIC1			
SIT4	1	1	SIT4	1	1	SIT4			SIT4			
HRD1	3	3	HRD1	2	2	HRD1			HRD1			**ERAD**
HRD3	7	7	HRD3	7	8	HRD3			HRD3			
YOS9	3	3	YOS9	4	4	YOS9			YOS9			
USA1	3	5	USA1	2	2	USA1			USA1			
CUE1	1	1	CUE1			CUE1			CUE1			
SSM4			SSM4	1	1	SSM4			SSM4			
DFM1	2	3	DFM1	2	2	DFM1			DFM1			
UBA1	2	3	UBA1	5	5	UBA1			UBA1			**Misc UPS**
UBA3	1	1	UBA3			UBA3			UBA3			
UBR1	1	1	UBR1			UBR1			UBR1			
UBP14	1	1	UBP14	2	2	UBP14			UBP14	1	1	
UBP15			UBP15	1	1	UBP15			UBP15			
CDC53	1	1	CDC53			CDC53	1	1	CDC53			
DOA1			DOA1	1	1	DOA1			DOA1			

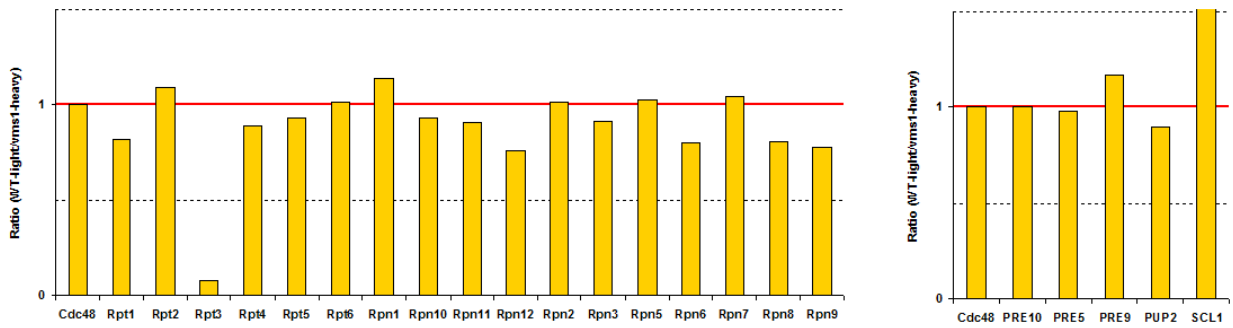

Figure 28. Cdc48p interaction with the proteasome is unaltered by the loss of VMS1

Wild-type and *vms1*Δ strains expressing Cdc48p-myc as their sole version of Cdc48p were grown in media containing standard and heavy ($^{13}C_6$,$^{15}N_2$) lysine, respectively. Extracts were prepared and Cdc48p-myc was immunoprecipitated with myc-agarose. Precipitated material was methanol/chloroform extracted and mass spectrometry was performed. The data from this SILAC analysis are presented as a ratio of WT (light) to *vms1*Δ (heavy). Ratios below "1" (horizontal red line) represent enrichment in *vms1*Δ (heavy-labeled) strain. Ratios above "1" represent enrichment in the wild-type (standard) strain.

3.3 DISCUSSION

3.3.1 Loss of *VMS1* increases cellular ubiquitinated proteins

As discussed in Chapter 2, loss of *VMS1* results in the accumulation of ubiquitinated proteins associated with Cdc48p. In this chapter, I report that the loss of *VMS1* also results in the accumulation of total cellular ubiquitinated proteins. This finding suggests that ubiquitinated protein homeostasis represents one of Vms1p's functions. Two apparent models can explain these data. In the first model, Vms1p modulates Cdc48p (or a Cdc48p cofactor) so that it promotes the efficient transfer or processing of ubiquitinated substrates. The second possibility is that Vms1p affects a downstream process such as proteasome function, which will in general increase the amount of ubiquitinated proteins in the cell. Using a panel of yeast strains mutated for various steps in the ERAD pathway, I discovered that the additional loss of *VMS1* consistently resulted in a further increase in ubiquitinated proteins (**Figure 22A**). This suggests that Vms1p functions in a largely additive parallel pathway with the tested genes. Interestingly, the level of ubiquitinated protein accumulation does not correlate with the presence of synthetic growth defects. For instance, *ubx2*Δ*vms1*Δ accumulate far more ubiquitin than *cdc48-3*,*vms1*Δ strains, yet the latter has a severe growth defect on rich media (**see Figure 14C, Chapter 2**). This likely reflects the additional functions of Cdc48p. Moreover, I found that loss of *VMS1* results in accumulation of total ubiquitinated proteins irrespective of strain background and

mating type (**Figure 22B and C**). This strongly suggests that ubiquitinated protein homeostasis is the conserved function of Vms1p.

3.3.2 Vms1p regulates proteasome subtype distribution

There are at least three scenarios which would result in the accumulation of total ubiquitinated protein: 1) defects in deubiquitinating enzymes, 2) aberrant regulation of ubiquitinated substrate transfer to the proteasome and 3) defects in proteasome function. While it is still possible that Vms1p plays a role in deubiquitination (but see **Figure 29**, in which no growth defect was observed in strains deleted for *VMS1* and the Cdc48p-associated DUB, *OTU1*) or substrate transfer, I chose to examine proteasome activity because this system was readily testable. In fact, I discovered that the distribution of proteasome subtypes was altered in *vms1*Δ mutants. The most prominent effect was with regard to the increase in the amount and activity of the 20S core as measured by both western blot analysis and Suc-LLVY AMC activity observed in the *vms1*Δ strain (**Figure 24A-C**). This was partially restored when the *vms1*Δ strain was supplied with a vector expressing wild-type Vms1p (**Figure 26A**). I also observed a significant decrease in proteasome activity associated with capped proteasomes in *vms1*Δ mutant cells, which is consistent with data showing an accumulation of ubiquitinated proteins. The former phenomenon was observed in 14 different experiments, without exception (**Figure 30, left**). By contrast, the decrease in 26S capped proteasome activity was observed in 8 out of 10 experiments (**Figure 30, right**). This might reflect the technically demanding nature of these experiments.

Surprisingly, I did not observe a decrease in the signal corresponding to 19S capped proteasomes when I compared wild-type and *vms1*Δ strains harboring an empty vector (grown in

a minimal media). In fact, the levels of capped proteasomes from *vms1*Δ cells expressing wild-type Vms1p-HA or the VIM mutant all appeared to increase. This phenomenon may be due in part to the effect of growth in minimal selective media. It is known that proteasomes play an important role in cell growth in minimal media (HEINEMEYER *et al.* 1991), where amino acids are limiting, but whether or not minimal media affects the distribution of proteasomes has not been tested, at least to my knowledge. At the most basic level, these data suggest that Vms1p affects the assembly or stability of the 26S proteasome.

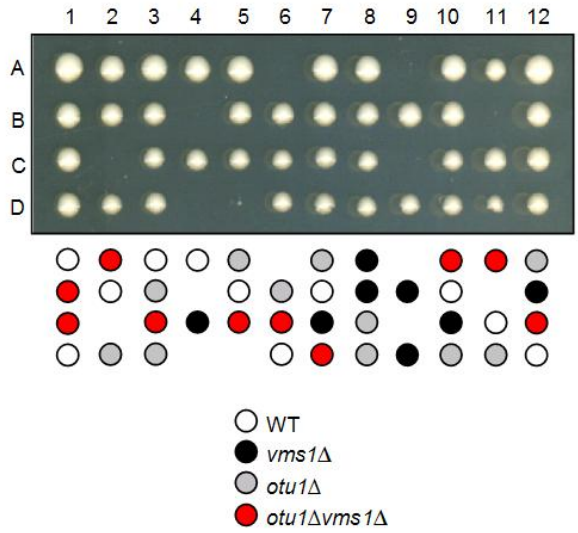

Figure 29. *VMS1* does not genetically interact with the gene encoding the deubiquitinating enzyme, *OTU1*

A genetic cross was performed between Mat alpha (BY4742) *vms1*Δ and Mat a (BY4741) *otu1*Δ strains. Diploid cells were sporulated and tetrads were dissected. White circles represent wild-type, black circles represent *vms1*Δ, grey circles represent *otu1*Δ, and red circles represent *otu1*Δ*vms1*Δ. The plate was incubated at 30°C.

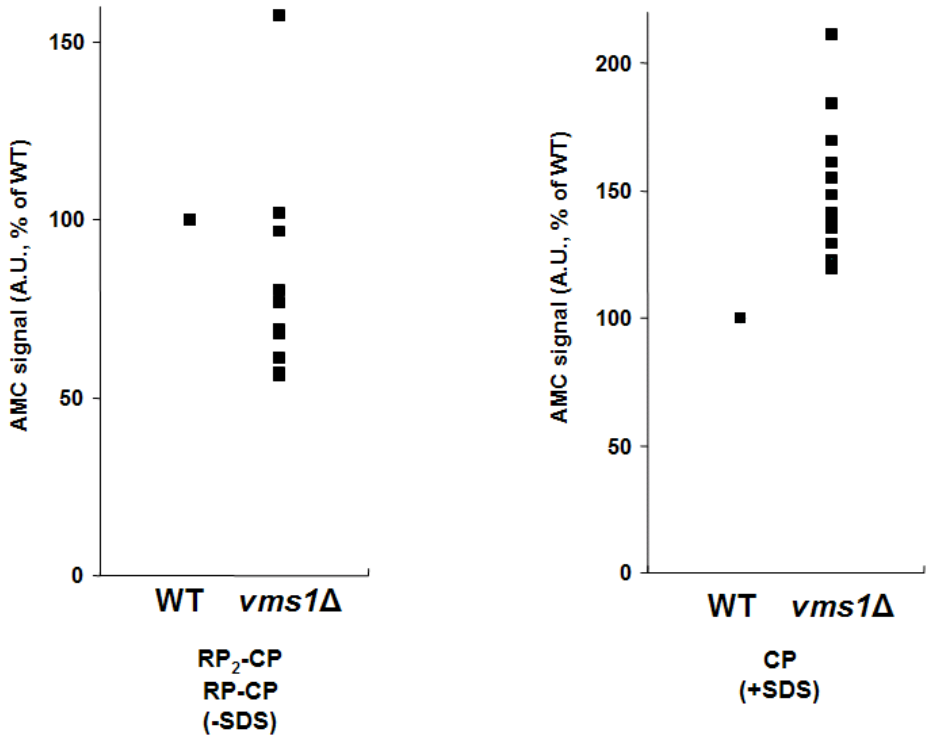

Figure 30. Individual experiments from Figure 24B

The individual experiments from Figure 24B are displayed as a scatter plot. The left plot is an assessment of 20S CP (Suc-LLVY-AMC) signal whereas the right plot is an assessment of 26S capped proteasome. In both examples, the strains used are wild-type and *vms1*Δ. The activity seen in the wild-type strain was set to 100%.

3.3.3 Vms1p most likely functions in proteasome stability

As mentioned above, my data can not rule out the possibility of defects in substrate transfer or DUB activity. I found that a strain double deleted for the genes encoding the ERAD DUB, *OTU1*, and *VMS1* showed no apparent growth defect (**Figure 29**). However, two other very prominent proteasome-associated DUBs exist (Ubp6p and Rpn11p), and these need to be tested. This could be done by: 1) examining the expression levels of these DUBs and 2) testing for the association of these DUBs with capped proteasomes in WT and *vms1*Δ yeast.

A defect in substrate transfer, due to loss of *VMS1*, was suggested in Chapter 2, and is based on the accumulation of ubiquitinated proteins associated with Cdc48p. This brings up the possibility that Vms1p serves as an escort factor or receptor for Cdc48p-ubiquitinated substrate complexes. This idea is further supported by the observation that both wild-type and a ΔVIM version of Vms1p co-migrated with the capped forms of the proteasome (**Figure 26A**). However, I have never been able to show association between Vms1p and ubiquitinated substrates as assessed by Vms1p immunoprecipitation followed by western blotting with antibodies against ubiquitin. Furthermore, the decrease in the amount of co-migrating Vms1p-ΔVIM with the proteasome suggests that Cdc48p may be required to link Vms1p with the proteasome, and this is further supported by the mass spectrometry data from (**Figure 28**) which indicates that the amount of Cdc48p-associated with the proteasome is unchanged in the *vms1*Δ background. This supports the possibility that Vms1p is recruited to the proteasome by Cdc48p, where Vms1p functions to maintain 26S proteasome homeostasis. The analysis of Vms1p-interaction partners

could validate this notion, especially if Vms1p is found in complex with Cdc48p and the proteasome, which is then reduced by a VIM mutant. Additionally, it would be interesting to see if gross overexpression of the Vms1p-ΔVIM mutant leads to any additional effects on the architecture of the 26S proteasome.

The co-migration of Vms1p with the 26S proteasome raises two exciting possibilities: 1) Vms1p plays a role in stabilizing the 26S proteasome, or 2) Vms1p helps assemble the 26S proteasome. Data from section 3.3.3 (**Figures 27A, B**) showed that there was no effect of doubly deleting between *VMS1* and select genes involved in proteasome assembly. While this result argues against a role in proteasome assembly, these experiments need to be further expanded to cover all possible proteasome chaperones (e.g., Pba1p-4p, Nas2, Nas6, Ecm29p) (FUNAKOSHI *et al.* 2009; KUSMIERCZYK *et al.* 2008; LE TALLEC *et al.* 2009; LEHMANN *et al.* 2010; LI and DEMARTINO 2009; PARK *et al.* 2009; ROELOFS *et al.* 2009; SAEKI *et al.* 2009; SCOTT *et al.* 2007). An alternative approach is to examine the proteins associated with Vms1p by immunoprecipitation under conditions that maintain proteasome stability (i.e., in the presence of ATP), or by yeast-two-hybrid. To date, there are no identified physical interactions between Vms1p and proteasome assembly chaperones, but these large-scale studies have relied on the bulky TAP tag for purification and conditions that deplete ATP (Biogrid) (STARK *et al.* 2006).

Notably, some mutants like *rpn10*Δ cells already showed very high levels of ubiquitin accumulation, and a further increase in ubiquitin accumulation caused by *VMS1* loss was modest (**Figure 27A**). The *rpn10*Δ*vms1*Δ double mutant, however, showed a pronounced increase in free 20S core particle. These data suggest that Vms1p functions in series with Rpn10p. In this

scenario, Rpn10p loss cripples ubiquitinated protein homeostasis because of the accumulation of non-, or partially functional proteasome intermediates that have the 19S base attached to the 20S CP. Vms1p loss further reduces the stability of the 19S base-20S CP intermediate, but the severity of the ubiquitin degradation defect is already maximal because the proteasome in *RPN10* mutants is defective. There is also evidence that overexpressed Dsk2p competes with Rpn10p for binding to substrate and this leads to the accumulation of ubiquitinated proteins (MATIUHIN *et al.* 2008). One possibility is that *vms1*Δ leads to Dsk2p overproduction, or prevents substrate association with Rpn10p. I have observed, on occasion, that Rpn10p distribution in a glycerol gradient is altered in *vms1*Δ lysates (see lower panel **Figure 27D for one example**).

3.3.4 Additional considerations

It is notable that mutations in genes encoding many proteasome-related factors showed a decrease in the amount of the di-ubiquitin signal (**Figure 27A, Ub x 2**). The relevance of this is not known.

Cdc48p immunoprecipitations yielded approximately 400 cytosolic and 350 membrane interactors (**Table 8**). However, only ~34% previously known interactors were identified. While the data from spectral counting and from the SILAC experiment differ, this is not uncommon and reflects the inaccuracy of using spectral counting for proteomic quantitation. I am currently working on improving the analysis of the SILAC data sets in collaboration with Dr. Woong Kim from the Gygi lab. The current hypothesis, which is based on the SILAC data, is that Cdc48p is at the proteasome at equal levels in WT and *vms1*Δ yeast. This can be examined by performing

the in gel proteasome substrate overlay assay, and then western blotting for Cdc48p and possibly other relevant cofactors such as Ufd1p. Finally, I have shown in Chapter 2 that *VMS1* genetically interacts with members of the UBX domain family. It would be interesting to see if the UBX family members, on their own, have any effect on the distribution of proteasome subtypes, as observed in this chapter for *vms1*Δ.

4.0 CONCLUSIONS AND FUTURE DIRECTIONS

4.1 CONCLUSIONS

In Chapters 2 and 3, I showed that the Vms1 protein, which was previously uncharacterized, functions in the ubiquitin proteasome system. Specifically, co-immunoprecipitation experiments show that Vms1p is a Cdc48p-interacting partner that resides in the cytoplasm and at intracellular membranes. I demonstrate that loss of *VMS1* results in an ERAD defect that is further exaggerated by the additional loss of select Cdc48p cofactors. Additionally, select double mutant combinations showed sensitivity to cellular stressors such as cadmium and tunicamycin. I showed that *VMS1* mutants accumulate total cellular ubiquitinated proteins, and accumulation was also evident in the population that is associated with Cdc48p. I also found that the accumulation of ubiquitinated proteins observed in the *VMS1* mutants can be mimicked by a yeast strain expressing only a version of Vms1p lacking its VIM domain, a Cdc48p interacting motif. These results indicate that ubiquitinated protein homeostasis requires the formation of the Cdc48p-Vms1p complex. Furthermore, I found that the ubiquitinated protein accumulation phenotype in *vms1*Δ yeast correlates with the accumulation of the latent 20S proteasome. I then showed that Vms1p co-migrates with the 26S proteasome and that the VIM mutant showed a reduced signal. Finally, I observed that the effect of *vms1*Δ on the proteasome was not due to changes in subunit expression, and did not appear to be the result of defects in the proteasome

assembly pathway. My data suggest, for the first time, that a complex of Cdc48p and Vms1p regulates the stability of the 26S proteasome. It is curious that the loss of *VMS1* leads to selective degradation defect of CFTR. This may imply that CFTR is hypersensitive to changes in proteasome levels in yeast.

4.2 FUTURE DIRECTIONS

4.2.1 Cycloheximide sensitivity

I have shown that the loss of *VMS1* on its own has only modest effects on protein degradation. Virtually all substrates tested to date had little to no detectable impairment in their degradation. A potential issue in these experiments is the use of the protein translation inhibitor, cycloheximide. *VMS1* mutant cells are extremely sensitive to cycloheximide. And, while this phenotype was not enough to occlude the ERAD defect for CFTR, it is evident that the effect of *vms1*Δ on CFTR degradation was better assessed in a pulse chase experiment (**Figure 16A and B**). One possible remedy would be to examine additional ERAD substrates, for instance, the ERAD-L substrate CPY* by pulse chase analysis. I would also be interested in performing a pulse chase, without cycloheximide, for the N-end rule substrate, Ub-pro-beta-gal. Alternatively, it is possible to define *in vivo* substrates that are dependent upon Vms1p for efficient degradation by mass spectrometry. This is currently under consideration and could be performed as a SILAC experiment using whole cell extracts, or isolated cellular fractions from wild-type and *vms1*Δ cells. Defining the *in vivo* substrates by this method is in theory applicable to any ERAD/UPS mutant, and would help characterize overlapping and unique pathways of protein degradation.

A prominent phenotype of *VMS1* loss is hypersensitivity to the protein translation inhibitor, cycloheximide. Cycloheximide exposure results in the depletion of ubiquitin and is suppressed by proteasome mutants (**Figure 31A**) (GERLINGER *et al.* 1997; HANNA *et al.* 2003). In my hands, *vms1*Δ yeast plated onto a low concentration of cycloheximide yielded suppressors of this phenotype, and indeed these suppressors accumulate ubiquitinated protein to a greater extent than the original mutants (**Figure 22C, Figure 31B**). This strongly suggests that cycloheximide sensitivity suppression is the result of proteasomal inactivation. My data indicate that proteasome instability is a relevant feature in the *vms1*Δ strain. It would be interesting to analyze proteasome distribution in *vms1*Δ strains that are sensitive and resistant to cycloheximide. If there is no effect, whole genome sequencing could be used to determine if these suppressors harbor mutations in additional proteasome components, or perhaps in novel genes that regulate the UPS. As an alternative to the whole genome approach, sequencing genes-encoding known proteasome genes could be performed. The spontaneous rescue of this phenotype has the potential to reveal much about regulation of proteasome function.

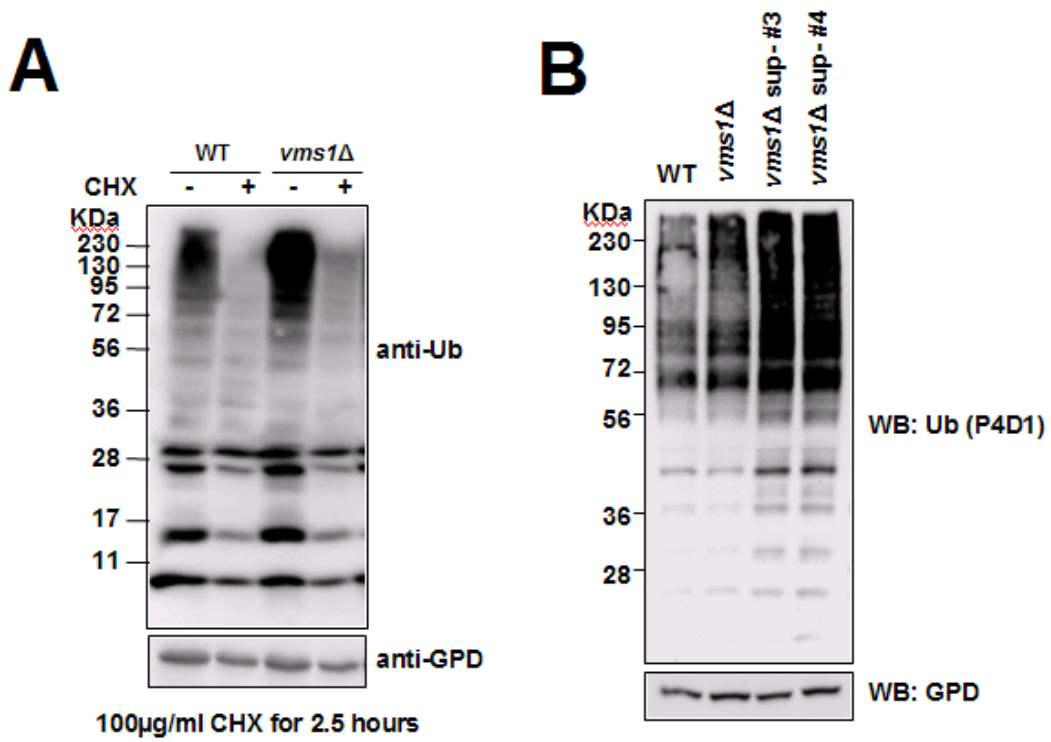

Figure 31. Suppressor mutants of the vms1Δ cycloheximide sensitive phenotype accumulate higher levels of ubiquitinated proteins

A. Cycloheximide depletes ubiquitin and ubiquitinated proteins in wild-type and *vms1*Δ yeast. Wild-type and *vms1*Δ cells were grown to log-phase and treated with 100µg of cycloheximide for 2.5 h. Cells before or after treatment were processed for western blot analysis with anti-ubiquitin antibodies. **B.** As seen in Figure 22C, *vms1*Δ yeast plated on cycloheximide show suppressor mutants. Suppressors (#3 and #4) were isolated and total protein was prepared by TCA precipitation. The protein extract was resolved by SDS-PAGE and subject to western blotting with anti-ubiquitin.

4.2.2 Cdc48p ATPase activity

VMS1 genetically interacts with many members of the UBX family of Cdc48p cofactors (**Table 5**). UBX family members from a diverse number of organisms have been shown to modulate Cdc48p/p97 ATPase activity (see section 1.4.2). In addition, *VMS1* genetically interacts with two different temperature sensitive *CDC48* alleles (*cdc48-2* and *cdc48-3*). The mutations have been partially characterized (see Figure 11), and affect the function of the first AAA-ATPase domain (D1). While the first ATPase domain is thought to be largely involved in hexamerization, there is evidence indicating that the ATPase domains communicate with each other during the hydrolysis cycle (DELABARRE and BRUNGER 2003; LI *et al.* 2012). It would be interesting to see if purified Vms1p can modulate the ATPase activity of Cdc48p in an *in vitro* assay. Currently, I have obtained purified Vms1p from our collaborator, Dr. Angela Gronenborn and with assistance from Dr. Leonardus Koharudin. Additionally, the Brodsky lab is well equipped to perform these assays as the lab routinely performs ATP- hydrolysis experiments for the HSP70s.

4.2.3 The Cdc48p-Vms1p complex at the proteasome

Recently, the Cdc48 hexamer was shown to form a tight functional complex with the 20S core particle in *Archaea* (BARTHELME and SAUER 2012). Three conclusions could be drawn from this elegant study. First, the Cdc48 complex dramatically increases 20S-mediated peptide degradation, suggesting that the peptide is being channeled into the 20S core by this ATPase. Second, the Cdc48 hexamer interaction with the 20S is not entirely dependent upon the HbYX

motif (see section 1.2.4). This result indicates that the Cdc48 hexamer has additional physical contacts with the proteasome that can stimulate the opening of the gate, and also alludes to the presence of additional bridging factors between the Cdc48 hexamer and the 20S core proteasome. Third, ATP, but not ADP binding to Cdc48 supported interaction with the 20S particle. This raises the possibility that UBX proteins, which are known to decrease the ATPase activity of yeast Cdc48p and genetically interact with *VMS1*, may be involved in modulation this type of interaction, or the interaction of the 19S cap and 20S core.

I have shown that Vms1p and a mutant version lacking the VIM domain co-migrate with the 26S proteasome (**Figure 26A**). Most interestingly, the Vms1-ΔVIM protein showed reduced co-migration compared to the wild-type version. This implies that Cdc48p may, in part, help recruit Vms1p to the proteasome to maintain proteasome stability. Further support for this hypothesis comes from the SILAC experiment, which showed that Cdc48p-association with proteasomal components was largely unaffected in the *vms1*Δ background (**Figure 28**). However, a major caveat with the SILAC data is that there are many different Cdc48p-complexes. It was simply not possible to determine whether Cdc48p-complexes were associated with the 19S cap and 20S core particle as a single entity or individually. Further, the conditions for the SILAC experiment were not optimal for maintaining the 26S proteasome complex and this apparent because the beta7 (Pre4p) subunit of the proteasome was never identified in any of my mass spectrometry experiment. It is likely then that Cdc48p interacts with the 19S and 20S particles individually.

Taking all these data into account, two formal possibilities exist: 1) Cdc48p may recruit Vms1p to the proteasome, and 2) Vms1p is recruited to the proteasome independent of the Cdc48p hexamer, and then recruits Cdc48p. The reason that the bulk of the Vms1-ΔVIM protein is reduced may be that the Cdc48p interaction prevents its degradation. To distinguish between these two possibilities, I would like to perform the native gel proteasome activity assay with lysates from wild-type and *vms1*Δ yeast expressing Cdc48p-myc followed by western blotting with the anti-myc serum. My expectation is that Cdc48p will co-migrate with the 20S core particle, and the interaction will be entirely unaffected by the *vms1*Δ genetic background. This would imply that the Cdc48p complex is at the proteasome to recruit Vms1p is a 26S stabilizing factor.

4.2.4 Testing additional fluorogenic substrates

I have shown that *VMS1* deletion leads to an increase in the amount of 20S activity for a fluorogenic substrate, Suc-LLVY-AMC. This substrate is specific only for the chymotryptic-like activity of the beta5 subunit of the proteasome. There are other substrates that can be used to test the additional activities of the proteasome. For instance, the Z-LLE-AMC substrate measures the PGPH-like activity and the BOC-RRL-AMC assesses the trypsin-like activity. I have recently purchased these substrates and plan on testing the affect of *VMS1* loss on their degradation.

4.2.5 An *in vitro* system for proteasome function

My work indicates that proteasome function is ultimately hampered by the loss of the *VMS1* gene. To further test this model, I would like to develop an *in vitro* assay for protein degradation.

The assay is based on a protocol originally developed to measure the *in vitro* degradation of a Cyclin inhibitor, Sic1p (SAEKI *et al.* 2005). Cdc48p complexed to ubiquitinated species can be purified from both wild-type and *vms1*Δ mutant yeast and can be used as a starting material, instead of the isolated ubiquitinated Sic1p (**see Figure 21B**). The precipitate can be mixed with purified 26S proteasome in the presence or absence of ATP to stimulate degradation (**Figure 32A**). In fact, I have attempted this assay. In **Figure 32B**, I found that mixing these components results in a reduction in the ubiquitinated signal (compare lanes 1-3 and 4-6). This might represent true substrate degradation, but I can not rule out DUB activity in this assay at the moment. Additionally, it is uncertain whether or not the ubiquitinated species are derived from Cdc48p or from the pool associated with the proteasome. To address this issue, I could in practice express an epitope-tagged form of ubiquitin (HA-tagged) along with Cdc48p-Myc, and purify the Cdc48-Myc complex as the starting material. This would let me monitor the ubiquitinated proteins specifically associated with Cdc48p. Regardless this is a very promising first step, and may allow the community to reconstitute the last steps prior to degradation in the ERAD pathway.

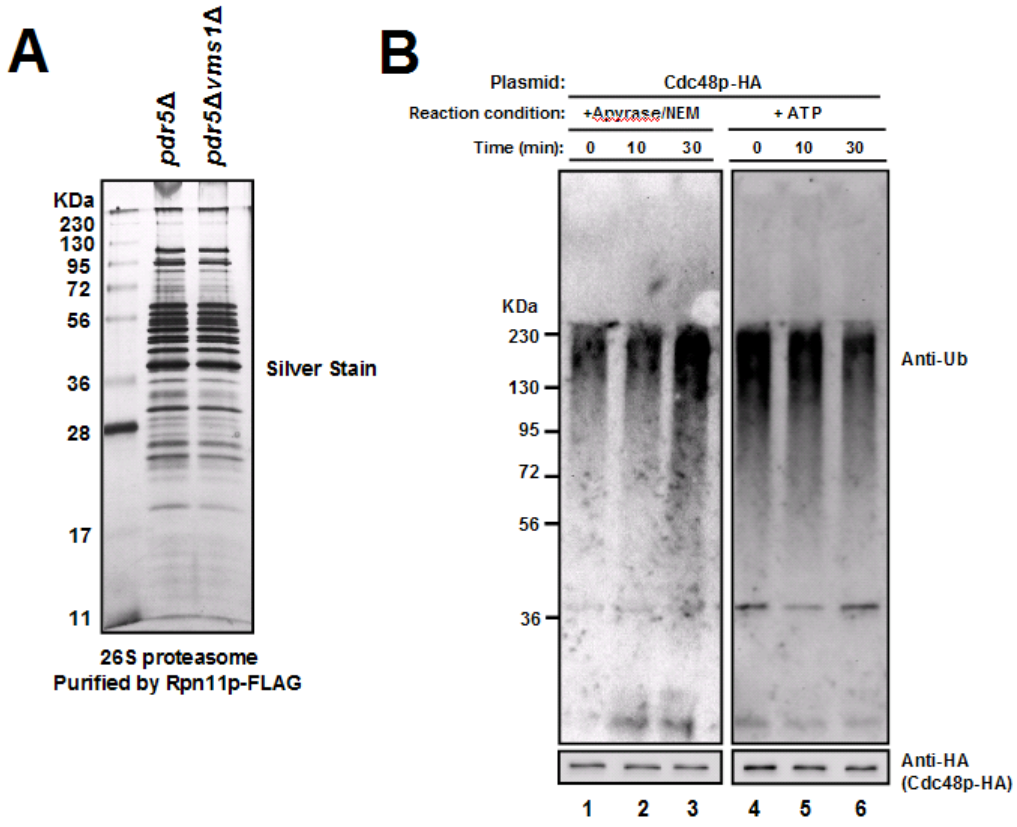

Figure 32. Development of an in vitro degradation assay

A. Lysates from yeast strains expressing Rpn11p-FLAG were prepared for affinity purification with FLAG-agarose. Affinity purified 26S proteasome was resolved, in duplicate, by SDS-PAGE and silver stained. **B.** In vitro degradation assay. Cdc48p-ubiquitinated protein complexes were purified as in Figure 21B. Affinity purified proteasome from (A) and either ATP or a cocktail of Apyrase/NEM was added to the Cdc48p-ubiquitinated protein precipitate, and the reaction was allowed to proceed at 30°C for the indicated times. The reaction was quenched by adding SDS-PAGE sample buffer, and resolved by SDS-PAGE for western blotting with anti-ubiquitin antibody.

Appendix A

MODELING IBMPFD MUTATIONS IN YEAST

The human homolog of Cdc48p, VCP/p97, has been linked to several diseases including a number of neuromuscular disorders (see section 1.4.1). A commonality among these diseases is the presence protein aggregates, suggesting that the pathology of the disease is caused by aberrant protein quality control (JU *et al.* 2009; WEIHL *et al.* 2006).

In this study, I used yeast to model the molecular pathology associated with the human disease, Inclusion Body Myopathy associated with Paget's disease of bone and Frontotemporal Dementia (IBMPFD). Specifically, I constructed several *CDC48* yeast mutants that corresponded to the most common IBMPFD mutations, R95G, R155H, and A232E (WATTS *et al.* 2004). I found that R95G and the A232E mutations caused temperature sensitivity in yeast and an autophagy-related defect. However, a more detailed analysis, which was done with the help of Bill Glassford (graduate rotation student, University of Pittsburgh), revealed that the temperature sensitivity of the R95G and R155H alleles were the result of the HA-epitope tag at the end of carboxy terminus of Cdc48p. A Myc-tagged version of these alleles displayed no temperature sensitivity and no defect in autophagy. Further, the Myc-tagged alleles showed no growth

phenotypes on various stress agents and no ERAD defects. This study, however, does reveal that epitope tagged versions of Cdc48p are very stable and thus the differences between these two versions of Cdc48p are likely related to some aspect of Cdc48p function. In fact, I discovered that there are differences in the apparent migration of the Cdc48p hexamer, depending upon the epitope tag used. Additionally, I show for the first time that a classic temperature sensitive allele of *CDC48*, *cdc48-3,* is devoid of detectable free hexamer. I conclude that the yeast model of IBMPFD might be used in the future to study basic Cdc48p function such as hexamer assembly and cofactor binding. (This study was started as a collaboration between the Brodsky lab and the lab of Dr. John Paul Taylor at St. Jude's Childrens Hospital (Memphis, Tennessee)).

A.1 EXPERIMENTAL PROCEDURES

A.1.1 Yeast strains, oligos, plasmids, and growth assays

Yeast strains used in this study are listed in Table 10. Strain construction and growth assays were performed as described in Chapter 2 section 2.1.1. A notable exception is that cells were selected on media lacking uracil to maintain the *CDC48* encoding plasmid. Schematic for creating yeast harboring IBMPFD mutations is shown in Figure 33. Plasmids and oligonucleotides used in this study are listed in Table 11 and 12.

Table 11. List of strains used in this study

Strain	Genotype	Reference
BY4742	*MATα, his3Δ1, leu2Δ0, ura3Δ0, lys2Δ0, MET15*	Open Biosystems
cdc48-3	*MATα, his3Δ1, leu2, ura3, lys2Δ0, MET15, cdc48-3*	Tran, et al., 2011
cdc48ΔWTMyc	*MATα, his3Δ1, leu2Δ0, ura3Δ0, lys2Δ0, MET15, cdc48Δ::KanMX, pRS315-CDC48Myc*	This study
cdc48ΔR95GMyc	*MATα, his3Δ1, leu2Δ0, ura3Δ0, lys2Δ0, MET15, cdc48Δ::KanMX, pRS315-CDC48Myc(R95G)*	This study
cdc48ΔR155HMyc	*MATα, his3Δ1, leu2Δ0, ura3Δ0, lys2Δ0, MET15, cdc48Δ::KanMX, pRS315-CDC48Myc(R155H)*	This study
cdc48ΔA232EMyc	*MATα, his3Δ1, leu2Δ0, ura3Δ0, lys2Δ0, MET15, cdc48Δ::KanMX, pRS315-CDC48Myc(A232E)*	This study
cdc48ΔWTHA	*MATα, his3Δ1, leu2Δ0, ura3Δ0, lys2Δ0, MET15, cdc48Δ::KanMX, pRS315-CDC48HA*	This study
cdc48ΔR95GHA	*MATα, his3Δ1, leu2Δ0, ura3Δ0, lys2Δ0, MET15, cdc48Δ::KanMX, pRS315-CDC48HA(R95G)*	This study
cdc48ΔR155HHA	*MATα, his3Δ1, leu2Δ0, ura3Δ0, lys2Δ0, MET15, cdc48Δ::KanMX, pRS315-CDC48HA(R155H)*	This study
cdc48ΔA232EHA	*MATα, his3Δ1, leu2Δ0, ura3Δ0, lys2Δ0, MET15, cdc48Δ::KanMX, pRS315-CDC48HA(A232E)*	This study
ufd2Δcdc48ΔWTHA	*MATα, his3Δ1, leu2Δ0, ura3Δ0, lys2Δ0, MET15, ufd2Δ::HIS3MX, cdc48Δ::KanMX, pRS315-CDC48HA*	This study
ufd2Δcdc48ΔR95GHA	*MATα, his3Δ1, leu2Δ0, ura3Δ0, lys2Δ0, MET15, ufd2Δ::HIS3MX, cdc48Δ::KanMX, pRS315-CDC48HA(R95G)*	This study
ufd2Δcdc48ΔR155HHA	*MATα, his3Δ1, leu2Δ0, ura3Δ0, lys2Δ0, MET15, ufd2Δ::HIS3MX, cdc48Δ::KanMX, pRS315-CDC48HA(R155H)*	This study
ufd2Δcdc48ΔA232EHA	*MATα, his3Δ1, leu2Δ0, ura3Δ0, lys2Δ0, MET15, ufd2Δ::HIS3MX, cdc48Δ::KanMX, pRS315-CDC48HA(A232E)*	This study
ufd2Δ::HIS3MX	*MATα, his3Δ1, leu2Δ0, ura3Δ0, lys2Δ0, MET15, ufd2Δ::HIS3MX*	This study

Table 12. Plasmids used in this study

Plasmid name	Description	Reference
pSM1911	PGK1 promoter, Ste6p*-HA expression plasmid, 2 micron	Huyer, et al., 2006
CPY*-3xHA	Endogenous promoter, CPY* 3xHA expression plasmid, CEN	Bhamidipati, et al., 2005
pRS315-CDC48myc	Endogenous promoter, c-terminal 1xmyc CDC48, CEN	Tran, et al., 2011
pRS315-CDC48myc(R95G)	Endogenous promoter, c-terminal 1xmyc CDC48 (R95G), CEN	This study
pRS315-CDC48myc(R155H)	Endogenous promoter, c-terminal 1xmyc CDC48 (R155H), CEN	This study
pRS315-CDC48myc(A232E)	Endogenous promoter, c-terminal 1xmyc CDC48 (A232E), CEN	This study
pRS316-CDC48HA	Endogenous promoter, c-terminal 1xHA tagged CDC48, CEN	Tran, et al., 2011
pRS316-CDC48HA(R95G)	Endogenous promoter, c-terminal 1xHA tagged CDC48 (R95G), CEN	This study
pRS316-CDC48HA(R155H)	Endogenous promoter, c-terminal 1xHA tagged CDC48 (R155H), CEN	This study
pRS316-CDC48HA(A232E)	Endogenous promoter, c-terminal 1xHA tagged CDC48 (A232E), CEN	This study

Table 13. List of oligonucleotides used in this study

Name	Sequence
R95G-F	agttcgtaacaatttacgtattgggctgggtgatttagttacaattcatc
R95G-R	gatgaattgtaactaaatcacccagcccaatacgtaaattgttacgaact
R155H-F	gaaaggcgaccattttgttgtccatggcggtatgagacaagtcgaattca
R155H-R	tgaattcgacttgtctcataccgccatggacaacaaaatggtcgcctttc
A232E-F	tgagacatcctcagttgttcaaggagatcggtatcaagccaccaagaggt
A232E-R	acctcttggtggcttgataccgatctccttgaacaactgaggatgtctca

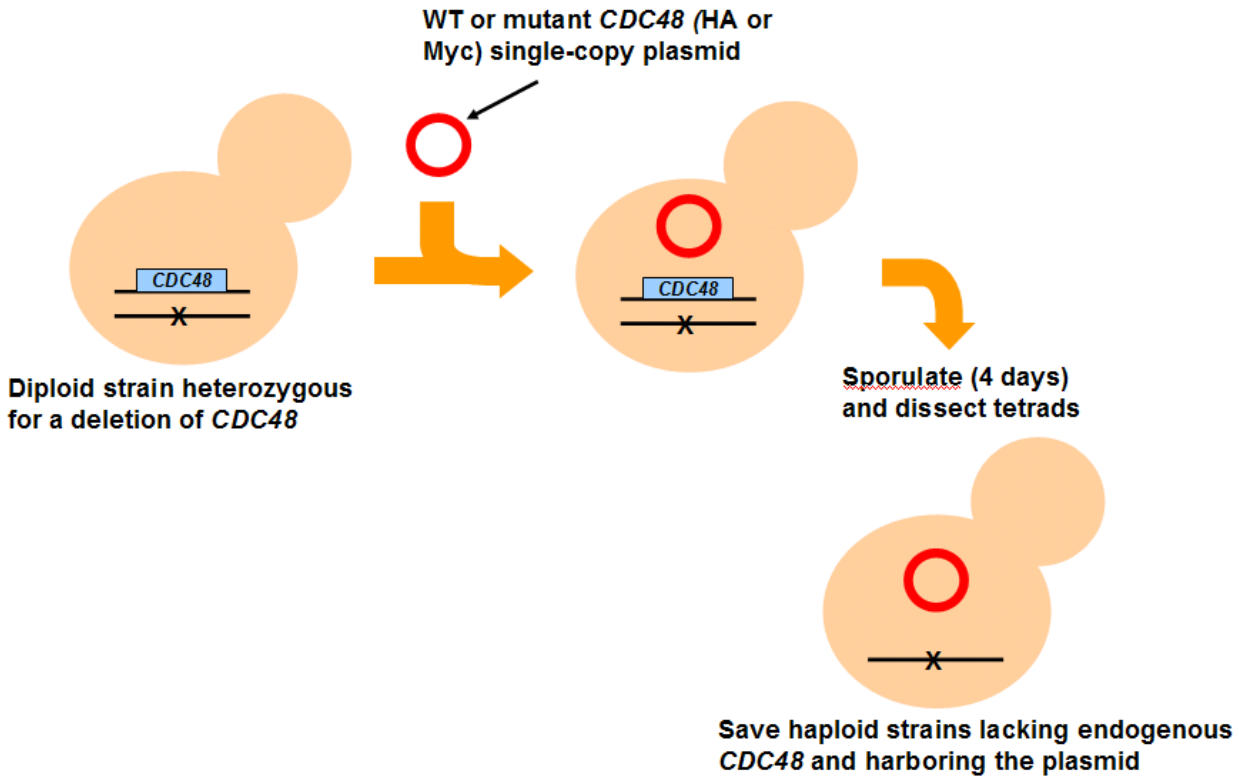

Figure 33. The general scheme used to model IBMPFD mutations in yeast

Diploid strains heterozygous for the deletion of *CDC48* (*cdc48*Δ::KanMX) were transformed with the indicated plasmids and grown on selective media. Diploids were then sporulated and tetrads were dissected on selective media to force the maintenance of the plasmid. Strains positive for growth on both G418 and the plasmid selective marker were saved. Total DNA was extracted from these strains and the *CDC48* gene was amplified and sequenced to ensure that the only allele present was from the plasmid.

A.1.2 Cycloheximide chase assay

Cycloheximide chase assays were performed as described in Chapter 2 section 2.1.2.

A.1.3 Assays to measure autophagy

Autophagy and CVT pathways were assessed using the assays described in Chapter 2 section 2.1.6.

A.1.4 Immunoprecipiation

Immunoprecipitation of the Cdc48p-HA and Cdc48p-Myc tagged constructs was done as described in Chapter 2 section 2.1.5.

A.1.5 Native PAGE

Cdc48p hexamers were analyzed using native PAGE. Briefly, 100ml of log-phase cells were harvested, resuspended in Buffer 88 (20mM HEPES pH 6.8, 150mM KOAc, 250mM sorbitol, 5mM MgOAc) supplemented with 1mM PMSF, 1µg/ml leupeptin, and 0.5µg/ml pepstatin A, and disrupted by glass bead lysis at 4°C. The unbroken cells were removed by low-speed centrifugation, and the resulting crude supernatant was centrifuged at 18,000g for 20 min in a refrigerated table top centrifuge to obtain the cytosolic fraction. The cytosolic fraction (25µg) was resuspended in native PAGE sample buffer (80mM Tris-HCl, pH 8.0, 8mM EDTA, 15% glycerol, 0.08% Tris base, 0.01% bromophenol blue) and resolved on a 6% native

polyacrylamide gel (8.5 x 10 cm). To denature select samples, SDS was added to a final concentration of 0.5% and the mixture was incubated at 75°C for 10 minutes. The samples were cooled on ice prior to loading. Proteins were then transferred on nitrocellulose and western blot analysis was performed with the indicated antibodies.

A.1.6 Gel filtration analysis

Gel filtration analysis was used to analyze the distribution of Cdc48p complexes. The source material was cytosolic extracts prepared as described in section 5.1.5. Sephacryl S300HR gel filtration media resuspended in Buffer 88 (~80ml) was packed by gravity in a 2.5 x 50 cm column. The column was flushed with 5-6 volumes of Buffer 88 prior to use, and stored in 10% ethanol. To fractionate the Cdc48p complex, 10mg of cytosol was applied to the column. A peristaltic pump (1mm tubing) was used at a setting of 150ml/h to flush the column with Buffer 88. Fractions were collected with an automated fraction collector at a setting of 1.5 min/fraction. The total protein from each fraction was isolated by TCA precipitation and resolved by SDS-PAGE. Western blotting was performed with the indicated antibodies.

A.1.7 Antibodies and western blot analysis

Antibodies used in this study included: Anti-HA (Roche, USA), anti-Myc (Santa Cruz, USA), anti-GFP (Roche, USA), anti-Ape1p (a kind gift from Dr. Daniel Klionsky), anti-Cdc48p (a kind gift from Dr. Rasmus Hartmann-Petersen) and Ubx1p (a kind gift from Dr. Alexander Buchberger). Western blots were decorated with the indicated primary antibodies and appropriate HRP-conjugated anti-mouse or anti-rabbit IgG secondary antibodies. The HRP-

chemiluminescent signal was visualized by enhanced chemiluminescence (Pierce, USA). Images were captured on a Kodak Image Station 440CF (Kodak, USA) and were analyzed using ImageJ v1.42q (**Abramoff**).

A.2 RESULTS

A.2.1 Yeast strains carrying IBMPFD mutations do not exhibit growth defects at permissive temperatures

The indicated IBMPFD mutation was introduced at the corresponding location in the yeast *CDC48* gene by site directed mutagenesis (Figure 34A). The mutagenized version of *CDC48* was cloned into a low-copy *CEN* plasmid and introduced into a diploid strain heterozygous for the deletion of *CDC48*. A single HA-epitope tag was also introduced at the carboxy terminus of the Cdc48 protein to facilitate detection. Haploid strains containing both a deletion of the *CDC48* chromosomal locus and the plasmid containing *CDC48* were selected for by the scheme seen in Figure 33. For convenience, the human nomenclature is used for the yeast-modeled IBMPFD alleles.

As seen in Figure 34B and 34C, yeast strains harboring the IBMPFD mutations in their only copy of Cdc48p displayed no obvious growth defect. Additionally, the expression level of Cdc48p-HA from the *CEN* plasmid in these strains was unaffected by the presence of the IMBPFD mutations, and comparable to a wild-type construct (Figure 34B, bottom panel). This

indicates that the IBMPFD mutations, under standard growing conditions, are not detrimental to cell viability and growth.

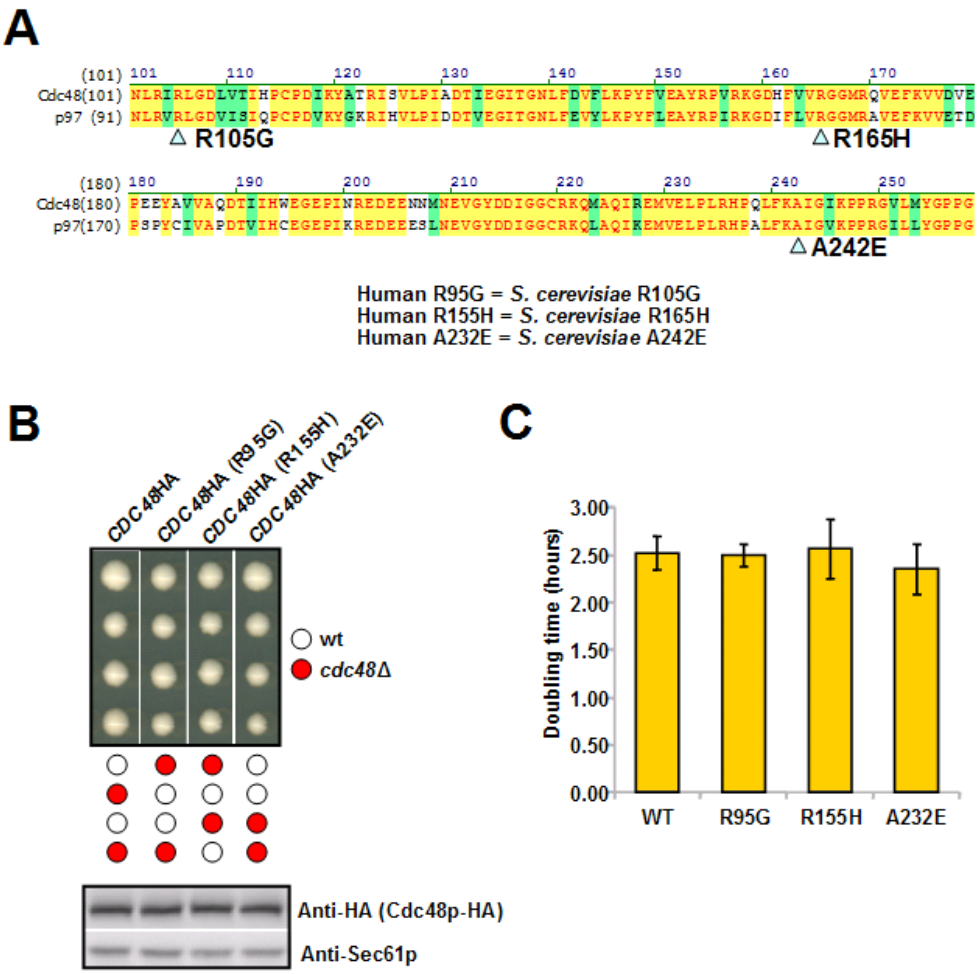

Figure 34. IBMPFD mutations modeled in the CDC48-HA gene show no viability or growth defects under standard growth conditions

A. The three different IBMPFD mutations selected are indicated by the upward pointing arrowheads. The alignment between human and yeast p97 and Cdc48p, respectively, was done using Vector NTI. These three mutations represent the most common IBMPFD mutations. **B.** Tetrads carrying the individual IBMPFD alleles were dissected and grown at 30ºC (top). Western blot analysis (anti-HA and anti-Sec61p) was performed on total protein from the indicated strains to determine their relative expression levels (bottom). **C.** Growth of the indicated strains was measured (OD_{600}) in liquid culture. The doubling times were calculated and plotted using Microsoft Excel.

A.2.2 Yeast strains carrying IBMPFD mutations are temperature

To test if IBMPFD mutations in the *CDC48-HA* gene compromise tolerance to general cell stress, 10-fold serial dilutions of the indicated strains were spot plated and grown at permissive (30ºC) and at high temperature (38ºC). The IBMPFD alleles R95G and A232E displayed a pronounced and reproducible temperature sensitive phenotype at high temperature (Figure 35A, right). High temperature is known to induce, among other things, the autophagic pathway (MELENDEZ and NEUFELD 2008). IBMPFD mutations in humans have also been shown to cause defects in the autophagic pathway (JU *et al.* 2009). I therefore analyzed the processing of an autophagic/CVT marker in IBMPFD-modeled *CDC48-HA* mutants. Consistent with the temperature sensitive phenotype, both the R95G and A232E mutants showed an increase in the processing of Ape1p, which indicated that the autophagic/CVT pathways were activated (Figure 35B, compare lanes 2 and 4). Interestingly, when these strains were challenged at higher temperature, the processing of Ape1p was reduced in both the R95G and A232E mutants (Figure 35B, compare lanes 6 and 8). This suggests that the temperature sensitivity observed in these select IBMPFD strains could be due to an autophagic defect.

One possible explanation for the temperature sensitivity seen in R95G and A232E *CDC48-HA* mutants is protein instability. Elevated temperature is known to exacerbate the misfolding of some proteins and promote their degradation (ZHANG *et al.* 2002). To test protein stability, I performed a cycloheximide chase analysis of the IBMPFD *CDC48-HA* mutants. As seen in Figure 36A and B, the IBMPFD mutants were not grossly unstable when compared to wild-type Cdc48p-HA. Thus, it is more likely that the observations of temperature sensitivity and the mild autophagic defect are due to the altered function of Cdc48p.

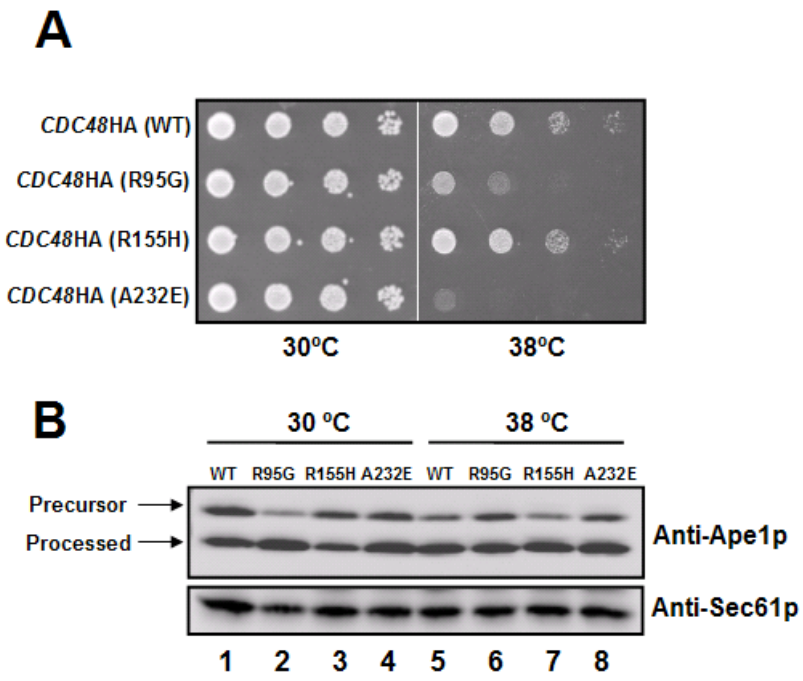

Figure 35. Select IBMPFD mutations modeled in the CDC48-HA gene show temperature sensitivity and autophagic defects

A. The indicated yeast stains were spot tested (10-fold serial dilutions) on the appropriate media and the plates were incubated at the indicated temperatures. **B.** Autophagic/CVT pathway was assessed as described in the Experimental Procedures section. Total TCA precipitated protein from the indicated strains was resolved by SDS-PAGE and western blotting was performed with the indicated antibodies.

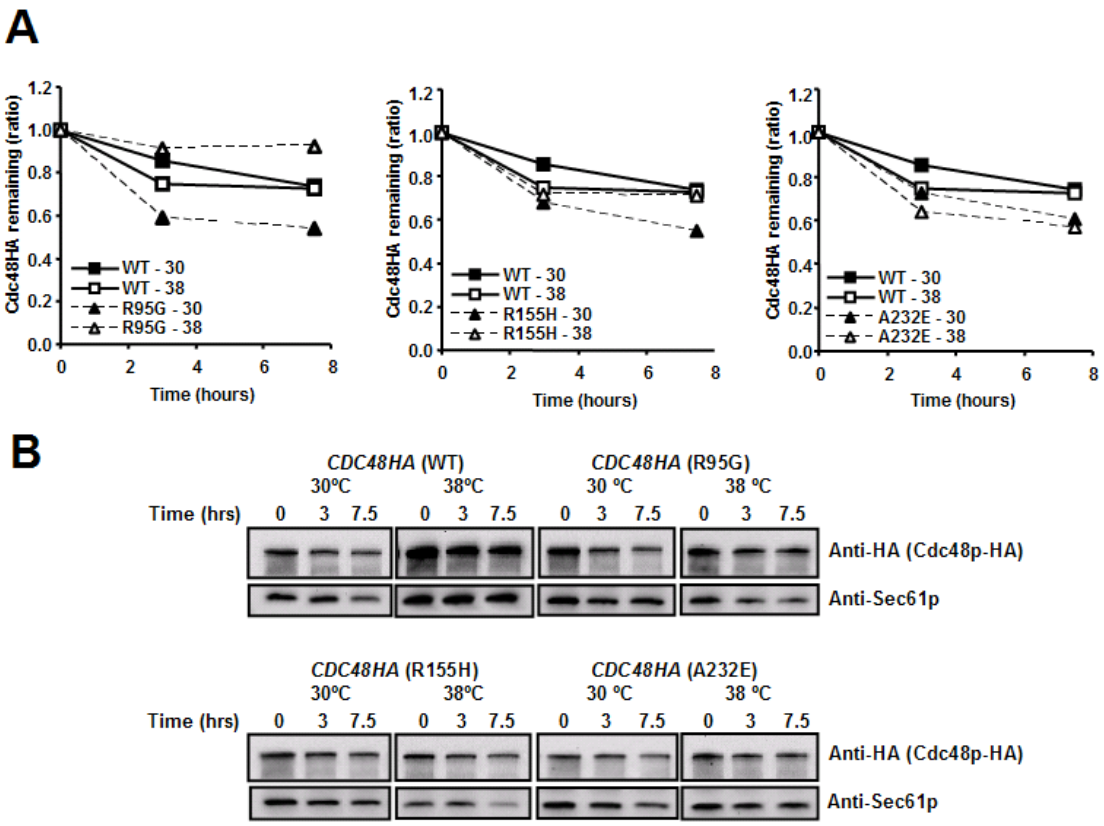

Figure 36. Cdc48p-HA is a stable protein

A and B. The stability of Cdc48p-HA was assessed by cycloheximide chase assay as described in the Experimental Procedures sections. **A.** represents the quantitation of two independent experiments and **B.** are representative figures from the experiment.

A.2.3 Temperature sensitive IBMPFD mutants are due to a genetic interaction between the mutant allele and the epitope tag

To ensure that effects seen in the IBMPFD mutations were due solely to the mutation, a graduate rotation student, Bill Glassford and I tested the recoverability of the temperature sensitive phenotype. This assessment was important because epitope tagging at the carboxy terminus of Cdc48p might impair the binding of select cofactors, such as (BOHM *et al.* 2011; RUMPF and JENTSCH 2006). In this experiment, the temperature sensitive R95G and A232E strains were transformed with an empty vector, or a vector designed to express wild-type versions of Cdc48p that were untagged, HA-tagged or Myc-tagged at the carboxy terminus. As seen in Figure 37, all strains grew normally at the permissive temperature (30ºC). However, when the strains were incubated at high temperature (38ºC), only the strains expressing the untagged or Myc-tagged versions of Cdc48p recovered the temperature sensitive phenotype of the R95G and A232E mutations. This result was quite surprising and suggested that the phenotype of the R95G and A232E *CDC48-HA* mutant constructs was due to a combined effect of the mutant allele and the epitope tag.

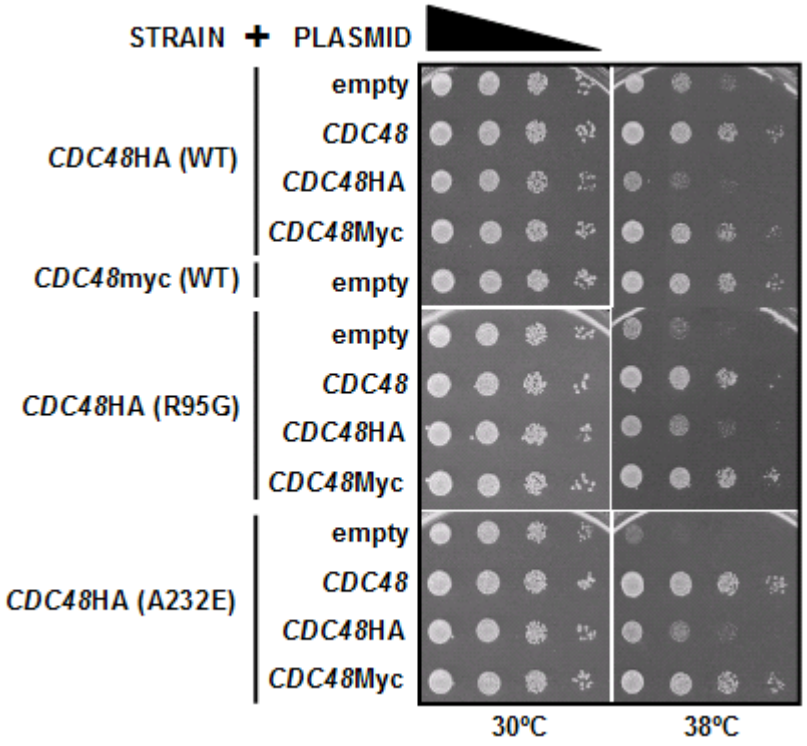

Figure 37. The temperature sensitivity seen in select IBMPFD-CDC48-HA alleles is the result of a compound effect of the mutant allele and the HA-epitope tag

The indicated strains (left of the vertical bar) were transformed with the indicated plasmids (right of the bar). The strains were spot plated (10-fold serial dilutions) and selective media and incubated at the indicated temperatures.

A.2.4 Cdc48p-HA hexamers exhibit slower migration than Cdc48p-Myc hexamers

Many IBMPFD mutations affect the amino-terminus and the first AAA ATPase domain of p97/Cdc48p (HALAWANI *et al.* 2009). A classic temperature sensitive of *CDC48, cdc48-3*, possesses mutations in the first AAA ATPase domain (see Figure 11 in Chapter 1). During the course of my studies, I discovered that the *cdc48-3* mutant, when incubated at a permissive temperature, lacked detectable free hexamers as assessed by native PAGE (Figure 38). Thus, one possible explanation for the temperature sensitivity of Cdc48p-HA is that free hexamers may be depleted. To test examine this, a graduate rotation student, Bill Glassford and I performed a native gel assay using lysates from yeast expressing Cdc48p-HA or Cdc48p-Myc alone, or both Cdc48p-HA and Cdc48p-Myc. We also assessed the effect of temperature on Cdc48p-HA and Cdc48p-Myc hexamers. As observed in Figure 39A, Cdc48p-HA hexamers showed a slower apparent migration when compared to Cdc48p-Myc hexamers (compare lanes 3, 4, 7, 8, 11-14 in Figure 39A). The signal corresponding to the Cdc48p-Myc hexamer consistently migrated faster than Cdc48p-HA hexamers (compare lanes 3 and 4 with 11 and 12 in Figure 39A). Cdc48p-HA and Cdc48p-Myc also displayed altered gel filtration profiles (Figure 39B). Interestingly, mixed Cdc48p-HA and Cdc48p-Myc hexamers also migrated with the same apparent mobility as the Cdc48p-Myc hexamer alone (compare lanes 7 and 8 with 11-14 in Figure 39A). The presence of mixed Cdc48p-HA and Cdc48p-Myc hexamers was confirmed by reciprocal immunoprecipation experiments (Figure 39C). These results indicate that Cdc48p-Myc confers this type of hexamer mobility even in the presence of temperature sensitive Cdc48p-HA subunits.

The incubation of cells at 38ºC led to a noticeable decrease in Cdc48p-HA hexamers (compare lanes 3 and 4 in Figure 39A), whereas Cdc48p-Myc hexamers appeared to increase with high temperature exposure (Figure 39A, lanes 11 and 12). Intriguingly, these two aforementioned properties were quite apparent when strains expressed both Cdc48p-HA and Cdc48p-Myc (compared the upper and lower bands seen in lanes 7 and 8 of Figure 39A). These data collectively suggest that temperature sensitivity of Cdc48p-HA may be caused by the loss of free hexamers, and that the R95G and A232E IBMPFD mutations further compromise a Cdc48p-HA hexamer-associated process.

In Figure 38, I found that the loss of *UFD2* results in faster Cdc48p hexamer migration. Given that Ufd2p binds to the carboxy terminus of Cdc48p, I wondered if the slower migration of the Cdc48p-HA hexamer was caused by the tight binding of Ufd2p to the carboxy terminus. The tight binding of Ufd2p to Cdc48p-HA would exclude the binding of the DUB, Otu1p (RUMPF and JENTSCH 2006). Thus the HA tag may lead to an overrepresentation of pro-degradative Cdc48p-Ufd2p within the cell. To test this idea, I deleted the *UFD2* gene in the different IBMPFD mutant *CDC48-HA* backgrounds and tested for the recovery of temperature sensitivity. As seen in Figure 40, the deletion of *UFD2* did not rescue temperature sensitivity in any of these strains tested.

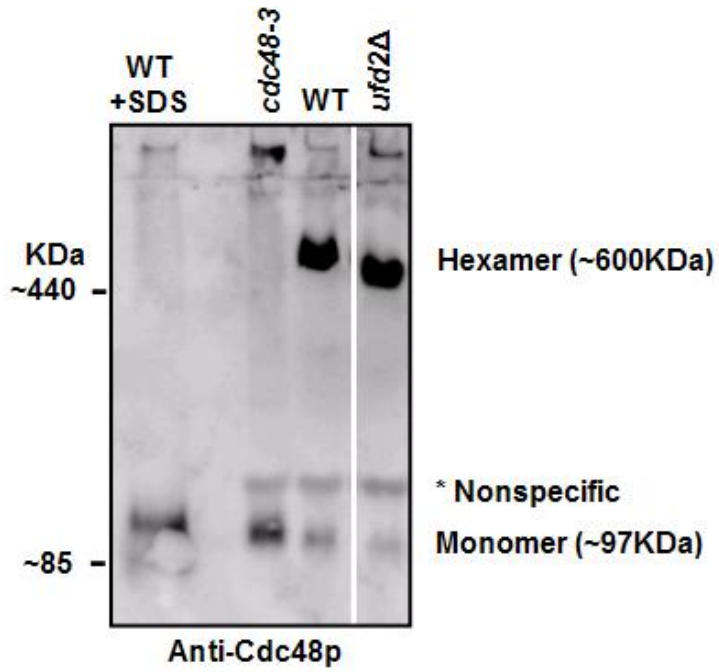

Figure 38. The cdc48-3 allele causes the loss of free hexamer

Cytosolic extracts were prepared from the indicated strains. A total of 25µg of protein was resolved by native PAGE as described in the Experimental Procedures section. Western blotting was performed with the anti-Cdc48p antibody (a kind gift from Dr. Rasmus Hartman-Petersen). For SDS treatment, SDS was added to a final concentration of 0.5% and the sample was incubated at 75ºC.

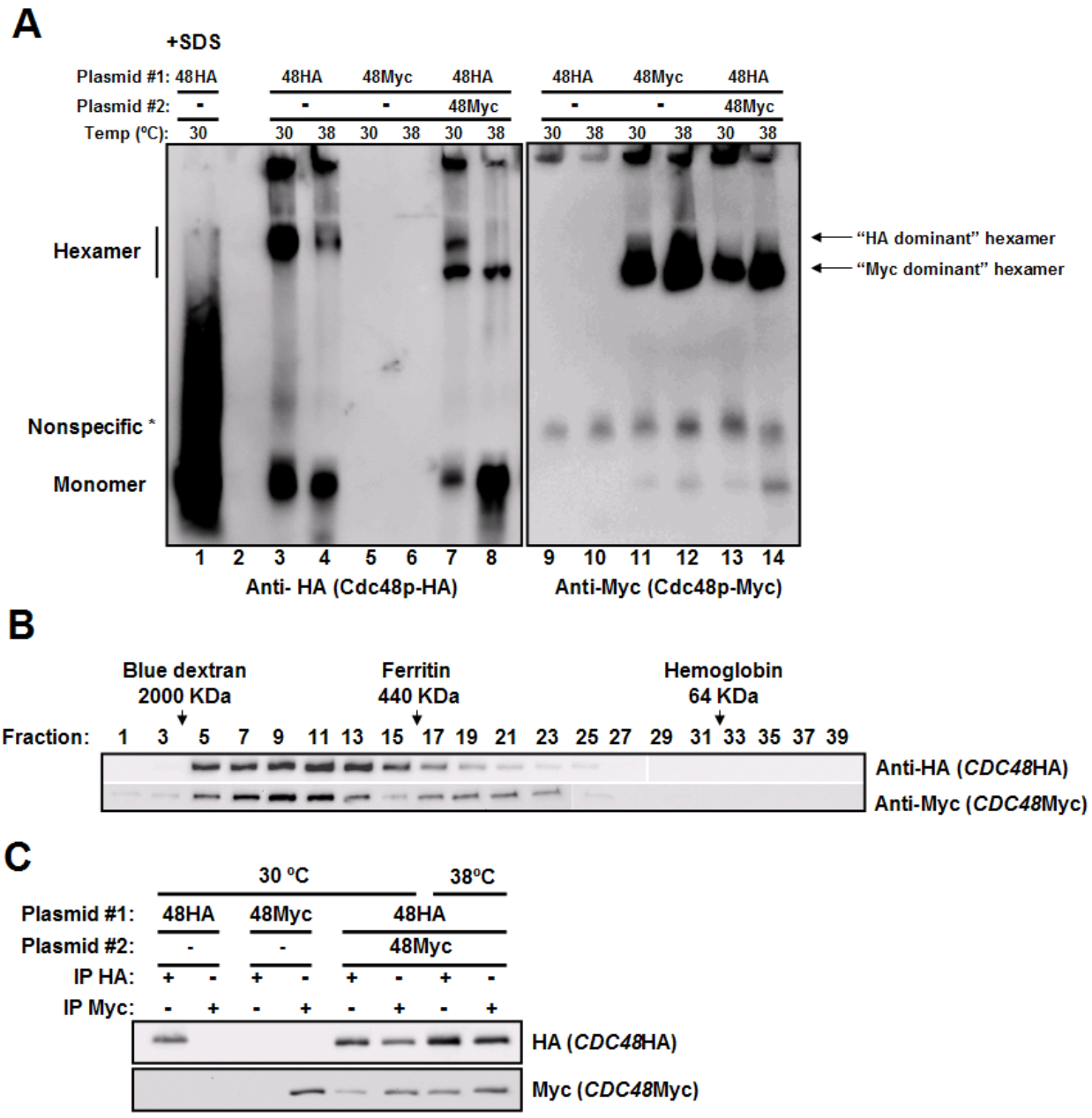

Figure 39. Cdc48p-HA hexamers display a different migration pattern than Cdc48p-Myc hexamers

A. The indicated cells were grown at either permissive (30ºC) or non-permissive (38ºC for 2-4 h) temperatures. Cytosolic extracts were prepared from the indicated strains and 25µg of the cytosolic extract was resolved by native PAGE as described in the Experimental Procedures section. Western blotting was performed with antibodies against the epitope tags found at the carboxy terminus of Cdc48p. **B.** A total of 10mg of cytosolic extract from wild-type Cdc48p-HA

and Cdc48p-Myc was separated by gel filtration (Sephacryl S300HR) column chromatography as described in the Experimental Procedures section. Total protein from each fraction was TCA precipitated and resolved by SDS-PAGE. Western blotting was performed with the indicated antibodies to assess the distribution of Cdc48p complexes. **C.** Immunoprecipitation experiments were performed to assess the formation of mixed hexamers and were done as described in the Experimental Procedures section. Immunoprecipitated proteins were resolved by SDS-PAGE and western blotted with the indicated antibodies.

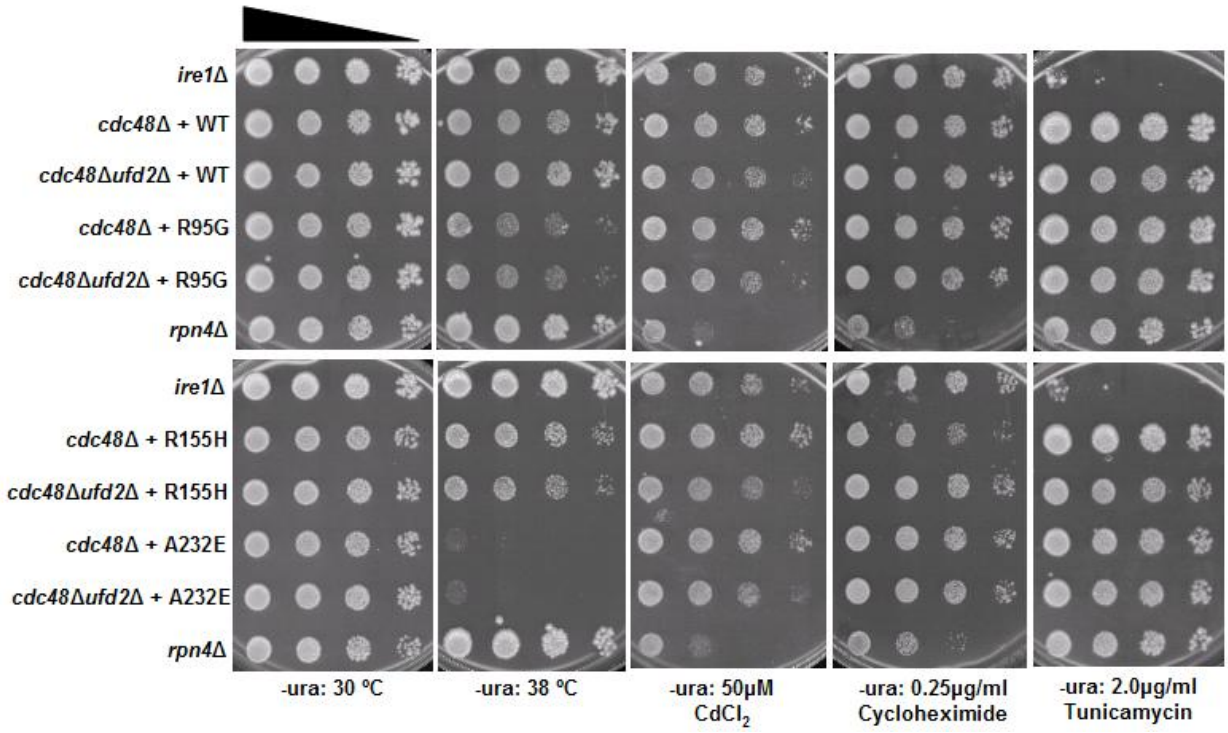

Figure 40. The loss of UFD2 does not rescue the temperature sensitive IBMPFD-CDC48-HA alleles

The indicated strains were spot tested (10-fold serial dilution) for sensitivity at permissive (30ºC) or non-permissive (38ºC) temperatures, and also for sensitivity towards the indicated chemical stress agents.

A.2.5 IBMPFD mutations modeled into *CDC48-MYC* are not temperature sensitive

Given that the original goal of this project was to model IBMPFD disease-causing mutations in yeast, I created a second series of strains containing IBMPFD mutations in a *CDC48-Myc* gene and tested for the expression of these alleles. The strategy was identical to that used to create the IBMPFD *CDC48-HA* strains (Figure 33). Like their IBMPFD *CDC48-HA* counterparts, the Cdc48p-Myc versions all expressed the mutant proteins to levels comparable to that of the wild-type protein (Figure 41A). To see if the IBMPFD *CDC48-Myc* strains had compromised stress tolerance, I performed the serial dilution spot test at permissive (30ºC) and non-permissive (38ºC) temperatures, and also on media containing different chemical stress agents. As observed in Figure 41B, the modeling of IBMPFD mutations in the *CDC48-Myc* gene did not lead to sensitivity at higher temperature or on any tested chemical stressors. Additionally, the IBMPFD-CDC48-Myc alleles displayed no apparent ERAD defect for two different substrates (Figure 42A and B) and no defect in autophagy (Figure 43). Thus, I conclude that select IBMPFD mutations when combined with the HA epitope tag at the carboxy terminus, mimic some aspects of the molecular pathology of IBMPFD.

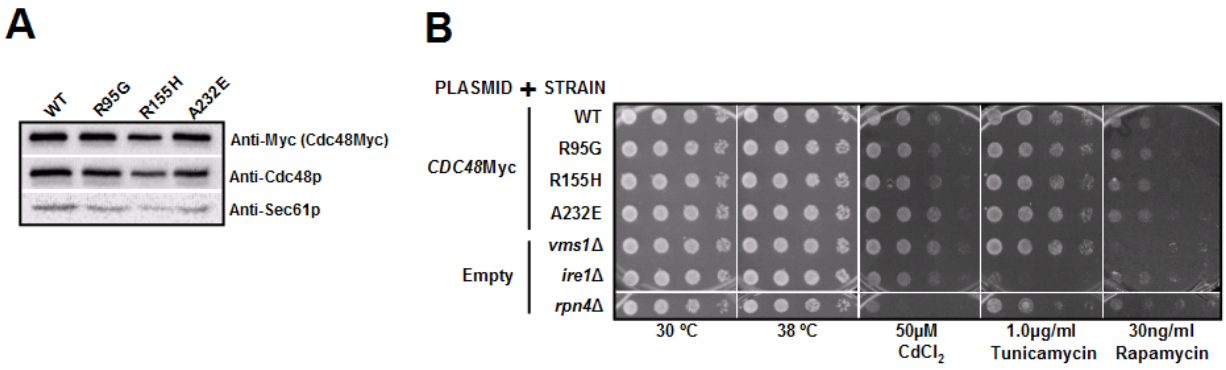

Figure 41. IBMPFD mutations modeled in the CDC48-Myc gene is not temperature sensitive

A. IBMPFD mutants were constructed as described in the Experimental Procedures section. The procedure is illustrated in Figure 1. Western blot was performed from total protein extracts from the indicated strains to assess the level of protein expression between the various IBMPFD alleles. **B.** The indicated strains were spot tested (10-fold serial dilution) for sensitivity at permissive (30ºC) or non-permissive (38ºC) temperatures, and also for sensitivity towards the indicated chemical stress agents.

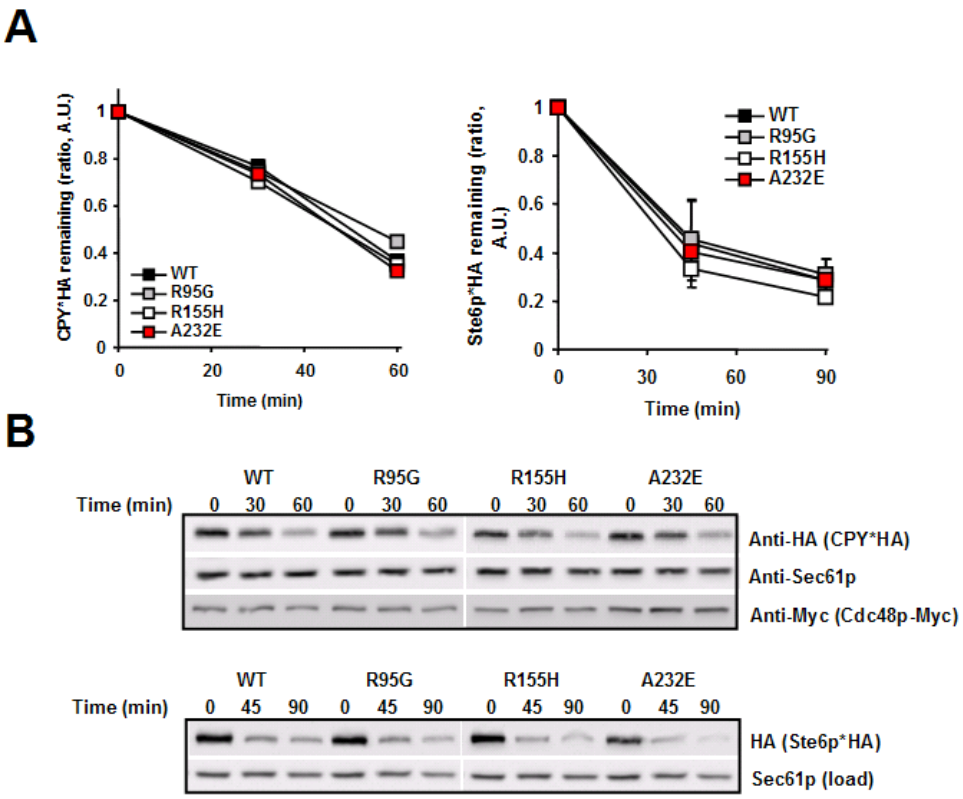

Figure 42. IBMPFD mutations modeled in the CDC48-Myc gene do not negatively affect the ERAD of two model substrates

A. and B. The ERAD of Ste6p*, a transmembrane substrate and CPY*, a soluble ER-lumenal substrate was assessed by cycloheximide chase as described in the Experimental Procedures section. **A.** Quantitation of protein levels from three independent experiments. Representative figures are shown in **B**.

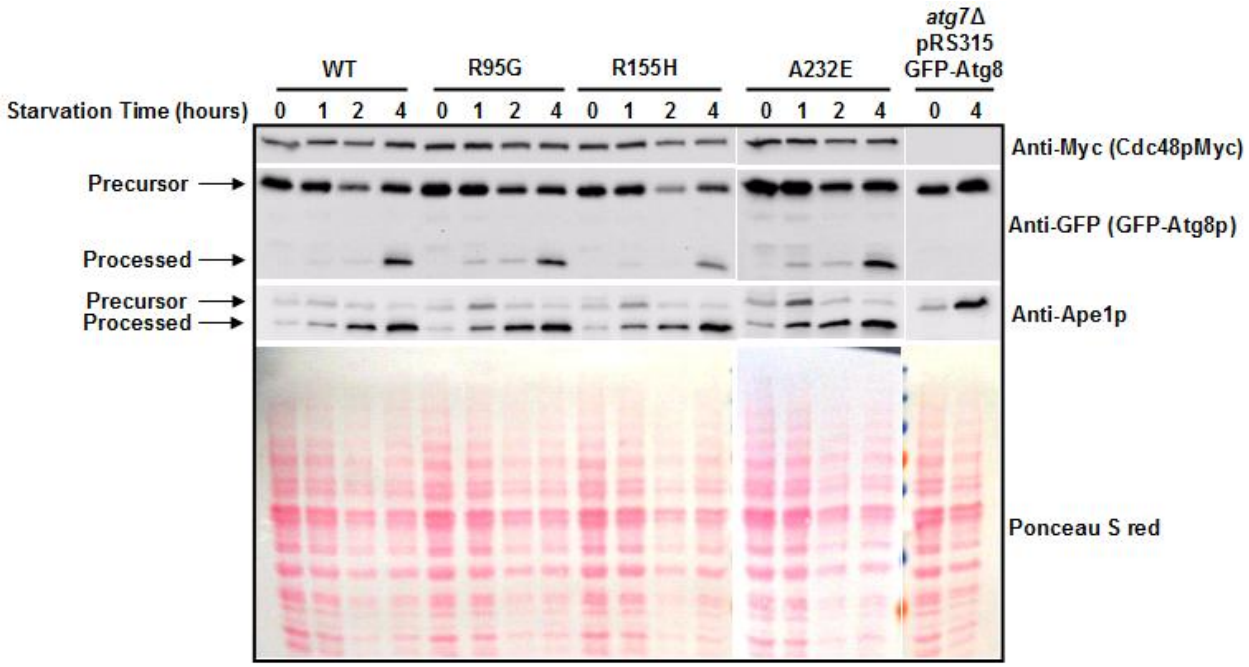

Figure 43. IBMPFD mutations modeled in the CDC48-Myc gene do not show autophagy defects

The indicated strains were transformed with a vector designed to express GFP-*ATG8*, a reporter of autophagy. The induction of autophagy was performed as a time-course experiment as described in the Experimental Procedures section. Total protein was precipitated and resolved by SDS-PAGE and western blotting was performed with the indicated antibodies. Ponceau S red staining is included as an indicator of relative protein loading.

A.3 DISCUSSION

The modeling of IBMPFD mutations in epitope tagged versions of the yeast *CDC48* gene has led to a number of insights. First, the HA-, but not the Myc-epitope tag compounds the effects of the R95G and A232E alleles to cause temperature sensitivity and autophagic defects. This finding is remarkable given the fact that the HA tag (amino acids sequence: YPYDVPDYA) is a single HA, which was presumed to be minimally obstructive to Cdc48p function. The Myc-tag (amino acid sequence: EQKLISEEDL) is also present as a single copy. The observed difference in temperature sensitivity is likely due to the sequence of the HA tag.

Incubating "wild-type" Cdc48p-HA yeast at high temperature led to a noticeable decrease in the amount of free hexamer (Figure 39A, lanes 3, 4, 7, 8). The classic temperature sensitive allele, *cdc48-3*, which possesses a pair of mutations in the first AAA ATPase domain, is largely devoid of free hexamers. Wild-type Cdc48p-HA, when incubated at high temperature, may mimic the *cdc48-3* allele at permissive temperature. This is conceptually interesting since the HA tag and *cdc48-3* allele reside on opposite ends of the protein. Given that the first AAA ATPase domain, which is the domain mutated in *cdc48-3*, is involved in hexamerization, this implies that the carboxy terminus affects the hexamerization domain. This is further supported by the fact that the R95G and A232E IBMPFD alleles and HA tag are on opposite ends the Cdc48p protein. Intriguingly, the R95G temperature sensitivity is less severe than that caused by the A232E allele, but more severe than the non-mutated version of *CDC48-HA*. The R95G mutation is in the

amino-terminus domain which binds cofactors. It is formally possible that the effects seen in the R95G mutant/HA-tag combination is due to changes in cofactor binding in addition to whatever effect the HA tag causes. One suggested experiment would be to immunoprecipitate the different mutant proteins and perform mass spectrometry. The expectation is that the R95G/HA-tag combination will show a different spectrum of associated cofactors.

Additionally, performing the native gel assay with both HA- and Myc- tagged versions of IBMPFD mutants might prove insightful. A comparison between the IBMPFD mutants and other temperature sensitive alleles of *CDC48*, such as *cdc48-1*, *2* and *10*, and mutants defective in nucleotide binding and hydrolysis would be most interesting. Further, assessing the distribution of hexamers in the *UFD2*/IBMPFD double mutants could shed light on the anomalous hexamer migration observed in yeast expressing Cdc48p-HA. In addition, overexpressing *UFD2* may be insightful.

The anomalous migration of Cdc48p-HA hexamer is particularly intriguing because it appears that incubation at high temperature causes a loss of free hexamer (Figure 39A lanes 3 and 4). I believe that this is a result of protein aggregation, which is supported by the following two reasons. First, the high temperature incubation does not lead to an increase in monomer or HA-reactive signal found in the loading well of the native gel. Second, the extracts are clarified cytosolic extracts, so insoluble material is largely removed. This notion could be easily tested by comparing the total Cdc48p-HA levels in insoluble and cytosolic fractions by SDS-PAGE.

BIBLIOGRAPHY

ABRAMOFF, M. D., M. P. J. and R. S. J., 2004 Image Processing with ImageJ. Biophotonics International **11:** 36-42.

ADAMS, A., GOTTSCHLING, D. E., KAISER, C. A., STEARNS, T., 1997 *Methods in Yeast Genetics*. Cold Spring Harbor Laboratory Press.

ADAMS, J., and M. KAUFFMAN, 2004 Development of the proteasome inhibitor Velcade (Bortezomib). Cancer Invest **22:** 304-311.

AHNER, A., K. NAKATSUKASA, H. ZHANG, R. A. FRIZZELL and J. L. BRODSKY, 2007 Small heat-shock proteins select DeltaF508-CFTR for endoplasmic reticulum-associated degradation. Mol Biol Cell **18:** 806-814.

ALBERTS, S. M., C. SONNTAG, A. SCHAFER and D. H. WOLF, 2009 Ubx4 modulates cdc48 activity and influences degradation of misfolded proteins of the endoplasmic reticulum. The Journal of biological chemistry **284:** 16082-16089.

ALEXANDRU, G., J. GRAUMANN, G. T. SMITH, N. J. KOLAWA, R. FANG *et al.*, 2008 UBXD7 binds multiple ubiquitin ligases and implicates p97 in HIF1alpha turnover. Cell **134:** 804-816.

AMERIK, A. Y., and M. HOCHSTRASSER, 2004 Mechanism and function of deubiquitinating enzymes. Biochim Biophys Acta **1695:** 189-207.

AMERIK, A. Y., J. NOWAK, S. SWAMINATHAN and M. HOCHSTRASSER, 2000 The Doa4 deubiquitinating enzyme is functionally linked to the vacuolar protein-sorting and endocytic pathways. Mol Biol Cell **11:** 3365-3380.

ARNASON, T., and M. J. ELLISON, 1994 Stress resistance in Saccharomyces cerevisiae is strongly correlated with assembly of a novel type of multiubiquitin chain. Mol Cell Biol **14:** 7876-7883.

ARRIBAS, J., and J. G. CASTANO, 1990 Kinetic studies of the differential effect of detergents on the peptidase activities of the multicatalytic proteinase from rat liver. J Biol Chem **265:** 13969-13973.

ASHER, G., P. TSVETKOV, C. KAHANA and Y. SHAUL, 2005 A mechanism of ubiquitin-independent proteasomal degradation of the tumor suppressors p53 and p73. Genes Dev **19:** 316-321.

BABBITT, S. E., A. KISS, A. E. DEFFENBAUGH, Y. H. CHANG, E. BAILLY *et al.*, 2005 ATP hydrolysis-dependent disassembly of the 26S proteasome is part of the catalytic cycle. Cell **121:** 553-565.

BACHMAIR, A., D. FINLEY and A. VARSHAVSKY, 1986 In vivo half-life of a protein is a function of its amino-terminal residue. Science **234:** 179-186.

BAILLY, V., S. LAUDER, S. PRAKASH and L. PRAKASH, 1997 Yeast DNA repair proteins Rad6 and Rad18 form a heterodimer that has ubiquitin conjugating, DNA binding, and ATP hydrolytic activities. J Biol Chem **272:** 23360-23365.

BALCH, W. E., R. I. MORIMOTO, A. DILLIN and J. W. KELLY, 2008 Adapting proteostasis for disease intervention. Science **319:** 916-919.

BALLAR, P., Y. SHEN, H. YANG and S. FANG, 2006 The role of a novel p97/valosin-containing protein-interacting motif of gp78 in endoplasmic reticulum-associated degradation. J Biol Chem **281:** 35359-35368.

BARTHELME, D., and R. T. SAUER, 2012 Identification of the Cdc48bullet20S Proteasome as an Ancient AAA+ Proteolytic Machine. Science.

BAUGH, J. M., E. G. VIKTOROVA and E. V. PILIPENKO, 2009 Proteasomes can degrade a significant proportion of cellular proteins independent of ubiquitination. J Mol Biol **386:** 814-827.

BAYS, N. W., R. G. GARDNER, L. P. SEELIG, C. A. JOAZEIRO and R. Y. HAMPTON, 2001a Hrd1p/Der3p is a membrane-anchored ubiquitin ligase required for ER-associated degradation. Nat Cell Biol **3:** 24-29.

BAYS, N. W., S. K. WILHOVSKY, A. GORADIA, K. HODGKISS-HARLOW and R. Y. HAMPTON, 2001b HRD4/NPL4 is required for the proteasomal processing of ubiquitinated ER proteins. Mol Biol Cell **12:** 4114-4128.

BECH-OTSCHIR, D., A. HELFRICH, C. ENENKEL, G. CONSIGLIERI, M. SEEGER *et al.*, 2009 Polyubiquitin substrates allosterically activate their own degradation by the 26S proteasome. Nat Struct Mol Biol **16:** 219-225.

BEN-SAADON, R., D. ZAAROOR, T. ZIV and A. CIECHANOVER, 2006 The polycomb protein Ring1B generates self atypical mixed ubiquitin chains required for its in vitro histone H2A ligase activity. Mol Cell **24:** 701-711.

BERTRAM, C., N. VON NEUHOFF, B. SKAWRAN, D. STEINEMANN, B. SCHLEGELBERGER *et al.*, 2008 The differentiation/retrodifferentiation program of human U937 leukemia cells is accompanied by changes of VCP/p97. BMC Cell Biol **9:** 12.

BESCHE, H. C., W. HAAS, S. P. GYGI and A. L. GOLDBERG, 2009a Isolation of mammalian 26S proteasomes and p97/VCP complexes using the ubiquitin-like domain from HHR23B reveals novel proteasome-associated proteins. Biochemistry **48:** 2538-2549.

BESCHE, H. C., A. PETH and A. L. GOLDBERG, 2009b Getting to first base in proteasome assembly. Cell **138:** 25-28.

BEURON, F., I. DREVENY, X. YUAN, V. E. PYE, C. MCKEOWN *et al.*, 2006 Conformational changes in the AAA ATPase p97-p47 adaptor complex. EMBO J **25:** 1967-1976.

BHAMIDIPATI, A., V. DENIC, E. M. QUAN and J. S. WEISSMAN, 2005 Exploration of the topological requirements of ERAD identifies Yos9p as a lectin sensor of misfolded glycoproteins in the ER lumen. Mol Cell **19:** 741-751.

BIEDERER, T., C. VOLKWEIN and T. SOMMER, 1997 Role of Cue1p in ubiquitination and degradation at the ER surface. Science **278:** 1806-1809.

BOGAN, J. S., N. HENDON, A. E. MCKEE, T. S. TSAO and H. F. LODISH, 2003 Functional cloning of TUG as a regulator of GLUT4 glucose transporter trafficking. Nature **425:** 727-733.

BOHM, S., G. LAMBERTI, V. FERNANDEZ-SAIZ, C. STAPF and A. BUCHBERGER, 2011 Cellular functions of Ufd2 and Ufd3 in proteasomal protein degradation depend on Cdc48 binding. Mol Cell Biol **31:** 1528-1539.

BRAUN, S., K. MATUSCHEWSKI, M. RAPE, S. THOMS and S. JENTSCH, 2002 Role of the ubiquitin-selective CDC48(UFD1/NPL4)chaperone (segregase) in ERAD of OLE1 and other substrates. Embo J **21:** 615-621.

BRODSKY, J. L., 2007 The protective and destructive roles played by molecular chaperones during ERAD (endoplasmic-reticulum-associated degradation). Biochem J **404:** 353-363.

BRODSKY, J. L., and R. SCHEKMAN, 1993 A Sec63p-BiP complex from yeast is required for protein translocation in a reconstituted proteoliposome. J Cell Biol **123:** 1355-1363.

BRODSKY, J. L., and W. R. SKACH, 2011 Protein folding and quality control in the endoplasmic reticulum: Recent lessons from yeast and mammalian cell systems. Current opinion in cell biology **23:** 464-475.

BRUDERER, R. M., C. BRASSEUR and H. H. MEYER, 2004 The AAA ATPase p97/VCP interacts with its alternative co-factors, Ufd1-Npl4 and p47, through a common bipartite binding mechanism. J Biol Chem **279:** 49609-49616.

BUCHBERGER, A., B. BUKAU and T. SOMMER, 2010 Protein quality control in the cytosol and the endoplasmic reticulum: brothers in arms. Mol Cell **40:** 238-252.

BUCHBERGER, A., M. J. HOWARD, M. PROCTOR and M. BYCROFT, 2001 The UBX domain: a widespread ubiquitin-like module. J Mol Biol **307:** 17-24.

BUCK, T. M., C. M. WRIGHT and J. L. BRODSKY, 2007 The activities and function of molecular chaperones in the endoplasmic reticulum. Semin Cell Dev Biol **18:** 751-761.

CAO, K., R. NAKAJIMA, H. H. MEYER and Y. ZHENG, 2003 The AAA-ATPase Cdc48/p97 regulates spindle disassembly at the end of mitosis. Cell **115:** 355-367.

CARROLL, S. M., and R. Y. HAMPTON, 2010 Usa1p is required for optimal function and regulation of the Hrd1p endoplasmic reticulum-associated degradation ubiquitin ligase. J Biol Chem **285:** 5146-5156.

CARVALHO, P., V. GODER and T. A. RAPOPORT, 2006 Distinct ubiquitin-ligase complexes define convergent pathways for the degradation of ER proteins. Cell **126:** 361-373.

CARVALHO, P., A. M. STANLEY and T. A. RAPOPORT, 2010 Retrotranslocation of a misfolded luminal ER protein by the ubiquitin-ligase Hrd1p. Cell **143:** 579-591.

CHANDRA, A., L. CHEN, H. LIANG and K. MADURA, 2010 Proteasome assembly influences interaction with ubiquitinated proteins and shuttle factors. J Biol Chem **285:** 8330-8339.

CHAU, V., J. W. TOBIAS, A. BACHMAIR, D. MARRIOTT, D. J. ECKER *et al.*, 1989 A multiubiquitin chain is confined to specific lysine in a targeted short-lived protein. Science **243:** 1576-1583.

CHEN, L., L. ROMERO, S. M. CHUANG, V. TOURNIER, K. K. JOSHI *et al.*, 2011 Sts1 plays a key role in targeting proteasomes to the nucleus. J Biol Chem **286:** 3104-3118.

CHEN, P., and M. HOCHSTRASSER, 1996 Autocatalytic subunit processing couples active site formation in the 20S proteasome to completion of assembly. Cell **86:** 961-972.

CHENG, Q., L. CHEN, Z. LI, W. S. LANE and J. CHEN, 2009 ATM activates p53 by regulating MDM2 oligomerization and E3 processivity. EMBO J **28:** 3857-3867.

CHENG, Y. L., and R. H. CHEN, 2010 The AAA-ATPase Cdc48 and cofactor Shp1 promote chromosome bi-orientation by balancing Aurora B activity. J Cell Sci **123:** 2025-2034.

CHEONG, H., and D. J. KLIONSKY, 2008 Biochemical methods to monitor autophagy-related processes in yeast. Methods Enzymol **451:** 1-26.

CHRISTIANSON, T. W., R. S. SIKORSKI, M. DANTE, J. H. SHERO and P. HIETER, 1992 Multifunctional yeast high-copy-number shuttle vectors. Gene **110:** 119-122.

CONFORTI, L., A. TARLTON, T. G. MACK, W. MI, E. A. BUCKMASTER *et al.*, 2000 A Ufd2/D4Cole1e chimeric protein and overexpression of Rbp7 in the slow Wallerian degeneration (WldS) mouse. Proc Natl Acad Sci U S A **97:** 11377-11382.

COSTANZO, M., A. BARYSHNIKOVA, C. L. MYERS, B. ANDREWS and C. BOONE, 2011 Charting the genetic interaction map of a cell. Current opinion in biotechnology **22:** 66-74.

COUGHLAN, C. M., J. L. WALKER, J. C. COCHRAN, K. D. WITTRUP and J. L. BRODSKY, 2004 Degradation of mutated bovine pancreatic trypsin inhibitor in the yeast vacuole suggests post-endoplasmic reticulum protein quality control. J Biol Chem **279:** 15289-15297.

COX, J. S., C. E. SHAMU and P. WALTER, 1993 Transcriptional induction of genes encoding endoplasmic reticulum resident proteins requires a transmembrane protein kinase. Cell **73:** 1197-1206.

CREWS, C. M., 2003 Feeding the machine: mechanisms of proteasome-catalyzed degradation of ubiquitinated proteins. Current opinion in chemical biology **7:** 534-539.

CROSAS, B., J. HANNA, D. S. KIRKPATRICK, D. P. ZHANG, Y. TONE *et al.*, 2006 Ubiquitin chains are remodeled at the proteasome by opposing ubiquitin ligase and deubiquitinating activities. Cell **127:** 1401-1413.

CSALA, M., G. BANHEGYI and A. BENEDETTI, 2006 Endoplasmic reticulum: a metabolic compartment. FEBS Lett **580:** 2160-2165.

CUI, D. Y., C. R. BROWN and H. L. CHIANG, 2004 The type 1 phosphatase Reg1p-Glc7p is required for the glucose-induced degradation of fructose-1,6-bisphosphatase in the vacuole. J Biol Chem **279:** 9713-9724.

DAHLMANN, B., M. RUTSCHMANN, L. KUEHN and H. REINAUER, 1985 Activation of the multicatalytic proteinase from rat skeletal muscle by fatty acids or sodium dodecyl sulphate. Biochem J **228:** 171-177.

DAI, R. M., E. CHEN, D. L. LONGO, C. M. GORBEA and C. C. LI, 1998 Involvement of valosin-containing protein, an ATPase Co-purified with IkappaBalpha and 26 S proteasome, in ubiquitin-proteasome-mediated degradation of IkappaBalpha. J Biol Chem **273:** 3562-3573.

DANGE, T., D. SMITH, T. NOY, P. C. ROMMEL, L. JURZITZA *et al.*, 2011 Blm10 protein promotes proteasomal substrate turnover by an active gating mechanism. J Biol Chem **286:** 42830-42839.

DANTUMA, N. P., C. HEINEN and D. HOOGSTRATEN, 2009 The ubiquitin receptor Rad23: at the crossroads of nucleotide excision repair and proteasomal degradation. DNA Repair (Amst) **8:** 449-460.

DECOTTIGNIES, A., A. EVAIN and M. GHISLAIN, 2004 Binding of Cdc48p to a ubiquitin-related UBX domain from novel yeast proteins involved in intracellular proteolysis and sporulation. Yeast **21:** 127-139.

DELABARRE, B., and A. T. BRUNGER, 2003 Complete structure of p97/valosin-containing protein reveals communication between nucleotide domains. Nat Struct Biol **10:** 856-863.

DELABARRE, B., J. C. CHRISTIANSON, R. R. KOPITO and A. T. BRUNGER, 2006 Central pore residues mediate the p97/VCP activity required for ERAD. Mol Cell **22:** 451-462.

DENIC, V., E. M. QUAN and J. S. WEISSMAN, 2006 A luminal surveillance complex that selects misfolded glycoproteins for ER-associated degradation. Cell **126:** 349-359.

DESHAIES, R. J., and C. A. JOAZEIRO, 2009 RING domain E3 ubiquitin ligases. Annu Rev Biochem **78:** 399-434.

DESHAIES, R. J., and R. SCHEKMAN, 1989 SEC62 encodes a putative membrane protein required for protein translocation into the yeast endoplasmic reticulum. J Cell Biol **109:** 2653-2664.

DRISCOLL, J., M. G. BROWN, D. FINLEY and J. J. MONACO, 1993 MHC-linked LMP gene products specifically alter peptidase activities of the proteasome. Nature **365:** 262-264.

DRISCOLL, J., and A. L. GOLDBERG, 1990 The proteasome (multicatalytic protease) is a component of the 1500-kDa proteolytic complex which degrades ubiquitin-conjugated proteins. J Biol Chem **265:** 4789-4792.

DUBIEL, W., K. FERRELL and M. RECHSTEINER, 1995 Subunits of the regulatory complex of the 26S protease. Molecular biology reports **21:** 27-34.

ELSASSER, S., R. R. GALI, M. SCHWICKART, C. N. LARSEN, D. S. LEGGETT *et al.*, 2002 Proteasome subunit Rpn1 binds ubiquitin-like protein domains. Nat Cell Biol **4:** 725-730.

ELSASSER, S., M. SCHMIDT and D. FINLEY, 2005 Characterization of the proteasome using native gel electrophoresis. Methods Enzymol **398:** 353-363.

ENENKEL, C., A. LEHMANN and P. M. KLOETZEL, 1998 Subcellular distribution of proteasomes implicates a major location of protein degradation in the nuclear envelope-ER network in yeast. Embo J **17:** 6144-6154.

EYTAN, E., D. GANOTH, T. ARMON and A. HERSHKO, 1989 ATP-dependent incorporation of 20S protease into the 26S complex that degrades proteins conjugated to ubiquitin. Proc Natl Acad Sci U S A **86:** 7751-7755.

FARESE, R. V., JR., and T. C. WALTHER, 2009 Lipid droplets finally get a little R-E-S-P-E-C-T. Cell **139:** 855-860.

FINLEY, D., 2009 Recognition and processing of ubiquitin-protein conjugates by the proteasome. Annu Rev Biochem **78:** 477-513.

FLEMING, J. A., E. S. LIGHTCAP, S. SADIS, V. THORODDSEN, C. E. BULAWA *et al.*, 2002 Complementary whole-genome technologies reveal the cellular response to proteasome inhibition by PS-341. Proc Natl Acad Sci U S A **99:** 1461-1466.

FREEMONT, P. S., I. M. HANSON and J. TROWSDALE, 1991 A novel cysteine-rich sequence motif. Cell **64:** 483-484.

FRICKE, B., S. HEINK, J. STEFFEN, P. M. KLOETZEL and E. KRUGER, 2007 The proteasome maturation protein POMP facilitates major steps of 20S proteasome formation at the endoplasmic reticulum. EMBO Rep **8:** 1170-1175.

FROHLICH, K. U., H. W. FRIES, M. RUDIGER, R. ERDMANN, D. BOTSTEIN *et al.*, 1991 Yeast cell cycle protein CDC48p shows full-length homology to the mammalian protein VCP and is a member of a protein family involved in secretion, peroxisome formation, and gene expression. J Cell Biol **114:** 443-453.

FUJII, K., M. KITABATAKE, T. SAKATA and M. OHNO, 2012 40S subunit dissociation and proteasome-dependent RNA degradation in nonfunctional 25S rRNA decay. EMBO J **31:** 2579-2589.

FUKUNAGA, K., T. KUDO, A. TOH-E, K. TANAKA and Y. SAEKI, 2010 Dissection of the assembly pathway of the proteasome lid in Saccharomyces cerevisiae. Biochem Biophys Res Commun **396:** 1048-1053.

FUNAKOSHI, M., X. LI, I. VELICHUTINA, M. HOCHSTRASSER and H. KOBAYASHI, 2004 Sem1, the yeast ortholog of a human BRCA2-binding protein, is a component of the proteasome regulatory particle that enhances proteasome stability. J Cell Sci **117:** 6447-6454.

FUNAKOSHI, M., R. J. TOMKO, JR., H. KOBAYASHI and M. HOCHSTRASSER, 2009 Multiple assembly chaperones govern biogenesis of the proteasome regulatory particle base. Cell **137:** 887-899.

GACZYNSKA, M., K. L. ROCK and A. L. GOLDBERG, 1993 Gamma-interferon and expression of MHC genes regulate peptide hydrolysis by proteasomes. Nature **365:** 264-267.

GANOTH, D., E. LESHINSKY, E. EYTAN and A. HERSHKO, 1988 A multicomponent system that degrades proteins conjugated to ubiquitin. Resolution of factors and evidence for ATP-dependent complex formation. J Biol Chem **263:** 12412-12419.

GARDNER, R. G., G. M. SWARBRICK, N. W. BAYS, S. R. CRONIN, S. WILHOVSKY *et al.*, 2000 Endoplasmic reticulum degradation requires lumen to cytosol signaling. Transmembrane control of Hrd1p by Hrd3p. J Cell Biol **151:** 69-82.

GARZA, R. M., B. K. SATO and R. Y. HAMPTON, 2009 In vitro analysis of Hrd1p-mediated retrotranslocation of its multispanning membrane substrate 3-hydroxy-3-methylglutaryl (HMG)-CoA reductase. J Biol Chem **284:** 14710-14722.

GAUSS, R., E. JAROSCH, T. SOMMER and C. HIRSCH, 2006 A complex of Yos9p and the HRD ligase integrates endoplasmic reticulum quality control into the degradation machinery. Nat Cell Biol **8:** 849-854.

GERLINGER, U. M., R. GUCKEL, M. HOFFMANN, D. H. WOLF and W. HILT, 1997 Yeast cycloheximide-resistant crl mutants are proteasome mutants defective in protein degradation. Mol Biol Cell **8:** 2487-2499.

GHAEMMAGHAMI, S., W. K. HUH, K. BOWER, R. W. HOWSON, A. BELLE *et al.*, 2003 Global analysis of protein expression in yeast. Nature **425:** 737-741.

GHISLAIN, M., R. J. DOHMEN, F. LEVY and A. VARSHAVSKY, 1996 Cdc48p interacts with Ufd3p, a WD repeat protein required for ubiquitin-mediated proteolysis in Saccharomyces cerevisiae. EMBO J **15:** 4884-4899.

GLICKMAN, M. H., D. M. RUBIN, O. COUX, I. WEFES, G. PFEIFER *et al.*, 1998a A subcomplex of the proteasome regulatory particle required for ubiquitin-conjugate degradation and related to the COP9-signalosome and eIF3. Cell **94:** 615-623.

GLICKMAN, M. H., D. M. RUBIN, V. A. FRIED and D. FINLEY, 1998b The regulatory particle of the Saccharomyces cerevisiae proteasome. Mol Cell Biol **18:** 3149-3162.

GNANN, A., J. R. RIORDAN and D. H. WOLF, 2004 Cystic Fibrosis Transmembrane Conductance Regulator Degradation Depends on the Lectins Htm1p/EDEM and the Cdc48 Protein Complex in Yeast. Mol Biol Cell **15:** 4125-4135.

GOECKELER, J. L., A. STEPHENS, P. LEE, A. J. CAPLAN and J. L. BRODSKY, 2002 Overexpression of yeast Hsp110 homolog Sse1p suppresses ydj1-151 thermosensitivity and restores Hsp90-dependent activity. Mol Biol Cell **13:** 2760-2770.

GONZALEZ, F., A. DELAHODDE, T. KODADEK and S. A. JOHNSTON, 2002 Recruitment of a 19S proteasome subcomplex to an activated promoter. Science **296:** 548-550.

GORBEA, C., G. M. GOELLNER, K. TETER, R. K. HOLMES and M. RECHSTEINER, 2004 Characterization of mammalian Ecm29, a 26 S proteasome-associated protein that localizes to the nucleus and membrane vesicles. J Biol Chem **279:** 54849-54861.

GREENBLATT, E. J., J. A. OLZMANN and R. R. KOPITO, 2011 Derlin-1 is a rhomboid pseudoprotease required for the dislocation of mutant alpha-1 antitrypsin from the endoplasmic reticulum. Nat Struct Mol Biol **18:** 1147-1152.

GROLL, M., M. BAJOREK, A. KOHLER, L. MORODER, D. M. RUBIN *et al.*, 2000 A gated channel into the proteasome core particle. Nat Struct Biol **7:** 1062-1067.

GROLL, M., L. DITZEL, J. LOWE, D. STOCK, M. BOCHTLER *et al.*, 1997 Structure of 20S proteasome from yeast at 2.4 A resolution. Nature **386:** 463-471.

GRZIWA, A., W. BAUMEISTER, B. DAHLMANN and F. KOPP, 1991 Localization of subunits in proteasomes from Thermoplasma acidophilum by immunoelectron microscopy. FEBS Lett **290:** 186-190.

GUINTO, J. B., G. P. RITSON, J. P. TAYLOR and M. S. FORMAN, 2007 Valosin-containing protein and the pathogenesis of frontotemporal dementia associated with inclusion body myopathy. Acta Neuropathol **114:** 55-61.

GUTERMAN, A., and M. H. GLICKMAN, 2004 Complementary roles for Rpn11 and Ubp6 in deubiquitination and proteolysis by the proteasome. J Biol Chem **279:** 1729-1738.

HAGLUND, K., P. P. DI FIORE and I. DIKIC, 2003 Distinct monoubiquitin signals in receptor endocytosis. Trends Biochem Sci **28:** 598-603.

HALAWANI, D., A. C. LEBLANC, I. ROUILLER, S. W. MICHNICK, M. J. SERVANT *et al.*, 2009 Hereditary inclusion body myopathy-linked p97/VCP mutations in the NH2 domain and the D1 ring modulate p97/VCP ATPase activity and D2 ring conformation. Mol Cell Biol **29:** 4484-4494.

HAMMAN, B. D., L. M. HENDERSHOT and A. E. JOHNSON, 1998 BiP maintains the permeability barrier of the ER membrane by sealing the lumenal end of the translocon pore before and early in translocation. Cell **92:** 747-758.

HAMPTON, R. Y., R. G. GARDNER and J. RINE, 1996 Role of 26S proteasome and HRD genes in the degradation of 3-hydroxy-3-methylglutaryl-CoA reductase, an integral endoplasmic reticulum membrane protein. Mol Biol Cell **7:** 2029-2044.

HAN, S., Y. LIU and A. CHANG, 2007 Cytoplasmic Hsp70 promotes ubiquitination for endoplasmic reticulum-associated degradation of a misfolded mutant of the yeast plasma membrane ATPase, PMA1. J Biol Chem **282:** 26140-26149.

HANNA, J., N. A. HATHAWAY, Y. TONE, B. CROSAS, S. ELSASSER *et al.*, 2006 Deubiquitinating enzyme Ubp6 functions noncatalytically to delay proteasomal degradation. Cell **127:** 99-111.

HANNA, J., D. S. LEGGETT and D. FINLEY, 2003 Ubiquitin depletion as a key mediator of toxicity by translational inhibitors. Mol Cell Biol **23:** 9251-9261.

HANNA, J., A. MEIDES, D. P. ZHANG and D. FINLEY, 2007 A ubiquitin stress response induces altered proteasome composition. Cell **129:** 747-759.

HANSON, P. I., and S. W. WHITEHEART, 2005 AAA+ proteins: have engine, will work. Nat Rev Mol Cell Biol **6:** 519-529.

HATAKEYAMA, S., and K. I. NAKAYAMA, 2003 U-box proteins as a new family of ubiquitin ligases. Biochem Biophys Res Commun **302:** 635-645.

HEINEMEYER, W., M. FISCHER, T. KRIMMER, U. STACHON and D. H. WOLF, 1997 The active sites of the eukaryotic 20 S proteasome and their involvement in subunit precursor processing. J Biol Chem **272:** 25200-25209.

HEINEMEYER, W., J. A. KLEINSCHMIDT, J. SAIDOWSKY, C. ESCHER and D. H. WOLF, 1991 Proteinase yscE, the yeast proteasome/multicatalytic-multifunctional proteinase: mutants unravel its function in stress induced proteolysis and uncover its necessity for cell survival. EMBO J **10:** 555-562.

HELENIUS, A., and M. AEBI, 2004 Roles of N-linked glycans in the endoplasmic reticulum. Annu Rev Biochem **73:** 1019-1049.

HENDIL, K. B., R. HARTMANN-PETERSEN and K. TANAKA, 2002 26 S proteasomes function as stable entities. J Mol Biol **315:** 627-636.

HENDIL, K. B., F. KRIEGENBURG, K. TANAKA, S. MURATA, A. M. LAURIDSEN *et al.*, 2009 The 20S proteasome as an assembly platform for the 19S regulatory complex. J Mol Biol **394:** 320-328.

HEO, J. M., N. LIVNAT-LEVANON, E. B. TAYLOR, K. T. JONES, N. DEPHOURE *et al.*, 2010 A stress-responsive system for mitochondrial protein degradation. Mol Cell **40:** 465-480.

HERSHKO, A., and A. CIECHANOVER, 1998 The ubiquitin system. Annu Rev Biochem **67:** 425-479.

HETZER, M., H. H. MEYER, T. C. WALTHER, D. BILBAO-CORTES, G. WARREN *et al.*, 2001 Distinct AAA-ATPase p97 complexes function in discrete steps of nuclear assembly. Nat Cell Biol **3:** 1086-1091.

HICKE, L., 2001 Protein regulation by monoubiquitin. Nat Rev Mol Cell Biol **2:** 195-201.

HILT, W., and D. H. WOLF, 1995 Proteasomes of the yeast S. cerevisiae: genes, structure and functions. Molecular biology reports **21:** 3-10.

HITCHCOCK, A. L., H. KREBBER, S. FRIETZE, A. LIN, M. LATTERICH *et al.*, 2001 The conserved npl4 protein complex mediates proteasome-dependent membrane-bound transcription factor activation. Mol Biol Cell **12:** 3226-3241.

HITT, R., and D. H. WOLF, 2004 Der1p, a protein required for degradation of malfolded soluble proteins of the endoplasmic reticulum: topology and Der1-like proteins. FEMS yeast research **4:** 721-729.

HOCHSTRASSER, M., 1996 Ubiquitin-dependent protein degradation. Annu Rev Genet **30:** 405-439.

HOCHSTRASSER, M., 2006 Lingering mysteries of ubiquitin-chain assembly. Cell **124:** 27-34.

HOCHSTRASSER, M., and A. VARSHAVSKY, 1990 In vivo degradation of a transcriptional regulator: the yeast alpha 2 repressor. Cell **61:** 697-708.

HOELLER, D., C. M. HECKER, S. WAGNER, V. ROGOV, V. DOTSCH *et al.*, 2007 E3-independent monoubiquitination of ubiquitin-binding proteins. Mol Cell **26:** 891-898.

HOFFMAN, L., G. PRATT and M. RECHSTEINER, 1992 Multiple forms of the 20 S multicatalytic and the 26 S ubiquitin/ATP-dependent proteases from rabbit reticulocyte lysate. J Biol Chem **267:** 22362-22368.

HOPPE, T., 2005 Multiubiquitylation by E4 enzymes: 'one size' doesn't fit all. Trends Biochem Sci **30:** 183-187.

HOPPE, T., K. MATUSCHEWSKI, M. RAPE, S. SCHLENKER, H. D. ULRICH *et al.*, 2000 Activation of a membrane-bound transcription factor by regulated ubiquitin/proteasome-dependent processing. Cell **102:** 577-586.

HORN, S. C., J. HANNA, C. HIRSCH, C. VOLKWEIN, A. SCHUTZ *et al.*, 2009 Usa1 functions as a scaffold of the HRD-ubiquitin ligase. Mol Cell **36:** 782-793.

HOUGH, R., G. PRATT and M. RECHSTEINER, 1986 Ubiquitin-lysozyme conjugates. Identification and characterization of an ATP-dependent protease from rabbit reticulocyte lysates. J Biol Chem **261:** 2400-2408.

HOUGH, R., G. PRATT and M. RECHSTEINER, 1987 Purification of two high molecular weight proteases from rabbit reticulocyte lysate. J Biol Chem **262:** 8303-8313.

HOYT, M. A., M. ZHANG and P. COFFINO, 2003 Ubiquitin-independent mechanisms of mouse ornithine decarboxylase degradation are conserved between mammalian and fungal cells. J Biol Chem **278:** 12135-12143.

HSIEH, M. T., and R. H. CHEN, 2011 Cdc48 and cofactors Npl4-Ufd1 are important for G1 progression during heat stress by maintaining cell wall integrity in Saccharomyces cerevisiae. PLoS ONE **6:** e18988.

HUANG, D. T., H. W. HUNT, M. ZHUANG, M. D. OHI, J. M. HOLTON *et al.*, 2007 Basis for a ubiquitin-like protein thioester switch toggling E1-E2 affinity. Nature **445:** 394-398.

HUIBREGTSE, J. M., M. SCHEFFNER, S. BEAUDENON and P. M. HOWLEY, 1995 A family of proteins structurally and functionally related to the E6-AP ubiquitin-protein ligase. Proc Natl Acad Sci U S A **92:** 2563-2567.

HUSNJAK, K., S. ELSASSER, N. ZHANG, X. CHEN, L. RANDLES *et al.*, 2008 Proteasome subunit Rpn13 is a novel ubiquitin receptor. Nature **453:** 481-488.

HUYER, G., W. F. PILUEK, Z. FANSLER, S. G. KREFT, M. HOCHSTRASSER *et al.*, 2004 Distinct Machinery Is Required in Saccharomyces cerevisiae for the Endoplasmic Reticulum-associated Degradation of a Multispanning Membrane Protein and a Soluble Luminal Protein. J Biol Chem **279:** 38369-38378.

IKEDA, F., and I. DIKIC, 2008 Atypical ubiquitin chains: new molecular signals. 'Protein Modifications: Beyond the Usual Suspects' review series. EMBO Rep **9:** 536-542.

IMAI, J., M. MARUYA, H. YASHIRODA, I. YAHARA and K. TANAKA, 2003 The molecular chaperone Hsp90 plays a role in the assembly and maintenance of the 26S proteasome. EMBO J **22:** 3557-3567.

ISMAIL, N., and D. T. NG, 2006 Have you HRD? Understanding ERAD is DOAble! Cell **126:** 237-239.

ISONO, E., Y. SAEKI, H. YOKOSAWA and A. TOH-E, 2004 Rpn7 Is required for the structural integrity of the 26 S proteasome of Saccharomyces cerevisiae. J Biol Chem **279:** 27168-27176.

ISONO, E., N. SAITO, N. KAMATA, Y. SAEKI and E. A. TOH, 2005 Functional analysis of Rpn6p, a lid component of the 26 S proteasome, using temperature-sensitive rpn6 mutants of the yeast Saccharomyces cerevisiae. J Biol Chem **280:** 6537-6547.

JANSE, D. M., B. CROSAS, D. FINLEY and G. M. CHURCH, 2004 Localization to the proteasome is sufficient for degradation. J Biol Chem **279:** 21415-21420.

JAROSCH, E., C. TAXIS, C. VOLKWEIN, J. BORDALLO, D. FINLEY *et al.*, 2002 Protein dislocation from the ER requires polyubiquitination and the AAA-ATPase Cdc48. Nat Cell Biol **4:** 134-139.

JOHNSON, E. S., P. C. MA, I. M. OTA and A. VARSHAVSKY, 1995 A proteolytic pathway that recognizes ubiquitin as a degradation signal. J Biol Chem **270:** 17442-17456.

JOHNSON, J. O., J. MANDRIOLI, M. BENATAR, Y. ABRAMZON, V. M. VAN DEERLIN *et al.*, 2010 Exome sequencing reveals VCP mutations as a cause of familial ALS. Neuron **68:** 857-864.

JOSHI, K. K., L. CHEN, N. TORRES, V. TOURNIER and K. MADURA, 2011 A proteasome assembly defect in rpn3 mutants is associated with Rpn11 instability and increased sensitivity to stress. J Mol Biol **410:** 383-399.

JU, J. S., R. A. FUENTEALBA, S. E. MILLER, E. JACKSON, D. PIWNICA-WORMS *et al.*, 2009 Valosin-containing protein (VCP) is required for autophagy and is disrupted in VCP disease. J Cell Biol **187:** 875-888.

JUNG, T., and T. GRUNE, 2008 The proteasome and its role in the degradation of oxidized proteins. IUBMB Life **60:** 743-752.

KABANI, M., J. M. BECKERICH and J. L. BRODSKY, 2002 Nucleotide exchange factor for the yeast Hsp70 molecular chaperone Ssa1p. Mol Cell Biol **22:** 4677-4689.

KAGANOVICH, D., R. KOPITO and J. FRYDMAN, 2008 Misfolded proteins partition between two distinct quality control compartments. Nature **454:** 1088-1095.

KALIES, K. U., S. ALLAN, T. SERGEYENKO, H. KROGER and K. ROMISCH, 2005 The protein translocation channel binds proteasomes to the endoplasmic reticulum membrane. EMBO J **24:** 2284-2293.

KANEKO, T., J. HAMAZAKI, S. IEMURA, K. SASAKI, K. FURUYAMA *et al.*, 2009 Assembly pathway of the Mammalian proteasome base subcomplex is mediated by multiple specific chaperones. Cell **137:** 914-925.

KIM, H. C., and J. M. HUIBREGTSE, 2009 Polyubiquitination by HECT E3s and the determinants of chain type specificity. Mol Cell Biol **29:** 3307-3318.

KIM, H. T., K. P. KIM, F. LLEDIAS, A. F. KISSELEV, K. M. SCAGLIONE *et al.*, 2007 Certain pairs of ubiquitin-conjugating enzymes (E2s) and ubiquitin-protein ligases (E3s) synthesize nondegradable forked ubiquitin chains containing all possible isopeptide linkages. J Biol Chem **282:** 17375-17386.

KIM, I., J. AHN, C. LIU, K. TANABE, J. APODACA *et al.*, 2006 The Png1-Rad23 complex regulates glycoprotein turnover. J Cell Biol **172:** 211-219.

KIM, I., K. MI and H. RAO, 2004 Multiple interactions of rad23 suggest a mechanism for ubiquitylated substrate delivery important in proteolysis. Mol Biol Cell **15:** 3357-3365.

KIM, I., and H. RAO, 2006 What's Ub chain linkage got to do with it? Sci STKE **2006:** pe18.

KIM, W., E. D. SPEAR and D. T. NG, 2005 Yos9p detects and targets misfolded glycoproteins for ER-associated degradation. Mol Cell **19:** 753-764.

KINCAID, E. Z., J. W. CHE, I. YORK, H. ESCOBAR, E. REYES-VARGAS *et al.*, 2012 Mice completely lacking immunoproteasomes show major changes in antigen presentation. Nat Immunol **13:** 129-135.

KISSELEV, A. F., W. A. VAN DER LINDEN and H. S. OVERKLEEFT, 2012 Proteasome inhibitors: an expanding army attacking a unique target. Chem Biol **19:** 99-115.

KLEIGER, G., A. SAHA, S. LEWIS, B. KUHLMAN and R. J. DESHAIES, 2009 Rapid E2-E3 assembly and disassembly enable processive ubiquitylation of cullin-RING ubiquitin ligase substrates. Cell **139:** 957-968.

KLEIJNEN, M. F., J. ROELOFS, S. PARK, N. A. HATHAWAY, M. GLICKMAN *et al.*, 2007 Stability of the proteasome can be regulated allosterically through engagement of its proteolytic active sites. Nat Struct Mol Biol **14:** 1180-1188.

KNOP, M., A. FINGER, T. BRAUN, K. HELLMUTH and D. H. WOLF, 1996 Der1, a novel protein specifically required for endoplasmic reticulum degradation in yeast. Embo J **15:** 753-763.

KOEGL, M., T. HOPPE, S. SCHLENKER, H. D. ULRICH, T. U. MAYER *et al.*, 1999 A novel ubiquitination factor, E4, is involved in multiubiquitin chain assembly. Cell **96:** 635-644.

KOHLER, A., P. CASCIO, D. S. LEGGETT, K. M. WOO, A. L. GOLDBERG *et al.*, 2001 The axial channel of the proteasome core particle is gated by the Rpt2 ATPase and controls both substrate entry and product release. Mol Cell **7:** 1143-1152.

KOLLER, K. J., and M. J. BROWNSTEIN, 1987 Use of a cDNA clone to identify a supposed precursor protein containing valosin. Nature **325:** 542-545.

KONDO, H., C. RABOUILLE, R. NEWMAN, T. P. LEVINE, D. PAPPIN *et al.*, 1997 p47 is a cofactor for p97-mediated membrane fusion. Nature **388:** 75-78.

KOPP, F., R. STEINER, B. DAHLMANN, L. KUEHN and H. REINAUER, 1986 Size and shape of the multicatalytic proteinase from rat skeletal muscle. Biochim Biophys Acta **872:** 253-260.

KRICK, R., S. BREMER, E. WELTER, P. SCHLOTTERHOSE, Y. MUEHE *et al.*, 2010 Cdc48/p97 and Shp1/p47 regulate autophagosome biogenesis in concert with ubiquitin-like Atg8. J Cell Biol **190:** 965-973.

KRIEGENBURG, F., M. SEEGER, Y. SAEKI, K. TANAKA, A. M. LAURIDSEN *et al.*, 2008 Mammalian 26S proteasomes remain intact during protein degradation. Cell **135:** 355-365.

KROGAN, N. J., G. CAGNEY, H. YU, G. ZHONG, X. GUO *et al.*, 2006 Global landscape of protein complexes in the yeast Saccharomyces cerevisiae. Nature **440:** 637-643.

KUSMIERCZYK, A. R., M. J. KUNJAPPU, M. FUNAKOSHI and M. HOCHSTRASSER, 2008 A multimeric assembly factor controls the formation of alternative 20S proteasomes. Nat Struct Mol Biol **15:** 237-244.

KWON, Y. T., Y. REISS, V. A. FRIED, A. HERSHKO, J. K. YOON *et al.*, 1998 The mouse and human genes encoding the recognition component of the N-end rule pathway. Proc Natl Acad Sci U S A **95:** 7898-7903.

LALONDE, D. P., and A. BRETSCHER, 2011 The UBX protein SAKS1 negatively regulates endoplasmic reticulum-associated degradation and p97-dependent degradation. J Biol Chem **286:** 4892-4901.

LANDER, E. S., L. M. LINTON, B. BIRREN, C. NUSBAUM, M. C. ZODY *et al.*, 2001 Initial sequencing and analysis of the human genome. Nature **409:** 860-921.

LANDER, G. C., E. ESTRIN, M. E. MATYSKIELA, C. BASHORE, E. NOGALES *et al.*, 2012 Complete subunit architecture of the proteasome regulatory particle. Nature **482:** 186-191.

LATTERICH, M., K. U. FROHLICH and R. SCHEKMAN, 1995 Membrane fusion and the cell cycle: Cdc48p participates in the fusion of ER membranes. Cell **82:** 885-893.

LE TALLEC, B., M. B. BARRAULT, R. COURBEYRETTE, R. GUEROIS, M. C. MARSOLIER-KERGOAT *et al.*, 2007 20S proteasome assembly is orchestrated by two distinct pairs of chaperones in yeast and in mammals. Mol Cell **27:** 660-674.

LE TALLEC, B., M. B. BARRAULT, R. GUEROIS, T. CARRE and A. PEYROCHE, 2009 Hsm3/S5b participates in the assembly pathway of the 19S regulatory particle of the proteasome. Mol Cell **33:** 389-399.

LEE, I., and H. SCHINDELIN, 2008 Structural insights into E1-catalyzed ubiquitin activation and transfer to conjugating enzymes. Cell **134:** 268-278.

LEE, J. R., A. J. OESTREICH, J. A. PAYNE, M. S. GUNAWAN, A. P. NORGAN *et al.*, 2009 The HECT domain of the ubiquitin ligase Rsp5 contributes to substrate recognition. J Biol Chem **284:** 32126-32137.

LEE, R. J., C. W. LIU, C. HARTY, A. A. MCCRACKEN, M. LATTERICH *et al.*, 2004 Uncoupling retro-translocation and degradation in the ER-associated degradation of a soluble protein. Embo J **23:** 2206-2215.

LEE, S. Y., A. DE LA MOTA-PEYNADO and J. ROELOFS, 2011 Loss of Rpt5 protein interactions with the core particle and Nas2 protein causes the formation of faulty proteasomes that are inhibited by Ecm29 protein. J Biol Chem **286:** 36641-36651.

LEGGETT, D. S., J. HANNA, A. BORODOVSKY, B. CROSAS, M. SCHMIDT *et al.*, 2002 Multiple associated proteins regulate proteasome structure and function. Mol Cell **10:** 495-507.

LEHMANN, A., K. JANEK, B. BRAUN, P. M. KLOETZEL and C. ENENKEL, 2002 20 S proteasomes are imported as precursor complexes into the nucleus of yeast. J Mol Biol **317:** 401-413.

LEHMANN, A., A. NIEWIENDA, K. JECHOW, K. JANEK and C. ENENKEL, 2010 Ecm29 fulfils quality control functions in proteasome assembly. Mol Cell **38:** 879-888.

LI, G., C. HUANG, G. ZHAO and W. J. LENNARZ, 2012 Interprotomer motion-transmission mechanism for the hexameric AAA ATPase p97. Proc Natl Acad Sci U S A **109:** 3737-3741.

LI, W., D. TU, A. T. BRUNGER and Y. YE, 2007a A ubiquitin ligase transfers preformed polyubiquitin chains from a conjugating enzyme to a substrate. Nature **446:** 333-337.

LI, X., and G. N. DEMARTINO, 2009 Variably modulated gating of the 26S proteasome by ATP and polyubiquitin. Biochem J **421:** 397-404.

LI, X., A. R. KUSMIERCZYK, P. WONG, A. EMILI and M. HOCHSTRASSER, 2007b beta-Subunit appendages promote 20S proteasome assembly by overcoming an Ump1-dependent checkpoint. EMBO J **26:** 2339-2349.

LIANG, J., C. YIN, H. DOONG, S. FANG, C. PETERHOFF *et al.*, 2006 Characterization of erasin (UBXD2): a new ER protein that promotes ER-associated protein degradation. J Cell Sci **119:** 4011-4024.

LILLEY, B. N., and H. L. PLOEGH, 2004 A membrane protein required for dislocation of misfolded proteins from the ER. Nature **429:** 834-840.

LIM, P. J., R. DANNER, J. LIANG, H. DOONG, C. HARMAN *et al.*, 2009 Ubiquilin and p97/VCP bind erasin, forming a complex involved in ERAD. J Cell Biol **187:** 201-217.

LIS, E. T., and F. E. ROMESBERG, 2006 Role of Doa1 in the Saccharomyces cerevisiae DNA damage response. Mol Cell Biol **26:** 4122-4133.

LIU, C., D. VAN DYK, V. CHOE, J. YAN, S. MAJUMDER *et al.*, 2011 Ubiquitin ligase ufd2 is required for efficient degradation of mps1 kinase. The Journal of biological chemistry **286:** 43660-43667.

LIU, C. W., L. MILLEN, T. B. ROMAN, H. XIONG, H. F. GILBERT *et al.*, 2002 Conformational remodeling of proteasomal substrates by PA700, the 19 S regulatory complex of the 26 S proteasome. J Biol Chem **277:** 26815-26820.

LOPEZ, A. D., K. TAR, U. KRUGEL, T. DANGE, I. G. ROS *et al.*, 2011 Proteasomal degradation of Sfp1 contributes to the repression of ribosome biogenesis during starvation and is mediated by the proteasome activator Blm10. Mol Biol Cell **22:** 528-540.

LOWE, J., D. STOCK, B. JAP, P. ZWICKL, W. BAUMEISTER *et al.*, 1995 Crystal structure of the 20S proteasome from the archaeon T. acidophilum at 3.4 A resolution. Science **268:** 533-539.

MA, C. P., C. A. SLAUGHTER and G. N. DEMARTINO, 1992 Identification, purification, and characterization of a protein activator (PA28) of the 20 S proteasome (macropain). J Biol Chem **267:** 10515-10523.

MADEO, F., J. SCHLAUER, H. ZISCHKA, D. MECKE and K. U. FROHLICH, 1998 Tyrosine phosphorylation regulates cell cycle-dependent nuclear localization of Cdc48p. Mol Biol Cell **9:** 131-141.

MARQUES, A. J., C. GLANEMANN, P. C. RAMOS and R. J. DOHMEN, 2007 The C-terminal extension of the beta7 subunit and activator complexes stabilize nascent 20 S proteasomes and promote their maturation. J Biol Chem **282:** 34869-34876.

MARTENS, S., M. M. KOZLOV and H. T. MCMAHON, 2007 How synaptotagmin promotes membrane fusion. Science **316:** 1205-1208.

MASTRANDREA, L. D., J. YOU, E. G. NILES and C. M. PICKART, 1999 E2/E3-mediated assembly of lysine 29-linked polyubiquitin chains. J Biol Chem **274:** 27299-27306.

MATIUHIN, Y., D. S. KIRKPATRICK, I. ZIV, W. KIM, A. DAKSHINAMURTHY *et al.*, 2008 Extraproteasomal Rpn10 restricts access of the polyubiquitin-binding protein Dsk2 to proteasome. Mol Cell **32:** 415-425.

MAYER, A. N., and K. D. WILKINSON, 1989 Detection, resolution, and nomenclature of multiple ubiquitin carboxyl-terminal esterases from bovine calf thymus. Biochemistry **28:** 166-172.

MCCRACKEN, A. A., and J. L. BRODSKY, 1996 Assembly of ER-associated protein degradation in vitro: dependence on cytosol, calnexin, and ATP. J Cell Biol **132:** 291-298.

MCGRATH, J. P., S. JENTSCH and A. VARSHAVSKY, 1991 UBA 1: an essential yeast gene encoding ubiquitin-activating enzyme. EMBO J **10:** 227-236.

MCGUIRE, M. J., M. L. MCCULLOUGH, D. E. CROALL and G. N. DEMARTINO, 1989 The high molecular weight multicatalytic proteinase, macropain, exists in a latent form in human erythrocytes. Biochim Biophys Acta **995:** 181-186.

MEDICHERLA, B., Z. KOSTOVA, A. SCHAEFER and D. H. WOLF, 2004 A genomic screen identifies Dsk2p and Rad23p as essential components of ER-associated degradation. EMBO Rep **5:** 692-697.

MEERANG, M., D. RITZ, S. PALIWAL, Z. GARAJOVA, M. BOSSHARD *et al.*, 2011 The ubiquitin-selective segregase VCP/p97 orchestrates the response to DNA double-strand breaks. Nat Cell Biol **13:** 1376-1382.

MELENDEZ, A., and T. P. NEUFELD, 2008 The cell biology of autophagy in metazoans: a developing story. Development **135:** 2347-2360.

METZGER, M. B., and S. MICHAELIS, 2009 Analysis of quality control substrates in distinct cellular compartments reveals a unique role for Rpn4p in tolerating misfolded membrane proteins. Mol Biol Cell **20:** 1006-1019.

MEYER, H. H., H. KONDO and G. WARREN, 1998 The p47 co-factor regulates the ATPase activity of the membrane fusion protein, p97. FEBS Lett **437:** 255-257.

MEYER, H. H., J. G. SHORTER, J. SEEMANN, D. PAPPIN and G. WARREN, 2000 A complex of mammalian ufd1 and npl4 links the AAA-ATPase, p97, to ubiquitin and nuclear transport pathways. EMBO J **19:** 2181-2192.

MEYER, H. H., Y. WANG and G. WARREN, 2002 Direct binding of ubiquitin conjugates by the mammalian p97 adaptor complexes, p47 and Ufd1-Npl4. EMBO J **21:** 5645-5652.

MIYACHI, K., Y. HIRANO, T. HORIGOME, T. MIMORI, H. MIYAKAWA *et al.*, 2004 Autoantibodies from primary biliary cirrhosis patients with anti-p95c antibodies bind to recombinant p97/VCP and inhibit in vitro nuclear envelope assembly. Clin Exp Immunol **136:** 568-573.

MIZUNO, M., and S. J. SINGER, 1993 A soluble secretory protein is first concentrated in the endoplasmic reticulum before transfer to the Golgi apparatus. Proc Natl Acad Sci U S A **90:** 5732-5736.

MOIR, D., S. E. STEWART, B. C. OSMOND and D. BOTSTEIN, 1982 Cold-sensitive cell-division-cycle mutants of yeast: isolation, properties, and pseudoreversion studies. Genetics **100:** 547-563.

MOLINEAUX, S. M., 2012 Molecular pathways: targeting proteasomal protein degradation in cancer. Clin Cancer Res **18:** 15-20.

MULLALLY, J. E., T. CHERNOVA and K. D. WILKINSON, 2006 Doa1 is a Cdc48 adapter that possesses a novel ubiquitin binding domain. Mol Cell Biol **26:** 822-830.

MURATA, H., B. TEFEREDEGNE, A. M. LEWIS, JR. and K. PEDEN, 2009 A quantitative PCR assay for SV40 neutralization adaptable for high-throughput applications. J Virol Methods **162:** 236-244.

NAKATSUKASA, K., G. HUYER, S. MICHAELIS and J. L. BRODSKY, 2008 Dissecting the ER-associated degradation of a misfolded polytopic membrane protein. Cell **132:** 101-112.

NAKATSUKASA, K., S. NISHIKAWA, N. HOSOKAWA, K. NAGATA and T. ENDO, 2001 Mnl1p, an alpha -mannosidase-like protein in yeast Saccharomyces cerevisiae, is required for endoplasmic reticulum-associated degradation of glycoproteins. J Biol Chem **276:** 8635-8638.

NEUBER, O., E. JAROSCH, C. VOLKWEIN, J. WALTER and T. SOMMER, 2005 Ubx2 links the Cdc48 complex to ER-associated protein degradation. Nat Cell Biol **7:** 993-998.

NEWTON, K., M. L. MATSUMOTO, I. E. WERTZ, D. S. KIRKPATRICK, J. R. LILL *et al.*, 2008 Ubiquitin chain editing revealed by polyubiquitin linkage-specific antibodies. Cell **134:** 668-678.

NIWA, H., C. A. EWENS, C. TSANG, H. O. YEUNG, X. ZHANG *et al.*, 2012 The role of the N-domain in the ATPase activity of the mammalian AAA ATPase p97/VCP. J Biol Chem **287:** 8561-8570.

ORINO, E., K. TANAKA, T. TAMURA, S. SONE, T. OGURA *et al.*, 1991 ATP-dependent reversible association of proteasomes with multiple protein components to form 26S complexes that degrade ubiquitinated proteins in human HL-60 cells. FEBS Lett **284:** 206-210.

ORME, C. M., and J. S. BOGAN, 2012 The ubiquitin regulatory X (UBX) domain-containing protein TUG regulates the p97 ATPase and resides at the endoplasmic reticulum-golgi intermediate compartment. J Biol Chem **287:** 6679-6692.

OSLEY, M. A., 2004 H2B ubiquitylation: the end is in sight. Biochim Biophys Acta **1677:** 74-78.

OSSAREH-NAZARI, B., M. BONIZEC, M. COHEN, S. DOKUDOVSKAYA, F. DELALANDE *et al.*, 2010 Cdc48 and Ufd3, new partners of the ubiquitin protease Ubp3, are required for ribophagy. EMBO Rep **11:** 548-554.

PANASENKO, O. O., and M. A. COLLART, 2011 Not4 E3 ligase contributes to proteasome assembly and functional integrity in part through Ecm29. Mol Cell Biol **31:** 1610-1623.

PAPA, F. R., and M. HOCHSTRASSER, 1993 The yeast DOA4 gene encodes a deubiquitinating enzyme related to a product of the human tre-2 oncogene. Nature **366:** 313-319.

PARK, S., D. M. RANCOUR and S. Y. BEDNAREK, 2007 Protein domain-domain interactions and requirements for the negative regulation of Arabidopsis CDC48/p97 by the plant ubiquitin regulatory X (UBX) domain-containing protein, PUX1. J Biol Chem **282:** 5217-5224.

PARK, S., J. ROELOFS, W. KIM, J. ROBERT, M. SCHMIDT *et al.*, 2009 Hexameric assembly of the proteasomal ATPases is templated through their C termini. Nature **459:** 866-870.

PARKER, J. L., and H. D. ULRICH, 2009 Mechanistic analysis of PCNA poly-ubiquitylation by the ubiquitin protein ligases Rad18 and Rad5. EMBO J **28:** 3657-3666.

PARSONS, A. B., A. LOPEZ, I. E. GIVONI, D. E. WILLIAMS, C. A. GRAY *et al.*, 2006 Exploring the mode-of-action of bioactive compounds by chemical-genetic profiling in yeast. Cell **126:** 611-625.

PATHARE, G. R., I. NAGY, S. BOHN, P. UNVERDORBEN, A. HUBERT *et al.*, 2012 The proteasomal subunit Rpn6 is a molecular clamp holding the core and regulatory subcomplexes together. Proc Natl Acad Sci U S A **109:** 149-154.

PATTERSON, C., 2002 A new gun in town: the U box is a ubiquitin ligase domain. Sci STKE **2002:** pe4.

PETERS, J. M., Z. CEJKA, J. R. HARRIS, J. A. KLEINSCHMIDT and W. BAUMEISTER, 1993 Structural features of the 26 S proteasome complex. J Mol Biol **234:** 932-937.

PETH, A., H. C. BESCHE and A. L. GOLDBERG, 2009 Ubiquitinated proteins activate the proteasome by binding to Usp14/Ubp6, which causes 20S gate opening. Mol Cell **36:** 794-804.

PICKART, C. M., 2001 Mechanisms underlying ubiquitination. Annu Rev Biochem **70:** 503-533.

PICKART, C. M., and R. E. COHEN, 2004 Proteasomes and their kin: proteases in the machine age. Nat Rev Mol Cell Biol **5:** 177-187.

PICKART, C. M., and D. FUSHMAN, 2004 Polyubiquitin chains: polymeric protein signals. Current opinion in chemical biology **8:** 610-616.

PICKART, C. M., and I. A. ROSE, 1985 Ubiquitin carboxyl-terminal hydrolase acts on ubiquitin carboxyl-terminal amides. J Biol Chem **260:** 7903-7910.

PLEASURE, I. T., M. M. BLACK and J. H. KEEN, 1993 Valosin-containing protein, VCP, is a ubiquitous clathrin-binding protein. Nature **365:** 459-462.

PLEMPER, R. K., P. M. DEAK, R. T. OTTO and D. H. WOLF, 1999 Re-entering the translocon from the lumenal side of the endoplasmic reticulum. Studies on mutated carboxypeptidase yscY species. FEBS Lett **443:** 241-245.

PLEMPER, R. K., R. EGNER, K. KUCHLER and D. H. WOLF, 1998 Endoplasmic reticulum degradation of a mutated ATP-binding cassette transporter Pdr5 proceeds in a concerted action of Sec61 and the proteasome. J Biol Chem **273:** 32848-32856.

PYE, V. E., I. DREVENY, L. C. BRIGGS, C. SANDS, F. BEURON *et al.*, 2006 Going through the motions: the ATPase cycle of p97. J Struct Biol **156:** 12-28.

QIAN, S. B., L. WALDRON, N. CHOUDHARY, R. E. KLEVIT, W. J. CHAZIN *et al.*, 2009 Engineering a ubiquitin ligase reveals conformational flexibility required for ubiquitin transfer. J Biol Chem **284:** 26797-26802.

RABINOVICH, E., A. KEREM, K. U. FROHLICH, N. DIAMANT and S. BAR-NUN, 2002 AAA-ATPase p97/Cdc48p, a cytosolic chaperone required for endoplasmic reticulum-associated protein degradation. Mol Cell Biol **22:** 626-634.

RADHAKRISHNAN, S. K., C. S. LEE, P. YOUNG, A. BESKOW, J. Y. CHAN *et al.*, 2010 Transcription factor Nrf1 mediates the proteasome recovery pathway after proteasome inhibition in mammalian cells. Mol Cell **38:** 17-28.

RAINA, S., and D. MISSIAKAS, 1997 Making and breaking disulfide bonds. Annu Rev Microbiol **51:** 179-202.

RAMADAN, K., R. BRUDERER, F. M. SPIGA, O. POPP, T. BAUR *et al.*, 2007 Cdc48/p97 promotes reformation of the nucleus by extracting the kinase Aurora B from chromatin. Nature **450:** 1258-1262.

RAMOS, P. C., J. HOCKENDORFF, E. S. JOHNSON, A. VARSHAVSKY and R. J. DOHMEN, 1998 Ump1p is required for proper maturation of the 20S proteasome and becomes its substrate upon completion of the assembly. Cell **92:** 489-499.

RANCOUR, D. M., S. PARK, S. D. KNIGHT and S. Y. BEDNAREK, 2004 Plant UBX domain-containing protein 1, PUX1, regulates the oligomeric structure and activity of arabidopsis CDC48. J Biol Chem **279:** 54264-54274.

RAO, H., and A. SASTRY, 2002 Recognition of specific ubiquitin conjugates is important for the proteolytic functions of the ubiquitin-associated domain proteins Dsk2 and Rad23. J Biol Chem **277:** 11691-11695.

RAPE, M., T. HOPPE, I. GORR, M. KALOCAY, H. RICHLY *et al.*, 2001 Mobilization of processed, membrane-tethered SPT23 transcription factor by CDC48(UFD1/NPL4), a ubiquitin-selective chaperone. Cell **107:** 667-677.

RAPOPORT, T. A., K. E. MATLACK, K. PLATH, B. MISSELWITZ and O. STAECK, 1999 Posttranslational protein translocation across the membrane of the endoplasmic reticulum. Biol Chem **380:** 1143-1150.

RAVID, T., S. G. KREFT and M. HOCHSTRASSER, 2006 Membrane and soluble substrates of the Doa10 ubiquitin ligase are degraded by distinct pathways. EMBO J **25:** 533-543.

REN, J., N. PASHKOVA, S. WINISTORFER and R. C. PIPER, 2008 DOA1/UFD3 plays a role in sorting ubiquitinated membrane proteins into multivesicular bodies. J Biol Chem **283:** 21599-21611.

REYES-TURCU, F. E., K. H. VENTII and K. D. WILKINSON, 2009 Regulation and cellular roles of ubiquitin-specific deubiquitinating enzymes. Annu Rev Biochem **78:** 363-397.

RICHLY, H., M. RAPE, S. BRAUN, S. RUMPF, C. HOEGE *et al.*, 2005 A series of ubiquitin binding factors connects CDC48/p97 to substrate multiubiquitylation and proteasomal targeting. Cell **120:** 73-84.

RIVETT, A. J., 1998 Intracellular distribution of proteasomes. Curr Opin Immunol **10:** 110-114.

RIVETT, A. J., A. PALMER and E. KNECHT, 1992 Electron microscopic localization of the multicatalytic proteinase complex in rat liver and in cultured cells. J Histochem Cytochem **40:** 1165-1172.

ROELOFS, J., S. PARK, W. HAAS, G. TIAN, F. E. MCALLISTER *et al.*, 2009 Chaperone-mediated pathway of proteasome regulatory particle assembly. Nature **459:** 861-865.

ROMISCH, K., 1999 Surfing the Sec61 channel: bidirectional protein translocation across the ER membrane. J Cell Sci **112 (Pt 23):** 4185-4191.

ROTIN, D., and S. KUMAR, 2009 Physiological functions of the HECT family of ubiquitin ligases. Nat Rev Mol Cell Biol **10:** 398-409.

ROUILLER, I., B. DELABARRE, A. P. MAY, W. I. WEIS, A. T. BRUNGER *et al.*, 2002 Conformational changes of the multifunction p97 AAA ATPase during its ATPase cycle. Nat Struct Biol **9:** 950-957.

RUMPF, S., and S. JENTSCH, 2006 Functional division of substrate processing cofactors of the ubiquitin-selective Cdc48 chaperone. Mol Cell **21:** 261-269.

RUSSELL, S. J., S. H. REED, W. HUANG, E. C. FRIEDBERG and S. A. JOHNSTON, 1999 The 19S regulatory complex of the proteasome functions independently of proteolysis in nucleotide excision repair. Mol Cell **3:** 687-695.

SACCONI, S., P. CAMANO, J. C. DE GREEF, R. J. LEMMERS, L. SALVIATI *et al.*, 2012 Patients with a phenotype consistent with facioscapulohumeral muscular dystrophy display genetic and epigenetic heterogeneity. J Med Genet **49:** 41-46.

SAEKI, Y., E. ISONO and E. A. TOH, 2005 Preparation of ubiquitinated substrates by the PY motif-insertion method for monitoring 26S proteasome activity. Methods Enzymol **399:** 215-227.

SAEKI, Y., T. SONE, A. TOH-E and H. YOKOSAWA, 2002 Identification of ubiquitin-like protein-binding subunits of the 26S proteasome. Biochem Biophys Res Commun **296:** 813-819.

SAEKI, Y., Y. TAYAMA, A. TOH-E and H. YOKOSAWA, 2004 Definitive evidence for Ufd2-catalyzed elongation of the ubiquitin chain through Lys48 linkage. Biochem Biophys Res Commun **320:** 840-845.

SAEKI, Y., E. A. TOH, T. KUDO, H. KAWAMURA and K. TANAKA, 2009 Multiple proteasome-interacting proteins assist the assembly of the yeast 19S regulatory particle. Cell **137:** 900-913.

SAKATA, E., S. BOHN, O. MIHALACHE, P. KISS, F. BECK *et al.*, 2012 Localization of the proteasomal ubiquitin receptors Rpn10 and Rpn13 by electron cryomicroscopy. Proc Natl Acad Sci U S A **109:** 1479-1484.

SAKATA, E., F. STENGEL, K. FUKUNAGA, M. ZHOU, Y. SAEKI *et al.*, 2011 The catalytic activity of Ubp6 enhances maturation of the proteasomal regulatory particle. Mol Cell **42:** 637-649.

SATO, B. K., and R. Y. HAMPTON, 2006 Yeast Derlin Dfm1 interacts with Cdc48 and functions in ER homeostasis. Yeast **23:** 1053-1064.

SCHAUBER, C., L. CHEN, P. TONGAONKAR, I. VEGA, D. LAMBERTSON *et al.*, 1998 Rad23 links DNA repair to the ubiquitin/proteasome pathway. Nature **391:** 715-718.

SCHEFFNER, M., U. NUBER and J. M. HUIBREGTSE, 1995 Protein ubiquitination involving an E1-E2-E3 enzyme ubiquitin thioester cascade. Nature **373:** 81-83.

SCHMIDT, M., W. HAAS, B. CROSAS, P. G. SANTAMARIA, S. P. GYGI *et al.*, 2005 The HEAT repeat protein Blm10 regulates the yeast proteasome by capping the core particle. Nat Struct Mol Biol **12:** 294-303.

SCHMIDT, W. E., V. MUTT, M. CARLQUIST, H. KRATZIN, J. M. CONLON *et al.*, 1985 Valosin: isolation and characterization of a novel peptide from porcine intestine. FEBS Lett **191:** 264-268.

SCHUBERTH, C., and A. BUCHBERGER, 2005 Membrane-bound Ubx2 recruits Cdc48 to ubiquitin ligases and their substrates to ensure efficient ER-associated protein degradation. Nat Cell Biol **7:** 999-1006.

SCHUBERTH, C., and A. BUCHBERGER, 2008 UBX domain proteins: major regulators of the AAA ATPase Cdc48/p97. Cell Mol Life Sci **65:** 2360-2371.

SCHUBERTH, C., H. RICHLY, S. RUMPF and A. BUCHBERGER, 2004 Shp1 and Ubx2 are adaptors of Cdc48 involved in ubiquitin-dependent protein degradation. EMBO Rep **5:** 818-824.

SCHULMAN, B. A., and J. W. HARPER, 2009 Ubiquitin-like protein activation by E1 enzymes: the apex for downstream signalling pathways. Nat Rev Mol Cell Biol **10:** 319-331.

SCHYMICK, J. C., K. TALBOT and B. J. TRAYNOR, 2007 Genetics of sporadic amyotrophic lateral sclerosis. Hum Mol Genet **16 Spec No. 2:** R233-242.

SCOTT, C. M., K. B. KRUSE, B. Z. SCHMIDT, D. H. PERLMUTTER, A. A. MCCRACKEN *et al.*, 2007 ADD66, a gene involved in the endoplasmic reticulum-associated degradation of alpha-1-antitrypsin-Z in yeast, facilitates proteasome activity and assembly. Mol Biol Cell **18:** 3776-3787.

SEEMULLER, E., A. LUPAS and W. BAUMEISTER, 1996 Autocatalytic processing of the 20S proteasome. Nature **382:** 468-471.

SEIFERT, U., L. P. BIALY, F. EBSTEIN, D. BECH-OTSCHIR, A. VOIGT *et al.*, 2010 Immunoproteasomes preserve protein homeostasis upon interferon-induced oxidative stress. Cell **142:** 613-624.

SHCHERBIK, N., and D. S. HAINES, 2007 Cdc48p(Npl4p/Ufd1p) binds and segregates membrane-anchored/tethered complexes via a polyubiquitin signal present on the anchors. Mol Cell **25:** 385-397.

SHI, D., M. S. POP, R. KULIKOV, I. M. LOVE, A. L. KUNG *et al.*, 2009 CBP and p300 are cytoplasmic E4 polyubiquitin ligases for p53. Proc Natl Acad Sci U S A **106:** 16275-16280.

SHIH, S. C., G. PRAG, S. A. FRANCIS, M. A. SUTANTO, J. H. HURLEY *et al.*, 2003 A ubiquitin-binding motif required for intramolecular monoubiquitylation, the CUE domain. EMBO J **22:** 1273-1281.

SIKORSKI, R. S., and P. HIETER, 1989 A system of shuttle vectors and yeast host strains designed for efficient manipulation of DNA in Saccharomyces cerevisiae. Genetics **122:** 19-27.

SKAAR, J. R., and M. PAGANO, 2009 Control of cell growth by the SCF and APC/C ubiquitin ligases. Curr Opin Cell Biol **21:** 816-824.

SMITH, D. M., S. C. CHANG, S. PARK, D. FINLEY, Y. CHENG *et al.*, 2007 Docking of the proteasomal ATPases' carboxyl termini in the 20S proteasome's alpha ring opens the gate for substrate entry. Mol Cell **27:** 731-744.

SMITH, M. H., H. L. PLOEGH and J. S. WEISSMAN, 2011 Road to ruin: targeting proteins for degradation in the endoplasmic reticulum. Science **334:** 1086-1090.

SONE, T., Y. SAEKI, A. TOH-E and H. YOKOSAWA, 2004 Sem1p is a novel subunit of the 26 S proteasome from Saccharomyces cerevisiae. J Biol Chem **279:** 28807-28816.

SONG, C., Q. WANG and C. C. LI, 2003 ATPase activity of p97-valosin-containing protein (VCP). D2 mediates the major enzyme activity, and D1 contributes to the heat-induced activity. J Biol Chem **278:** 3648-3655.

SPENCE, J., S. SADIS, A. L. HAAS and D. FINLEY, 1995 A ubiquitin mutant with specific defects in DNA repair and multiubiquitination. Mol Cell Biol **15:** 1265-1273.

STAPF, C., E. CARTWRIGHT, M. BYCROFT, K. HOFMANN and A. BUCHBERGER, 2011 The general definition of the p97/valosin-containing protein (VCP)-interacting motif (VIM) delineates a new family of p97 cofactors. J Biol Chem **286:** 38670-38678.

STARK, C., B. J. BREITKREUTZ, T. REGULY, L. BOUCHER, A. BREITKREUTZ *et al.*, 2006 BioGRID: a general repository for interaction datasets. Nucleic Acids Res **34:** D535-539.

STIRLING, C. J., J. ROTHBLATT, M. HOSOBUCHI, R. DESHAIES and R. SCHEKMAN, 1992 Protein translocation mutants defective in the insertion of integral membrane proteins into the endoplasmic reticulum. Mol Biol Cell **3:** 129-142.

STOLZ, A., R. S. SCHWEIZER, A. SCHAFER and D. H. WOLF, 2010 Dfm1 forms distinct complexes with Cdc48 and the ER ubiquitin ligases and is required for ERAD. Traffic **11:** 1363-1369.

SUZUKI, M., T. OTSUKA, Y. OHSAKI, J. CHENG, T. TANIGUCHI *et al.*, 2012 Derlin-1 and UBXD8 are engaged in dislocation and degradation of lipidated ApoB-100 at lipid droplets. Mol Biol Cell **23:** 800-810.

SWAMINATHAN, S., A. Y. AMERIK and M. HOCHSTRASSER, 1999 The Doa4 deubiquitinating enzyme is required for ubiquitin homeostasis in yeast. Mol Biol Cell **10:** 2583-2594.

SWANSON, R., M. LOCHER and M. HOCHSTRASSER, 2001 A conserved ubiquitin ligase of the nuclear envelope/endoplasmic reticulum that functions in both ER-associated and Matalpha2 repressor degradation. Genes Dev **15:** 2660-2674.

SZATHMARY, R., R. BIELMANN, M. NITA-LAZAR, P. BURDA and C. A. JAKOB, 2005 Yos9 protein is essential for degradation of misfolded glycoproteins and may function as lectin in ERAD. Mol Cell **19:** 765-775.

TAN, X., P. A. OSMULSKI and M. GACZYNSKA, 2006 Allosteric regulators of the proteasome: potential drugs and a novel approach for drug design. Curr Med Chem **13:** 155-165.

THOMS, S., 2002 Cdc48 can distinguish between native and non-native proteins in the absence of cofactors. FEBS Lett **520:** 107-110.

THROWER, J. S., L. HOFFMAN, M. RECHSTEINER and C. M. PICKART, 2000 Recognition of the polyubiquitin proteolytic signal. Embo J **19:** 94-102.

TOMKO, R. J., JR., and M. HOCHSTRASSER, 2011 Incorporation of the Rpn12 subunit couples completion of proteasome regulatory particle lid assembly to lid-base joining. Mol Cell **44:** 907-917.

TONE, Y., and E. A. TOH, 2002 Nob1p is required for biogenesis of the 26S proteasome and degraded upon its maturation in Saccharomyces cerevisiae. Genes Dev **16:** 3142-3157.

TRAN, J. R., L. R. TOMSIC and J. L. BRODSKY, 2011 A Cdc48p-associated factor modulates endoplasmic reticulum-associated degradation, cell stress, and ubiquitinated protein homeostasis. The Journal of biological chemistry **286:** 5744-5755.

TRESSE, E., F. A. SALOMONS, J. VESA, L. C. BOTT, V. KIMONIS *et al.*, 2010 VCP/p97 is essential for maturation of ubiquitin-containing autophagosomes and this function is impaired by mutations that cause IBMPFD. Autophagy **6:** 217-227.

UCHIYAMA, K., G. TOTSUKAWA, M. PUHKA, Y. KANEKO, E. JOKITALO *et al.*, 2006 p37 is a p97 adaptor required for Golgi and ER biogenesis in interphase and at the end of mitosis. Developmental cell **11:** 803-816.

VALLE, C. W., T. MIN, M. BODAS, S. MAZUR, S. BEGUM *et al.*, 2011 Critical role of VCP/p97 in the pathogenesis and progression of non-small cell lung carcinoma. PLoS ONE **6:** e29073.

VAN NOCKER, S., S. SADIS, D. M. RUBIN, M. GLICKMAN, H. FU *et al.*, 1996 The multiubiquitin-chain-binding protein Mcb1 is a component of the 26S proteasome in Saccharomyces cerevisiae and plays a nonessential, substrate-specific role in protein turnover. Mol Cell Biol **16:** 6020-6028.

VAN NOCKER, S., and R. D. VIERSTRA, 1993 Multiubiquitin chains linked through lysine 48 are abundant in vivo and are competent intermediates in the ubiquitin proteolytic pathway. J Biol Chem **268:** 24766-24773.

VASHIST, S., and D. T. NG, 2004 Misfolded proteins are sorted by a sequential checkpoint mechanism of ER quality control. J Cell Biol **165:** 41-52.

VELICHUTINA, I., P. L. CONNERLY, C. S. ARENDT, X. LI and M. HOCHSTRASSER, 2004 Plasticity in eucaryotic 20S proteasome ring assembly revealed by a subunit deletion in yeast. EMBO J **23:** 500-510.

VEMBAR, S. S., and J. L. BRODSKY, 2008 One step at a time: endoplasmic reticulum-associated degradation. Nat Rev Mol Cell Biol **9:** 944-957.

VERDECIA, M. A., C. A. JOAZEIRO, N. J. WELLS, J. L. FERRER, M. E. BOWMAN *et al.*, 2003 Conformational flexibility underlies ubiquitin ligation mediated by the WWP1 HECT domain E3 ligase. Mol Cell **11:** 249-259.

VERMA, R., L. ARAVIND, R. OANIA, W. H. MCDONALD, J. R. YATES, 3RD *et al.*, 2002 Role of Rpn11 metalloprotease in deubiquitination and degradation by the 26S proteasome. Science **298:** 611-615.

VERMA, R., S. CHEN, R. FELDMAN, D. SCHIELTZ, J. YATES *et al.*, 2000 Proteasomal proteomics: identification of nucleotide-sensitive proteasome-interacting proteins by mass spectrometric analysis of affinity-purified proteasomes. Mol Biol Cell **11:** 3425-3439.

VERMA, R., R. OANIA, R. FANG, G. T. SMITH and R. J. DESHAIES, 2011 Cdc48/p97 mediates UV-dependent turnover of RNA Pol II. Mol Cell **41:** 82-92.

VOGES, D., P. ZWICKL and W. BAUMEISTER, 1999 The 26S proteasome: a molecular machine designed for controlled proteolysis. Annu Rev Biochem **68:** 1015-1068.

VON MIKECZ, A., 2006 The nuclear ubiquitin-proteasome system. J Cell Sci **119:** 1977-1984.

WALCZAK, H., K. IWAI and I. DIKIC, 2012 Generation and physiological roles of linear ubiquitin chains. BMC Biol **10:** 23.

WALZ, J., A. ERDMANN, M. KANIA, D. TYPKE, A. J. KOSTER *et al.*, 1998 26S proteasome structure revealed by three-dimensional electron microscopy. J Struct Biol **121:** 19-29.

WANG, C. W., and S. C. LEE, 2012 The ubiquitin-like (UBX)-domain-containing protein Ubx2/ Ubxd8 regulates lipid droplet homeostasis. J Cell Sci.

WANG, M., and C. M. PICKART, 2005 Different HECT domain ubiquitin ligases employ distinct mechanisms of polyubiquitin chain synthesis. EMBO J **24:** 4324-4333.

WANG, Q., C. SONG, X. YANG and C. C. LI, 2003 D1 ring is stable and nucleotide-independent, whereas D2 ring undergoes major conformational changes during the ATPase cycle of p97-VCP. J Biol Chem **278:** 32784-32793.

WANG, X., J. YEN, P. KAISER and L. HUANG, 2010 Regulation of the 26S proteasome complex during oxidative stress. Sci Signal **3:** ra88.

WATTS, G. D., J. WYMER, M. J. KOVACH, S. G. MEHTA, S. MUMM *et al.*, 2004 Inclusion body myopathy associated with Paget disease of bone and frontotemporal dementia is caused by mutant valosin-containing protein. Nature genetics **36:** 377-381.

WEIHL, C. C., S. DALAL, A. PESTRONK and P. I. HANSON, 2006 Inclusion body myopathy-associated mutations in p97/VCP impair endoplasmic reticulum-associated degradation. Hum Mol Genet **15:** 189-199.

WICKLIFFE, K. E., A. WILLIAMSON, H. J. MEYER, A. KELLY and M. RAPE, 2011 K11-linked ubiquitin chains as novel regulators of cell division. Trends Cell Biol **21:** 656-663.

WILK, S., and M. ORLOWSKI, 1983 Evidence that pituitary cation-sensitive neutral endopeptidase is a multicatalytic protease complex. J Neurochem **40:** 842-849.

WILSON, J. D., Y. LIU, C. M. BENTIVOGLIO and C. BARLOWE, 2006 Sel1p/Ubx2p participates in a distinct Cdc48p-dependent endoplasmic reticulum-associated degradation pathway. Traffic **7:** 1213-1223.

WINBORN, B. J., S. M. TRAVIS, S. V. TODI, K. M. SCAGLIONE, P. XU *et al.*, 2008 The deubiquitinating enzyme ataxin-3, a polyglutamine disease protein, edits Lys63 linkages in mixed linkage ubiquitin chains. J Biol Chem **283:** 26436-26443.

WOJCIK, C., and G. N. DEMARTINO, 2003 Intracellular localization of proteasomes. Int J Biochem Cell Biol **35:** 579-589.

WRIGHT, R., M. L. PARRISH, E. CADERA, L. LARSON, C. K. MATSON *et al.*, 2003 Parallel analysis of tagged deletion mutants efficiently identifies genes involved in endoplasmic reticulum biogenesis. Yeast **20:** 881-892.

WU, H., S. L. POMEROY, M. FERREIRA, N. TEIDER, J. MARIANI *et al.*, 2011 UBE4B promotes Hdm2-mediated degradation of the tumor suppressor p53. Nat Med **17:** 347-355.

XIE, Y., and A. VARSHAVSKY, 2000 Physical association of ubiquitin ligases and the 26S proteasome. Proc Natl Acad Sci U S A **97:** 2497-2502.

XIE, Y., and A. VARSHAVSKY, 2001 RPN4 is a ligand, substrate, and transcriptional regulator of the 26S proteasome: a negative feedback circuit. Proc Natl Acad Sci U S A **98:** 3056-3061.

XU, P., D. M. DUONG, N. T. SEYFRIED, D. CHENG, Y. XIE *et al.*, 2009 Quantitative proteomics reveals the function of unconventional ubiquitin chains in proteasomal degradation. Cell **137:** 133-145.

YAMAMOTO, S., Y. TOMITA, S. NAKAMORI, Y. HOSHIDA, H. NAGANO *et al.*, 2003 Elevated expression of valosin-containing protein (p97) in hepatocellular carcinoma is correlated with increased incidence of tumor recurrence. J Clin Oncol **21:** 447-452.

YAO, T., and R. E. COHEN, 2002 A cryptic protease couples deubiquitination and degradation by the proteasome. Nature **419:** 403-407.

YE, Y., H. H. MEYER and T. A. RAPOPORT, 2001 The AAA ATPase Cdc48/p97 and its partners transport proteins from the ER into the cytosol. Nature **414:** 652-656.

YE, Y., H. H. MEYER and T. A. RAPOPORT, 2003 Function of the p97-Ufd1-Npl4 complex in retrotranslocation from the ER to the cytosol: dual recognition of nonubiquitinated polypeptide segments and polyubiquitin chains. J Cell Biol **162:** 71-84.

YE, Y., and M. RAPE, 2009 Building ubiquitin chains: E2 enzymes at work. Nat Rev Mol Cell Biol **10:** 755-764.

YE, Y., Y. SHIBATA, C. YUN, D. RON and T. A. RAPOPORT, 2004 A membrane protein complex mediates retro-translocation from the ER lumen into the cytosol. Nature **429:** 841-847.

YEUNG, H. O., P. KLOPPSTECK, H. NIWA, R. L. ISAACSON, S. MATTHEWS *et al.*, 2008 Insights into adaptor binding to the AAA protein p97. Biochem Soc Trans **36:** 62-67.

YOU, J., and C. M. PICKART, 2001 A HECT domain E3 enzyme assembles novel polyubiquitin chains. J Biol Chem **276:** 19871-19878.

YU, Z., O. KLEIFELD, A. LANDE-ATIR, M. BSOUL, M. KLEIMAN *et al.*, 2011 Dual function of Rpn5 in two PCI complexes, the 26S proteasome and COP9 signalosome. Mol Biol Cell **22:** 911-920.

ZETTL, M., C. ADRAIN, K. STRISOVSKY, V. LASTUN and M. FREEMAN, 2011 Rhomboid family pseudoproteases use the ER quality control machinery to regulate intercellular signaling. Cell **145:** 79-91.

ZHANG, S., S. GUHA and F. C. VOLKERT, 1995 The Saccharomyces SHP1 gene, which encodes a regulator of phosphoprotein phosphatase 1 with differential effects on glycogen metabolism, meiotic differentiation, and mitotic cell cycle progression. Mol Cell Biol **15:** 2037-2050.

ZHANG, Y., S. MICHAELIS and J. L. BRODSKY, 2002 CFTR expression and ER-associated degradation in yeast. Methods Mol Med **70:** 257-265.

ZHANG, Y., G. NIJBROEK, M. L. SULLIVAN, A. A. MCCRACKEN, S. C. WATKINS *et al.*, 2001 Hsp70 molecular chaperone facilitates endoplasmic reticulum-associated protein degradation of cystic fibrosis transmembrane conductance regulator in yeast. Mol Biol Cell **12:** 1303-1314.

ZHAO, G., G. LI, H. SCHINDELIN and W. J. LENNARZ, 2009 An Armadillo motif in Ufd3 interacts with Cdc48 and is involved in ubiquitin homeostasis and protein degradation. Proc Natl Acad Sci U S A **106:** 16197-16202.